UDC 533.9(063)(082) YU ISSN 0373-3742

ПУБЛИКАЦИЈЕ АСТРОНОМСКЕ ОПСЕРВАТОРИЈЕ У БЕОГРАДУ
PUBLICATIONS OF THE ASTRONOMICAL OBSERVATORY OF BELGRADE

Sv. 61 No. 61

PROCEEDINGS

of the 2nd Yugoslav – Belarussian Symposium on Physics & Diagnostics of Laboratory & Astrophysical Plasmas

September 5-6, 1998, Zlatibor, Yugoslavia

Edited by M. S. Dimitrijević and V. S. Burakov

БЕОГРАД
1998

PUBL. ASTRON. OBS. BELGRADE No. 61, 1–197 BELGRADE AUGUST 1998

PUBLICATIONS OF THE ASTRONOMICAL OBSERVATORY OF BELGRADE

FOUNDED IN 1947

Director of the Astronomical Observatory: Dr M. S. Dimitrijević

The publication of this issue is financially supported by the Ministry of Sciences and Technology of Serbia, the Federal Ministry of Science and Technology and the Serbian-Belarussian Friendship Society.

Number of copies / тираж : 500

Production: Portal Co., Kosovska 51, Belgrade

UDC 533.9(063)(082) YU ISSN 0373-3742

ПУБЛИКАЦИЈЕ АСТРОНОМСКЕ ОПСЕРВАТОРИЈЕ У БЕОГРАДУ
PUBLICATIONS OF THE ASTRONOMICAL OBSERVATORY OF BELGRADE

Sv. 61 No. 61

PROCEEDINGS

of the 2nd Yugoslav – Belarussian Symposium on Physics & Diagnostics of Laboratory & Astrophysical Plasmas

September 5-6, 1998, Zlatibor, Yugoslavia

Edited by M. S. Dimitrijević and V. S. Burakov

БЕОГРАД
1998

PUBL. ASTRON. OBS. BELGRADE No. 61, 1–197 BELGRADE AUGUST 1998

The 2nd Yugoslav–Belarussian Symposium on Physics & Diagnostics of Laboratory & Astrophysical Plasmas

Zlatibor, Yugoslavia

5th – 6th September, 1998

Honorary Committee:

Prof. Dr B. Ivković (President, Minister of Science and Technology of Republic Serbia)

V. Brilev (Ambassador of Belarus in Yugoslavia)

Dr V. S. Burakov (Institute of Molecular and Atomic Physics of Belarus Academy of Sciences, Belarus)

Academician A. Despić (President of Serbian Academy of Sciences and Arts)

Dr M. S. Dimitrijević (Director of the Belgrade Astronomical Observatory)

Ž. Jovanović (Minister of Foreign Affaires of Yugoslavia)

L. Ya. Min'ko (Institute of Molecular and Atomic Physics of Belarus Academy of Sciences, Belarus)

Prof. Dr J. Purić (Rector of Belgrade University, Yugoslavia)

Academician A. P. Vojtovich (President of National Belarus Academy of Sciences, Belarus)

Prof. Dr J. Zelenović (Minister of Development, Science and Ecology of Yugoslavia)

Scientific Organizing Committee:

M. S. Dimitrijević (Co-chairman, Astronomical Observatory, Belgrade, Yugoslavia)

V. S. Burakov (Co-chairman, Institute of Molecular and Atomic Physics of Belarus Academy of Sciences, Belarus)

J. Purić (Vice-chairman, Faculty of Physics, Belgrade, Yugoslavia)

L. Ya. Min'ko (Vice-chairman, Institute of Molecular and Atomic Physics of Belarus Academy of Sciences, Belarus)

N. Konjević (Faculty of Physics, Belgrade, Yugoslavia)

T. Nenadović (Institute of Nuclear Sciences "Vinča", Belgrade, Yugoslavia)

S. Djurović (Institute of Physics, Faculty of Sciences, Novi Sad, Yugoslavia)

L. Č. Popović (Astronomical Observatory, Belgrade, Yugoslavia)

M. Ćuk (Faculty of Physics, Belgrade, Yugoslavia)

V. I. Arkhipenko (Institute of Molecular and Atomic Physics of Belarus Academy of Sciences, Belarus)

A. N. Chumakov (Institute of Molecular and Atomic Physics of Belarus Academy of Sciences, Belarus)

V. K. Goncharov (Research Institute of Applied Physical Problems at Belarus State University, Belarus)

G. S. Romanov (Institute of Molecular and Atomic Physics of Belarus Academy of Sciences, Belarus)

V. D. Shimanovich (Institute of Molecular and Atomic Physics of Belarus Academy of Sciences, Belarus)

Local Organizing Committee:

L. Č. Popović (Co-chairman)
M. Ćuk (Co-chairman)

D. Tankosić
N. Trajković
T. Milovanov

Editors of the Symposium Proceedings:

M. S. Dimitrijević
V. S. Burakov

CONTENTS

FOREWORD

The First Belarussian-Yugoslav Symposium on Physics and Diagnostics of Laboratory and Astrophysical Plasma was held in Minsk, 1-3 July 1996, as an effectuation of the desire of Yugoslav and Belarussian scientists to collaborate and contribute to the strengthening of mutual ties between Yugoslavia and Belarus. On the Yugoslav side the scientists concerned were associated with: Astronomical Observatory (Belgrade), Institute of Physics (Zemun), Faculty of Physics (Belgrade), Institute of Nuclear Sciences (Vinča) and Institute of Physics of the Faculty of Sciences (Novi Sad), while on the Belarussian side the scientists associations were with: Institute of Molecular and Atomic Physics of the Belarussian Academy of Sciences (Minsk), Institute of Applied Physical Problems of the Belarussian State University (Minsk) and Astronomical Observatory (Minsk).

This First Symposium has been dedicated to the memory of M. A. Elyashevich, academician of the Belarussian Academy of Sciences. Co-chairmen and editors of the Symposium proceedings were V. S. Burakov and the undersigned. The proceedings were published by the Belgrade Observatory – PUBLICATIONS BAO No. 53.

The Serbian delegation comprised 12 scientists. Presented at the Symposium were 52 contributions by authors from Belarus, Serbia, Russia, Ukraine, France, Syria and Czech Republic. The opportunity was take at the Symposium for founding the Belarus-Yugoslav Friendship Society, the guests of honour at the ceremony being M. S. Dimitrijević, J. Purić and M. Ćuk. As our desire was to stimulate mutual ties between our peoples not only in science but in other activities as well, a Serbian-Belarussian Friendship Society was founded in Belgrade too, the guests of honour at the ceremony being L. Ya. Min'ko, A. Chumakov and I. Filatova.

This Second Symposium is a continuation of our common activity aimed at developing mutual collaboration and the ties for the benefit of our countries and science in general.

MILAN S. DIMITRIJEVIĆ

INVITED LECTURES

Publ. Astron. Obs. Belgrade No. 61 (1998), 9 – 12 *Invited lecture*

THE EFFECT OF CATHODE TEMPERATURE ON THE ELECTRIC FIELD DISTRIBUTION IN CATHODE FALL REGION OF THE KISELEVSKII PLASMA SOURCE

V.I.ARKHIPENKO, L.V.SIMONCHIK, S.M.ZGIROVSKII

Institute of Molecular and Atomic Physics NASB, Scorina av. 70, Minsk 22072, Belarus
E-mail: simon@imaph.bas-net.by

The glow discharges at atmospheric pressure and higher are characterized by some typical features of cathode region such as small spatial size of layers (about tens microns) and high gradients of temperature, particle concentration, electric fields etc. It is result in significant deviation of plasma from equilibrium state. It is the reason of different plasma instabilities in cathode region and results in the contraction and arc breakdown.

In the present work the effect of cathode temperature on parameters of cathode fall region and negative glow is investigated in glow discharge in helium at atmospheric pressure named as Kiselevskii plasma source (KPS) (Kiselevskii et al 1983, Arkhipenko et al 1997). This discharge is unique in itself, because it exists at atmospheric pressure and higher, has the stable characteristics and can be used as spectral source of line and continuous spectrum and the source of excitation of spectra in atomic emission spectroscopy as well.

The discharge was produced in hermetic chamber between round anode and flat copper cathode. The flow of working gas helium was ~ 4 l/min. The impurity concentration in helium flow was not over 0.01%. The discharge was formed by source of direct current varying from 0.05 up to 15 A. The distance between electrodes can be change from 0,5 up to 8 mm.

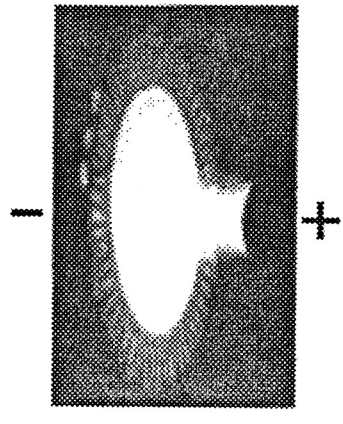

Fig.1.

The image of discharge is shown in Fig.1 One can see, that it has the following structure: the luminous thin disk (less than 1 mm) of negative glow is located above cathode surface, and the luminous column by a diameter of 3-5 mm is propagated toward the anode. There is dark space between these luminous regions. The end of the anode is covered with a bright luminous layer. Negative cathode glow has ring structure, which is created by zones of different plasma luminescence. The luminescence at the disk edge is

nonuniform and also consists of alternating dark and light zones.

The diameter of a negative glow depends on a discharge current and

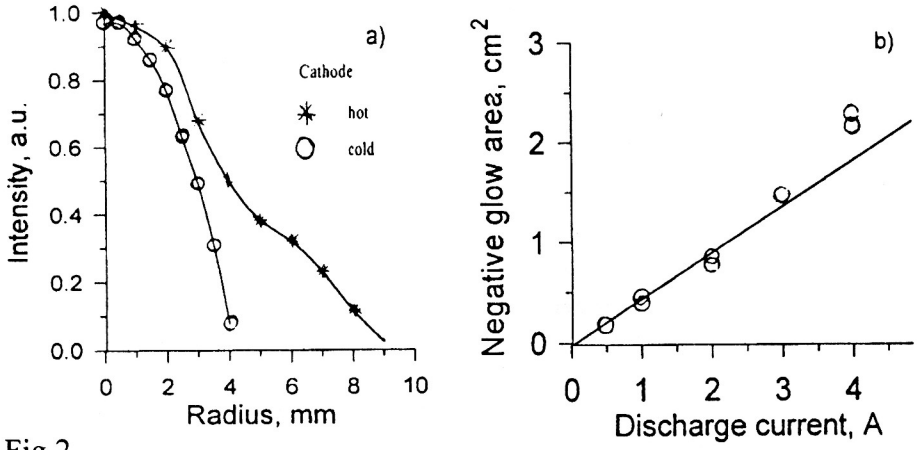

Fig.2.

cathode temperature. In a Fig. 2a the cross distributions of He I (450.1 nm) line intensity in negative cathode glow for two regimes: at cold and hot cathodes are shown. The cold cathode regime was realized by special design cathode with water cooling. Thus the cathode temperature did not exceed 100 °C. At the hot cathode the heat was took away from cathode surface by central tube, which was used as cathode holder. In this case the cathode temperature was about 500 °C. At the cold cathode and current 1 A the negative glow has a diameter about 7-8 mm. In case of hot cathode the luminescence is spreaded on the cathode and can reach about 20 mm in dia. At that the cathode luminescence diameter practically does not depend on the distance between electrodes (2 - 10 mm).

The dependence of the cathode negative glow size on current was investigated in cold cathode regime (Fig.2b). In this case the bounds of negative glow in radial direction rather sharp and luminescence size can be determined. The area of negative cathode glow region grows linearly when the current increases up to 3 A and grows faster at currents higher than 3 A that, apparently, is connected with heating of cathode.

In papers Suzdalov I. I. (1972) and (Kiselevskii et al 1983) the voltage-current characteristic of glow discharge at atmospheric pressure was investigated as $U = f(I)$. It grows in the current range from 0.3 up to 2 A (Suzdalov I. I. 1972) and up to 5 A (Kiselevskii et al 1983). Thus the discharge voltage increases from 180 up to 250 V (Fig.3a, crosses). When current exceeds these values, glow discharge breakdown in arc regime (Fig.3a, bottom curve). One of the reasons of this breakdown can be heating of the cathode. At such conditions, apparently, the emitting properties of cathode and conditions in cathode fall region are changed. It is demonstrated by changes of discharge

characteristics such as: the negative glow region size and potential fall on electrodes. At once after discharge ignition at current 1 A the diameter of negative glow is about 8-9 mm. When the cathode temperature increases up to ~ 500 °C the luminous area is increased more than two times. Thus the discharge voltage is increased on 10 – 20 V.

In Fig.3b the dependencies of voltage fall on electrodes for two cathode regimes are shown. At the minimal interval, the voltage on electrodes, apparently, corresponds to cathode voltage fall, because in this case the positive column does not exist, and the type of negative glow practically does not depended on distance between electrodes. One can see, that in case of the hot cathode the voltage fall on 80 V higher than at cold cathode. In both cases the increase of distance between electrodes as well as positive column grows result

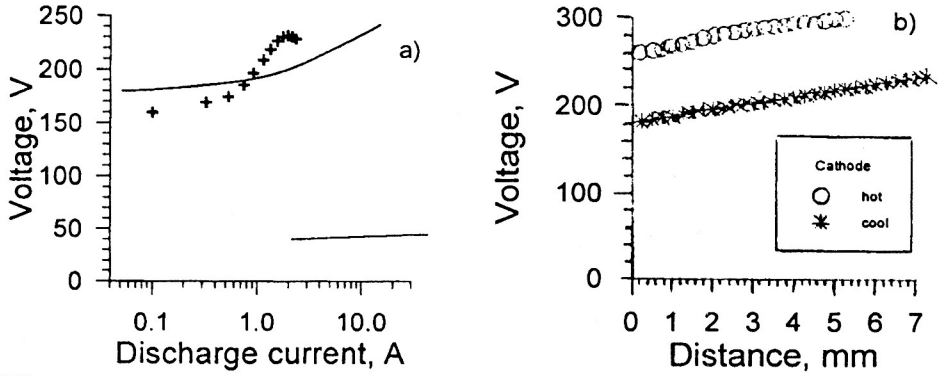

Fig.3.

in the approximately identical increase of voltage about 50V.

Using the cathode special designed by authors for effective cooling of cathode the glow discharge having the rise current-voltage characteristic was produced in more widely current range (Fig.3a). So at current increase from 0.05 up to 15 A the voltage) on electrodes is increased from 180 up to 240 V (Fig.3a, continuous curve). At that the discharge breakdown is not occurred. To increase the current over 15 A in our experiment was impossible because of insufficient parameters of current source, and small cathode cross size. The applied electric power was reached of ~ 4 kW.

The potential distribution of KPS is typical for glow discharges i.e. there is significant cathode fall (Kiselevskii et al 1983). The electric field distribution in cathode fall region was measured by H_β line broadening. The experimental H_β line profiles registered in the KPS cathode fall region contained the two broadening peaks. The distance between peaks and line center is defined by constant electrical field resulting in the Stark splitting of the H_β line. Electric field value measured by H_β line Stark broadening is ~ 60 kV/cm. Its distributions along anode-cathode axis for cold and hot cathodes are

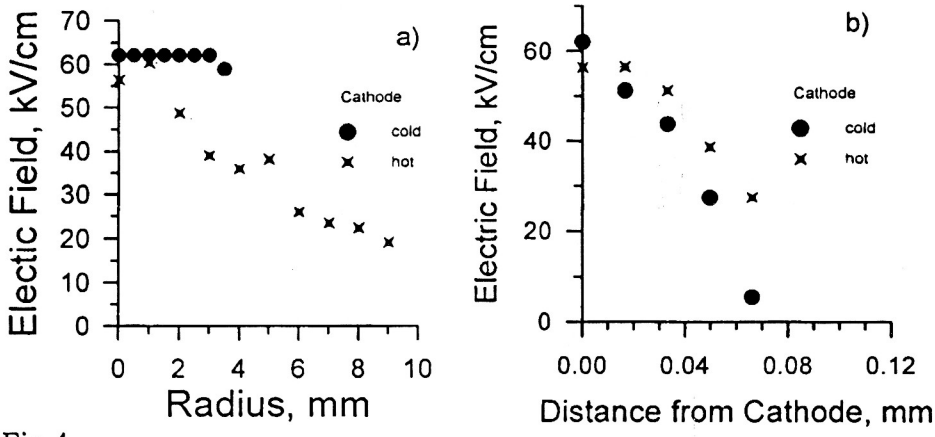

Fig.4.

shown in Fig.4. One can see, that cathode fall region has about 100 microns long for hot cathode and less than 80 microns long for cold. The maximum electric field in cathode fall region in both cases is practically equal. It gives that the longitudinal size of cathode fall for hot cathode is higher than for cold that well corresponds to applied voltage at these regimes (Fig.3b).

The essential difference in field distribution in cathode area between cold and hot regimes is observed in radial direction (Fig4b). When cathode is cold the magnitude of field in a radial direction does not change right up till the luminescence bound. In this case, as already mentioned above, the luminescence has sharp bounds. That is why the field was determined on distance less than 4 mm from axis.

At the hot cathode the field is decreased in radial direction more smoothly: in distance of 5 mm the magnitude of electric field decreases twice in comparison with one at axis, and at edge of negative glow in three times. It should be noted, that the feature of radial distribution at 4 mm is connected to dark ring zone of negative glow (Fig.1).

Thus, the received results show that the cathode temperature essentially effects on the KPS cathode fall region and spatial potential distribution.

The work have been performed at financial support of Belarussian Found of Fundamental Researches (project Φ96-086).

References

Kiselevskii L. I., Mazurenko S. L., Makarevich A. N. and Solovianchik D. A. : 1983,\journal{Technic. Phys. Letters}, \vol{9}, 1401
Arkhipenko V.I. et al: 1997,\Proc.of Intern. Confer. PPPT-2\ vol{1},5
Suzdalov I. I.:1972, \journal {Journ. Appl. Spectr.} \vol {17} 977

Publ. Astron. Obs. Belgrade No. 61 (1998), 13 – 16 *Invited lecture*

МНОГОИМПУЛЬСНЫЙ ПРИПОВЕРХНОСТНЫЙ ОПТИЧЕСКИЙ РАЗРЯД КАК ЭФФЕКТИВНЫЙ ИСТОЧНИК ЭРОЗИОННОЙ ПЛАЗМЫ

А.Н.ЧУМАКОВ, Н.А.БОСАК
Институт молекулярной и атомной физики Национальной Академии наук Беларуси, 220082 Минск, Беларусь
E-mail: chumakov@imaph.bas-net.by

Резюме. Выявлены условия эффективного образования эрозионной плазмы и управления ее параметрами в многоимпульсном приповерхностном оптическом разряде.

1. ВВЕДЕНИЕ

Многоимпульсное лазерное воздействие на поглощающие материалы при относительно низких плотностях мощности лазерного излучения (ЛИ) $q < 10^7$ Вт/см^2 (λ=1,06 мкм), когда процессы плазмообразования протекают в парах мишени без перехода в окружающий мишень газ, в значительной мере исследовано и широко применяется в технологии. В этих условиях частота следования лазерных импульсов влияет преимущественно на процессы разрушения облучаемого материала и сказывается прежде всего на выносе массы, форме лунки и т.д. Анализ динамики плазменных образований в таких условиях привел к развитию представлений о режиме последовательного выталкивания воздуха и эрозионных паров периодическими плазменными сгустками (Минько Л.Я. и др., 1989).

При более высоких плотностях мощности ЛИ $q \sim 10^8 \div 10^9$ Вт/см^2 энерговклад в мишень ограничивается развитием экранировки мишени плазмой и формированием лазерных волн поглощения в газах (Немчинов И.В., 1982). Процессы лазерного приповерхностного плазмообразования протекают при этом уже не только в эрозионной плазме, а преимущественно в окружающем мишень атмосферном газе. В таких условиях переход от одноимпульсного лазерного воздействия к многоимпульсному должен, вероятно, приводить к существенной неаддитивности действия отдельных лазерных импульсов серии, особенно при высоких частотах их повторения.

В работе рассмотрены возможности направленного выбора плазмообразующей среды (пары мишени или атмосферный газ), в которой реализуется оптический разряд, и управления параметрами образующейся плазмы на основании исследований одно- и многоимпульсного лазерного воздействия на материалы в газах.

2.ЭКСПЕРИМЕНТАЛЬНЫЕ РЕЗУЛЬТАТЫ И ИХ ОБСУЖДЕНИЕ

Проведены систематические исследования воздействия ЛИ на ряд мишеней (металлы, стеклотекстолит, графит, эбонит) при различных давлениях воздуха 0,1-10 атм и плотностях мощности ЛИ $10^7 < q \leq 10^9$ Вт/см^2 (λ=1,06 мкм) в режимах одиночных, двойных, а также серий лазерных импульсов с частотами повторения $f \leq 200$ кГц. Управление режимом генерации лазера осуществлялось с помощью крупногабаритных пассивных затворов с F_2^- - центрами окраски (Босак Н.А. и др., 1987). Динамика лазерных плазмообразований исследовалась методами высокоскоростной фотографии и киноспектрографии, регистрировалось давление и потенциалы на поверхности металлических мишеней.

Показано, что в воздухе атмосферного давления при интенсивности ЛИ $q<2 \cdot 10^7$ Вт/см^2 независимо от частоты следования лазерных импульсов приповерхностный оптический разряд развивается в эрозионной плазме. При достаточно высокой частоте повторения лазерных импульсов ~50-100 кГц над эрозионным плазменным факелом образуется область повышенной плотности воздуха, обусловленная взаимодействием ударных волн, инициируемых отдельными лазерными импульсами, с атмосферным воздухом (Костюкевич Е.А. и др., 1980). В такой "пробке" сжатого воздуха над эрозионным плазменным образованием уже при интенсивности ЛИ $q \sim 2 \div 5 \cdot 10^7$ Вт/см^2 может инициироваться низкопороговый оптический пробой (Минько Л.Я. и др., 1989), приводящий к одновременному существованию эрозионной и воздушной плазмы в различных областях плазменного факела.

С повышением интенсивности ЛИ $q > 5 \cdot 10^7$ Вт/см^2 преимущественное плазмообразования перемещается из паров в воздух еще на фронте лазерного импульса, приводя к экранировке мишени воздушной плазмой (Минько Л.Я. и др., 1994). Более 10% энергии лазерного импульса конвертируется в излучение плазмы в видимой и инфракрасной областях спектра, интенсивность которого квазилинейно растет с плотностью мощности ЛИ (Чумаков А.Н. и др., 1994, 1997). Такая физическая картина характерна как для одиночных лазерных импульсов, так и для серии, если частота их повторения не превышает ~1÷5 кГц. В этих условиях оптический разряд осуществляется преимущественно в воздухе.

При более высоких частотах повторения лазерных импульсов $f \geq 5$ кГц обнаруживается неаддитивность действия отдельных лазерных импульсов серии, которая проявляется при измерениях давления на мишени (рис.1), ее потенциалов (рис.2), а также при регистрации спектров. Это приводит к тому, что в определенном диапазоне параметров лазерных импульсов ($q > 0,2$ ГВт/см^2; $f > 5$ кГц)

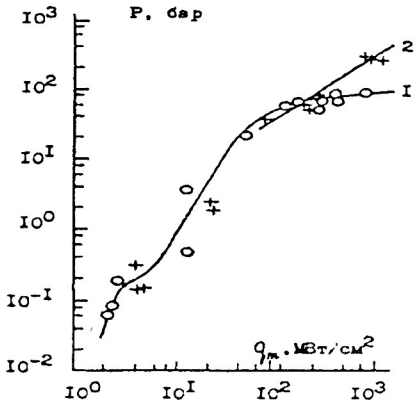

Рис.1. Давление на Al-мишени при воздействии первого (1) и второго (2) импульсов ЛИ

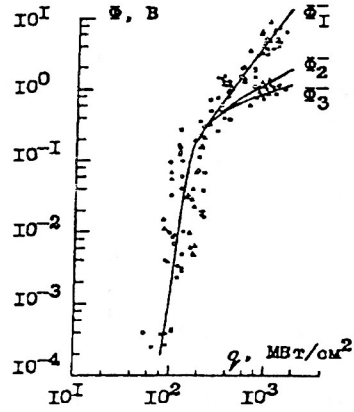

Рис.2.Потенциалы Al-мишени при воздействии первого (Φ_1^-) и последующих импульсов ЛИ

реализуется режим эффективного эрозионного плазмообразования, который сопровождается повышением эффективности возбуждения давления на поверхности мишени, усилением эрозионного плазмообразования и сменой плазмообразующей среды (Минько Л.Я., Чумаков А.Н. и Босак Н.А., 1990). Воздушная плазма, образованная первым лазерным импульсом, обладает специфической пространственной структурой, обусловленной инициированием радиационной, либо светодетонационой лазерных волн поглощения, и в дальнейшем при воздействии последующих лазерных импульсов почти полностью вытесняется эрозионной плазмой. При этом в плазменном факеле образуются устойчивые вихревые структуры, препятствующие смешиванию эрозионной и воздушной плазмы в течение интервала между лазерными импульсами. Иначе говоря, создается лазерно-плазменный насос, отсасывающий воздух из области воздействия вблизи мишени. В этих условиях реализуется специфический приповерхностный оптический разряд в эрозионной плазменной среде. Анализ динамики плазменного фронта показал, что светодетонационные волны поглощения ЛИ формируются и распространяются при этом и в эрозионной плазме, а не только в воздухе (Минько Л.Я., Чумаков А.Н. и др., 1993). Выяснено, что описанная физическая картина сохраняется и при понижении давления воздуха до ~ 0,1 атм.

С увеличением давления атмосферного газа (азот) уменьшается скорость разлета плазмы, приводя к накоплению в области каустики линзы нескольких плазменных сгустков от ряда лазерных импульсов, а также

изменяется структура приповерхностных лазерных плазмообразований. Кроме того над ними обнаруживаются локальные плазменные образования в окружающем мишень газе, количество которых становится особенно значительным при увеличении давления до 8 - 10 атмосфер. Поэтому эффективность образования эрозионной плазмы с повышением давления уменьшается. При давлении $p \geq 10$ атм (азот) в приповерхностном оптическом разряде одновременно сосуществуют области как с эрозионной, так и с азотной плазмой даже при плотности мощности ЛИ $q \sim 50$ МВт/см^2 в хаотическом режиме генерации (Al-мишень).

Высокая эрозионная эффективность многоимпульсного приповерхностного оптического разряда обеспечивает широкие возможности его применения в технологии. Так двухимпульсный оптический разряд уже применяется в лазерном спектральном анализе (Першин С.М., 1989; Петух П.Л. и др., 1994), а высокочастотный многоимпульсный - в лазерных технологиях обработки материалов (Минько Л.Я., Чумаков А.Н., Босак Н.А. и др., 1995).

Литература

Босак Н.А., Мартыненко О.Г., Чумаков А.Н. и др.: 1987, Препринт №43 Института тепло- и массообмена им. А.В.Лыкова, Минск.

Костюкевич Е.А., Минько Л.Я., Чумаков А.Н.: 1980, Препринт № 211 Института физики АН БССР, Минск.

Минько Л.Я., Бакеев А.А., Чумаков А.Н.: 1989, *ЖПС*, **51**, 403.

Минько Л.Я., Чумаков А.Н., Босак Н.А.: 1990, *Квант.электр.*, **17**, 480.

Минько Л.Я., Чумаков А.Н., Босак Н.А., Авраменко В.Б.: 1993, *Хим. физика*, **12**, 1500.

Минько Л.Я., Чумаков А.Н., Баканович Г.И.: 1994, *ЖПС*, **61**, 476.

Минько Л.Я., Чумаков А.Н., Босак Н.А. и др.: 1995, V Межд. конф. "Лазерные технологии'95". Тез. докл., 38, Шатура.

Немчинов И.В.: 1982, *Изв. АН СССР. Сер.физич.*, **46**, 1026.

Першин С.М. : 1989, *Квантовая электроника*, **16**, 325.

Петух П.Л., Широканов А.Д., Янковский А.А.: 1994, *ЖПС*, **61**, 340.

Чумаков А.Н., Ефремов В.В., Босак Н.А. и др.: 1994, *Квант. электр.*, **21**, 773.

Чумаков А.Н.: 1997, Физика плазмы и плазменные технологии, (Мат. конф.), **3**, 547, Минск.

Publ. Astron. Obs. Belgrade No. 61 (1998), 17 – 20 *Invited lecture*

EMISSION OF AN ATMOSPHERIC PRESSURE ARC IN A GAS FLOW

E.A. ERSHOV-PAVLOV*, K.L. STEPANOV, Yu.A.STANKEVICH, L.K.STANCHITS

Heat & Mass Transfer Institute, 15, P. Brovka str., 220072 Minsk, Belarus
E-mail: kls@hmti.ac.by
*Institute of Molecular & Atomic Physics, 70, F. Scaryna Ave., 220072 Minsk, Belarus
E-mail: ershov@imaph.bas-net.by

Abstract. Techniques and results are presented of the emission calculation for an atmospheric pressure arc stabilized with a gas flow. Local thermodynamic equilibrium (LTE) is used as an approximation for the arc positive column. Spectral (in visible and UV region), as well as total emission parameters are studied using the approximation for the arc plasma volume having two-dimensional temperature distribution of an axial symmetry. A radiative-collisional model is formulated for the arc near cathode region, where a departure from LTE is observed. The model accounts a population of excited particles on energy levels and the plasma emission. Air plasma is taken to fit for the analysis of the arcs in air and nitrogen gas flows.

Arc plasma parameters. The study is limited with positive columns and near cathode regions of transferred arcs. Here the plasma is mainly composed of the flow gas particles. Moreover, at a constant pressure the arc positive column is a stationary non-uniform plasma volume of an axial or conical geometry. Usually the arc axial gradient is much lower of the radial one even for the near cathode regions. A typical temperature distribution is shown in Fig. 1 for the transferred arc in nitrogen at 250 A current. (Megy, 1995).

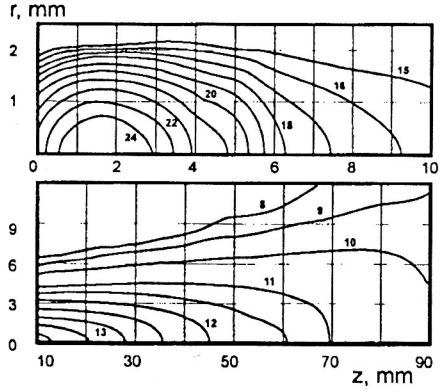

Fig. 1. Arc temperature distribution (kK).

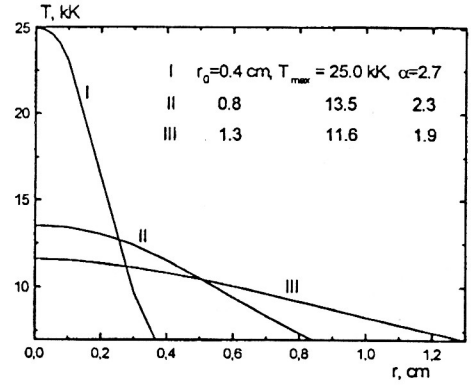

Fig. 2. Radial temperature profiles.

Radial temperature profiles of the arcs can be presented in a parametrical form, e.g., $T(r) = T_0\left[1 + A(r / r_0)^{\alpha}\right]^{-1}$ (Bousrih, 1995). Here T_0 is the plasma axial temperature, r_0 is the arc radius, α determins the temperature profile form (from a uniform at $\alpha \to \infty$ up

to a very steep one, when $\alpha \sim 1$), $A = T_0 / T(r_0) - 1$. The temperature two-dimensional profile T(r,z) also can be easily presented with this expression, if one takes into account, that T_0, r_0, α and A depend on z. In Fig. 2 radial temperature profiles are shown for three axial positions (I - z = 0.16 cm, II - z = 2 and III - z = 6 cm) of the arc (Megy, 1995).

Radiation transfer calculations. Theoretical (Avilova, 1970, Romanov 1995) and experimental (Shimanovich, 1997) data on optical properties of air plasma have been used for the radiation transfer consideration. Measured spectral absorption coefficients are presented in Fig. 3 for atmospheric pressure air plasma at different temperatures (Shimanovich, 1997).

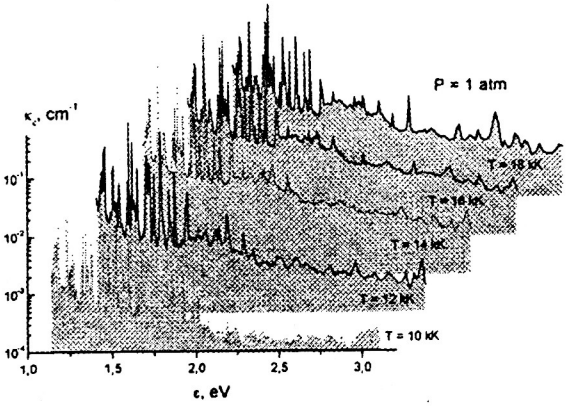

Fig. 3. Spectral absorption coefficients of air plasma at P= 1atm, T=10-18 kK.

The radiation transfer equation has been solved supposing two- or one-dimensional cylindrical geometry of the arc plasma volume for the temperature profiles, shown in Figs. 1, 2.

$$\left(\mu \frac{\partial I_\varepsilon}{\partial r} - \frac{1-\mu^2}{r}\frac{\partial I_\varepsilon}{\partial \mu}\right)\mathrm{Sin}\theta + \frac{\partial I_\varepsilon}{\partial z}\mathrm{Cos}\theta = \kappa_\varepsilon (I_{pc} - I_\varepsilon). \quad (1)$$

The solution has been found along the eq.(1) characteristics, which correspond to Gauss knots of the angle variables determining the radiation flux from the plasma

$$d\Omega = d\chi\,\mathrm{Sin}\Psi\, d\Psi, \qquad \mathrm{Cos}\Psi = \mathrm{Sin}\theta\mathrm{Cos}\varphi, \qquad \mathrm{Sin}\psi\mathrm{Cos}\chi = \mathrm{Sin}\theta\mathrm{Sin}\varphi. \quad (2)$$

Taking into account the symmetry, the flux has been determined from a one-dimensional cylinder surface using the following expression

$$S_\varepsilon = 4\int_0^{\pi/2} d\chi \int_0^{\pi/2} \mathrm{Cos}\Psi\,\mathrm{Sin}\Psi\, I_\varepsilon(\chi,\psi)\, d\Psi = \frac{\pi^2}{4}\sum_i W_i \sum_j \mathrm{Cos}\Psi_j\,\mathrm{Sin}\Psi_j\, I_\varepsilon(\chi_i,\Psi_j)\, W_j, \quad (3)$$

(W_i are weights of the Gauss quadrature formulas) providing 64 rays pass in $\pi/2$ solid angle. Separately, radiation intensity has also been calculated in the plane normal to the cylinder axis and in the direction passing through the axis. At the integration (1) along the ray, the source function in a calculation cell has been approximated with the linear dependence.

$$I_\varepsilon(\tau_i) = I_\varepsilon(\tau_{i-1})e^{(-\Delta\tau_i)} + I_{pc}(\tau_i)\left[1 - e^{(-\Delta\tau_i)}\right] - \left(\frac{dI_{pc}}{d\tau}\right)_i \left[1 - e^{(-\Delta\tau_i)}(1+\Delta\tau_i)\right], \quad (4)$$

It provided true asymptotics $I_\varepsilon(\tau_i)$ in small and large τ limits.

Emission of the arc positive column. Data on group (for 6 spectral intervals) and total radiation fluxes from the positive column surface of the arc are presented in Table 1.

Note the following. Inspite of the equilibrium emission maximum corresponding to axial temperatures is observed in the spectral interval $\varepsilon \approx 2.5 - 6$ eV, the plasma radiation flux in shorter wavelengths (groups 5 and 6) is rather important. It is due to the plasma large opacity in these spectral regions, as well as because of strong spectral lines, which totally determine the radiation output. In the visible region ($\varepsilon \approx 1.15$-4.5 eV) the flux falls with the plasma mean temperature decrease. At a time its part in the total flux increases up to 5.2, 25 и 35.5% for the profiles I, II, III, respectively. Total power (per length unit) decreases monotonously (6.3, 2.1 и 0.99 kW/cm). On the contrary in visible region of the spectrum the value increases to 0.25, 0.55 and 0.35 kW/cm, respectively.

Table 1. Radiation fluxes from the arc positive column, kW/cm^2

S, kW/cm^2							
$\Delta\varepsilon$, eV	0.03-1.15	1.15-3.16	3.16-4.52	4.52-6.51	6.51-11	11-17	0-∞
$\Delta\lambda$, nm	>1078	1078-392	392-274	274-190	190-113	113-73	∞-0
I	$6.5\cdot10^{-2}$	$1.21\cdot10^{-1}$	$1.03\cdot10^{-2}$	$7.98\cdot10^{-3}$	$7.23\cdot10^{-1}$	1.58	2.51
II	$3.87\cdot10^{-2}$	$9.63\cdot10^{-2}$	$7.60\cdot10^{-3}$	$5.29\cdot10^{-3}$	$1.74\cdot10^{-1}$	$9.73\cdot10^{-2}$	$4.19\cdot10^{-1}$
III	$1.22\cdot10^{-2}$	$3.81\cdot10^{-2}$	$4.78\cdot10^{-3}$	$2.85\cdot10^{-3}$	$4.81\cdot10^{-2}$	$1.55\cdot10^{-2}$	$1.21\cdot10^{-1}$

Fig. 4 gives an idea about a role of different radial parts of the positive column in the output radiation formation. Here directed radiation intensity is shown in the points of the normal ray with $\xi = 0.5r_0, r_0, 1.5r_0, 2r_0$ (section II). One can see from the spectra comparison in the ray points at $0.5r_0$, r_0 и $2r_0$, that the emission in periphery layers of the column practically do not give any input in the radiation with $\varepsilon \le 10$ eV energy. The same layers shield VUV radiation, which is generated in the column hot regions, with the radiation in free-bound continuum falling down up to the order and more of the value at the axis, and spectral lines are totally reabsorbed.

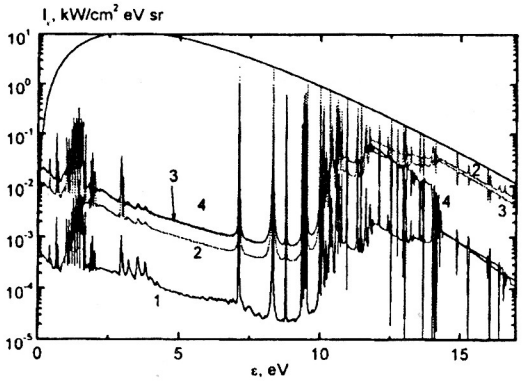

Fig. 4. Spectral intensity in different ray points.

Arc emission in the near-cathode region. The results above are based on the LTE approximation, that is limited for the plasma near the arc cathode region. Here at the space scale of the cathode spot dimension, temperatures of electrons and heavy particles can differ much, and the exited particles distribution on energy levels does not obligatory corresponds to the Boltzmann-Saha law. One of the evidence of the LTE deviation is an "unusual" behaviour of the maximum emissivity of atomic lines with the distance from

the cathode, see, e.g, Haddad (1984), Pellerin (1992), Razafinimanana (1994) for argon and Megy (1995) for nitrogen plasmas. Closer to the cathode, the line emissivity maxima become lower, and the temperatures, at which they are observed, are higher. As a result it causes a difference in temperatures measured using atom and ion spectral lines (e.g., NI λ =746.8 nm and NII λ =399.5 nm, Megy, 1995). There are some processes which can cause the plasma state deviation of the equlibrium one near the cathode. We note the following possible important reasons: emission of non-termal electrons from the cathode, very high current density at the cathode tip, non-compensated spontaneous radiative decay of the excited levels.

We used radiative-collisional model (RCM) to account a population kinetics of the atomic excited levels and to evaluate the arc radiation in the near-cathode region. The kinetics equations content basical elementary acts and processes responsible for the level population (collisional ionization and triple recombination, excitation and de-excitation by electron impacts, radiative level decay, photo- and dielectron recombination).

Stationary approximation RCM (Romanov, 1991)

$$\sum_n K^{(i)}_{mn} N^{(i)}_n + D^{(i)}_m = 0 \qquad (5)$$

corresponds to an instantaneous reaction of the populations on ambiant conditions (electron temperature T_e and density N_e) and accounts the collisional-radiative equilibrium states in a large interval of plasma parameters. In the limiting case of low and high densities coronal and thermodynamic equilibriums, respectively, are realized.

Results of our calculations using the model show, that for plasmas near the arc cathode (T~2 eV, N_e~(2-4)$\cdot 10^{17}$ cm^{-3}) there is a rather strong deviation from the equilibrium not only of the excited levels population, but also of the plasma charge composition. One can see a relative increase of the plasma electron density due to a difference in electron and heavy particle temperatures at a constant pressure, as well as an intensity fall of the atomic lines because of the excited levels de-population. So, the results show qualitatively the phenomena previously observed experimentally (Megy, 1995). The equilibrium deviation results in lower emission of the near-cathode arc parts, than one can expect for LTE plasmas with such high parameters.

References

Avilova I.V., Biberman L.M., Vorob'ev V.S. at al.: 1970, The Optical Properties of Hot Air. Moscow, Nauka.

Bousrih S., Megy S., Ershov-Pavlov E., and Baronnet J.-M.: 1995, Proc. ISPC-12, Minneapolis, **4**, 1819.

Haddad G.H. and Farmer A.J.: 1984, J. Phys. D: Appl. Phys., **17**, 1189.

Megy S., Ershov-Pavlov E., Baronnet J.-M.: 1995, J. Phys. D: Appl. Phys., **28**, 344.

Pellerin S., Musiol K., Pokrzywka B., Chapelle J.: 1994, J. Phys.D: Appl. Phys., **27**, 522.

Razafinimanana M., Gudzy P., Gleizes A. et al.: 1994, J. High Temp. Chem. Proc., **4**, 51.

Romanov G.S., Stankevich Yu.A., Stanchits L.K., and Stepanov K.L.: 1995, Int. J. Heat Mass Transfer, **38**, 545.

Romanov G.S., Stepanov K.L., Stanchits L.K.: 1991, J. of Applied Spectroscopy (in Russian), **54**, 825.

Shimanovich V., Ershov-Pavlov E., Azharonok V. et al.: 1997, Preprint of the Institute of Molecular & Atomic Physics, No4, Minsk.

Publ. Astron. Obs. Belgrade No. 61 (1998), 21 – 24 *Invited lecture*

THE PARAMETERS AND PHASE COMPOSITION CONTROL OF LASER EROSION JETS WITH AN EMPLOYMENT ELECTRIC AND ELECTROMAGNETIC FIELDS.

V.K.Goncharov, M.V.Puzyrev, A.F.Chernyavskii.
Scientific-Research Institute of Applied Physical Problems, Kurchatova 7, 220106, Minsk, Belarus, Tel: (017) 2-77 - 56-44, E-mail: pfp@llpd.bsu.minsk.by.

Abstract. We have found possibility to control composition of the erosion laser jets with an employment external electric and electromagnetic fields. Erosion laser plasma with a minimal composition of the liquid drop phase have been obtained.

1. INTRODUCTION

The products of damage caused by moderate-intensity (10^5 - 10^8 W cm^{-2}) laser radiation to metals is two-phase jets. These jets consist of a vapour, a plasma, and liquid drops. It is interesting to use an external electric and electromagnetic fields to control parameters and composition of these erosion jets.

Lead target was placed between two plates. An external electric field was applied to these plates. It allowed to determine an influence of the external electric field on dynamics of a fine-disperse liquid-drop phase formation. The target was damaged by near-rectangular neodymium laser pulses of a power density $4{,}6\times10^5$ W cm^{-2}. The monitoring of sizes and liquid drops density was carried out by transverse probing the erosion products with radiation from an auxiliary ruby laser. The probing was carried out on the distance 1 mm from a targets surface. Electric field was changed from 0 up to 4 kV cm. Investigation results we can see on fig.1. The solid curve is result of measurements when field is absence, large dashes at E=1 kV cm, small dashes - E=4 kV cm. They show that at exposure laser radiation to the lead target drop density (N) increase in erosion laser jet if electric field was applied in comparison when electric field was absence, and drop diameters (d) decrease. It can be explained by a drop fragmentation as charges appear on these drops. It can be used for a control of erosion jets parameters.

Another control method of the erosion plasma jets parameters and composition is exposure to jets by rather intensity electromagnetic radiation. The investigation in crossed laser beams have been made when the interacting laser radiation was directed perpendicular to the target surface and radiation from an auxiliary laser propagated parallel to the surface at some distance

from it. Auxiliary laser radiation interacted with the erosion products and evaporated additionally the condensed phase without altering the conditions on the target surface.

We used a lead target. The interacting radiation was in the form of near-rectangular neodymium laser pulses of 400-500 μs duration. The intensity of this radiation was 1.4×10^6 W cm^{-2} in all experiments and the irradiation spot diameter was 6 mm. The additional evaporation was caused by radiation from a free-running pulsed neodymium laser generation pulses of ~ 10^{-3} s duration. The diameter of the laser beam in the evaporation zone was 8 mm. The center of this beam was 2 mm above the target surface, so that the lower part of the beam was screened by the target itself and the rest interacted with the erosion jet. The intensity of the radiation causing additional evaporation was varied, depending on the experimental conditions. The monitoring condensed phase parameters was on the distance 2 mm from a targets surface.

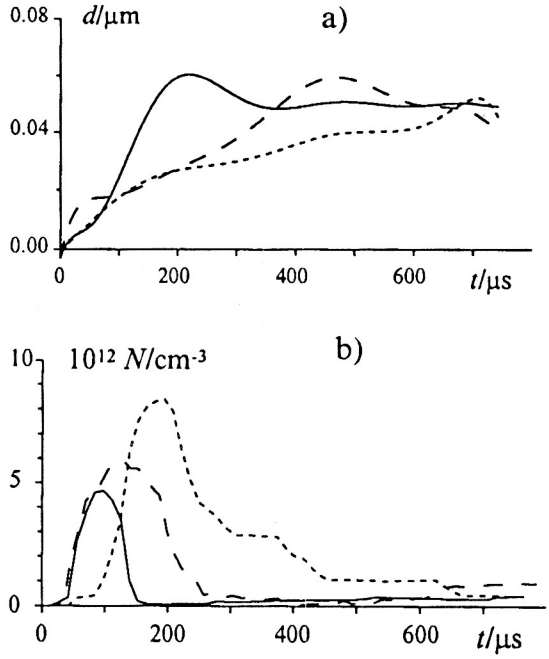

Fig. 1.

Kinetics of the condensed phase can highly depend on particles sizes and consequence on particle formation mechanism. Therefore, it is useful to consider three cases: case 1, when an erosion jet contains small particles generated by bulk vapour formation (during the action of plasma-forming neodymium laser pulse); case 2, when an erosion jet contains particles formed by both mechanisms (it follow 450 - 500 μs from beginning of a laser pulse); case 3, when an erosion jet contains primarily large particles formed by the hydrodynamic mechanism (it follow after 650 - 700 μs from beginning of a laser pulse acting on the target).

Experiments showed that the additional evaporation of the condensed-phase particles in case 1 began at the laser radiation intensities causing additional evaporation as low as ~ 10^5 W cm^{-2} and, when power density reached ~ 5×10^5 W cm^{-2}, particles became so small that probe ruby

laser radiation scattered by them was below the sensitivity limit of our measuring system, which was 10^8 cm^{-3}.

Fig.2 gives results of our experiments on a laser target exposed to neodymium laser pulses of 1.4×10^6 W cm^{-2} intensity in the absence of the radiation causing additional evaporation (solid curve) and in the presence of such radiation of ~ 2.3×10^5 W cm^{-2} intensity (dashed curve). We found that even when the intensity of the radiation causing additional evaporation was low (compared with the intensity of radiation producing the initial damage), the dimensions of the condensed-phase particles and their concentration fell significantly.

Experimental results for case 2 was showed fig 3a. The interacting radiation once again had the intensity 1.4×10^6 W cm^{-2}. The intensity of the radiation causing additional evaporation was varied from zero to ~ 10^6 W cm^{-2}. The size of the particles first increased with increase in the intensity of radiation causing additional evaporation. This was observed because the smallest particles formed by bulk vapour formation were evaporated completely and a major fraction of the large particles formed by the hydrodynamics mechanism remained in the jet. A further increase in the intensity of the radiation causing additional evaporation reduced the particle size. A reduction in volume concentration C (ratio of the volume occupied by the condensed-phase particles in the investigated zone to the total volume of this zone) indicated sufficiently effective additional evaporation of the condensed phase of the target material when the intensity of the radiation causing additional evaporation was increased.

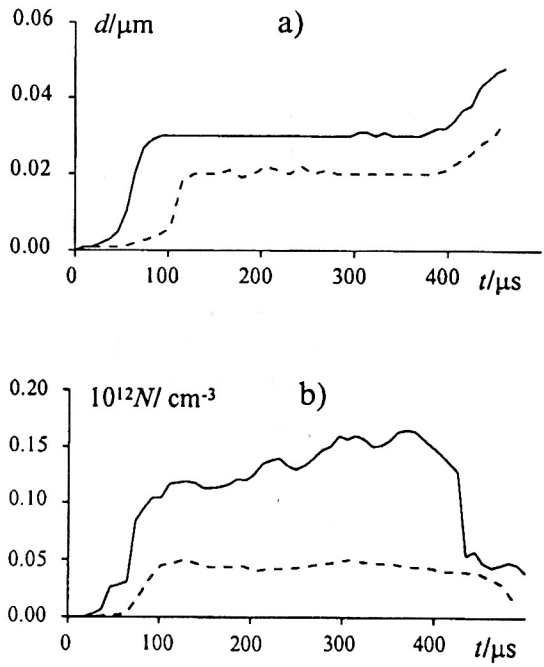

Fig. 2.

For case 3 (fig.3b) particle size decreased with increase in the intensity of the radiation causing additional evaporation. The behavior of the volume concentration indicated that the mass of the material concentrated in the

condensed-phase particles decreased significantly with increase in the intensity of the radiation causing additional evaporation and at some intensity of this radiation the particles could evaporate completely.

2. RESULTS

Our investigation of the kinetics of the condensed-phase particles in erosion jets in crossed laser beams showed that radiation from an auxiliary laser could be used to control effectively the parameters of the liquid-drop phase particles and thus the parameters of the erosion jets themselves. Radiation of lower intensity should be sufficient for this purpose and radiation of much lower intensity should be for particles generated bulk vapour formation. It have been shown that the simultaneous interacting of crossed laser beams and external electric field on erosion jets can be used for an effective of the material target condensed phase in erosion jets. Electric field allow decrease of the particles sizes and small particles can be effectively to evaporate the auxiliary laser radiation.

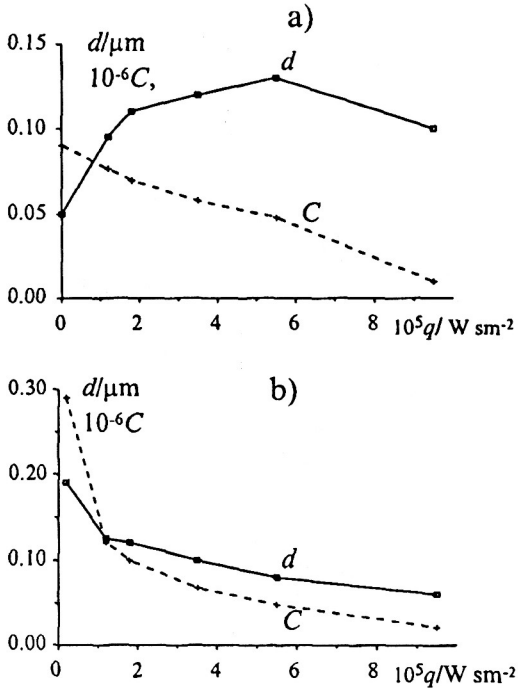

Fig. 3.

References

Влияние внешних электрических полей на динамику жидкокапельной фазы лазерных эрозионных факелов / В.К.Гончаров, М.В.Пузырев, А.В.Иовлев, А.В.Сметанников // II-я Международная конференция по лазерной физике и спектроскопии: Тез. докл. - Гродно, 1995. - С.242.

Goncharov V and Puzyrev M.: 1997, \ journal {Quantum Electronics}\ vol {27}, 319-321.

Publ. Astron. Obs. Belgrade No. 61 (1998), 25 – 26 *Invited lecture*

ELECTRIC CHARACTERISTICS OF THE TOTAL IONIZED PLASMAS IN CONSTANT AND TIME-VARIABLE EXTERNAL FIELDS

A. A. MIHAJLOV[1] and Z. DJURIĆ[2]

[1]*Institute of Physics, P.O.Box 57, 11001 Beograd, Yugoslavia*
[2]*Dept. of Materials, Oxford University, Parks Road, Oxford OX1 3PH*

In this work we have treated the conductivity and some other electrical characteristics of fully ionized non-ideal plasmas in external electric and magnetic fields. The cases of time-independent electric and magnetic fields have been discussed, as well as the case of time-depending high-freqency (HF) electric field. Presented work is continuation of previous work (Mihajlov *et al.* 1993), treating static conductivity of the fully-ionized plasmas. In the work just mentioned a method of determining this conductivity was developed. This method is a semiclassical analog of previously developed version of the RPA method (Djurić *et al.* 1991; Adamyan *et al.* 1994). Employing this method, the expression for static electrical conductivity, σ_0, is obtained in the form

$$\sigma_0 = -\frac{4e^2}{3m}\int_0^\infty E\rho(E)\tau\frac{dw}{dE}dE, \tag{1}$$

where $\rho(E)$ is the density of one-electron states in the energy space, $w(E)$ is the Fermi-Dirac distribution and τ is the relaxation time. In this theory the quantity τ is obtained by expresion

$$\tau = \frac{1}{\nu_e(E)}, \tag{2}$$

where $\nu_e(E)$ is the semiclassical analog of the corresponding RPA effective frequency of electron scattering in plasma. Full expressions for $\nu_e(E)$ are given in the paper mentioned (Mihajlov *et al.* 1993).

This semiclasical method has been tested in the previous work (Adamyan *et al.* 1994) in the case of determination of static electrical conductivity of fully ionized plasmas in the presence of an external static magnetic field. In this case, the components of the tensor of static electrical conductivity $\sigma_{ij}(\omega_c)$ are being expressed through qantities $\sigma_l(\omega_c)$, defined by expression

$$\sigma_l = \frac{4e^2}{3m}\int_0^\infty \frac{(\omega_c\tau)^{l-1}}{1+(\omega_c\tau)^2} E\rho\tau\frac{dw}{dE}dE, \tag{3}$$

where ω_c is the cyclotron frequency ($\omega_c = eB/mc$, where B is magnetic inductivity and $l = 1, 2, 3$. It is supposed here that the relaxation time τ is given by the same expression as when σ_0 was determined.

The developed formalism may be extended to fully ionized plasmas in an external, time-dependent electric field that varies with frequency ω. For this purpose, the real and imaginary parts of electrical conductivity, here denoted by $\sigma_r(\omega)$ and $\sigma_i(\omega)$ respectivelly, must be calculated. These quantities are determined in a way that is similar to the one described above for the electrical conductivity in the presence of a magnetic field, and are being expressed through the quantities σ_l with $l = 1, 2$. Thus, the following expressions are obtained for $\sigma_r(\omega)$ and $\sigma_i(\omega)$:

$$\sigma_r = -\frac{4e^2}{3m}\int_0^\infty \frac{1}{1+(\omega\tau)^2} E\rho\tau\frac{dw}{dE}dE, \qquad \sigma_i = -\frac{4e^2}{3m}\int_0^\infty \frac{\omega\tau}{1+(\omega\tau)^2} E\rho\tau\frac{dw}{dE}dE, \tag{4}$$

where τ is again given by the expression (2).

Using the expressions presented above, we have calculated the values of $\sigma_{ij}(\omega_c)$, and $\sigma_r(\omega)$ and $\sigma_i(\omega)$ in the range of electron densities from 10^{18} to 10^{22} cm^{-3}, and in the temperature range $5 \cdot 10^3 - 5 \cdot 10^5 K$. Besides, we determined the values of the generalized Holl's constant (in the case of the static magnetic field), HF dielectric permitivity $\epsilon(\omega)$, reflexion coefficient $R(\omega)$ and some other characteristics of fully ionized plasmas as well. For each electron density and temperature, calculations have been performed for ω_c and ω between $0.1\omega_p - 1.5\omega_p$, where ω_p is the plasma frequency.

The obtained results make it possible to study the influence of the plasma's inner conditions over the relaxation time τ as well as the behaviour of the conductivity when the frequency of the external electric field ω approaches the plasma frequency ω_p. Besides, determining values of the reflexion coefficient $R(\omega)$ allowes comparison of the results obtained by this theory with the existing experimental results (Mintsev and Zaporogets, 1989).

References

Adamyan, V.M., Djurić, Z., Ermolaev, A.M., Mihajlov, A.A. and Tkachenko, I.M.: 1994, *J. Phys. D*, **27**, 111–118.

Djurić, Z., Mihajlov, A.A., Nastasyuk, V.A., Popović, M. and Tkachenko, I.M.: 1991, *Phys. Lett. A*, **155** (6,7), 415–418.

Mihajlov, A.A., Ermolaev, A.M., Djurić, Z. and Ignjatović, Lj.: 1993, *J. Phys. D*, **26**, 1041–1047.

Mintsev, V.B., Zaporogets, Yu.B.: 1989, *Contrib. Plasma Phys.*, **29**, 493–501.

Publ. Astron. Obs. Belgrade No. 61 (1998), 27 *Invited lecture*

STARK BROADENING OF NEUTRAL ARGON LINES IN PLASMAS

Z. MIJATOVIĆ[1], D. NIKOLIĆ[1], S. DJUROVIĆ[1], R. KOBILAROV[1] and N. KONJEVIĆ[2]
[1]*Institute of Physics, Trg D. Obradovića 4, 21000 Novi Sad, Yugoslavia*
[2]*Institute of Physics, P.O. Box 68, 11080 Belgrade, Yugoslavia*

Stark broadening of twelve neutral argon lines has been experimentally studied. This study is performed to obtain new and reliable data of Stark broadening parameters (widths and shifts of the lines and ion-broadening parameter A). Some of the studied lines has not been measured before. As a plasma source wall-stabilized arc operated with 99 % Ar - 1 % H_2 mixture under atmospheric pressure, was used. In order to avoid possible adiative transfer problems when radiation is recorded end-on, plasma observation was performed side-on. The other reason for side-on observation was to obtain relativelly wide range of plasma electron density (0.74×10^{16} - 2.9×10^{16} cm^{-3}) and temperature (9300 - 10800 K). For the shift measurements Geissler tube was used as a reference plasma source.

Attention was paid on precise spectral intensity measurements (with the error $< 1\%$) and wavelength settings (within 0.0025 nm). Recorded profiles were Abel inverted and then precise numerical procedure for line separation and deconvolution was applied.

Obtained results for width and shift measurements are presented and compared with the theoretical ones and experimental results of other authors when they were available.

Publ. Astron. Obs. Belgrade No. 61 (1998), 28 – 31 *Invited lecture*

РАДИАЦИОННАЯ ПЛАЗМОДИНАМИКА - НОВОЕ НАУЧНОЕ НАПРАВЛЕНИЕ В ФИЗИКЕ ПЛАЗМЫ

Л.Я.МИНЬКО
Институт молекулярной и атомной физики
Национальной Академии наук Беларуси,
220082 Минск, Беларусь
E-mail: lrpd@imaph.bas-net.by

Радиационная плазмодинамика (РПД) изучает динамику плазменных потоков в условиях, когда в их энергетике важна роль радиационных процессов, или другими словами, перенос излучения играет существенную роль в энергетике плазменных потоков. РПД начала формироваться как новое самостоятельное научное направление исследований в физике плазмы в середине 70-х годов прежде всего на основе работ МГТУ им. Н.Э.Баумана, Института физики земли им. О.Ю.Шмидта, ФИАНа, ИОФАНа, ИВТАН, Института физики им. Б.И.Степанова (ИМАФ) АН БССР, НИИПФП им. А.Н.Севченко при БГУ (ИТМО им. А.В.Лыкова АН БССР).

Основные принципы РПД были сформулированы на I Всесоюзном симпозиуме по РПД (1989 г., г.Москва). С тех пор симпозиум регулярно проводится МГТУ им. Н.Э.Баумана. На III симпозиуме (1994 г.) ему придан статус Межгосударственного и образован постоянно действующий Организационный комитет, в котором представлен и ИМАФ НАНБ. Прошедший в 1997 году IV Межгосударственный симпозиум, а также большое количество принципиально новых физических результатов исследований, публикуемых в периодической печати в последнее время, свидетельствуют, что фундаментальные и прикладные исследования по РПД ведутся достаточно активно.

Концепция РПД состоит в изучении радиационно-плазмодинамических процессов, сопровождающих взаимодействие высокоэнергетических источников энергии с веществом всех агрегатных состояний, и разработке на основе этих исследований физико-технических принципов создания новых плазменных и лазерно-плазменных энергетических и технологических устройств, а также систем высокоэнергетических потоков, предназначенных для решения ряда актуальных задач лазерной физики и фотохимии, высокотемпературной теплофизики и радиационной метрологии, медико-биологических

исследований и прогрессивных технологий.

РПД включает следующие разделы (Радиационная плазмодинамика, Москва, Энергоатомиздат, 1991 г.):

- экспериментальные и теоретические исследования радиационно-плазмодинамических процессов взаимодействия теплового и когерентного излучения и сильных ударных волн с веществом различных агрегатных состояний;
- диагностика радиационно-плазмодинамических процессов;
- численное моделирование и теория радиационно-плазмодинамических процессов в различных условиях;
- термодинамические и оптические свойства излучающей плазмы;
- плазмодинамические источники излучения высокой спектральной яркости и генераторы сильных ударных волн;
- радиационно-плазмодинамические системы промышленного назначения.

Исследования по РПД в ИФ им. Б.И.Степанова (ИМАФ) НАНБ явились естественным продолжением наших работ по физике и диагностике импульсных плазменных ускорителей, начатых в начале 60-х годов под руководством академика Михаила Александровича Ельяшевича и обобщенных в монографии (Л.Я.Минько "Получение и исследование импульсных плазменных потоков", Изд. Наука и техника, Минск, 1970). РПД зародилась у нас еще в начале 70-х годов как лазерная плазмодинамика, в последующем трансформировавшаяся в радиационную лазерную плазмодинамику, а затем несколько позже с 1975 г. начались исследования по плазмодинамике квазистационарных плазменных ускорителей (КСПУ) с ионным токопереносом.

Основные этапы исследований:

- **Динамика лазерных плазмодинамических процессов или лазерная плазмодинамика.** Сформулированы принципы и созданы научные основы. Впервые в наших работах введено в научную литературу понятие лазерная плазмодинамика, сущность которой состоит в том, что с созданием лазеров появились новые возможности в динамике плазмы. Стало возможным получать самоподжигающиеся импульсные оптические разряды, т.е. поджигаемые собственной лазерной плазмой, создаваемой в начале лазерного импульса, воздействующего на твердое тело. Появилась возможность создавать лазерные источники плазмы, генерирующие эрозионные плазменные потоки с управляемыми параметрами, а также ударные волны (Л.Я.Минько. Лазерные плазменные ускорители и

(большие пятна облучения) одномерного разлета образующейся эрозионной плазмы, позволившая установить эрозионную природу начального плазмообразования и выявить турбулентную неустойчивость приповерхностных плазменных образований и влияние химического состава материала на характер распространения лазерных волн поглощения. В условиях образования крупномасштабных лазерных приповерхностных плазменных образований обнаружено испарение мишени (стеклотекстолит) радиационными потоками, испускаемыми плазмой, что проявляется в оттеснении ее от мишени холодными парами с нарастанием в процессе лазерного воздействия удаления контактной границы пары-плазма. Установлено влияние резонансного взаимодействия лазерного излучения с парами материала мишени на процессы начального эрозионного плазмообразования, заключающееся в снижении порога плазмообразования в тех случаях, когда длина волны взаимодействующего лазерного излучения совпадает с длинами волн спектральных линий атомов материала мишени.

Исследованы свойства лазерно-плазменных источников оптического излучения в атмосфере и вакууме.

- Динамика формирования, структура и свойства крупномасштабных квазистационарных компрессионных плазменных потоков. Создана картина оптико-плазмодинамических процессов и впервые получена компрессия в эрозионных плазменных ускорителях и плазмогенераторах двухступенчатого квазистационарного плазменного ускорителя (КСПУ) и самом КСПУ (энергозапас 250 кДж), позволяющем получать крупномасштабные плазменные потоки протяженностью до 100 см с характерной скоростью свыше 100 км/с и концентрацией элктронов в области компрессии ~ 10^{18} $см^{-3}$. Установлена связь между магнито- и плазмодинамическими процессами и свойствами квазистационарных компрессионных плазменных потоков в КСПУ.

Одновременно шло развитие оптико-спектроскопических и интерферометрических способов и средств диагностики быстропротекающих плазмодинамических процессов. В настоящее время тематика наших исследований составляет самостоятельные разделы РПД:

- Радиационная плазмодинамика импульсных источников плазменных потоков при различных давлениях окружающей среды.
- Радиационная плазмодинамика импульсного высокоэнергетического воздействия на твердое тело и плазму.

плазмотроны. В сб.: "Плазменные ускорители и их применение", Изд. Наука и техника, Минск, 1974). Получены важные результаты по нелинейному взаимодействию лазерного излучения с собственными эрозионными плазменными факелами при наличии конденсированной дисперсной фазы и по их экранирующему действию.

- Динамика компрессионных плазменных потоков, генерируемых одноступенчатыми коаксиальными плазменными ускорителями так называемыми магнитоплазменными компрессорами (МПК). Проведенные экспериментальные исследования МПК, представляющего самостоятельный интерес как система, в которой ускорение плазмы сопровождается ее сжатием, позволили впервые детально изучить динамику формирования компрессионного плазменного потока (КПП), выявить трубчатую структуру на стадии его распада, получить распределение основных газодинамических и термодинамических параметров КПП. Проведенные ранее исследования впервые полученных в воздухе при атмосферном давлении компрессионных эрозионных плазменных потоков, состав которых определяется материалом внутреннего электрода, позволили изучить радиационно-плазмодинамические процессы, ответственные за формирование таких потоков, найти способы увеличения эффективности ввода энергии непосредственно в компрессионный эрозионный плазменный поток, определить его основные газодинамические, термодинамические и излучательные характеристики.

- Динамика лазерных радиационно-плазмодинамических процессов или радиационная лазерная плазмодинамика. Изучены динамика плазмообразования и лазерных приповерхностных плазменных образований. Введено понятие и дано обоснование и экспериментальное подтверждение "самоподдерживающихся низкопороговых оптических разрядов ", динамика которых определяется в основном тепловым излучением собственной лазерной плазмы. Впервые с высокой надежностью благодаря высокоскоростным спектроскопическим исследованиям с высоким пространственно-временным разрешением установлена общая эрозионная природа низкопороговых приповерхностных оптических разрядов в широком диапазоне длин волн (от УФ до среднего ИК) и длительностей импульсов воздействующего на поверхность лазерного излучения.

Развита радиационно-плазмодинамическая картина взаимодействия лазерного излучения с поверхностью в реальных условиях

Publ. Astron. Obs. Belgrade No. 61 (1998), 32 *Invited lecture*

SPECTRAL LINE INVESTIGATION OF ACTIVE GALACTIC NUCLEI AT BELGRADE ASTRONOMICAL OBSERVATORY

L. Č. POPOVIĆ
Astronomical Observatory, Volgina 7, 11160 Belgrade 74, Yugoslavia
E-mail lpopovic@aob.aob.bg.ac.yu

The spectral line investigation, theoretically and experimentally, helps us to understand physical properties of plasmas in celestial bodies. Practically, we can diagnose the emitting plasma from outside of the Solar system only by using spectral lines and continnum. Consequently, the spectral line investigation is very important for numerous astrophysical problems.

Among the most interesting objects in Cosmos are the Active Galactic Nuclei (AGNs). Their radiation comes from a compact very luminous center of a galaxy, and in their spectra very broad emission lines are observed. These lines come from a very extensive emitting line region, where plasma has very various parametes; the electron density from $10^2 cm^{-3}$ to $10^{12} cm^{-3}$ and electron temperature from several hundreds to tens thousand kelvins. The investigation of line shapes as well as of variability of line and continuum flux helps us to model these object.

We have been investigating the spectral line shapes of Seyfert galaxies and quasars since 1994 (Popović *et al.* 1994ab, Popović *et al.* 1995ab, Popović 1996, Popović and Mediavilla 1997, Popović *et al.* 1998abc). In the begining, the research was mainly theoretical. Afterwards it has been extended to use Crimean Astrophysical Observatory observational data base (see Popović 1996). Also, the spectra from other observational data bases have been used (see e.g. Popović *et al.* 1995b). Now, we are trying to model the very complex lines of several typical Seyfert 1 galaxies and quasars (see Popović *et al.* 1998a) as well as to model double peaked lines of some of these objects (see Popović *et al.* 1998c).

References

Popović, L.Č., Vince, I., Kubičela, A.: 1994a, In: Multi – Wavelength Continuum emission of AGN, (eds. T.J.-L. Courvoisier and A. Blecha), Kluwer Academic Publishers, Dordrecht-Boston-London, p.456.

Popović, L.Č., Vince I., Kubičela, A., Atanacković-Vukmanović, O. and Samurović, S.: 1994b, *Bull. Astron. Belgrade* **149**, 9.

Popović, L.Č., Vince, I., Atanacković-Vukmanović, O. and Kubičela, A.: 1995a, *Astron. Astrophys.* **293**, 309.

Popović, L.Č., Jevremović, D., Vince, I. and Milovanov, T.: 1995b, *Publ. Obs. Astron. Belgrade* **50**, 103.

Popović, L.Č.: 1996, *Publ. Obs. Astron. Belgrade* **54**, 49.

Popović, L.Č. and Mediavilla, E.: 1997, *Publ. Obs. Astron. Belgrade* **57**, 95.

Popović, L.Č., Trajković, N. and Kubičela, A.: 1998a, *Publ. Obs. Astron. Belgrade* **60**, 67.

Popović, L.Č., Vince, I., Kubičela, A. and Salim, S.: 1998b, *Proc. of IAU 184* (in press).

Popović, L.Č., Pavlović, R., Živkov, V., Djurašević, G. and Kubičela, A.: 1998c, *Proc. of SPIG'98* (in press).

Publ. Astron. Obs. Belgrade No. 61 (1998), 33 – 34 *Invited lecture*

PLASMA FOCUS EXPERIMENT IN YUGOSLAVIA

J. PURIĆ[1], R. ANTANASIJEVIĆ[2] and M. ĆUK[1]
[1]*Faculty of Physics, University of Belgrade, P. O. Box 368, 11000 Belgrade, Yugoslavia*
[2]*Institute of Physic, P. O. Box 55, 11084 Zemun, Yugoslavia*

The first experiment with a modified plasma focus device up to 2kJ input energy was performed in the Laboratory for plasma spectroscopy at Faculty of Physics, University of Belgrade, in 1985 (Purić *et al.* 1986). The experiments on the model of plasma focus device in the connection with nuclear aspects, in 1989 were provided when D^+ ions of the energy about MeV were detected using the SND (CR-39) detectors (Antanasijević *et al.* 1991). During the next several years the new plasma focus device was built. The plasma focus chamber is the Mather type and consists of two brass coaxial electrodes (the outer electrode consists of 18 cylindrically positioned brass roads). The chamber has been designed for current up to 1 MA and 10^{10} n/pulse.

For producing a current up to 1MA and 1μs electrical discharges, a low inductance capacitor bank (C = 45 μF, L = 62 nH, R = 15 mΩ, M_{max} = 40 kV, E_{max} = 36 kJ) with triggered spark gap as a switching device is used as an energy source with a power supply and two coaxial electrodes.

The voltage measurement was performed with high voltage probes. A Rogovski coil monitoring the variations with time of electrode current was used.

Acceleration of the plasma focus current sheet has been measured with optic cables "looking" at certain spots inside the chamber. For neutron yield measurements a large (600 l) liquid scinttilator (NE 343) surrounded with 12 photomultipliers (Antanasijević *et al.* 1993) with efficiency of 80% for unique neutron was used.

Device is designed so that we have 8 windows on the plasma focus chamber and we can measure different processes during the single shot:

- positive particles produced from D-D reactions and its discrimination using the NTD (NC and CR-39), (Antanasijević *et al.* 1997) and Al foil of different ticknes, (Vuković and Antanasijević, 1995)
- X-ray "optics" using the mica sheet;
- Angular distribution of deuterons, and products of the D-D reactions. (Antanasijević *et al.* 1996) and
- Electromagnetic interference analysis on the current profile during the plasma focus collapse phase (Šević *et al.* 1998).

Finally, during this year, two new corresponding channels have been mounted on the appropriate windows, for optical measurements with spectrograph and X-ray ra-

diography with soft X-ray. Also, a small liquid detector (NE 343) of 12 l volume for neutron angular distribution measurement from D-D reactions.

Although the plasma focus experiment can be regarded as the simplest of all the fusion approaches based on self-magnetic field confinement there are a lot of unresolved problems intrinsic to such an approach. For instance, the plasma focus is considered as an impedance converter, which gives a fast rising high current at the final pinch phase. In spite of this, it is questionable whether the plasma focus can be revived as a fusion approach. The future of the plasma focus depends on whether the leakage current, which increases with he discharge energy, is intrinsic in the plasma focus device. We have tried to analyze the proceses of selforganisation in the collapse phase of the plasma focus operation in which the neutrons begin to be emitted if the working gas is deuterium. Therefore the role of the radiation collapse in the plasma focus device and theoretical explanations to the scaling law obtained experimentally is still very important subjects to be studied (Miyamoto, 1996).

References

Antanasijević, R., Vuković, J., Popović, S. Popović, M., Purić, J., Ćuk, M.: 1991, *Nucl. Track. and Rad. Meas.*, **19**, 555.

Antanasijević, R., Vuković, J., Šević, D. Joksimović, D., Dragić, A., Udovičić, V., Purić, J., Ćuk, M.: 1997, *Rad. Measurements*, **28**, 75.

Antanasijević, R., Lakićević, I., Marić, Z., Vigier, J.P.: 1993, *Phys. Lett.* **180**, 25.

Antanasijević, R., Todorović, Z., Šević, D. Joksimović, D., Dragić, A., Udovičić, V., Marić, Z.: 1996, *Rad. Measurements*, **28**, 241.

Vuković, J., Antanasijević, R.: 1996, *Rad. Measurements*, **28**, 141.

Miyamoto, T.: 1996, NIFS-PROC-26 Research Report, Nagoja, Japan, pp 71.

Šević, D., Antanasijević, R., Dragić, A. Udovičić, V, Purić, J., Ćuk, M.: 1996, *18th SPIG Contributed Papers*, 469.

Publ. Astron. Obs. Belgrade No. 61 (1998), 35 – 38 *Invited lecture*

ТЕОРЕТИЧЕСКИЕ ИССЛЕДОВАНИЯ ВЫСОКОТЕМПЕРАТУРНОЙ МНОГОЗАРЯДНОЙ ПЛАЗМЫ (ОБЗОР)

Г.С. РОМАНОВ

Академический научный комплекс " Институт тепло- и массообмена им.А.В.Лыкова "Академии наук Беларуси.

220072, Республика Беларусь, г.Минск, ул. П.Бровки,15,
E - mail mgv @ hmti. ac.by

АННОТАЦИЯ. Рассматриваются методы расчета оптико-физических параметров нагретых газов и многозарядной плазмы, необходимых для решения задач воздействия концентрированных потоков энергии на вещество. Приводятся примеры таких расчетов, а также решения ряда задач динамики лабораторной и натурной плазмы (действие лазерного излучения и электронных пучков на мишень, электрический взрыв проводников, движение в атмосфере и удар по поверхности Земли космических объектов).

Одной из актуальных проблем современной физики и новых технологий является изучение процессов, протекающих при действии лазерного излучения, пучков заряженных частиц и других высококонцентрированных потоков энергии на конденсированные поглощающие среды. Вопросы, возникающие при анализе процессов воздействия, весьма сложны и далеки от полного разрешения. Это связано с многообразием наблюдаемых явлений, их многопараметричностью, зависимостью от большого числа внешних факторов, трудностями в организации физического эксперимента и комплексной диагностики высокотемпературных, высокоэнергетичных быстропротекающих процессов. Все это делает актуальной разработку и создание численных моделей процессов и явлений, которые позволяли бы дополнять физический эксперимент адекватным ему численным, способным прогнозировать представляющие интерес параметры и закономерности. В данной работе возможности, лежащие на пути решения указанной проблемы, анализируются на примерах нескольких задач динамики плотной среды и плазмы, выбор и постановка которых обусловлены их практическим значением, обеспечившим достаточно полные и разносторонние экспериментальные исследования. Это задачи о действии мощных потоков лазерного излучения и сильноточных электронных пучков на поглощающие (в основном металлические) массивные и тонкие мишени. В этих задачах, благодаря высокой удельной концентрации энергии, значительную роль могут играть процессы тепло- и массопереноса, связанные с интенсивным нагревом, плавлением, испарением вещества мишени, распространением в ней мощных ударных волн, ионизацией паров, возникновением мощных потоков собственного теплового излучения образующей плазмы. Количественное изучение указанных процессов требует привлечения данных об индивидуальных оптико-физических характеристиках рассматриваемых сред в широком диапазоне изменения определяющих параметров, таких, например, как температура и плотность. Поэтому вначале кратко рассмотрим имеющиеся здесь данные и методы их получения.

1. Оптико-физические параметры высокотемпературных сред.

Для расчетов термодинамических характеристик плазмы при температурах, реализующихся в лабораторных условиях (до десятков электрон-вольт) в настоящее время используются модели Саха с поправками на кулоновское взаимодействие в области неидеальности и Томаса-Ферми при высоких плотностях вещества, а в области параметров исследовавшейся в ударно-волновых и других экспериментах -- полуэмпирические модели. Имеющаяся информация о структуре уровней энергии атомов и ионов, а также существующие методы расчета и экспериментальные данные позволяют в значительном числе случаев считать вопрос о нахождении уравнения состояния с требующейся для практических приложений точностью решенным. При решении газодинамических задач уравнения состояния

используется обычно в калорической форме, причем удобно пользоваться давлением P в функции внутренней энергии ε и плотности среды ρ: $P = P(\varepsilon, \rho)$. Для определения температуры T и других связанных с нею величин термическое уравнение состояния задается в виде: $T = T(P, \rho)$ или, что более предпочтительно, в виде $T = T(\varepsilon, \rho)$.

Иначе обстоит дело с оптическими характеристиками плазмы и, более того, оптическими характеристиками нагретых молекулярных газов - спектральными коэффициентами поглощения при температурах ~ 10^3 К и выше - в области однократной и многократной ионизации. Ввиду отсутствия исходной спектроскопической информации для многих ионов, а в ряде случаев для молекул и атомов, а также трудностей, связанных с необходимостью учета возмущающего действия заряженных частиц на структуру спектров испускания и поглощения в плазме, количество данных, достаточно полных для того, чтобы их можно было использовать в газодинамических расчетах, в настоящее время ограничено. Здесь можно указать на банки данных такого рода для воздуха и некоторых других молекулярных газов, некоторых металлов и диэлектриков, ряда инертных газов и смесей. В отношении публикаций по коэффициентам поглощения плазмы *He, C, Al, Ne, Ar, Xe, Bi* и некоторым другим приходится констатировать, что эти результаты в том объеме, который необходим для приложений, продолжают оставаться в основном достоянием тех коллективов исследователей, в которых они были получены. Трудности представления детальной спектральной информации в обозримом виде пока препятствуют ее широкому распространению и использованию, заставляя прибегать к различного рода усреднениям по спектру. Примерами таких усреднений служат хорошо известные росселандов пробег излучения I_R и усредненный по Планку коэффициент поглощения K_{Pl}, используемые, соответственно, для описания радиационной диффузии в оптически толстой среде и объемного лучеиспускания в оптически тонкой среде. Более аккуратным способом усреднения является усреднение (росселандово, планковское или с единичной весовой функцией) по отдельным спектральным интервалам (группам фотонов), внутри которых коэффициент поглощения может считаться приблизительно постоянным. Расчет спектральных коэффициентов поглощения связан с суммированием вкладов большого числа компонентов и учетом для них многочисленных переходов, каждый из которых в определенном спектральном диапазоне при определенной температуре может играть доминирующую роль. Основными механизмами, определяющими поглощение излучения в газах и плазме, являются процессы тормозного поглощения в полях ионов, атомов и молекул, фотоионизация из основных и возбужденных состояний атомов и ионов, поглощение в процессах фотоионизации и фотодиссоциации молекул, фотоионизация внутренних электронных оболочек частиц, поглощение в электронно-колебательных переходах молекул, поглощение в спектральных линиях атомов и ионов. Сечения всех элементарных процессов при расчетах коэффициентов поглощения брались из известной справочной литературы, а при отсутствии их для атомов и ионов рассчитывались по методу квантового дефекта, методам Хартри-Фока и Хартри-Фока-Слетера.

2. Расчетно - теоретические модели процессов.

Возвращаясь теперь к вопросам разработки физических и математических моделей процессов, сопровождающих воздействие концентрированных потоков энергии на преграду, укажем, что такие модели, помимо адекватного учета основных физических процессов, не должны накладывать существенных ограничений на геометрические и временные масштабы явлений. Учитывая также тот факт, что экспериментальное изучение проводится в большинстве случаев в условиях, когда важны эффекты нестационарности и неодномерности, достаточно полное сопоставление возможно только на основании нестационарных и неодномерных численных моделей.

Опишем наиболее существенные особенности численных моделей, разработанных для решения указанных задач. Учитывая, что действующие на поверхность пучки имеют, как правило, осевую симметрию и направлены к ней по нормали, соответствующую систему уравнений динамики сплошной среды, описывающую движение возникающих у поверх-

ности паров (или, в общем случае, продуктов разрушения) запишем в эйлеровых переменных в цилиндрической системе координат rOz с осью z, направленной по внешней нормали к поверхности:

$$\frac{\partial\rho}{\partial t}+div(\rho\vec{w})=0$$

$$\frac{\partial(\rho v)}{\partial t}+div(\rho v\vec{w})+\frac{\partial}{\partial r}(P-S_{11}-S_{13})-\frac{S_{22}-S_{11}}{r}=0$$

$$\frac{\partial(\rho u)}{\partial t}+div(\rho u\vec{w})+\frac{\partial}{\partial z}(P-S_{33})-\frac{1}{r}\frac{\partial}{\partial r}(rS_{13})=0$$

$$\frac{\partial(\rho E)}{\partial t}+div(\rho E\vec{w})+\frac{\partial}{\partial z}\left[(P-S_{33})u-S_{13}v\right]+$$

$$+\frac{1}{r}\frac{\partial}{\partial r}\left[(P-S_{11})vr-S_{13}ur\right]+div\vec{F}=\frac{dq}{dz}$$

$$E=\varepsilon+w^2/2;\qquad P=P(\rho,\varepsilon);\qquad T=T(\rho,\varepsilon);$$

Здесь u и v - осевая и радиальная компоненты скорости w, E - полная, ε - внутренняя удельная энергия, S_{ik} - компоненты девиатора напряжений, $\vec{F}$ - интегральный поток энергии за счет механизмов переноса ее теплопроводностью и излучением, dq/dz - энергия, выделяемая внешним источником в единице объема в данной точке пространства (r,z) в единицу времени.

К системе (1) необходимо присоединить определяющее уравнение, описывающее свойства материала при сдвиге, из которого можно получить связь девиатора напряжений с тензором скоростей деформаций ε_{ij}:

$$S_{ij}=S_{ij}(\varepsilon) \tag{2}$$

Для оптически толстых сред поток энергии $\vec{F}$ в (1) определяется электронной (коэффициент κ_e) и лучистой (коэффициент κ_L) теплопроводностью:

$$\vec{F}=\vec{F}_e+\vec{F}_L=-(k_e+k_L)\Delta T \tag{3}$$

В общем случае сред с произвольной прозрачностью лучистый поток определяется через спектральную интенсивность излучения J_e:

$$\vec{F}_L=\int_0^\infty d\varepsilon\int_{(4\pi)}d\vec{\Omega}\cdot\vec{\Omega}\cdot I_e \tag{4}$$

для нахождения которой следует решить уравнение переноса излучения :

$$(\vec{\Omega}\nabla)I_\varepsilon=ck_\varepsilon(I_{\varepsilon p}-I_\varepsilon) \tag{5}$$

В (4, 5) $\vec{\Omega}$ - единичный вектор направления, c - скорость света, $I_{\varepsilon p}$ - равновесная (планковская) интенсивность излучения для фотонов с энергией ε, k_ε - монохроматический коэффициент поглощения фотонов с энергией ε, исправленный на вынужденное испускание. При изучении движения сред, в которых пробеги собственного излучения сравнимы с характерными размерами задачи, используется описание переноса излучения в приближении "вперед-назад" вдоль каждой из осей координат r, z. Зависимость интенсивности излучения от энергии фотонов учитывается введением нескольких спектральных групп, в пределах которых коэффициент поглощения среды можно считать постоянным, равным его планковскому среднему. Мощность dq/dz источника энерговыделения в (1) определяется характером рассматриваемой задачи. Например:

а) При действии на преграду пучка лазерного излучения с плотностью потока энергии $q_\infty(r)$ в точке (r,z) получим:

$$q(r,z)=q_{\infty}(r)\exp(-\int_{z}^{\infty}k_{\varepsilon_0}dz)\left[1-R(T_s)\exp(-r\int_{0}^{z}k_{\varepsilon_0}dz')\right] \quad (6)$$

В (6) k_{ε_0} - коэффициент поглощения лазерного излучения, энергия фотонов которого ε_0, продуктами разрушения преграды, $R(T_s)$ - коэффициент отражения излучения от преграды, определяемый ее температурой T_s. Отражение предполагается зеркальным.

б) При действии на преграду пучка заряженных частиц (электронов) энерговыделение следует считать объемным. Поэтому структура зоны энерговыделения в преграде и выброшенном из формирующего в ней кратера веществе пересчитывалась по методу Монте-Карло каждый раз, когда изменение плотности вещества в какой-либо расчетной точке за счет движения достигало 10%. Величина dq/dz в этом случае равна:

$$dq/dz=\rho a_t\cdot j_o\cdot f(r)\cdot\varphi(t) \quad (7)$$

где $a_t(z)$ - энергия, теряемая одной частицей в веществе при прохождении ею массового пути $dx=\rho\,dz$ на глубине z, j_o - максимальная плотность тока в пучке, $f(r)$ и $\varphi(t)$ - функции, определяющие пространственно-временную зависимость плотности тока.

При численном интегрировании системы (1) вместе с определяющими задачу выражениями $\vec{F}$ и dq/dz материальные характеристики среды задаются в виде сеточных функций $\ln P$, $\ln k$, $\ln T$, $\ln k_\varepsilon$ логарифмических переменных $\ln\rho$, $\ln\varepsilon$ с равным шагом и разрешением, обеспечивающим достаточную точность при линейной интерполяции между узлами.

Для решения системы (1) используется конечно-разностный метод "крупных частиц" и TVD - схема, в которых предусмотрены специальные процедуры выделения контактных поверхностей, разделяющих вещества, отличающиеся своими теплофизическими и оптическими характеристиками. Решение уравнения переноса осуществляется методом характеристик или методом дискретных ординат

3. Решение конкретных задач.

В качестве примера использования разработанных методик приводятся решения следующих радиационно-плазмодинамических задач, полученные для реальных оптико-физических параметров материалов:

1. Воздействие лазерного излучения умеренной плотности потока $q<10^9\,BT/cm^2$ на металлические преграды в воздухе (технологические применения).
2. Воздействие лазерного излучения большой мощности $q\le10^{13}-10^{14}\,BT/cm^2$ на многослойные мишени (конверсия лазерного излучения в рентгеновское).
3. Воздействие на преграду сильноточного пучка электронов (обработка материалов, получение рентгеновского теплового излучения).
4. Электрический взрыв плоских и цилиндрических проводников и его применения в качестве мощных источников излучения в видимой, ультрафиолетовой и рентгеновской областях спектра.
5. Динамика излучения, возникающего при движении в атмосфере Земли космических объектов со скоростями до 50 км/сек.
6. Динамика и излучение плазмы, возникающей при ударе о поверхность Земли космических объектов со скоростями до 50 км/сек.

Работа выполнена при финансовой поддержке Международного научно-технического Центра (г.Москва), - Проект В23 - 96.

Publ. Astron. Obs. Belgrade No. 61 (1998), 39 *Invited lecture*

SELF-ORGANIZATION PROCESSES IN PLASMAS

M. M. ŠKORIĆ
Institute of Nuclear Sciences "Vinča", POB 522, 11001 Belgrade, Yugoslavia
and
**National Institute for Fusion Science, Toki-shi, 509- 5292, Japan*

A large amount of effort put into studies of complexity and self-organization in plasmas has revealed a profound underlying structure in diverse and seemingly irregular phenomena. Self-organization is a generic process of a creation of order in a nonlinear far-from-equilibrium system, open to an environment. Energy input, nonlinear instability which leads to dissipation, entropy production and its removal from a system are key governing points (Sato *et al.* 1996). We shall briefly discuss basic concepts to focus at an example of a stimulated Raman backscattering in laser plasmas. At high intensities, anomalous Raman backscattering, turbulent spectra and hot electrons, detrimental to laser fusion are often observed. We introduce a fluid-hybrid and particle simulations in order to model and explain nonlinear Raman complexities.In a broader context, we study long-time saturated Raman states to find a consistency with a general scenario (Sato *et al.* 1996). An interplay between self-organization at micro (kinetic) and macro (wave- fluid) scales is revealed through quasi-periodic and intermittent evolution of physical variables,related dissipative structures and entropy changes (Škorić *et al.* 1998).

References

Sato, T. and the Complexity Group: 1996, Physics of Plasmas v.3, 2135.
Škorić, M.M., Sato, T., Maluckov, A.M. and Jovanović, M.S.: 1998, NIFS Report-549.

* visiting professor, Ministry of Education, Science and Culture of Japan; partial support by the Ministry of Science and Technology of the Republic of Serbia; under project 01E11 is acknowledged

Publ. Astron. Obs. Belgrade No. 61 (1998), 40 *Invited lecture*

CHARACTERISTICS OF GUIDING VLF WAVES BY FIELD-ALIGNED IRREGULARITIES IN THE MAGNETOSPHERE

D. M. ŠULIĆ

Astronomical Observatory, Volgina 7, 11160 Belgrade 74, Yugoslavia

It is well known that under reasonable initial conditions an electric field in the equatorial plane can produce electron density enhancements and depressions in the magnetosphere. Plasma diffuses along field lines rather than across them, so enhancement or depression in plasma density tends to be field- aligned. The first ray theory of VLF waves propagation shows that trapping is possible by irregularities manifested as enhancement or depression of electron density

In our ray tracing calculations we have supposed that VLF waves propagate in two dimensions in inhomogeneous cold plasma. The electron density and ion densities used here are represented by a field-aligned isothermal diffusive equilibrium model. The electron density at any point in the magnetosphere is calculated from electron, ion (H^+, He^+ and O^+) and temperature profiles at a reference level of 900 km altitude. In this paper the geomagnetic field is assumed to be a dipole field.

In the present paper we have examined the guiding of VLF waves by troughs (waveguide with depression of electron density to the background of electron density) which are located in different models of the magnetosphere. The main feature for a trough extending along the geomagnetic field line is very variable electron plasma frequency and electron gyrofrequency along its length. Electron gyrofrequency is approximately $\sim$ 1MHz near the ends of trough in the bottom of the magnetosphere. As VLF wave is trapped and travels up to the equatorial region the gyrofrequency slowly decreases and has values comparable with wave frequency.

The principal idea of our work is calculation of the absolute value of group velocity for wave frequencies, which are in different ratio to the minimum value of gyrofrequency along ray path. In many practically important cases of guiding VLF waves we are also interested in the direction of group velocity with respect to direction of geomagnetic induction or wave normal.

CONTRIBUTED PAPERS

Publ. Astron. Obs. Belgrade No. 61 (1998), 43 *Contributed paper*

ЧИСЛЕННОЕ МОДЕЛИРОВАНИЕ ПРОЦЕССОВ В КСПУ С ПРОНИЦАЕМЫМИ ТРАНСФОРМЕРАМИ

АНАНИН С.И.

Институт молекулярной и атомной физики НАН Беларуси
220072, Беларусь, г. Минск, пр. Ф. Скарыны 70
Email: lrpd@imaph.bas-net.by

В современных квазистационарных сильноточных плазменных ускорителях (КСПУ) типа П-50 ускорительный канал образован «прозрачными» стержневыми трансформерами (электродами) с изменяющейся степенью магнитной экранировки, зависящей от соотношения полного разрядного тока и тока, текущего по отдельным стержням. В работе [1] была предложена двумерная модель, позволившая описать структуру течения плазмы в КСПУ с проницаемым катодным трансформером. В рамках такой модели течение плазмы описывается системой уравнений нестационарной магнитной гидродинамики в приближении кольцевого ввода [2]. При этом катод моделируется профилированной поверхностью с концентрическими отверстиями, ширина которых характеризует степень неполноты магнитной экранировки. В данной работе эта модель была дополнена так, чтобы включить в рассмотрение всю разрядную камеру ускорителя, в том числе и пространство, расположенное снаружи анодных стержней. Кроме того, рассмотрено влияние на структуру и параметры плазмы сценария течения, то есть всей последовательности его эволюции, начиная с заполнения разрядной камеры плазмой ВИБ. Проведено сравнение с экспериментальными данными, показана адекватность представленной модели.

Литература

1. Ананин С.И., Асташинский В.М. Физика плазмы, 1997, том 23, № 1, с.37.
2. Ананин С.И. Физика плазмы, 1992, том 18, № 3, с. 388.

Publ. Astron. Obs. Belgrade No. 61 (1998), 44 – 47 *Contributed paper*

ИНТЕРФЕРЕНЦИОННО-ТЕНЕВАЯ ДИАГНОСТИКА ПЛАЗМЕННЫХ ПОТОКОВ С ЦИФРОВОЙ ОБРАБОТКОЙ ИЗОБРАЖЕНИЙ

С.И.АНАНИН, В.М.АСТАШИНСКИЙ, Е.А.КОСТЮКЕВИЧ, А.А.МАНЬКОВСКИЙ

Институт молекулярной и атомной физики НАН Беларуси,

проспект Ф.Скарыны, 70, Минск, 220072, Беларусь

Резюме. Представлен обзор исследований импульсной и стационарной плазмы, выполненных с применением методов визуализации оптических неоднородностей.

I. ВВЕДЕНИЕ

В арсенале диагностических средств, нашедших применение в изучении плазмодинамических процессов, заметное место занимают методы визуализации оптических неоднородностей, основанные на измерении рефракции плазмы, зная которую, можно рассчитать значения N_e с точностью, не доступной другим методам (Грим, 1969). Наиболее универсальным в этом отношении является интерференционный метод благодаря возможности менять в широких пределах его чувствительность и однозначности трактовки получаемых данных. Вместе с тем его реализация достаточно трудна, что объясняется в первую очередь сложностью схемы стандартных приборов. Громоздкость интерферометра служит причиной повышенной восприимчивости прибора к вибрациям и затрудняет его размещение на установке. Колебания зеркал хотя и не мешают регистрации интерферограмм с высоким временным разрешением, но без принятия дополнительных мер не позволяют юстировать прибор. Для преодоления этого неудобства стандартные приборы строят на массивных основаниях с применением виброзащитных развязок. В итоге, например, интерферометр ИТ-42 с полем зрения 225 мм имеет габариты 3x3x1 м при массе около 3 тонн.

Положение значительно осложняется при исследовании процессов в крупных вакуумных камерах. Здесь, как правило, возникают новые, не менее серьезные проблемы. Прежде всего, в случае расположения зеркал прибора снаружи камеры ее смотровые окна по качеству и точности изготовления должны быть сравнимы с самими зеркалами. Далее, при откачке камеры смотровые окна деформируются, внося сильные искажения в поле интерференции, для устранения которых требуется изготовление компенсационных пластин. Альтернативный вариант с размещением зеркал внутри камеры снижает остроту проблемы смотровых окон, но существенно осложняет процедуру юстировки прибора за счет необходимости каж-

дый раз производить разгерметизацию камеры. Наконец, нельзя не упомянуть и о том, что обработка интерферограмм достаточно сложна и отнимает немало времени. Все эти факторы сдерживают распространение метода оптической интерферометрии в диагностике плазмы.

Ниже представлен краткий обзор работ, выполненных с применением автоколлимационного интерферометра (Костюкевич и Минько, 1981), конструктивные особенности которого упрощают реализацию метода. Прибор состоит из источника света, коллиматора, светоделителя и двух полупрозрачных зеркал, отражающих опорный и предметный пучки. Светоделитель направляет их в съемочную камеру, где наблюдается результат их интерференции в виде системы параллельных полос, частота и ориентация которых задается поворотами одного из зеркал. За счет одноосности схемы и использования принципа автоколлимирования прибор отличается компактностью и легко монтируется практически на любой установке. Так, габариты самого крупного из применявшихся в экспериментах интерферометра с полем зрения 200 мм составляли всего 80x40x40 см.

Покадровая съемка интерферограмм с частотой до 250000 кадр/с проводилась фоторегистратором СФР. Использовавшиеся для зондирования плазмы лазеры на рубине и неодиме, работавшие в режиме свободной генерации с селекцией мод, обеспечивали временное разрешение не хуже 100 нс при частоте съемки до 250000 кадр/с.

Для обработки интерферограмм была создана автоматизированная система (Ананин и др., 1994), в состав которой входят видеокамера на ПЗС-матрице, блок управления, монитор и компьютер. На видеокамеру записывается нужный кадр киноинтерферограммы. Блок управления оцифровывает сигналы с матрицы, запоминает изображение, выводит его на монитор и обеспечивает выполнение операций ввода-вывода.

Программа обработки интерферограмм, создававшаяся с учетом особенностей эксперимента, включает процедуру автоматизированного поиска максимумов интерференционных полос в заданных сечениях, интерактивную коррекцию полученной матрицы и последующие машинные вычисления, дающие в итоге распределение Ne в визуализируемой области.

II. ЭКСПЕРИМЕНТ

1. Взаимодействие лазерного излучения с веществом

Анализ киноинтерферограмм воздействия сфокусированного излучения Nd-лазера в пичковом режиме на алюминиевую мишень (Костюкевич и др., 1980) позволил проследить динамику развития лазерного факела и выявить характер распространения ударных волн. При их взаимодействии в надфакельной области образуется плотная воздушная «пробка», которая

может существенно влиять на процесс взаимодействия лазерного излучения с собственной плазмой. Применение интерферометрии на двух длинах волн позволило найти распределение N_e, максимальное значение которой составило $2x10^{18}$ $см^{-3}$. При воздействии на мишень 1-мкс импульсом высокое временное разрешение достигалось за счет щелевой развертки полос. В результате измерены скорости ударных фронтов и найден временной ход Ne на оси факела.

2. Дуговой плазмотрон

При исследованиях стабилизирующего действия электрической дуги на течение плазмы в канале стационарного дугового плазмотрона со стержневым катодом и трубчатым анодом (Алешин и др., 1983) окна смотровой секции были заменены зеркалами интерферометра (диаметром 10 мм), крепившимися к фланцам через эластичные уплотнения, обеспечивавшие герметичность канала и возможность юстировки прибора. В результате были установлены факторы, определяющие переход режима течения от турбулентного к ламинарному.

3. МПК и КСПУ

Магнитоплазменный компрессор (МПК) представляет собой электроразрядную систему, содержащую разрядное устройство с коаксиально расположенными электродами, которая позволяет получать импульсные плазменные потоки, сжатые собственным магнитным полем (Асташинский и др., 1991).

Четыре таких устройства используются в принципиально новой двухступенчатой системе - квазистационарном сильноточном плазменном ускорителе (КСПУ) - в качестве первой ступени. Они инжектируют полностью ионизированные плазменные потоки во вторую ступень - ускорительный канал, образованный внешним электродом длиной 120 см и диаметром 50 см и центральным электродом сложного профиля. Таким образом, разряд второй ступени происходит в предварительно разогретой среде, чем обеспечивается достижение высоких параметров на выходе ускорителя.

Чтобы исключить влияние деформаций смотровых окон, зеркала 200-мм интерферометра жестко крепились изнутри камеры к оправам окон. Специальная конструкция оправ окон позволяла юстировать зеркала снаружи, не прибегая к разгерметизации камеры. Кроме того, жесткая связь зеркал со стенками вакуумной камеры обеспечивала надежную защиту от вибраций: юстировка прибора не нарушалась даже после продолжительной работы вакуумных агрегатов.

Предварительные расчеты показали, что в условиях МПК и КСПУ рефракция плазмы в области компрессии определяется главным образом

свободными электронами, а вклад тяжелых частиц не превышает погрешности измерений. Это давало возможность определять N_e по однодлинноволновым интерферограммам.

T_e в области компрессии КСПУ определяли по скорости звука в плазме, которая однозначно связана с углом отхождения скачка уплотнения, образующегося при набегании плазменного потока на тонкий клин, установленный под нулевым углом атаки. Для визуализации скачков уплотнения интерферометр был переоборудован в теневой прибор посредством замены заднего полупрозрачного зеркала глухим.

В результате проведенных экспериментов прослежена динамика формирования области компрессии в МПК и КСПУ, найдено пространственно-временное распределение N_e в потоке, обнаружено, что на стадии развала область компрессии приобретает трубчатую структуру. По значениям N_e в канале и за срезом ускорителя определена степень сжатия плазменного потока в области компрессии. На основании тенеграмм взаимодействия потока с клином рассчитаны значения T_e (Ананин и др., 1998).

III. ЗАКЛЮЧЕНИЕ

Результаты проведенных исследований показали высокую гибкость и универсальность автоколлимационного интерферометра, позволяющую применять его в самых разнообразных условиях.

Литература

Грим Г.: 1969, *Спектроскопия плазмы*. Атомиздат, М., 243.

Костюкевич Е.А., Минько Л.Я.: 1981, *Журнал прикладной спектроскопии*, **34**, № 3, 551.

С.И.Ананин, В.М.Асташинский, Е.А.Костюкевич и др.: 1994, в сб. *Физика и техника плазмы. Материалы конференции.* т.1, Минск, Беларусь, 336.

Костюкевич Е.А., Минько Л.Я., Чумаков А.Н.: 1980, *Препринт/АН БССР. Институт физики*; № 211.

Алешин Н.Ф., Лизунков Г.П., Костюкевич Е.А.: 1983, в сб. *Тепло- и массоперенос: экспериментальные и теоретические исследования.* Минск, ИТМО им.Лыкова АН БССР, 75.

Асташинский В.М., Ефремов В.В., Костюкевич Е.А. и др.: *Физика плазмы*, **17**, № 9, 1111.

Ананин С.И., Асташинский В.М., Костюкевич Е.А. и др.: *Физика плазмы*, 1998, в печати.

Publ. Astron. Obs. Belgrade No. 61 (1998), 48 – 50 *Poster paper*

ON THE CHARACTERISTICS OF X-RAYS EMITTED FROM THE PLASMA FOCUS DEVICE

R.Antanasijević, D.Đorđević and D.Joksimović
Institute of Physics, Pregrevica 118, Zemun,
11080 Beograd, Yugoslavia
E-mail: antanasijevic@atom.phy.bg.ac.yu

J.Purić, M.Ćuk
Faculty of Physics, PO Box 368, 11001 Belgrade, Yugoslavia

Abstract: On the plasma focus device we investigated the X-ray emission of different gases: H,D,N and the mixture H+Ar(25%Ar, 75%H). For the detection of X-ray roentgenographic method was employed with use of Al absorbers of different thickness. Only the soft X-rays (up to E=18 KeV) were detected.

1. INTRODUCTION

For diagnostics of plasma focus (PF) good knowledge of emitted X-rays is of exceptional importance, both its energy spectrum and exact lateral position of the emission source. By some results we can see (Katsumi 1995) that PF "hot spots" from which X-ray emission occurs, coincide with these where the neutrons are emitted.

2. EXPERIMENTAL METHOD

The plasma focus we used is of the Mather type (Mather 1965) and consists of two brass coaxial electrodes (the outer electrode consists of 18 cylindrically positioned brass roads) separated by a glass insulator sleeve at one end, where the breakdown of a gas discharge takes place.
The dimensions of PF chamber are chosen for its optimized operation at an energy up to 40kJ and a charging voltage up to 40 kV. Pressure

inside the chamber varied between 1-10 mbar. Development and acceleration of the plasma focus current sheet have been measured by means of the fiber optic cables that are "looking" at certain points inside the chamber.

Electrical circuit parameters are chosen in such a way that the radial compression starts near the current maximum. For the X-ray detection we used the roentgenographic method. In order to determine the maximum energy of emitted X-rays, we used Al absorbers of different thickness.

Roentgenographic films were protected from the influence of visible light emitted in PF, placed on the windows inside the PF chamber with a thin Al foil (20 μm).

In this work, knowing the space above the electrode from which X-rays are emitted, we simplified the method of detection which is seen from Fig.1. The lateral resolution of detected X-radiation in front of the film colimators (2 cm long; ϕ1 mm) is placed (in form of stainless steel disk) which was described in the previous work. Film and colimator are positioned so that they could observe the space around the top of central electrode. Distance between colimator and central electrode is 130 mm. Aluminium absorbers of different thickness (maxim. 1000 μm) were used for analysis of emitted X-radiation.

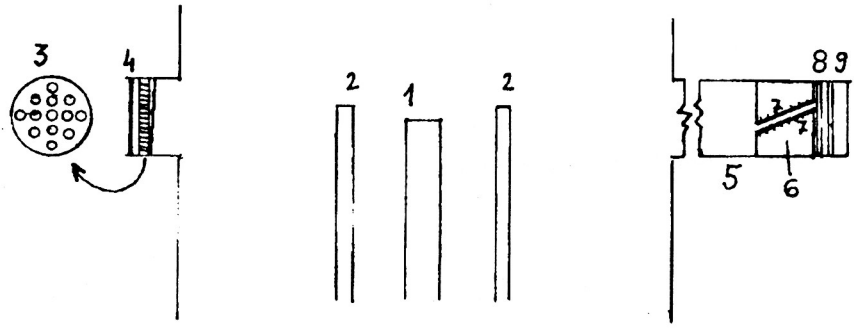

Fig.1. Cross-section of PF chamber 1-central electrode, 2-outer electrode, 3-stainless steel disk, with Al absorbers, 4-X-ray film. 5-tube (up to 2 m long) 6-beam devider, 7-mica sheets, 8-Al absorber, 9-X-ray film

On disk in front of the film there are 13 holes covered with Al of different thickness (50-1500 μm). Energy of X-radiation is calculated on the basis of absorber thickness used.

In the experiment with pure D or in the mixture Ar+H we confirmed an important fact that the X-rays emission, in both cases occurs in a narrow zone around the central electrode, this zone is greater than that corresponding to "hot spot" from D-D reaction products, including the neutrons emitted (Antanasijević at all, 1997).

3. RESULTS

Blackness obtained on the X-ray films after passing through the MICA sheets (8 on Fig.1), shows that in the X-ray spectra emitted from PF, λ corresponding to MICA latice constant exists.

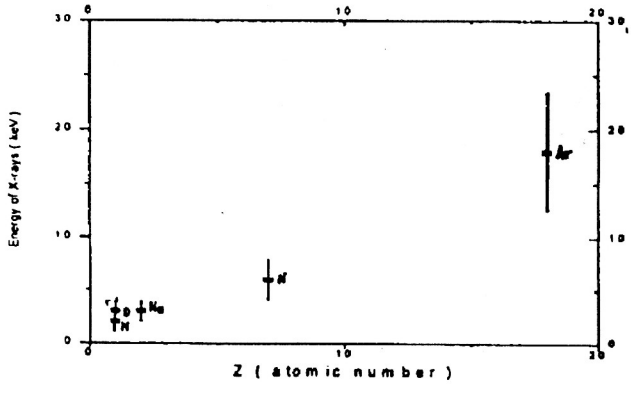

Fig.2. Dependence of energy X-ray on gas atomic number

In Fig.2 we show dependence of energy of emitted X-rays on the gas atomic number Z. For the X-rays emission of mixture Ar+H we obtain larger energy value in comparison with the previous results (Antanasijević 1995), but at the same time concentration of Ar in this experiment was much larger. Estimated error in this experiment is around ±30%.

References

Katsumi H. and Hiroyuki K.: 1995, J.Phys.Soc.Jpn.65, 139.
Mather J.W.: 1965, Phys. of Fluids, vol.8, no.2.
Antanasijević R. et all: 1995, 5th ICCF, Monte Carlo, p.505.
Antanasijević R. et all: 1997, Rad.Meas., vol 28, 241

Publ. Astron. Obs. Belgrade No. 61 (1998), 51 – 54 *Poster paper*

LINEAR OPTICAL POLARIZATION OF P Cygni IN 1986-1992

J. ARSENIJEVIĆ and S. MARKOVIĆ
Astronomical Observatory, Volgina7, 11160 Belgrade 74, Yugoslavia
E–mail jarsenijevic@aob.aob.bg.ac.yu
E–mail smarkovic@aob.aob.bg.ac.yu

1. INTRODUCTION

Luminous blue variable P Cygni (HD 193237, B1-B2, Ia) has been showing irregular brightness changes and mass loss about $10^{-5} M_{\odot}$ per year. It has an extended and expanding atmosphere. Undisplaced emission lines are flanked by shortward displaced absorption lines, typical P Cygni-like line profile was first noted in 1888. Because of its brightness, P Cyg was the object frequently studied during more then hundred years.

Polarimetric studies of P Cygni were sporadic till the end of seventies. Hayes (1985) started more intensive polarimetric monitoring of the star by observing linear polarization in B spectral region. During the last decade, polarimetric observations provided the complete wavelength coverage from 1400 to 7600 Å (Taylor *et al.*, 1991). The brightness variations of different time scales exist mainly of an irregular character.

Belgrade linear polarimetric data in V spectral region, collected during seven years, cover the period of time in which many other different observations of P Cyg were done. Belgrade measurements will be useful in the analyses of long-term (years) and short-term (months) variability of the star.

2. OBSERVATIONS

The observations of the visual linear polarization of the star P Cyg were performed with the Zeiss 65 cm-refractor and the D.C. one-channel polarimeter at Belgrade Observatory. The observations were done between July 12, 1986 and August 31, 1992. One 8-minute measurement of the Stokes parameters Q and U has a typical r.m.s. error not larger then 0.07%.

The observed values of visual linear polarization percentage P and position angles Θ of the star P Cygni during the period 1986-1992 are presented in Figures 1 and 2 respectively. Polarization parameters are on the y-axes and Julian days on the x-axes.

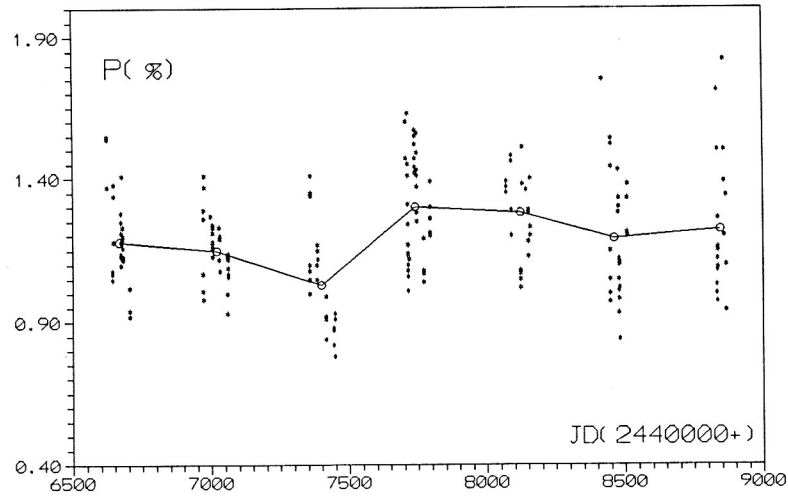

Fig. 1. The observed polarization percentage of P Cyg in V filter during the period 1984-1991.

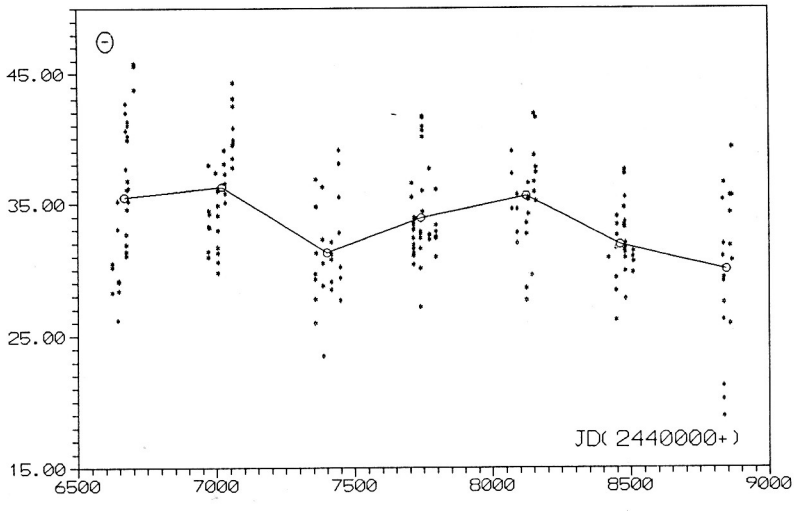

Fig. 2. The position angle of the observed polarization of P Cyg in V filter during the period 1984-1991.

The annual mean values of the observed polarization parameters P, Θ and Stokes parameters, Q and U, are presented in Table 1. Julian days in Table correspond to the middle of the season of the observation. The interstellar component of P Cygni is normally rather high, Taylor *et al.* (1991) derived the interstellar component. But, having in mind many different problems in finding interstellar polarization for one star we prefer using the observed polarization, at least in this kind of work where only time-variability analysis is concerned.

TABLE I

Yearly mean values of polarization percentage (P), position angle (Θ), and Stokes parameters (Q, U) for the star P Cyg. n - the number of observations per each year.

JD (2440000+)	P(%)	$\Theta(^o)$	Q(%)	U(%)	n
6667	1.18 ± 0.34	35.5 ± 4.6	0.387 ± 0.244	1.118 ± 0.128	29
7019	1.15 ± 0.23	36.3 ± 3.0	0.345 ± 0.157	1.097 ± 0.096	32
7398	1.03 ± 0.29	31.3 ± 1.3	0.475 ± 0.141	0.920 ± 0.168	25
7740	1.30 ± 0.33	33.9 ± 1.6	0.490 ± 0.152	1.205 ± 0.181	40
8122	1.28 ± 0.28	35.6 ± 1.7	0.413 ± 0.131	1.209 ± 0.157	23
8473	1.19 ± 0.32	31.9 ± 0.4	0.525 ± 0.121	1.071 ± 0.208	28
8845	1.22 ± 0.48	30.0 ± 2.2	0.612 ± 0.244	1.060 ± 0.237	18

3. DISCUSSION

The observed polarization percentage varies with time as does the position angle. The long-term variations (from year to year) are with small amplitudes for both parameters. The amplitude of percentage changes is under 0.3%. For the position angles the changes are not greater then 5°. The short-term changes (during one season of observations) are considerably larger. The percentage values are between 0.5 and 1.0%. The position angle varies between 11° and 26°. The Belgrade observed values of V polarization parameters are in very good agreement with Hayes' (1985) values in B spectral region. This is in accordance with the known polarization wavelength dependence.

During first three years of observations, 1986-1988, the polarization percentage slowly decreases. For the period 1985-1989 Groot (1989) found an increase of visual brightness of P Cygni. So, we could conclude that for the star P Cygni an anticorrelation between long-term visual polarization percentage variation and visual brightness changes exists.

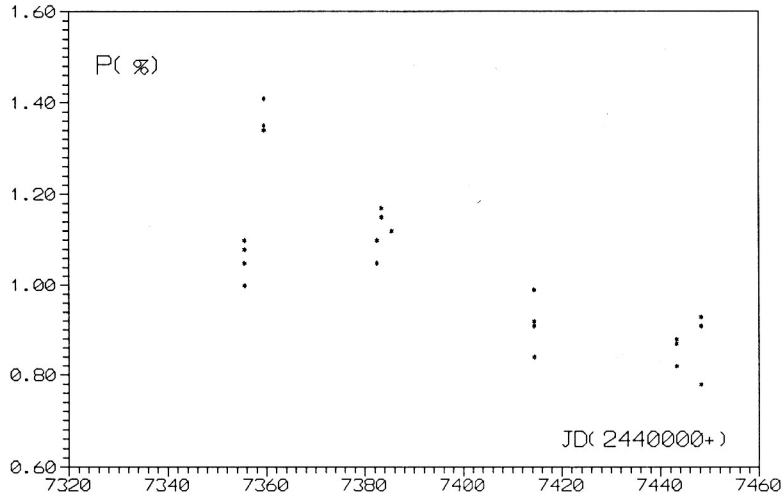

Fig. 3. The observed polarization percentage of P Cyg in V filter during 1988.

As the short-term polarization percentage variations are concerned the situation is the opposite. During 1988, the star varied in brightness (Groot, 1989) and in polarization, Figure 3, but with a positive correlation. Of course, it is seen in the period JD 2447355-7448 when polarimetric and photoelectric observations were done almost simultaneously. The different behaviour of the short-term and long-term polarization percentage variations with respect to the photometric variations should has to be confirmed with a larger quantity of the observed data.

Acknowledgements

We would like to express our appreciation to our colleagues A. Kubičela, I. Vince and S. Jankov for the help in observations and reduction of data. We are also thankful to R. Dümmler who suggested the polarimetric observations of this star.

References

Groot de: 1989, *Preprint Series* **96**, Armagh Observatory.
Hayes, D.P.: 1985, *Ap. J.* **289**, 726-731.
Taylor, M., Code, A.D., Hardsieek, K.H., Anderson, C.M., Babler, B.L., Bjorkman, K.S., Clayton, G.C., Magalhaes, A.M., Meade, M.R., Schulte-Ladbeck, R.E. and Whitney, B.A.: 1991, *Ap. J.* **382**, L85-L88.

Publ. Astron. Obs. Belgrade No. 61 (1998), 55 – 58 *Contributed paper*

КВАЗИСТАЦИОНАРНЫЙ ПЛАЗМЕННЫЙ УСКОРИТЕЛЬ КОМПАКТНОЙ ГЕОМЕТРИИ КАК ИСТОЧНИК ПЛАЗМЫ ДЛЯ АТОМНОЙ СПЕКТРОСКОПИИ

В.М.АСТАШИНСКИЙ, Л.Я.МИНЬКО,
*М.ЧУК, *М.М.КУРАИЦА, *Я.ПУРИЧ

Институт молекулярной и атомной физики
Национальной академии наук Беларуси
Пр. Ф.Скарыны, 70, 220072 Минск, Беларусь
E-mail: lrpd@imaph.bas-net.by

*Физический факультет Белградского университета
P.O.BOX 368, 11001 Белград, Югославия
E-mail: epuric@rudjer.ff.bg.ac.yu

Резюме. Рассмотрены возможности квазистационарных плазменных ускорителей компактной геометрии (КПУ-КГ) газоразрядного и эрозионного типов, генерирующих компрессионные плазменные потоки (КПП) заданного состава, как источников плазмы для атомной спектроскопии.

1.ВВЕДЕНИЕ

Для исследований в области атомной спектроскопии необходимы плазменные источники излучения, обеспечивающие возможность определения вероятностей оптических переходов в атомах и ионах, сил осцилляторов, коэффициентов переноса, а также изучения закономерностей уширения спектральных линий, в том числе в электромагнитных полях различной конфигурации.

Такие источники при своей относительной простоте должны иметь достаточно широкий диапазон термодинамических параметров, быть осесимметричными и обеспечивать хорошую воспроизводимость.

К устройствам, удовлетворяющим таким требованиям, можно отнести квазистационарные плазменные ускорители (КПУ), в которых ускорение плазмы сопровождается ее сжатием собственным азимутальным магнитным полем (Морозов, 1978). Пожалуй наибольший интерес для атомной спектроскопии представляют квазистационарные газоразрядные и эрозионные

плазменные ускорители компактной геометрии (Асташинский и др., 1989, Минько и др., 1991) с относительно небольшим энергозапасом накопителей (10 - 30 кДж), генерирующие компрессионные плазменные потоки заданного состава, характеризующиеся достаточно высокими термодинамическими параметрами плазмы. Характерная длительность квазистационарной стадии развития компрессионных потоков рассматриваемых систем составляет ~ 50 - 100 мкс.

2. ТЕРМОДИНАМИЧЕСКИЕ ПАРАМЕТРЫ И СВОЙСТВА КПП ЗАДАННОГО СОСТАВА

Газоразрядные КПУ-КГ позволяют получать плазменные потоки практически из любых газов и их смесей, составленных в любых пропорциях. Рабочий газ подается в разрядное устройство ускорителя либо с помощью импульсного электродинамического клапана, либо предварительно откачанная вакуумная камера заполняется газом до заданного давления (так называемый режим "остаточного газа").

Следует отметить, что в системах с собственным азимутальным магнитным полем, к которым относятся и рассматриваемые КПУ, наблюдается сепарация ионов по массе и заряду, т.е. происходит "самоочищение" компрессионного потока от тяжелых ионов примесей, в основном, продуктов разрушения электродов (Морозов, 1978).

Проведенные ранее исследования таких ускорителей высокоскоростными фотографическими, спектроскопическими и интерференционно-теневыми методами позволили изучить динамику формирования, структуру и свойства компрессионных плазменных потоков, определить их основные газодинамические и термодинамические параметры (Асташинский и др., 1991, Асташинский и др, 1992, Минько и др., 1992).

При работе на водороде за срезом КПУ-КГ формируется компрессионный плазменный поток диаметром ~ 1 см и длиной ~ 4-5 см. В регистрируемых спектрах испускания плазмы компрессионного потока в области 300-700 нм наблюдаются в основном сплошное излучение и линии атомарного водорода. При малых расходах рабочего газа наблюдаются также наиболее интенсивные (резонансные) линии атомов элементов, входящих в состав материала электродов. В зависимости от начальных

параметров разряда температура плазмы составляет ~ $(1\text{-}3)\cdot 10^4$ К, а концентрация электронов — $(1\text{-}2)\cdot 10^{17}$ см$^{-3}$.

При работе КПУ с воздухом в режиме остаточного газа в диапазоне давлений 1-5 тор, температура плазмы компрессионного потока составляла ~ $(3\text{-}4)\cdot 10^4$ К, а концентрация электронов ~ $(1\text{-}3)\cdot 10^{18}$ см$^{-3}$ (Асташинский и др., 1984). В спектрах испускания наблюдаются в основном сплошное излучение и линии ионов азота и кислорода, вплоть до 3-й кратности ионизации. Осевое ограничение компрессионного потока неподвижной преградой позволило сформировать в течение одного разряда два взаимосвязанных, одновременно существующих источника излучения в видимой области спектра с яркостной температурой ~ $3\cdot 10^4$ К (компрессионный поток; состав плазмы определяется, в основном, рабочим газом) и $5\cdot 10^4$ К (ударносжатый приповерхностный слой плазмы, состав которой преимущественно определяется материалом преграды).

Исследования газоразрядных КПУ позволили установить критерии получения при фиксированном уровне запасаемой в ускорителе энергии максимальных параметров плазмы с малым количеством примесей в зависимости от макроскопических параметров разряда (максимального значения разрядного тока, массового расхода рабочего вещества и начального напряжения накопителя энергии).

Предложенные оригинальные КПУ эрозионного типа (Минько и др., 1991) впервые обеспечили возможность получения в воздухе при атмосферном давлении (т.е. в условиях свободного доступа к плазме) компрессионных эрозионных плазменных потоков заданного состава, определяемого материалом внутреннего электрода. Проведенные исследования позволили установить физические процессы, ответственные за формирование таких потоков, найти способы увеличения эффективности ввода энергии непосредственно в компрессионный поток, определить основные газодинамические и термодинамические параметры эрозионной плазмы (Минько и др., 1991, Асташинский и др., 1995).

Компрессионный поток в таких системах имеет длину ~ 15 см при диаметре 1-2 см. В случае, когда внутренний электрод выполнен из меди, в спектре излучения плазмы наблюдаются только линии атомов и ионов меди. Концентрация электронов плазменного потока составляет при этом ~ $(1\text{-}2)\cdot 10^{17}$ см$^{-3}$, а температура плазмы - $(2{,}5 - 4)\cdot 10^4$ К.

Анализ приведенных выше параметров плазмы эрозионных и газоразрядных компрессионных потоков показывает, что в них устанавливается локальное термодинамическое равновесие.

3. ЗАКЛЮЧЕНИЕ

Проведенные исследования квазистационарных газоразрядных и эрозионных плазменных ускорителей компактной геометрии позволили установить основные закономерности в физических процессах, определяющих режимы работы такого рода плазмодинамических систем, найти способы управления параметрами формирующихся компрессионных плазменных потоков заданного состава. Рассмотрение свойств КПУ-КГ показывает перспективность их использования для атомной спектроскопии.

Литература

Морозов А.И.:1978, Физические основы космических электрореактивных двигателей, Атомиздат, Москва.

Асташинский В.М., Баканович Г.И., Костюкевич Е.А. и др.:1989, Журнал прикладной спектроскопии, 50, 887.

Минько Л.Я., Асташинский В.М., Маньковский А.А.: 1991, Журнал прикладной спектроскопии, 55, 903.

Асташинский В.М., Ефремов В.В., Костюкевич Е.А. и др.: 1991, Физика плазмы, 17, 1111.

Асташинский В.М., Баканович Г.И., Кузьмицкий А.М. и др.: 1992, Инженерно-физический журнал, 62, 386.

Минько Л.Я., Асташинский В.М.: 1992, Инженерно-физический журнал, 62, 714.

Асташинский В.М., Баканович Г.И., Минько Л.Я.: 1984, Физика плазмы,10, 1058.

Асташинский В.М., Баканович Г.И., Минько Л.Я.: 1984, Журнал прикладной спектроскопии, 40, 540.

Минько Л.Я., Асташинский В.М.: 1991, Вакуумная техника, 1, 50.

Асташинский В.М., Маньковский А.А., Минько Л.Я.: 1995, Материалы конф. “Физика низкотемпературной плазмы”, 1, 98, Петрозаводск.

Publ. Astron. Obs. Belgrade No. 61 (1998), 59 – 62 *Poster paper*

ПРИМЕНЕНИЕ УШИРЕНИЯ СПЕКТРАЛЬНЫХ ЛИНИЙ В ДИАГНОСТИКЕ ЭЛЕКТРОРАЗРЯДНЫХ ЭРОЗИОННЫХ ПЛАЗМЕННЫХ ПОТОКОВ

Авраменко В.Б., Кузьмицкий А.М., Минько Л.Я.
Институт молекулярной и атомной физики НАН Беларуси
220072, Минск, пр. Ф. Скорины 70
Email: lrpd@imaph.bas-net.by

Спектроскопическими методами можно проводить исследования в широком интервале основных параметров плазмы. Использование в диагностических целях различных спектральных линий позволяет получать сведения о параметрах плазмы в тех областях источника, где происходит их эффективное возбуждение. В неоднородном источнике плазмы распределение зон высвечивания спектральных линий обуславливается различными факторами – потенциалом возбуждения, постоянной квадратичного эффекта Штарка и др., которые и определяют аналитические возможности спектральных линий.

В настоящей работе приводятся результаты экспериментальных исследований параметров плазмы различных источников с использованием квадратичного эффекта Штарка. Концентрация электронов определялась по различным спектральным линиям, обладающим значительной величиной постоянной уширения.

Концентрация заряженных частиц в эрозионном плазменном ускорителе определялась по уширению спектральных линий атомов и ионов элементов, входящих в состав материала подложки: SiII 637,1нм ($E_в$=12,07эВ), FI 623,9 (14,68), FII 429,9 (29,55), CII 426,7 (20,95), обусловленных квадратичным эффектом Штарка. Концентрация электронов определялась как по пересчитанным на радиальное распределение контурам, так и по непересчитанным

(табл.1).

Во всех исследуемых случаях в качестве накопителя энергии использовалась конденсаторная батарея емкостью 24 мкФ, которая заряжалась до напряжения U_0 =5кВ, однако, в зависимости от величины начальной индуктивности разрядного контура величина разрядного тока могла существенно изменяться.

ТАБЛИЦА 1

Распределение концентрации электронов вдоль радиуса, измеренное по различным спектральным линиям

радиус, мм	$N_e \cdot 10^{-17}$ см$^{-3}$ (U_o=5кВ)					
	SiII637,1		FI623,9		FII429,9	
	без пересчета контуров	с пересчетом контуров	без пересчета контуров	с пересчетом контуров	без пересчета контуров	с пересчетом контуров
0	3,9	-	4,2	-	5,9	-
1	4,4	4,7	4,0	-	4,8	4,0
2	4,3	4,8	4,2	4,2	4,8	4,0
3	3,9	4,7	4,0	4,0	6,6	4,0
4	3,5	4,1	3,9	4,0	-	-
5	3,5	3,8	3,9	3,8	-	-

Заметного изменения концентрации электронов (N_e) вдоль радиуса плазменной струи не происходит. Малое отличие N_e при измерении по пересчитанным по радиусу и непересчитанным контурам указывает на высокую однородность источника. В этих условиях определение концентрации электронов с использованием уширения различных линий дает близкие по величине значения.

Вдоль оси струи на расстоянии 0,6 см от среза сопла N_e заметно ниже по сравнению с ее величиной у среза и уменьшается вдоль радиуса. Измерение концентрации электронов методами

голографической интерферометрии и по уширению спектральной линии FI 623,9 дает близкие результаты. N_e, измеренное методом голографической интерферометрии достигает $1{,}7 \cdot 10^{18}$ $см^{-3}$, а максимальное значение N_e, измеренное по уширению спектральной линии FI 623,9, достигает $1{,}4 \cdot 10^{18}$ $см^{-3}$. Такое согласие указывает на высокую достоверность полученных результатов.

Измерения концентрации заряженных частиц с пространственно–временным разрешением проводились по штарковскому уширению спектральной линии атома фтора FI 623,9нм (табл.2).

ТАБЛИЦА 2

Распределение концентрации электронов вдоль радиуса для различных моментов времени

радиус, мм	$N_e \cdot 10^{-17}$ $см^{-3}$ (U_o=5кВ)		
	1 кадр	3 кадр	5 кадр
0	14	6,2	6,2
1	15	6,7	6,2
2	13	6,2	6,2
3	11	6,2	6,2
4	10	5,7	6,7
4,5	-	5,2	6,7

Концентрация частиц имеет максимальное значение в начале высвечивания линии. В это же время наблюдается некоторое уменьшение концентрации вдоль радиуса, однако через 4 мкс она не только уменьшается по абсолютному значению ~2 раза, но и несколько выравнивается вдоль радиуса. Спустя ~8 мкс концентрация электронов имеет не только более выровненный постоянный характер вдоль радиуса струи, но и обнаруживается максимальное значение вдали от оси.

Использование квадратичного эффекта Штарка спектральной линии FII 429,9 нм в импульсном приповерхностном разряде позволило обнаружить одновременное существование двух максимумов концентрации заряженных частиц на различных расстояниях (h) от поверхности стенки, соответствующим двум каналам разряда (середина межэлектродного промежутка, экспозиция 4мкс, U_0=5кВ) (см. рис.).

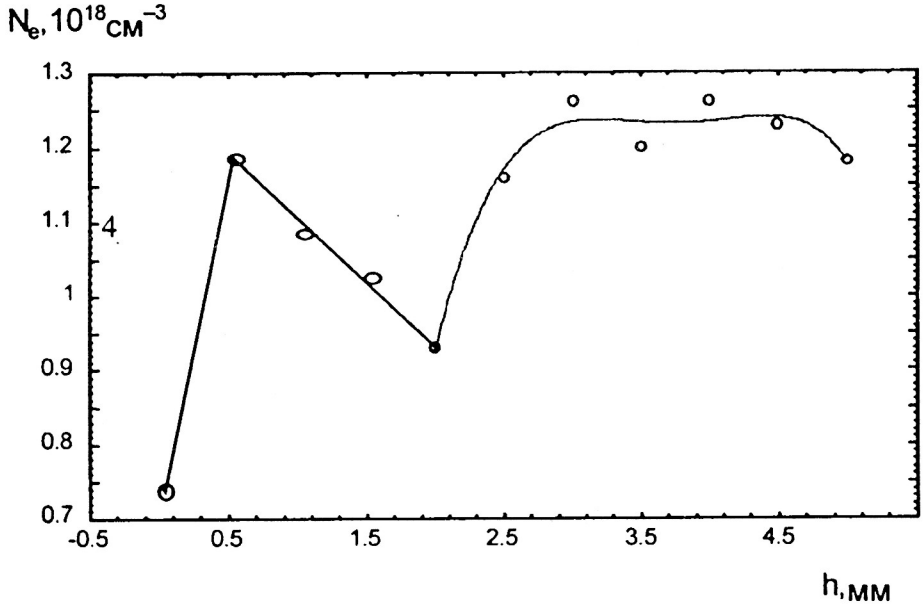

Рис. Распределение электронной концентрации

Анализ распределения интенсивностей спектральных линий показал, что первый максимум электронной концентрации соответствует высвечиванию атомных спектральных линий, а второй максимум – ионных спектральных линий. Ход концентрации электронов соответствует наблюдаемой на СФР–граммах картине течения разряда.

Publ. Astron. Obs. Belgrade No. 61 (1998), 63 – 66 *Poster paper*

ИМПУЛЬСНЫЙ КОАКСИАЛЬНЫЙ ПЛАЗМЕННЫЙ ИЗЛУЧАТЕЛЬ ДЛЯ НАКАЧКИ МОЩНЫХ ЛАЗЕРОВ НА КРАСИТЕЛЯХ

Б.А. БАРИХИН., Е.З. ПАНУСЕВИЧ
Гродненский госуниверситет, 230023, ул. Ожешко, 22, Гродно, Белоруссия
boyarkin@univer.belpak.grodno.by

Аннотация. Рассматривается плазменный электроразрядный излучатель, оптические свойства которого удовлетворяют требованиям, предъявляемым к источнику накачки лазеров на красителях. Приводятся электрические и световые характеристики излучателя. Особое внимание уделено условиям формирования однородного плазменного образования.

Обычно лазерный модуль на растворах красителей построен по следующей схеме разрядного контура: "система управления режимом работы разрядного контура ↔ емкостной накопитель → управляемый высоковольтный коммутатор → токоведущая линия → нагрузка". В данной работе в качестве нагрузки рассматривается плазма электрического разряда в импульсной коаксиальной лампе (ИКЛ). Источник питания лазерного модуля должен обеспечивать возможность оперативного маневра величиной энергии, выделяемой на нагрузке, и длительностью импульса, в течение которого она выделяется. Энергия импульса определяется уровнем рабочего напряжения источника и электрической емкостью накопителя. Изменение длительности импульса в схеме разрядного контура обеспечивается изменением волнового сопротивления токоведущей линии.

Поскольку для возбуждения активной среды лазера используется излучение плазмы (оптическая накачка), свойства этого излучения можно изменять в соответствии с условиями поставленной задачи, выбирая необходимые уровень напряжения, приложенного к электродам разрядной полости (РП), и давление рабочего газа (Балтаков и др., 1975). Электрическая емкость описываемого разрядного контура определяется емкостью накопителя, который представляет собой батарею из конденсаторов, соединенных параллельно, общей емкостью (в секции) $C_0 \sim 10^2$ мкФ. Индуктивность контура обусловлена собственными индуктивностями токоведущей линии и нагрузки и составляет L_0 = 0,1 мкГн. Нагрузкой служит ИКЛ, у которой активное сопротивление разрядной плазмы $R_a \sim 10^{-2}$ Ом в

максимуме импульса тока. Накопитель заряжается до рабочего напряжения $0 \le u_0 \le$ 40 кВ. Разрядная полость ИКЛ после эвакуации заполняется Xe, рабочее давление газа $P_0 \ge 1$ кПа. Указанное выше значение R_a реализуется в диапазоне $1 \le P_0 \le 10$ кПа.

Условия и требования к источнику накачки лазера на красителях в максимальной степени учтены в конструкции ИКЛ, в которой в отличие от ранее использованных конструкций (Маршак, 1978) предусмотрены:

1) Развязка металлических и кварцевых элементов для повышения механической прочности ИКЛ при импульсных нагрузках с крутым передним фронтом.
2) Возможность изменения геометрических размеров разрядной полости для повышения механической прочности ИКЛ и расширения диапазона управления спектром излучения накачки.
3) Возможность уменьшения давления рабочего газа в разрядной полости независимо от напряжения на источнике питания для повышения механической прочности ИКЛ и расширения диапазона управления спектром излучения накачки.
4) Конструктивное решение обратного токопровода ИКЛ для обеспечения равномерного освещения излучением накачки активной среды лазера.

Обычное техническое решение конструкции ИКЛ предусматривает обратный токопровод в виде сплошной проводящей цилиндрической трубы, которое одновременно является несущей конструкции лампы. Однако при этом упускается из вида то обстоятельство, что в сплошной трубе возможно возникновение азимутальных, т.е. непараллельных оси трубы, токов, приводящее к контракции разряда в отдельных областях по периметру РП, что снижает однородность разряда в РП и равномерность освещения боковой поверхности активного элемента. Тем самым ухудшаются пространственные характеристики излучения лазера, в частности угловая расходимость, изменяется распределение накачки по объему активной среды, что приводит к снижению выходной энергии и к.п.д. лазера.

Прямыми измерениями в схеме с постоянной активной нагрузкой $R_a = 10^{-2}$ Ом установлено, что индуктивность цепи L_0 = 0,3 мкГ, волновое сопротивление контура $Z_k = 5 \cdot 10^{-2}$ Ом, разряд - периодический, затухающий, постоянная затухания $\gamma_p = 5{,}81 \cdot 10^4$ с$^{-1}$, добротность разрядного контура $Q \approx 3{,}5$, отношение энергии, вводимой в разряд за первый полупериод импульса тока (21,8 мкс), к энергии, запасенной в конденсаторной батарее равно 0,6. На рис. 1 приводится осциллограмма разрядного тока, на импульс которого

наложена рассчитанная кривая интегрального по объёму межэлектродного промежутка электрического сопротивления R_a электроразрядной плазмы. На рис. 2 приводятся осциллограммы

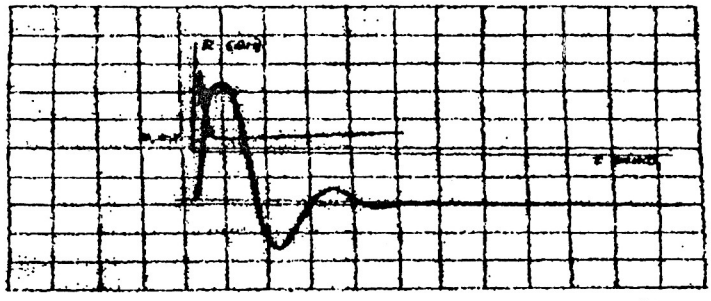

Рис.1

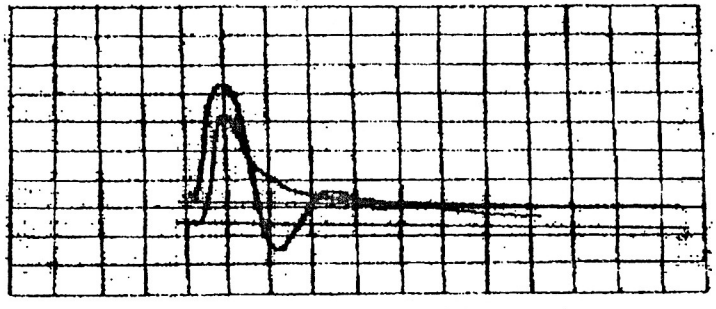

Рис.2

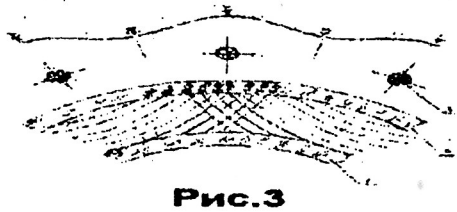

Рис.3

разрядного тока (нижний луч) и импульса оптического излучения плазмы (верхний луч).

В экспериментах с секционированным накопителем исследован режим работы разрядного контура при коммутации на ИКЛ двух секций накопителя. Обработка полученных данных показывает, что в этом случае параметры второго импульса разряда несколько отличаются от параметров первого. Отличия состоят в том, что в исследованном диапазоне задержек между импульсами (до ~1 мс) активное сопротивление плазмы разряда во втором импульсе $R_{a2} \approx 0{,}8\ R_{a1}$. Кроме того, длительность первого полупериода тока во втором импульсе больше, чем в первом $T_{i2} \approx T_{i1}$. Однако принципиального характера эти отличия не носят.

Параллельно с измерениями параметров электрического разряда в ИКЛ проводились измерения ее световых характеристик. Форма импульса излучения плазмы электрического разряда (верхний луч на рис. 2) регистрировалась коаксиальными вакуумными фотоэлементами типа ФЭК. Из полученных данных можно сделать вывод о подобии передних фронтов импульсов тока и светового излучения (в спектральной области 320 – 600 нм в пределах точности измерений). Яркостная температура разряда T определялась по результатам калориметрических и калибровочных измерений.

Для получения больших значений выходной энергии лазера необходимо среди прочих решить задачи равномерности освещения раствора красителя по периметру поперечного сечения активной среды и обеспечения высокой механической прочности конструкции ИКЛ при ударных нагрузках. Первая задача имеет решающее значение для эффективного преобразования оптической накачки в генерируемое излучение.

С целью улучшения пространственных и энергетических характеристик излучения ЛОК путем повышения равномерности освещения боковой поверхности активного элемента, обратный токопровод ИКЛ выполняется в виде набора высоковольтных коаксиальных кабелей. В этом случае повышение однородности разряда достигается тем, что обратный токопровод в виде набора кабелей обеспечивает "принудительную" устойчивость тока в нем по сравнению со сплошным, т.к. изолированные промежутки между кабелями препятствуют развитию азимутальных неустойчивостей. На рис. 3 показаны линии равного магнитогидродинамического давления в плазме электрического разряда в объеме РП. Кривая верхней части рисунка описывает распределение давления в поперечном сечении ИКЛ, рассчитанное в рамках обычной магнитогидродинамической модели (Кнопфель, 1978). Легко видеть, что такое распределение обеспечивает продольную устойчивость полого цилиндрического столба плазмы и исключает развитие азимутальных неустойчивостей при стационарном протекании разрядного тока.

Литература:

Балтаков Ф.Н., Барихин Б.А.: 1975, *Кв. электроника*, **2**, 822.

Кнопфель Г.: 1972, Сверхсильные импульсные магнитные поля, Москва, изд. "Мир".

Маршак И.С. : 1978, Импульсные источники света, Москва, изд. "Энергия".

Publ. Astron. Obs. Belgrade No. 61 (1998), 67 – 70 *Poster paper*

INVESTIGATION OF LS COUPLING IN CARBON II

B.Blagojević, M.V.Popović and N.Konjević

Institute of Physics, 11080 Belgrade, P.O.Box 68, Yugoslavia

1. INTRODUCTION

LS or Russell-Saunders coupling is dominant for many transitions in the spectra of light elements. This is the case spin-orbit interaction in atomic Hamiltonian is more important than the electrostatic separation between levels of the same principal quantum number n. Since electrostatic separation increases as Z while the spin-orbit interaction grows as $Z^4\alpha^2$ where α is fine structure constant, the LS-coupling scheme becomes inappropriate at a certain point. Systematic failure of the LS-coupling approximation is expected from lower to higher elements of an isoelectronic sequence for nl-nl' transitions. The aim of this paper is to test predictions of LS-coupling theory for the transitions within $3s^2S$-$3p^2P^0$ and $3p^2P^0$-$3d^2D$ multiplets of singly ionized carbon. In addition we tested whether plasma electron density influences spontaneous emission coefficients as suggested by Chung et al.

2. THEORY

For LS coupling theory see e.g. Glenzer et al. Theoretical values calculated from multiconfiguration Dirac-Fock (MCDF) wave function of moderate accuracy are compared with our measured intensity ratios. For the case of pure LS coupling the relative line strength for a transition between levels J_1 and J_2 is proportional to the factor (Cowan, Appendix I)

$$D^2_{line} = (2J_1+1)(2J_2+1)\begin{Bmatrix} L_1 & S_1 & J_1 \\ J_1 & 1 & L_2 \end{Bmatrix}^2 \qquad (1)$$

Values of the 6j symbol are given in Appendix D of Cowan. The intensity ratio of two multiplet components is represented by Glenzer et al

$$\frac{I}{I'} = \left(\frac{\lambda'}{\lambda}\right)^4 \left(\frac{D_{line}}{D'_{line}}\right)^2 \exp\left(\frac{E'-E}{kT_e}\right) \qquad (2)$$

where I, λ and I', λ' are the total intensities and wavelengths of the two components, and E and E' are the energies of the upper levels of the two components, respectively.

3. EXPERIMENT

The light source was a low pressure pulsed arc with quartz discharge tube 24 mm internal diameter. The distance between aluminum electrodes was 16.2 cm and 3 mm diameter holes were located at the center of both electrodes to allow end-on plasma observations to be made. The central part around the pulsed arc axis was imaged 1 : 1 onto the entrance slit of the 1 m monochromator by means of the concave 1 m focal length, focusing mirror. A 30 mm diaphragm placed in front of the focusing mirror ensures that light comes from the narrow cone about the arc axis.

The monochromator with inverse linear dispersion 0.833 nm/mm in the first order of the diffraction grating was equipped with the photomultiplier tube (PMT) and a stepping motor. Signals from the PMT were led to a digital storage oscilloscope, which was triggered by the voltage pulse from the Rogowski coil induced by the current pulse through the discharge tube. The discharge was driven by a 15.2 μF low inductance capacitor charged to 2.2 kV (peak current 15 kA) and fired by an ignitron. Greatest care was taken to find the optimum conditions with the least line self-absorption. It was found that the percentage of oxygen in the mixture was of crucial importance for the elimination of self-absorption. The ratio C_2H_2 : He = 4.8 : 95.2 was determined after a number of experiments in which C_2H_2 was diluted gradually until strong line intensities C II are find proportional to the concentration of C in the gas mixture. During the spectral line recording continuous flow of acetylene-helium mixture was maintained at a pressure of about 400 Pa.

4. PLASMA DIAGNOSTICS

For the electron-density measurements we use the width of He II P 468.6 nm line. The full width at half-maximum $\Delta\lambda_{FWHM}$ of this line is related to the electron density N_e using the following relationship (Büscher et al)

$$N_e(cm^{-3}) = 2.238 * 10^{16} \Delta\lambda^{1.204}{}_{FWHM} \qquad (3)$$

where $\Delta\lambda_{FWHM}$ is in 0.1 nm units. This equation is based on the fitting of the experimental data, and in fact closely agrees with calculations by Griem and Shen. Our main concern in electron-density measurements is a possible presence of self-absorption of the 468.6 nm line, which may distort the line profile. This would result in erroneous reading of the line half width, which, after the use of Eq.(3), introduces an error in electron-density measurements. There are several experimental methods which can be used for self-absorption check (Konjević and Wiese) but unfortunately,

none of them is convenient for the He II 468.6 nm line or for our long, pulsed plasma source. Recently, in order to determine the optical thickness of the investigated line Kobilarov et al have introduced in the discharge an additional movable electrode. By positioning the movable electrode at two different positions and by recording the line profiles from two plasma lengths it is possible to determine $k_\lambda l$ where k_λ is the spectral line absorption coefficient and l is the plasma length along the direction of observation. If $k_\lambda l$ is not large ($k_\lambda l < 1$, Wiese) it is possible to recover the line profile (Fig.2 of Kobilarov et al) for the optically thin case. The same method is used here for the He II 468.6 nm line self absorption testing. For this purpose an additional aluminum electrode (10 mm thick) is located inside the discharge tube and the profiles of 468.6 nm line are recorded with two plasma lengths. Since the measured $k_\lambda l$ was smaller than 0.64 it was possible to recover the line profile for the optically thin case.

5. EXPERIMENTAL RESULTS AND DISCUSSION

The experimental intensity ratios R_m for $3s^2S$-$3p^2P^0$ and $3p^2P^0$-$3d^2D$ multiplet of C II ions are given in Table 1 together with theoretical ratio R_{th} and electron concentration. The agreement between averaged $\langle R_m \rangle$ and theoretical R_{th} ratios for both multiplets are within ±9%.

Table 1.

$N_e(10^{16}cm^{-3})$	$R_{m\ 3s\text{-}3p}$	$R_{th\ 3s\text{-}3p}$	$R_{m\ 3p\text{-}3d}$	$R_{th\ 3p\text{-}3d}$
4.70	1.82		1.61	
4.38	1.83		1.66	
3.89	1.82		1.68	
3.08	1.83		1.66	
2.33	1.88	2.00	1.63	1.80
3.11	1.82		1.58	
3.06	1.98		1.65	
2.45	1.94		1.68	
	$\langle R_m \rangle$=1.87		$\langle R_m \rangle$=1.64	

This is good indication that theory (Wiese et al) predicts well spectral line intensity ratios within multiplets. Within the investigated plasma electron density range spontaneous emission coefficients remain constant what is

in agreement with results and discussion in Griem et al (1996) and Griem (1991).

REFERENCES

Chung Y., Lemaire P. and Sucewer S.: 1988, Phys.Rev.Lett. **60**, 1122.
Glenzer S., Kunze H.-J.,Musielok J., Kim Y.-K. and Wiese W.L.,: 1994, Phys.Rev.A **49**, 221.
Cowan R.D.,: 1981, *The Theory of Atomic Structure and Spectra* (University of California Press, Berkeley).
Büscher S., Glenzer S., Wrubel Th. and Kunze H.-J.,: 1996, J.Phys.B, **29**, 4107.
Griem H.R. and Shen K.Y.,: 1961, Phys.Rev. **122**, 1490.
Konjević N. and Wiese L.W.,: 1976, J.Phys. Chem. Ref. Data **5**, 259.
Kobilarov R., Konjević N., and Popović M.V.,: 1981, Phys.Rev.A **40**, 3871.
Wiese W.L.,: 1965, in *Plasma Diagnostic Techniques*, edited by R.M. Huddleston and S.L.Leonard, Academic, New York.
Wiese W.L., Fuhr J.R. and Deters T.M.,: 1996, *Atomic Transition Probabilities of Carbon, Nitrogen and Oxygen*, J.Phys.Chem.Ref.Data Monograph No.7.
Griem H.R., Huang Y.W., Wang J.-S. and Moreno J.C.,: 1991, Phys.Fluids B **3**, 2430.
Griem H.R.,: 1991, Phys.Rev.Lett. **66**, 521.

Publ. Astron. Obs. Belgrade No. 61 (1998), 71 – 74 *Poster paper*

ФОРМИРОВАНИЕ КРАТЕРА НА ПОВЕРХНОСТИ МЕТАЛЛИЧЕСКОГО ОБРАЗЦА, ОБЛУЧАЕМОГО ПОВТОРЯЮЩИМИСЯ ЛАЗЕРНЫМИ ИМПУЛЬСАМИ

Н.А.БОСАК, С.В.ВАСИЛЬЕВ, А.Ю.ИВАНОВ, В.И.НЕДОЛУГОВ, Л.Я.МИНЬКО, А.Н.ЧУМАКОВ.
Институт молекулярной и атомной физики Национальной Академии наук Беларуси, 220082 Минск, Беларусь
E-mail: lrpd@imaph.bas-net.by

Резюме. Экспериментально и теоретически исследованы особенности формирования кратера на металлических мишенях при лазерном воздействии в режиме повторяющихся лазерных импульсов.

Расширение сферы применения лазерной обработки материалов требует подробного изучения механизмов воздействия мощных световых потоков на поверхности твердых тел. Целью настоящей работы является исследование формирования рельефа как внешней (наплавленной), так и внутренней зоны кратера на поверхности металлов (In, Pb, Sn), облучаемых повторяющимися относительно короткими (несколько десятков наносекунд) гладкими лазерными импульсами с $q \sim 10^9$ Вт/см^2.

Схема экспериментальной установки для исследования формирования кратеров на поверхности твердых тел, была подобна использованной в работе Васильева С.В. и др. (1995). В качестве источника воздействующего на образец излучения был применен модуль, созданный на основе лазера ГОС - 1001 (λ = 1,06 мкм). Для получения моноимпульсного и импульсно - периодического режима генерации применялись крупногабаритные пассивные затворы из фтористого лития с F_2^-- центрами окраски (Басиев Т.Т. и др., 1982; Минько Л.Я., Чумаков А.Н. и Босак Н.А., 1990). Управление частотой повторения лазерных импульсов в диапазоне 5 - 50 кГц осуществлялось изменением уровня накачки и оптической плотности пассивных затворов. Длительность отдельного лазерного импульса определялась параметрами резонатора и характеристиками используемого затвора (Минько Л.Я. и др., 1990) и составляла τ = 80 нс. Излучение лазерного модуля при помощи фокусирующей системы направлялось на поверхность исследуемого образца. Сменные отражающие системы, включающие призму полного внутреннего отражения, позволяли направлять световой пучок на образец под произвольным углом, в том числе по нормали, как вертикально (снизу вверх или сверху вниз), так и горизонтально. Для получения на образце относительно однородного пятна фокусировки лазерного излучения (ЛИ) с резкими границами диаметром d = 2,0 мм использовалась диафрагма

диаметром 10 мм, изображение которой строилось на поверхности мишени. Часть лазерного излучения, отраженная от передней грани стеклянного клина, направлялась на измеритель энергии ИМО-2Н ; световой поток, отраженный от задней грани клина, направлялся на коаксиальный фотоэлемент ФК-19, что позволяло визуализировать временную форму лазерного импульса при помощи осциллографа С8-14. Энергия одного импульса ЛИ изменялась в пределах от 2 до 6 Дж; временная форма его была близка к гауссовой; средняя плотность мощности излучения в отдельном импульсе составляла примерно (0,8 - 2,5) $\cdot 10^9$ Вт/см^2 . Суммарная энергия лазерного импульса варьировалась от 4 Дж (моноимпульс) до 150 Дж (n=35 импульсов).

Для определения рельефа облучаемого образца нами использовался метод проекции полос, который реализовывался на установке, описанной в работе Васильева С.В. и др., (1993), позволявшей определять глубину (во внешней зоне - высоту) h любой точки кратера по отношению к необлученной плоской поверхности мишени с погрешностью, не превышающей 50 мкм. Обнаружено, что внутренняя или "отрицательная" зона кратера (откуда металл в ходе воздействия лазерного излучения выносился) имеет достаточно гладкую и ровную куполообразную поверхность (значительно более гладкую, чем в работе Васильева С.В. и др. (1995), причем как глубина зоны, так и ее диаметр возрастают с увеличением n (рис. 1). Внешняя, или "положительная" зона (на которую вынесенный металл наплавлен) имеет форму, близкую к округлой. Следует отметить, что при воздействии ЛИ на вещество горизонтально или сверху вниз для $n > 6 - 8$ внешняя зона представляет собой набор выбросов ("блинов") толщиной от 50 до 250 мкм, наплавленных друг на друга. Значение n, начиная с которого наблюдается формирование "стопы" выбросов, определяется энергиями (и отношением энергий) n-го и (n-1) -го пичков. При воздействии лазерного излучения снизу вверх формирование "стопы" не наблюдалось. На краю каждого округлого выброса имелся небольшой (высотой ≤ 100 мкм) буртик.

На "внешних" выбросах (в случае воздействия снизу вверх - на периферии единственного "блина"), а также на поверхности образца за пределами наиболее крупного округлого выброса имеются наплавленные "лучи". Исследования поверхности кратера при помощи оптического микроскопа показали, что указанные лучи представляют собой цепочки отдельных достаточно крупных (диаметром от 100 до 500 мкм) капель. Более мелкие капли наблюдаются и вне лучей, в том числе и на поверхности внешней зоны кратера.

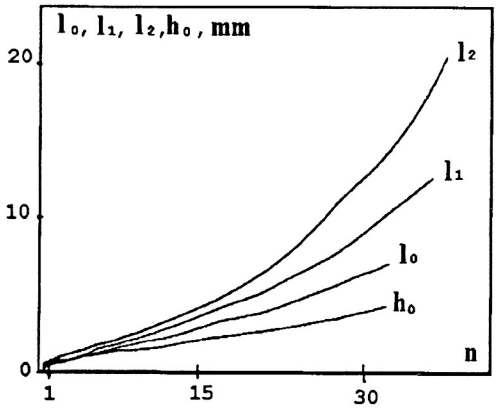

Рис.1. Зависимость поперечного размера наиболее крупного выброса l_1, зоны отжига на поверхности мишени l_2, внутренней зоны кратера l_0 и глубины кратера h_0 от числа пичков n в импульсе ЛИ.

Отметим, что размеры внешней зоны растут значительно быстрее, чем глубина и особенно диаметр внутренней зоны. При этом масса внешней зоны кратера составляет примерно 80% от массы вынесенного материала. Обращает внимание и то, что при воздействии ЛИ на образец снизу вверх размеры внешней зоны примерно в 1,5 раза больше, чем при воздействии в горизонтальном направлении и сверху вниз. Все это подтверждает, что при рассматриваемом режиме воздействия световых импульсов на вещество внутренняя зона образуется за счет "выплескивания" (вытекания) материала из ванны расплава, а не за счет испарения и тем более не за счет разбрызгивания (суммарная масса капель составляет менее 1% от массы вынесенного вещества).

Для выяснения причин формирования кратеров с указанными формами нами был проведен расчет изменения температуры T индиевого образца, облучаемого лазерными импульсами с использованными в эксперименте параметрами. Показано, что T быстро возрастает до значения превышающего температуру плавления индия и довольно быстро; при подаче через ~ 20 мкс 2-го лазерного импульса временная зависимость ΔT остается такой же, меняется только T_0. Таким образом, после подачи 8 лазерных импульсов температура мишени до подачи следующего импульса не опускается ниже температуры плавления индия.

На наш взгляд, данные экспериментальных исследований и результаты расчетов свидетельствуют о следующем механизме формирования кратера. Первый лазерный импульс прогревает, но не расплавляет металл. При подаче 2-го импульса ~ 2 мг металла плавится и выплескивается за пределы пятна фокусировки излучения (о выплескивании, а не о ламинарном вытекании говорит наличие буртика на периферии каждого выброса). Такие же выбросы производятся 3-м, 4-м, 5-м пичками, причем из-за более высокой начальной температуры и малой

глубины лунки масса выплескиваемого металла с каждым разом увеличивается. Поэтому диаметр каждого следующего "блина" превышает диаметр предыдущего; кроме того, из-за большой теплопроводимости индия (~ 48 Вт/м · К) металл перемешивается и выравнивается по высоте. Так формируется внешняя зона кратера при $n \leq$ 6–8.

Направление расположенных на поверхности наиболее крупного выброса и за его пределами "лучей" определяется градиентом освещенности в облучаемой зоне мишени, что согласуется с данными работы Васильева С.В. и др. (1995). Вероятно, механизм их образования аналогичен указанному в этой работе. Капли, вылетевшие под углами, отличающимися от оптимального, а также имеющие малые начальные скорости, не вылетали за пределы плазменного облака и в течение всего времени полета подвергались действию лазерного излучения. Металл в каплях частично испарялся, капли уменьшались и дробились. Поэтому центральная зона кратера имеет более гладкую поверхность, чем периферийная.

Таким образом, при воздействи лазерного излучения на металлы в режиме повторяющихся лазерных импульсов кратер формируется в основном путем многократного выплескивания расплава из облучаемой зоны мишени. Форма внешней зоны кратера определяется временной зависимостью температуры в освещенной области мишени и условиями вытекания металла - глубиной лунки, поверхностной энергией и направлением воздействия излучения на образец.

ЛИТЕРАТУРА

Басиев Т.Т.,Воронько Ю.В., Миров Б.С. и др.: 1982, *Изв. АН СССР. Сер. Физич.*, **46**, 1600.

Васильев С..В., Иванов А.Ю., Ляликов А.М.: 1993, *Квантовая электроника*, **20**, 616.

Васильев С.В., Иванов А.Ю., Ляликов А.М.: 1995, *Квантовая электроника*, **22**, 830.

Ельяшевич М.А., Минько Л.Я., Романов Г.С., Станкевич Ю.А., Чивель Ю.А., Чумаков А.Н.: 1985, *Изв. АН СССР. Сер.физич.*, **49**, 1132.

Минько Л.Я., Чумаков А.Н., Босак Н.А.: 1990, *Квантовая электроника*, **17**, 1480.

Publ. Astron. Obs. Belgrade No. 61 (1998), 75 – 77 *Poster paper*

THE ELECTRON GAS IN A MAGNETIC FIELD: THE EQUATION OF STATE

V. ČELEBONOVIĆ
Institute of Physics, Pregrevica 118, 11080 Zemun-Beograd, Yugoslavia
E-mail celebonovic@exp.phy.bg.ac.yu
E-mail vcelebonovic@sezampro.yu

Abstract. Continuing previous work, and using a simple change of variables proposed in existing literature, an analytical equation of state for a non-relativistic degenerate Fermi gas in a magnetic field is developed.

1. INTRODUCTION

This paper is a continuation of previous work (Celebonovic, 1998a) on the equation of state (EOS) of a degenerate non-relativistic Fermi gas. In that paper, an analytical expression for the Fermi-Dirac (FD) integrals of arbitrary order was proposed and applied in obtaining the EOS. The purpose of the present paper is to propose an analogous expression, but applicable in the case of a degenerate Fermi gas in a magnetic field. The nature of the source of the field is irrelevant.

2. CALCULATIONS

The FD integrals have the following form (for example, Cloutman, 1989)

$$F_n(\eta) = \int_0^\infty f(\varepsilon)d\varepsilon/[1+\exp[\beta(\varepsilon-\mu)]] \tag{1}$$

In this expression $f(\varepsilon) = \varepsilon^l$, l is a real number, μ is the chemical potential β denotes the inverse temperature and $\eta = \beta\mu$. The EOS of a degenerate Fermi gas is (for example, Cloutman, 1989)

$$n = (4\pi/h^3)(2mk_BT)^{3/2}F_{1/2}(\eta) \tag{2}$$

All the symbols in this equation have their standard meanings. It has recently been shown (Celebonovic, 1998a) that the FD integrals of arbitrary order can be expressed as

$$F_n(\eta) = \int_0^\mu (\varepsilon)d\varepsilon + T\sum_{n=0}^{\infty}(f^{(n)}(\mu)/n!)[1-(-1)^n]T^n[1-2^{-n}]\Gamma(n+1)\zeta(n+1) \tag{3}$$

The symbols Γ and ζ denote the gamma and zeta functions. How does this equation change when an external magnetic field is applied to the system? It has been proposed (Landau and Lifchitz, 1976) that the influence of such a field an be described by the following change of variables:

$$\mu \rightarrow \mu \mp \mu_B H = \mu(1 \mp \alpha) \tag{4}$$

where $\mu_B = e\hbar/2m_e c$ is the Bohr magneton, H is the magnetic field and $\alpha = \mu_B H/\mu$. The sign in eq. (4) depends on the orientation of the electronic magnetic moments with respect to the field. Inserting eq. (4) into eq. (3), and using the definition of $f(\epsilon)$, one gets the following form of a FD integral of arbitrary order in the presence of a magnetic field:

$$\begin{gathered} F_n(\eta) = [\mu(1 \mp \alpha)]^{l+1}/(l+1) + \\ T\sum_{n=0}^{\infty}(f^{(n)}(\mu(1 \mp \alpha))/n!)[1-(-1)^n]T^n[1-2^{-n}]\Gamma(n+1)\zeta(n+1) \end{gathered} \tag{5}$$

Using the result for the chemical potential of the electron gas (Celebonovic, 1998a), the parameter α can be expressed as follows

$$\alpha = \mu_B H/[\mu_0(1-(1/12)(\pi T/\mu_0)^2 + (1/720)(\pi T/\mu_0)^4 - (1/162)(\pi T/\mu_0)^6 + ...)] \tag{6}$$

In this equation $\mu_0 = An^{2/3}$ and $A = (3pi^2)^{2/3}\hbar^2/2m_e$. Inserting eq. (6) into eq. (5), and choosing the positive sign in eq. (4), one arrives at:

$$\begin{gathered} F_(1/2)(\eta) = (2/3)[(\mu_B H) + An^{2/3} - (\pi T)^2/(12An^{2/3}) + (\pi T)^4/(720A^3n^2) - \\ (\pi T)^6/(162A^5n^{10/3}) + (\pi T)^8/(754A^7n^{14/3})]^{3/2}(1 + << 3 >>) \end{gathered} \tag{7}$$

The symbol << .. >> denotes the number of omitted terms. Expanding eq. (7) in its full form, it follows that the FD integral of the order 1/2 can be expressed as:

$$\begin{gathered} F_{1/2}(\eta) = (\mu_B H)/(54 \times 1885^{1/2})[(2442960(\mu_B H)A^7n^{14/3} + \\ << 5 >>)/A^7n^{14/3}] + << 23 >> \end{gathered} \tag{8}$$

Inserting eq. (8) in its full form into eq. (2), it follows that the number density of the electron gas can be expressed as the following function:

$$\begin{gathered} n = 23.6954(\mu_B H) \times (m_e T)^{3/2} \times [((\mu_B H)A^7n^{14/3} + A^8n^{16/3} - \\ 0.822467n^4T^2A^6 + 0.13529A^4n^{8/3}T^4 - 5.9345A^2n^{4/3}T^6 + \\ 12.5843T^8)/(A^7n^{14/3})]^{1/2}/h^3 + << 23 >> \end{gathered} \tag{9}$$

This equation, especially in its full form, is far too complex to be solvable analytically. However, its low temperature limit can be solved analytically. Developing the full form of eq. (9) in series in T up to and including terms of the order T^2, one arrives

at the following implicit form of the EOS of a degenerate non-relativistic electron gas in a magnetic field

$$n = (\pi 2^{9/2}/3 \times h^3) \times (mn^{2/3}AT)^{3/2}(1 + (\mu_B H)/(An^{2/3}))^{3/2} \tag{10}$$

This can be solved analytically under the assumption that $x = \mu_B H/An^{2/3} \rightarrow 0$. Physically, this limitation means that the solution is valid when the numbre density of the electron gas is high, or when the magnetic field in which it is placed is weak. Developing now eq. (10) into series in x, up to and including terms of the order x^2, the following expression is obtained:

$$(1 - BT^{3/2})y^2 = (Fy + G)T^{3/2} \tag{11}$$

where the following symbols were used

$$\begin{aligned} &y = n^{2/3}; B = (2^{9/2}\pi/3)(m_e^{1/2}/h)^3 A^{3/2}; F = (3B/2)(\mu_B H/A) \\ &G = (3B/8)(\mu_B H/A)^2 \end{aligned} \tag{12}$$

Solving eq. (11) within S. Wolfram's MATHEMATICA 2.2 software package on a Pentium 166/MMX with a RAM of 32 MBytes, one gets that:

$$y = [-(FT)^{3/2} \pm \sqrt{F^2T^3 - 4GT^{3/2}(-1 + BT^{3/2})}]/(2(-1 + BT^{3/2})) \tag{13}$$

We have thus obtained the EOS of the non-relativistic degenerate Fermi gas in a magnetic field. This is the implicit form of the EOS. Using the changes of variables defined in eq. (12) it becomes possible to obtain the explicite form of the EOS.

What about the applications of the EOS derived in this paper? Equation (13) was derived for the low-temperature regime, assuming that $\mu_B H/An^{2/3} \rightarrow 0$. It follows from this assumption that eq. (13) is applicable to the low temperature electron gas whose number density is limited by $n \gg (\mu_B H/A)^{3/2}$. In astrophysics, situations like this can be expected to arise in accretion disks around compact objects. Having in mind laboratory work they can appear in high pressure experiments performed under external magnetic fields (like, for example, in studies of organic metals in solid state physics).

References

Cloutman, L.D.: 1989, *Astrophys. J. Suppl. Ser.*, **71**, 677.
Celebonovic, V.: 1998a, *Publ. Astron. Obs. Belgrade*, **16**, 18 and preprint astro-ph/9802279.
Landau, L.D. and Lifchitz, E.M.: 1976, Statistical Physics, **I**, Nauka, Moscow.

Publ. Astron. Obs. Belgrade No. 61 (1998), 78 – 80 *Poster paper*

ON THE STARK BROADENING OF K VIII LINES

M. S. DIMITRIJEVIĆ[1] and S. SAHAL-BRÉCHOT[2]
[1]*Astronomical Observatory, Volgina 7, 11160 Belgrade 74, Yugoslavia*
E-mail mdimitrijevic@aob.aob.bg.ac.yu

[2]*Observatoire de Paris, 92195 Meudon Cedex, France*
E-mail sahal@obspm.fr

Abstract. Using a semiclassical approach, we have calculated electron-, proton-, and doubly charged helium-impact line widths and shifts for 4 K VIII multiplets, for perturber densities 10^{18}– 10^{22} cm^{-3} and temperatures T = 200,000 – 3,000,000 K.

1. INTRODUCTION

Spectral lines of potassium are present in Solar (Moore, Minnaert and Houtgast, 1966) and stellar spectra (Merrill, 1956). For example, potassium has been found in the ejecta of SN 1987 A supernova (Trimble, 1991). Potassium is a product of alpha processes - neutron capture on slow time scale, and the data on the spectral line broadening parameters of potassium in various ionization stages are of interest for the considering and modelling of subphotospheric layers (Seaton, 1987), particularly radiative transfer in stellar interiors. Such data are also of interest for the fusion plasmas and laser-produced plasmas research and for the investigation of soft X-ray lasers (see e.g. Griem and Moreno, 1990; Fill and Schöning, 1994).

Within the the semiclassical-perturbation formalism (Sahal-Bréchot 1969ab), we have calculated electron-, proton-, and He III-impact line widths and shifts for 4 potassium XI multiplets. The used semiclassical perturbation formalism has been discussed and reviewed e.g. in Dimitrijević *et al.* (1991) and Dimitrijević and Sahal - Bréchot (1996).

2. RESULTS AND DISCUSSION

Energy levels for potassium VIII lines have been taken from Bashkin and Stoner (1978). All other details of calculations are given in Dimitrijević and Sahal-Bréchot (1998a).

Table 1

This Table shows electron- and proton-impact broadening full half-widths (FWHM) and shifts for K VIII for a perturber density of 10^{19} cm^{-3} and temperatures from 200,000 up to 3,000,000 K. By deviding C with the full linewidth we obtain an estimate for the maximum perturber density for which the line may be treated as isolated and tabulated data may be used.

PERTURBER DENSITY = 1.E+19cm-3

PERTURBERS ARE:		ELECTRONS		PROTONS	
TRANSITION	T(K)	WIDTH(Å)	SHIFT(Å)	WIDTH(Å)	SHIFT(Å)
KVIII 3s 3p	200000.	0.445E-01	-0.444E-03	0.672E-03	-0.262E-03
519.4Å	500000.	0.291E-01	-0.466E-03	0.168E-02	-0.616E-03
C=0.52E+22	1000000.	0.218E-01	-0.551E-03	0.250E-02	-0.969E-03
	1500000.	0.187E-01	-0.517E-03	0.297E-02	-0.118E-02
	2000000.	0.169E-01	-0.506E-03	0.316E-02	-0.133E-02
	3000000.	0.148E-01	-0.490E-03	0.345E-02	-0.149E-02
KVIII 3p 4s	200000.	0.141E-01	0.903E-03	0.464E-03	0.945E-03
221.3 Å	500000.	0.983E-02	0.108E-02	0.120E-02	0.156E-02
C=0.25E+21	1000000.	0.772E-02	0.104E-02	0.185E-02	0.194E-02
	1500000.	0.677E-02	0.102E-02	0.219E-02	0.215E-02
	2000000.	0.620E-02	0.989E-03	0.244E-02	0.233E-02
	3000000.	0.549E-02	0.888E-03	0.284E-02	0.256E-02
KVIII 3p 5s	200000.	0.135E-01	0.183E-02	0.142E-02	0.194E-02
142.8 Å	500000.	0.985E-02	0.174E-02	0.264E-02	0.273E-02
C=0.41E+20	1000000.	0.794E-02	0.171E-02	0.342E-02	0.331E-02
	1500000.	0.703E-02	0.159E-02	0.391E-02	0.368E-02
	2000000.	0.646E-02	0.146E-02	0.430E-02	0.391E-02
	3000000.	0.573E-02	0.127E-02	0.508E-02	0.418E-02
KVIII 3p 3d	200000.	0.391E-01	0.513E-03	0.982E-03	0.226E-03
441.4 Å	500000.	0.255E-01	0.658E-03	0.212E-02	0.521E-03
C=0.38E+22	1000000.	0.192E-01	0.754E-03	0.298E-02	0.801E-03
	1500000.	0.166E-01	0.803E-03	0.329E-02	0.973E-03
	2000000.	0.150E-01	0.768E-03	0.350E-02	0.110E-02
	3000000.	0.133E-01	0.752E-03	0.376E-02	0.122E-02

The complete results of our calculations of electron-, proton-, and He III-impact line widths and shifts for 4 potassium VIII multiplets, for perturber densities 10^{18}–10^{22} cm^{-3} and temperatures T = 200,000 – 3,000,000 K, will be published elsewhere (Dimitrijević and Sahal-Bréchot, 1998ab). Here, in Table 1, only data for perturber density of 10^{19} cm^{-3}, as a sample of obtained results are shown. We also specify the parameter C (Dimitrijević and S.Sahal-Bréchot, 1984), which gives an estimate of the maximum perturber density for which the line may be treated as isolated when divided by the corresponding full width at half maximum.

The results shown here are the first Stark broadening data concerning potassium VIII spectral lines. Besides the interest of such data for astrophysical and laboratory plasma research, they are of significance for the theoretical considerations of systematic trends along isoelectronic sequences and development and rafinement of the Stark broadening theory for multiply charged ion lines.

References

Bashkin, S., Stoner, J.O.Jr.: 1978, Atomic Energy Levels and Grotrian Diagrams, Vol. 2, North Holland, Amsterdam.

Dimitrijević, M.S., and Sahal-Bréchot, S.: 1984, *JQSRT* **31**, 301.

Dimitrijević, M.S., and Sahal-Bréchot, S.: 1996, *Physica Scripta* **54**, 50.

Dimitrijević, M.S. and Sahal-Bréchot, S.: 1998a, *Astron. Astrophys. Suppl. Series* to be submitted.

Dimitrijević, M.S. and Sahal-Bréchot, S.: 1998b, *Bull. Astron. Belgrade* **158**, to be published.

Dimitrijević, M.S., Sahal-Bréchot, S. and Bommier, V.: 1991, *Astron. Astrophys. Suppl. Series* **89**, 581.

Fill, E.E., Schöning, T.: 1994, *J. Appl. Phys.*, **76**, 1423.

Griem, H.R., Moreno, J.C.: 1990, in: X-Ray Lasers, ed. G. Tallents, Institute of Physics, Bristol, 301.

Merrill, P W.: 1956, Lines of the Chemical Elements in Astronomical Spectra, Carnegie Inst. of Washington, Publication 610, Washington D. C.

Moore, C.E., Minnaert, M.G.J., Houtgast, J.: 1966, The Solar Spectrum 2935Å to 8770 Å, NBS Monographs 61, U. S. Department of Commerce, NBS, Washington D.C.

Sahal-Bréchot, S.: 1969a, *Astron.Astrophys.* **1**, 91.

Sahal-Bréchot, S.: 1969b, *Astron.Astrophys.* **2**, 322.

Seaton, M.J.: 1987, *J. Phys. B* **20**, 6363.

Trimble, V.: 1991, The Origin and Abundance of the Chemical Elements Revisited, *Astron. Astrophys. Review*, **3**, 1.

Publ. Astron. Obs. Belgrade No. 61 (1998), 81 – 83 *Poster paper*

ON THE STARK BROADENING OF Tl III AND Pb IV LINES

M. S. DIMITRIJEVIĆ[1] and S. SAHAL-BRÉCHOT[2]
[1]*Astronomical Observatory, Volgina 7, 11160 Belgrade 74, Yugoslavia*
E-mail mdimitrijevic@aob.aob.bg.ac.yu

[2]*Observatoire de Paris, 92195 Meudon Cedex, France*
E-mail sahal@obspm.fr

Abstract. Using a semiclassical approach, we have calculated electron-, proton-, and ionized helium-impact line widths and shifts for 2 Tl III, and electron-, proton-, and He III-impact line widths and shifts for 2 Pb IV multiplets, for perturber densities 10^{17}– 10^{20} cm^{-3} and temperatures T = 20,000 – 500,000 K, and T = 50,000 – 1,000,000 K, respectively.

1. INTRODUCTION

The interest for a very extensive list of line broadening data is particularly stimulated by the developement of space astronomy where an extensive amount of spectroscopic information over large spectral regions of all kind of celestial objects has been and will be collected, stimulating the spectral–line–shape research. Not only in astrophysics, but also in physics and plasma technology, a number of problems depend on very extensive list of elements and line transitions with their atomic and line broadening parameters. One may mention as examples calculation of stellar opacities, stellar atmospheres modelling and investigations, abundance determinations, interpretation and modelling of stellar spectra, laboratory plasma diagnostic, research and modelling, radiative transfer calculations and investigation of laser produced plasmas (not only in laboratory but as well in industry during the laser welding, melting and evaporation of different targets), and plasmas created in fusion research (particularly inertial confinement and pellet compression fusion), development and modelling of lasers, as well as of light sources.

In order to provide to astrophysicists and physicists the needed Stark broadening data, we have calculated within the semi-classical perturbation method (Sahal-Bréchot, 1969ab) Stark broadening parameters for 79 He I, 62 Na, 51 K, 61 Li, 25 Al, 24 Rb, 3 Pd, 19 Be, 270 Mg, 31 Se, 33 Sr, 14 Ba, 28 Ca II, 30 Be II, 29 Li II, 66 Mg II, 64 Ba II, 19 Si II, 3 Fe II, 2 Ni II, 12 B III, 27 Be III, 23 Al III, 10 Sc III, 32 Y III, 10 Ti IV, 39 Si IV, 90 C IV, 5 O IV, 114 P IV, 19 O V, 30 N V, 25 C V, 51 P V, 34 S V, 26 V V, 2 F VI, 30 O VI, 21 S VI, 14 O VII, 10 F VII, 10 Cl VIII, 20 Ne VIII, 4 K VIII, 30 K IX, 4 Ca IX, 8 Na IX, 48 Ca X, 57 Na X, 4 Sc X, 18 Mg XI, 7 Al XI, 4 Si XI, 10 Sc XI, 4 Ti XI, 9 Si XII, 27 Ti XII, 61 Si XIII and 33 V XIII multiplets.

Data for particular lines of F I, Ga II, Ga III, Cl I, Br I, I I, Cu I, Hg II, N III, F V and S IV also have been provided by us.

By using the semiclassical-perturbation formalism (Sahal-Bréchot 1969ab), we have calculated electron-, proton-, and ionized helium-impact line widths and shifts for 2 Tl III and electron-, proton- and He III-impact line widths and shifts for 2 Pb IV multiplets, in order to continue our attempt to obtain a large set of reliable Stark broadening data. The used formalism has been reviewed shortly e.g. in Dimitrijević *et al.* (1991) and Dimitrijević and Sahal - Bréchot (1996).

2. RESULTS AND DISCUSSION

Energy levels for Tl III and Pb IV lines have been taken from Gutmann and Crooker (1973). All other details of calculations are given in Dimitrijević and Sahal-Bréchot (1998). Our results for electron-, proton-, and ionized helium-impact line widths

Table 1

This table shows electron- and proton-impact broadening full half-widths (FWHM) and shifts for Tl III for a perturber density of 10^{17} cm^{-3} and temperatures from 20,000 up to 500,000 K. By deviding C with the full linewidth, we obtain an estimate for the maximum perturber density for which the line may be treated as isolated and tabulated data may be used.

PERTURBER DENSITY = 1.E+17cm-3

PERTURBERS ARE:		ELECTRONS		PROTONS	
TRANSITION	T(K)	WIDTH(Å)	SHIFT(Å)	WIDTH(Å)	SHIFT(Å)
TlIII 6S 6P	20000.	0.170E-01	-0.341E-04	0.436E-03	-0.106E-04
1350.7 A	50000.	0.110E-01	-0.538E-04	0.822E-03	-0.270E-04
C= 0.12E+21	100000.	0.820E-02	-0.531E-04	0.109E-02	-0.483E-04
	200000.	0.650E-02	-0.726E-04	0.123E-02	-0.730E-04
	300000.	0.584E-02	-0.660E-04	0.132E-02	-0.887E-04
	500000.	0.523E-02	-0.657E-04	0.141E-02	-0.105E-03
TlIII 6S 7P	20000.	0.999E-02	0.653E-04	0.914E-03	-0.840E-05
618.6 A	50000.	0.746E-02	0.209E-04	0.120E-02	-0.200E-04
C= 0.59E+19	100000.	0.634E-02	0.103E-03	0.135E-02	-0.318E-04
	200000.	0.556E-02	0.649E-04	0.147E-02	-0.439E-04
	300000.	0.520E-02	0.662E-04	0.151E-02	-0.494E-04
	500000.	0.481E-02	0.745E-04	0.154E-02	-0.566E-04

and shifts for two Tl III multiplets, for perturber densities 10^{17}– 10^{20} cm^{-3} and temperatures T = 20,000 – 500,000 K, and electron-, proton-, and He III-impact line widths and shifts for two Pb IV multiplets, for perturber densities 10^{17}– 10^{20} cm^{-3} and temperatures T = 50,000 – 1,000,000 K, will be published elsewhere (Dimitrijević and Sahal-Bréchot, 1998). We present here in Tables 1 and 2, only data for perturber density of 10^{17} cm^{-3}, for Tl III and Pb IV respectively. We also specify a parameter C (Dimitrijević and S.Sahal-Bréchot, 1984), which gives an estimate for the maximum

perturber density for which the line may be treated as isolated when it is divided by the corresponding full width at half maximum.

There is no experimental data concerning Tl III and Pb IV Stark broadening parameters. There is however a theoretical result (Purić, Dimitrijević and Lakićević (1978) for Tl III $6s^2S$-$6p^2P^o$ multiplet, obtained within the semiempirical approach (Griem, 1968). The obtained width for 15000 K is two times smaller than our lowest value at 20000 K. We hope that the presented results will be useful for astrophysical and laboratory plasma research, as well as for the theoretical considerations of systematic trends along isoelectronic sequences.

Table 2

This table shows electron- and proton-impact broadening full half-widths (FWHM) and shifts for Pb IV for a perturber density of 10^{17} cm^{-3} and temperatures from 50,000 up to 1,000,000 K. By deviding C with the full linewidth, we obtain an estimate for the maximum perturber density for which the line may be treated as isolated and tabulated data may be used.

PERTURBER DENSITY = 1.E+17cm-3

PERTURBERS ARE:		ELECTRONS		PROTONS	
TRANSITION	T(K)	WIDTH(Å)	SHIFT(Å)	WIDTH(Å)	SHIFT(Å)
Pb IV 6S 6P	50000.	0.737E-02	-0.545E-04	0.290E-03	-0.272E-04
1108.7 A	100000.	0.534E-02	-0.647E-04	0.449E-03	-0.508E-04
C= 0.11E+21	200000.	0.404E-02	-0.750E-04	0.595E-03	-0.807E-04
	300000.	0.352E-02	-0.785E-04	0.641E-03	-0.978E-04
	500000.	0.304E-02	-0.723E-04	0.699E-03	-0.120E-03
	1000000.	0.259E-02	-0.687E-04	0.768E-03	-0.144E-03
Pb IV 6S 7P	50000.	0.347E-02	0.358E-04	0.390E-03	0.124E-04
464.8 A	100000.	0.276E-02	0.160E-04	0.470E-03	0.213E-04
C= 0.63E+19	200000.	0.228E-02	0.357E-04	0.530E-03	0.307E-04
	300000.	0.208E-02	0.260E-04	0.562E-03	0.367E-04
	500000.	0.188E-02	0.269E-04	0.586E-03	0.423E-04
	1000000.	0.166E-02	0.272E-04	0.610E-03	0.503E-04

References

Dimitrijević, M.S. and Sahal-Bréchot, S.: 1984, *JQSRT* **31**, 301.

Dimitrijević, M.S. and Sahal-Bréchot, S.: 1996, *Physica Scripta* **54**, 50.

Dimitrijević, M.S. and Sahal-Bréchot, S.: 1998, *Zh. Prikl. Spektrosk.* to be submitted.

Dimitrijević, M.S., Sahal-Bréchot, S. and Bommier, V.: 1991, *Astron. Astrophys. Suppl. Series* **89**, 581.

Griem, H.R.: 1968, *Phys. Rev.* **165**, 258.

Gutmann, F., Crooker, A.M.: 1973, *Can. J. Phys.* **51**, 1823.

Purić, J., Dimitrijević, M.S., Lakićević, I.S.: 1978, *Phys. Lett.* **67A**, 189.

Sahal-Bréchot, S.: 1969a, *Astron.Astrophys.* **1**, 91.

Sahal-Bréchot, S.: 1969b, *Astron.Astrophys.* **2**, 322.

Publ. Astron. Obs. Belgrade No. 61 (1998), 84 – 86 *Poster paper*

ON THE STARK BROADENING OF Ti XI LINES

M. S. DIMITRIJEVIĆ[1] and S. SAHAL-BRÉCHOT[2]
[1]*Astronomical Observatory, Volgina 7, 11160 Belgrade 74, Yugoslavia*
E-mail mdimitrijevic@aob.aob.bg.ac.yu

[2]*Observatoire de Paris, 92195 Meudon Cedex, France*
E-mail sahal@obspm.fr

Abstract. Using a semiclassical approach, we have calculated electron-, proton-, and doubly charged helium-impact line widths and shifts for 4 Ti XI multiplets, for perturber densities 10^{18}– 10^{22} cm^{-3} and temperatures T = 500,000 – 5,000,000 K.

1. INTRODUCTION

Stark broadening of spectral lines for titanium ion in various ionisation stages is of interest for the investigation and modeling of stellar plasma, since this element is present in stars. E.G. Rogerson and Ewell (1985) have found 7 Ti IV lines in the τ Sco spectrum. Stark broadening parameters for 10 Titanium IV multiplets, have been calculated within the semiclassical perturbation approach by Dimitrijević and Sahal - Bréchot (1992). Such data for higher ionization stages are of interest for the consideration of subphotospheric layers (Seaton, 1987), as well as e.g. for fusion plasma research and for investigations of systematic trends along isoelectronic sequences. Conjointly with Ti IV Stark broadening parameters, Dimitrijević and Sahal - Bréchot (1992) have determined also Stark broadening parameters for 10 scandium III multiplets, belonging to the same isoelectronic sequence. Moreover, Stark broadening parameters for 27 titanium XII multiplets have been determined recently (Dimitrijević and Sahal - Bréchot (1998ab)).

By using the semiclassical-perturbation formalism (Sahal-Bréchot 1969ab), we have calculated electron-, proton-, and He III-impact line widths and shifts for 4 titanium XI multiplets. The used semiclassical perturbation formalism has been discussed and reviewed e.g. in Dimitrijević *et al.* (1991) and Dimitrijević and Sahal - Bréchot (1996).

2. RESULTS AND DISCUSSION

Energy levels for titanium XI lines have been taken from Wiese and Musgrove (1989). All other details of calculations are given in Dimitrijević and Sahal-Bréchot (1998a).

Table 1

This Table shows electron- and proton-impact broadening full half-widths (FWHM) and shifts for Ti XI for a perturber density of 10^{19} cm^{-3} and temperatures from 500,000 up to 5,000,000 K. By deviding C with the full linewidth we obtain an estimate of the maximum perturber density for which the line may be treated as isolated and tabulated data may be used.

PERTURBER DENSITY = 1.E+19cm-3

PERTURBERS ARE:		ELECTRONS		PROTONS	
TRANSITION	T(K)	WIDTH(Å)	SHIFT(Å)	WIDTH(Å)	SHIFT(Å)
Ti XI3S 3P	500000.	0.129E-01	-0.142E-03	0.258E-03	-0.140E-03
386.1 A	750000.	0.107E-01	-0.155E-03	0.401E-03	-0.204E-03
C=0.39E+22	1000000.	0.943E-02	-0.179E-03	0.518E-03	-0.258E-03
	2000000.	0.704E-02	-0.174E-03	0.802E-03	-0.400E-03
	3000000.	0.601E-02	-0.171E-03	0.986E-03	-0.486E-03
	5000000.	0.500E-02	-0.162E-03	0.113E-02	-0.589E-03
Ti XI3P 4S	500000.	0.213E-02	0.161E-03	0.113E-03	0.211E-03
123.9 A	750000.	0.181E-02	0.165E-03	0.171E-03	0.258E-03
C=0.11E+21	1000000.	0.162E-02	0.159E-03	0.218E-03	0.297E-03
	2000000.	0.126E-02	0.154E-03	0.352E-03	0.373E-03
	3000000.	0.110E-02	0.149E-03	0.423E-03	0.416E-03
	5000000.	0.932E-03	0.131E-03	0.515E-03	0.473E-03
Ti XI3P 5S	500000.	0.177E-02	0.245E-03	0.245E-03	0.352E-03
81.1 A	750000.	0.153E-02	0.243E-03	0.351E-03	0.417E-03
C=0.25E+20	1000000.	0.139E-02	0.239E-03	0.405E-03	0.447E-03
	2000000.	0.111E-02	0.230E-03	0.541E-03	0.540E-03
	3000000.	0.985E-03	0.208E-03	0.633E-03	0.600E-03
	5000000.	0.843E-03	0.177E-03	0.776E-03	0.667E-03
Ti XI3P 3D	500000.	0.104E-01	-0.560E-04	0.325E-03	-0.509E-04
327.2 A	750000.	0.858E-02	-0.450E-04	0.476E-03	-0.757E-04
C=0.28E+22	1000000.	0.753E-02	-0.568E-04	0.595E-03	-0.978E-04
	2000000.	0.560E-02	-0.614E-04	0.859E-03	-0.164E-03
	3000000.	0.478E-02	-0.531E-04	0.985E-03	-0.200E-03
	5000000.	0.398E-02	-0.532E-04	0.109E-02	-0.256E-03

Our results for electron-, proton-, and He III-impact line widths and shifts for 4 titanium XI multiplets, for perturber densities 10^{18}– 10^{22} cm^{-3} and temperatures T = 500,000 – 5,000,000 K, will be published elsewhere (Dimitrijević and Sahal-Bréchot, 1998). We will show here in Table 1, data for perturber density of 10^{19} cm^{-3}, while the complete results will be published in Dimitrijević and Sahal-Bréchot (1998ab). We also specify the parameter C (Dimitrijević and S.Sahal-Bréchot, 1984), which gives an estimate of the maximum perturber density for which the line may be treated as isolated when divided by the corresponding full width at half maximum.

The results shown here are the first Stark broadening data concerning titanium XI spectral lines. Such data are of interest for astrophysical and laboratory plasma research, as well as for the theoretical considerations of systematic trends along isoelectronic sequences and development and rafinement of the Stark broadening theory for multiply charged ion lines. Such data are of interest also for fusion plasma research and for the consideration of laser produced plasmas. Experimental Stark broadening data for titanium XI spectral lines will be of course very interesting also for the above mentioned topics as well as for the further checking of the semiclassical perturbation method.

References

Dimitrijević, M.S. and Sahal-Bréchot, S.: 1984, *JQSRT* **31**, 301.
Dimitrijević, M.S. and Sahal-Bréchot, S.: 1992, *Astron. Astrophys. Suppl. Series* **95**, 121.
Dimitrijević, M.S. and Sahal-Bréchot, S.: 1996, *Physica Scripta* **54**, 50.
Dimitrijević, M.S. and Sahal-Bréchot, S.: 1998a, *Astron. Astrophys. Suppl. Series* to be submitted.
Dimitrijević, M.S. and Sahal-Bréchot, S.: 1998b, *Bull. Astron. Belgrade* **157**, in press.
Dimitrijević, M.S., Sahal-Bréchot, S. and Bommier, V.: 1991, *Astron. Astrophys. Suppl. Series* **89**, 581.
Rogerson, Jr. J. B. and Ewell, Jr. M. W.: 1985, *Astrophys. J. Suppl. Series* **58**, 265.
Sahal-Bréchot, S.: 1969a, *Astron.Astrophys.* **1**, 91.
Sahal-Bréchot, S.: 1969b, *Astron.Astrophys.* **2**, 322.
Seaton, M.J.: 1987, *J. Phys. B* **20**, 6363.
Wiese, W. L., Musgrove, A.: 1989, "Atomic Data for Fusion", Vol. VI: Spectroscopic Data for Titanium, Chromium and Nickel, Vol. 1. Titanium, ORNL-6551/V1, Controled Fusion Atomic Data Center, Oak Ridge National Laboratory, Oak Ridge.

Publ. Astron. Obs. Belgrade No. 61 (1998), 87 – 90 *Poster paper*

ON THE STARK BROADENING OF F VI AND Cl VII LINES

M. S. DIMITRIJEVIĆ[1] and S. SAHAL-BRÉCHOT[2]
[1]*Astronomical Observatory, Volgina 7, 11160 Belgrade 74, Yugoslavia*
E–mail mdimitrijevic@aob.aob.bg.ac.yu

[2]*Observatoire de Paris, 92195 Meudon Cedex, France*
E–mail sahal@obspm.fr

Abstract. Using a semiclassical approach, we have calculated electron-, proton-, and doubly charged helium-impact line widths and shifts for 2 F VI and 10 Cl VII multiplets, for perturber densities 10^{17}– 10^{22} cm^{-3} and temperatures T = 100,000 – 2,000,000 K.

1. INTRODUCTION

Chlorine and fluorine spectral lines have been observed in Solar (Moore, Minnaert and Houtgast, 1966), as well as in stellar spectra (Merrill, 1956). Trimble (1991) reports that chlorine and fluorine have been found in the ejecta of SN 1987 A supernova. Fluorine is a product of hydrogen burning in stellar interiors and envelopes and chlorine a product of alpha processes - neutron capture on slow time scale. Consequently, the data on the spectral line broadening parameters of fluorine and chlorine at various ionization stages are of interest for the considering and modelling of stellar plasma, particularly subphotospheric layers (Seaton, 1987) and radiative transfer in stellar interiors. For the investigation and developing of soft X-ray lasers, such data are also of interest (see e.g. Griem and Moreno, 1990; Fill and Schöning, 1994). Line broadening data for multiply charged ions are equally of significance for the fusion plasmas and laser-produced plasmas research and for the investigation of Stark broadening parameter systematic trends along isoelectronic sequences.

Within the semiclassical-perturbation formalism (Sahal-Bréchot 1969ab), we have calculated electron-, proton-, and He III-impact line widths and shifts for 2 fluorine VI and 10 chlorine VII multiplets. The used semiclassical perturbation formalism has been discussed and reviewed e.g. in Dimitrijević *et al.* (1991) and Dimitrijević and Sahal - Bréchot (1996).

2. RESULTS AND DISCUSSION

Energy levels for fluorine VI and chlorine VII lines have been taken from Bashkin and Stoner (1978). All other details of calculations are given in Dimitrijević and Sahal-Bréchot (1998a).

Table 1

This Table shows electron- and proton-impact broadening full half- widths (FWHM) and shifts for F VI for a perturber density of 10^{19} cm^{-3} and temperatures from 100,000 up to 2,000,000 K. By deviding C with the full linewidth, we obtain an estimate of the maximum perturber density for which the line may be treated as isolated and tabulated data may be used.

PERTURBER DENSITY = 1.E+19cm-3

PERTURBERS ARE:		ELECTRONS		PROTONS	
TRANSITION	T(K)	WIDTH(Å)	SHIFT(Å)	WIDTH(Å)	SHIFT(Å)
F VI 2S 2P	100000.	0.322E-01	-0.329E-03	0.117E-03	-0.174E-03
535.2 A	200000.	0.229E-01	-0.549E-03	0.322E-03	-0.366E-03
C=0.54E+22	500000.	0.149E-01	-0.586E-03	0.899E-03	-0.780E-03
	1000000.	0.111E-01	-0.608E-03	0.142E-02	-0.112E-02
	1500000.	0.953E-02	-0.574E-03	0.175E-02	-0.133E-02
	2000000.	0.859E-02	-0.567E-03	0.190E-02	-0.142E-02
F VI 2P 3S	100000.	0.928E-02	0.613E-03	0.279E-03	0.655E-03
173.1 A	200000.	0.699E-02	0.795E-03	0.667E-03	0.102E-02
C=0.70E+20	500000.	0.500E-02	0.760E-03	0.136E-02	0.149E-02
	1000000.	0.397E-02	0.736E-03	0.185E-02	0.180E-02
	1500000.	0.349E-02	0.670E-03	0.218E-02	0.199E-02
	2000000.	0.319E-02	0.617E-03	0.238E-02	0.210E-02

Table 2

This Table shows electron- and proton-impact broadening full half- widths (FWHM) and shifts for Cl VII for a perturber density of 10^{19} cm^{-3} and temperatures from 100,000 up to 2,000,000 K. By deviding C with the full line width we obtain an estimate of the maximum perturber density for which the line may be treated as isolated and tabulated data may be used.

PERTURBER DENSITY = 1.E+19cm-3

PERTURBERS ARE:		ELECTRONS		PROTONS	
TRANSITION	T(K)	WIDTH(Å)	SHIFT(Å)	WIDTH(Å)	SHIFT(Å)
Cl VII 3S 3P	100000.	0.183	-0.160E-02	0.149E-02	-0.859E-03
804.8 A	200000.	0.131	-0.211E-02	0.350E-02	-0.180E-02
C=0.80E+22	500000.	0.879E-0	1-0.262E-02	0.711E-02	-0.366E-02
	1000000.	0.674E-0	1-0.236E-02	0.997E-02	-0.510E-02
	1500000.	0.586E-0	1-0.234E-02	0.110E-01	-0.585E-02
	2000000.	0.534E-0	1-0.227E-02	0.117E-01	-0.633E-02

Table 2 continued

PERTURBER DENSITY = 1.E+19cm-3

PERTURBERS ARE:		ELECTRONS		PROTONS	
TRANSITION	T(K)	WIDTH(Å)	SHIFT(Å)	WIDTH(Å)	SHIFT(Å)
Cl VII 3S 4P	100000.	0.277E-01	0.264E-03	0.102E-02	0.129E-03
196.2 A	200000.	0.204E-01	0.211E-03	0.165E-02	0.256E-03
C=0.18E+21	500000.	0.143E-01	0.297E-03	0.235E-02	0.455E-03
	1000000.	0.114E-01	0.280E-03	0.267E-02	0.608E-03
	1500000.	0.102E-01	0.268E-03	0.286E-02	0.678E-03
	2000000.	0.942E-02	0.271E-03	0.299E-02	0.727E-03
Cl VII 4S 4P	100000.	4.35	-0.842E-01	0.132	-0.643E-01
2190.4 A	200000.	3.24	-0.983E-01	0.217	-0.112
C=0.22E+23	500000.	2.33	-0.966E-01	0.320	-0.176
	1000000.	1.88	-0.949E-01	0.377	-0.211
	1500000.	1.68	-0.938E-01	0.413	-0.234
	2000000.	1.56	-0.861E-01	0.441	-0.251
Cl VII 3P 4S	100000.	0.416E-01	0.236E-02	0.637E-03	0.149E-02
294.3 A	200000.	0.308E-01	0.255E-02	0.170E-02	0.252E-02
C=0.40E+21	500000.	0.218E-01	0.277E-02	0.352E-02	0.387E-02
	1000000.	0.174E-01	0.266E-02	0.466E-02	0.463E-02
	1500000.	0.154E-01	0.261E-02	0.536E-02	0.515E-02
	2000000.	0.141E-01	0.247E-02	0.598E-02	0.549E-02
Cl VII 3P 3D	100000.	0.114	-0.447E-03	0.171E-02	-0.147E-03
602.6 A	200000.	0.814E-0	1-0.418E-03	0.359E-02	-0.317E-03
C=0.45E+22	500000.	0.543E-0	1-0.484E-03	0.641E-02	-0.731E-03
	1000000.	0.416E-0	1-0.380E-03	0.807E-02	-0.111E-02
	1500000.	0.363E-0	1-0.405E-03	0.872E-02	-0.136E-02
	2000000.	0.332E-0	1-0.395E-03	0.915E-02	-0.153E-02
Cl VII 3P 4D	100000.	0.403E-01	0.685E-03	0.158E-02	0.112E-02
224.8 A	200000.	0.302E-01	0.870E-03	0.262E-02	0.182E-02
C=0.75E+20	500000.	0.214E-01	0.809E-03	0.402E-02	0.275E-02
	1000000.	0.172E-01	0.750E-03	0.499E-02	0.332E-02
	1500000.	0.153E-01	0.660E-03	0.564E-02	0.369E-02
	2000000.	0.141E-01	0.576E-03	0.620E-02	0.395E-02
Cl VII 4P 4D	100000.	3.11	0.119E-01	0.143	0.525E-01
1680.4 A	200000.	2.34	0.239E-01	0.217	0.875E-01
C=0.42E+22	500000.	1.69	0.120E-01	0.293	0.134
	1000000.	1.37	0.111E-01	0.345	0.161
	1500000.	1.23	0.706E-02	0.379	0.179
	2000000.	1.14	0.239E-02	0.404	0.192

The complete results of our calculations of electron-, proton-, and He III- impact line widths and shifts for 2 fluorine VI and 10 chlorine VII multiplets, for perturber densities 10^{17}– 10^{22} cm^{-3} and temperatures T = 100,000 – 2,000,000 K, will be published elsewhere (Dimitrijević and Sahal-Bréchot, 1998ab). Here, in Tables 1 and 2, only data for perturber density of 10^{19} cm^{-3}, as a sample of obtained results are shown for fluorine VI and chlorine VII respectively. We also specify a parameter C (Dimitrijević and S.Sahal-Bréchot, 1984), which gives an estimate for the maximum perturber density for which the line may be treated as isolated when it is divided by the corresponding full width at half maximum.

There is not experimental results concerning F VI and Cl VII. However, predictions on the basis of systematic trends along isoelectronic sequences exist for F VI $3s^1S$ - $3p^1P^o$, 2464.8 Å line for T = 45000 K and the electron density of $10^{17}cm^{-3}$ and for Cl VII $4s^2S$ - $4p^2P^o$, 2178.8 Å line for T = 60000 K and the electron density of $10^{17}cm^{-3}$ (Purić et al., 1988). Electron temperatures in this paper are too low for the comparison with our data.

We hope that the obtained results are of interest for astrophysical and laboratory plasma research, as well as for the theoretical considerations of systematic trends along isoelectronic sequences.

References

Bashkin, S., Stoner, J.O.Jr.: 1978, Atomic Energy Levels and Grotrian Diagrams, Vol. 2, North Holland, Amsterdam.

Dimitrijević, M.S. and Sahal-Bréchot, S.: 1984, *JQSRT* **31**, 301.

Dimitrijević, M.S. and Sahal-Bréchot, S.: 1996, *Physica Scripta* **54**, 50.

Dimitrijević, M.S. and Sahal-Bréchot, S.: 1998a, *Physica Scripta* to be submitted.

Dimitrijević, M.S. and Sahal-Bréchot, S.: 1998b, *Bull. Astron. Belgrade* **158**, to be published.

Dimitrijević, M.S., Sahal-Bréchot, S. and Bommier, V.: 1991, *Astron. Astrophys. Suppl. Series* **89**, 581.

Fill, E. E., Schöning, T.: 1994, *J. Appl. Phys.* **76**, 1423.

Griem, H.R., Moreno, J.C.: 1990, in: X-Ray Lasers, ed.G. Tallents, Institute of Physics, Bristol, 301.

Merrill, P.W.: 1956, Lines of the Chemical Elements in Astronomical Spectra, Carnegie Inst. of Washington, Publication 610, Washington D.C.

Moore, C.E., Minnaert, M.G.J., Houtgast, J.: 1966, The Solar Spectrum 2935Å to 8770 Å, NBS Monographs 61, U. S. Department of Commerce, NBS, Washington D.C.

Purić, J., Djeniže, S., Labat, J., Platiša, M., Srećković, A., Ćuk, M.: 1988, *Z. Phys. D* **10**, 431.

Sahal-Bréchot, S.: 1969a, *Astron.Astrophys.* **1**, 91.

Sahal-Bréchot, S.: 1969b, *Astron.Astrophys.* **2**, 322.

Seaton, M.J., 1987, *J. Phys. B* **20**, 6363.

Trimble, V., 1991, The Origin and Abundance of the Chemical Elements Revisited, *Astron. Astrophys. Review*, **3**, 1.

Publ. Astron. Obs. Belgrade No. 61 (1998), 91 – 94 *Poster paper*

ON THE STARK BROADENING OF Sc XI LINES

M. S. DIMITRIJEVIĆ[1] and S. SAHAL-BRÉCHOT[2]
[1]*Astronomical Observatory, Volgina 7, 11160 Belgrade 74, Yugoslavia*
E-mail mdimitrijevic@aob.aob.bg.ac.yu

[2]*Observatoire de Paris, 92195 Meudon Cedex, France*
E-mail sahal@obspm.fr

Abstract. Using a semiclassical approach, we have calculated electron-, proton-, and doubly charged helium-impact line widths and shifts for 10 Sc XI multiplets, for perturber densities 10^{18}– 10^{22} cm^{-3} and temperatures T = 500,000 – 5,000,000 K.

1. INTRODUCTION

The various atomic data concerning scandium element, including Stark broadening parameters of its spectral lines for various ionization stages are of interest for astrophysical plasma research and modeling, since this element is present in stellar plasma. Stark broadening data for higher ionization stages are additionaly of interest for the modelling and theoretical considerations of subphotospheric layers (Seaton, 1997), as well as for investigations of systematic trends along isoelectronic sequences.

By using the semiclassical-perturbation formalism (Sahal-Bréchot 1969ab), we have calculated electron-, proton-, and He III-impact line widths and shifts for 10 scandium XI multiplets. A short review of the formalism is given e.g. in Dimitrijević *et al.* (1991) and Dimitrijević and Sahal - Bréchot (1996).

2. RESULTS AND DISCUSSION

Energy levels for scandium XI lines have been taken from Bashkin and Stoner (1978). All other details of calculations are given in Dimitrijević and Sahal-Bréchot (1998). Our results for electron-, proton-, and He III-impact line widths and shifts for 10 scandium XI multiplets, for perturber densities 10^{18}– 10^{22} cm^{-3} and temperatures T = 500,000 – 5,000,000 K, will be published elsewhere (Dimitrijević and Sahal-Bréchot, 1998). We present here, in Table 1, only data for perturber density of 10^{19} cm^{-3}. We also specify the parameter C (Dimitrijević and Sahal-Bréchot, 1984), which gives an estimate of the maximum perturber density for which the line may be treated as isolated when divided by the corresponding full width at half maximum.

Table 1

This Table shows electron- and proton-impact broadening full half- widths (FWHM) and shifts for Sc XI for a perturber density of 10^{19} cm^{-3} and temperatures from 500,000 up to 5,000,000 K. By deviding C with the full line width, we obtain an estimate for the maximum perturber density for which the line may be treated as isolated and tabulated data may be used.

PERTURBER DENSITY = 1.E+19cm-3

PERTURBERS ARE:		ELECTRONS		PROTONS	
TRANSITION	T(K)	WIDTH(Å)	SHIFT(Å)	WIDTH(Å)	SHIFT(Å)
ScXI 3S-3P	500000.	0.247E-01	-0.340E-03	0.526E-03	-0.406E-03
510.9 A	750000.	0.205E-01	-0.413E-03	0.816E-03	-0.579E-03
C=0.51E+22	1000000.	0.181E-01	-0.439E-03	0.106E-02	-0.711E-03
	2000000.	0.136E-01	-0.413E-03	0.165E-02	-0.105E-02
	3000000.	0.116E-01	-0.400E-03	0.202E-02	-0.128E-02
	5000000.	0.966E-02	-0.389E-03	0.237E-02	-0.147E-02
ScXI 3S-4P	500000.	0.215E-02	0.174E-04	0.150E-03	0.216E-04
95.0 A	750000.	0.181E-02	0.205E-04	0.185E-03	0.299E-04
C=0.68E+20	1000000.	0.161E-02	0.173E-04	0.215E-03	0.367E-04
	2000000.	0.125E-02	0.176E-04	0.259E-03	0.523E-04
	3000000.	0.109E-02	0.166E-04	0.282E-03	0.617E-04
	5000000.	0.930E-03	0.156E-04	0.315E-03	0.707E-04
ScXI 4S-4P	500000.	0.511	-0.142E-01	0.321E-01	-0.207E-01
1327.8 A	750000.	0.435	-0.137E-01	0.404E-01	-0.256E-01
C=0.13E+23	1000000.	0.390	-0.133E-01	0.475E-01	-0.296E-01
	2000000.	0.306	-0.129E-01	0.601E-01	-0.374E-01
	3000000.	0.268	-0.126E-01	0.674E-01	-0.419E-01
	5000000.	0.230	-0.107E-01	0.790E-01	-0.476E-01
ScXI 3P-4S	500000.	0.240E-02	0.184E-03	0.130E-03	0.236E-03
127.9 A	750000.	0.204E-02	0.190E-03	0.192E-03	0.288E-03
C=0.12E+21	1000000.	0.183E-02	0.182E-03	0.246E-03	0.332E-03
	2000000.	0.142E-02	0.177E-03	0.391E-03	0.415E-03
	3000000.	0.124E-02	0.172E-03	0.470E-03	0.461E-03
	5000000.	0.105E-02	0.152E-03	0.575E-03	0.523E-03
ScXI 3P-3D	500000.	0.146E-01	-0.714E-04	0.477E-03	-0.729E-04
378.7 A	750000.	0.121E-01	-0.609E-04	0.692E-03	-0.108E-03
C=0.28E+22	1000000.	0.107E-01	-0.870E-04	0.861E-03	-0.140E-03
	2000000.	0.795E-02	-0.831E-04	0.123E-02	-0.233E-03
	3000000.	0.679E-02	-0.750E-04	0.140E-02	-0.283E-03
	5000000.	0.566E-02	-0.726E-04	0.155E-02	-0.361E-03

Table 1 continued

PERTURBER DENSITY = 1.E+19cm-3

PERTURBERS ARE:		ELECTRONS		PROTONS	
TRANSITION	T(K)	WIDTH(Å)	SHIFT(Å)	WIDTH(Å)	SHIFT(Å)
ScXI 3P-4D	500000.	0.261E-02	0.374E-04	0.186E-03	0.116E-03
104.9 A	750000.	0.220E-02	0.315E-04	0.234E-03	0.145E-03
C=0.37E+20	1000000.	0.196E-02	0.333E-04	0.279E-03	0.167E-03
	2000000.	0.152E-02	0.345E-04	0.365E-03	0.214E-03
	3000000.	0.133E-02	0.282E-04	0.419E-03	0.239E-03
	5000000.	0.113E-02	0.224E-04	0.498E-03	0.272E-03
ScXI 3P-5D	500000.	0.335E-02	0.867E-04	0.430E-03	0.319E-03
78.8 A	750000.	0.288E-02	0.935E-04	0.521E-03	0.379E-03
C=0.11E+20	1000000.	0.260E-02	0.941E-04	0.574E-03	0.406E-03
	2000000.	0.207E-02	0.787E-04	0.720E-03	0.489E-03
	3000000.	0.183E-02	0.668E-04	0.830E-03	0.541E-03
	5000000.	0.159E-02	0.574E-04	0.968E-03	0.603E-03
ScXI 4P-4D	500000.	0.364	0.190E-03	0.296E-01	0.813E-02
1042.3 A	750000.	0.310	-0.108E-02	0.367E-01	0.106E-01
C=0.37E+22	1000000.	0.278	-0.620E-03	0.415E-01	0.121E-01
	2000000.	0.218	-0.432E-03	0.495E-01	0.162E-01
	3000000.	0.192	-0.880E-03	0.550E-01	0.181E-01
	5000000.	0.165	-0.129E-02	0.636E-01	0.205E-01
ScXI 4P-5D	500000.	0.361E-01	0.633E-03	0.445E-02	0.293E-02
242.7 A	750000.	0.311E-01	0.660E-03	0.525E-02	0.349E-02
C=0.10E+21	1000000.	0.281E-01	0.681E-03	0.577E-02	0.373E-02
	2000000.	0.225E-01	0.539E-03	0.717E-02	0.449E-02
	3000000.	0.200E-01	0.435E-03	0.818E-02	0.498E-02
	5000000.	0.174E-01	0.355E-03	0.946E-02	0.549E-02
ScXI 3D-4P	500000.	0.672E-02	0.106E-03	0.512E-03	0.120E-03
168.6 A	750000.	0.566E-02	0.122E-03	0.631E-03	0.162E-03
C=0.21E+21	1000000.	0.504E-02	0.120E-03	0.731E-03	0.192E-03
	2000000.	0.389E-02	0.117E-03	0.875E-03	0.264E-03
	3000000.	0.340E-02	0.111E-03	0.954E-03	0.297E-03
	5000000.	0.291E-02	0.106E-03	0.106E-02	0.341E-03

There is no experimental data or results of other calculations, concerning scandium XI Stark broadening parameters. We hope that presented data will be of interest for astrophysical and laboratory plasma research, as well as for the theoretical considerations of systematic trends along isoelectronic sequences. The corresponding experimental data will be of interest for checking and rafinement of the Stark broadening theory for multicharged ion lines.

References

Bashkin, S., Stoner, J.O.Jr.: 1978, "Atomic Energy Levels and Grotrian Diagrams", Vol. 2, North Holland, Amsterdam.

Dimitrijević, M.S. and Sahal-Bréchot,S.: 1984, *JQSRT* **31**, 301.

Dimitrijević, M.S. and Sahal-Bréchot,S.: 1996, *Physica Scripta* **54**, 50.

Dimitrijević M.S. and Sahal-Bréchot, S.: 1998, *Astron. Astrophys. Suppl. Series* to be submitted.

Dimitrijević, M.S., Sahal-Bréchot, S. and Bommier, V.: 1991, *Astron. Astrophys. Suppl. Series* **89**, 581.

Sahal-Bréchot, S.: 1969a, *Astron.Astrophys.* **1**, 91.

Sahal-Bréchot, S.: 1969b, *Astron.Astrophys.* **2**, 322.

Seaton, M.J., 1987, *J. Phys. B* **20**, 6363.

Publ. Astron. Obs. Belgrade No. 61 (1998), 95 – 98 *Poster paper*

SPATIAL DISTRIBUTION OF ARGON EMISSION IN RF DISCHARGE

S. DJUROVIĆ

Institute of Physics, Trg Dositeja Obradovića 4, 21000 Novi Sad, Yugoslavia

1. INTRODUCTION

Radio frequency (rf) discharges are useful for many applications in material processing such as etching, sputtering, thin film deposition, treatment of surfaces etc. (Powell, 1984; Einspruch, 1984; Morgan, 1985; Miyake, 1992; Tokonami, 1992). Knowledge about processes inside of radio frequency discharges even of simple system such as argon discharges is still far from satisfactory.

In this paper results of spatially resolved optical emission measurements from pure argon rf discharge are reported. The radiation of neutral and ionic argon spectral lines is emitted from well defined 13.56 Mhz rf reactor in pressure range from 6.67 to 66.67 Pa and 200 V applied rf voltage. The time averaged spectroscopic measurements showed that different spectral lines have different positions of the peaks of the emission distribution.

2. EXPERIMENTAL

As the plasma source the Gaseous Electronic Conference (GEC) Radio Frequency Reference Cell was used. The details of the design of the Cell are given in Ref. Hargis et al. (1994). Briefly, the GEC RF Reference Cell is a parallel plate discharge chamber with 102 mm diameter electrodes separated by 25 mm. The electrodes are cylindrically symmetric and their surfaces are horizontal. The top electrode contains 169 holes 380 μm in diameter to provide a showerhead gas inlet. The cylindrical vacuum chamber is constructed of stainless steel and has 8 cooper gasket side ports symmetrically positioned to the chamber midplane. Two 203 mm diameter ports are fitted with 136 mm diameter quartz windows for spectroscopic observations. Two additional ports, orthogonal to these, are 152 mm diameter flanges, one of which accommodates a turbo molecular pump for establishing a base pressure of $< 10^{-5}$ Pa. The bottom of the vacuum chamber is constructed so the pumpout of the gas is accomplished by four symmetrically placed 70 mm diameter ports piped into a single exhaust line to a mechanical vacuum pump. The top electrode is grounded to the chamber on the outside of the vacuum interface. The bottom electrode is powered by a 13.56 Mhz rf power

supply isolated by a filter box in external circuit. The flow rates were 10 standard cubic centimeters per minute.

The experimental setup for spectroscopic measurements is described elsewhere (Djurović *et al.*, 1993). The monochromator is equipped with a cooled 5 cm diameter end-on photomultiplier for detection of the optical signal. The photomultiplier tube is connected to a picoameter and signal from the picoameter is fed to a personal computer through IEEE-488 interface.

3. RESULTS

The Ar I 750.4 nm and Ar II 427.8 nm lines were observed in the pressure range of 6.67 to 66.67 Pa. The time averaged intensity distributions along the discharge axis for Ar I 750.4 nm line for different pressures are shown in Fig 1. To obtain good signal-to-noise ratio every experimental point in Fig. 1 represents the average value of 40 readings from the picoameter.

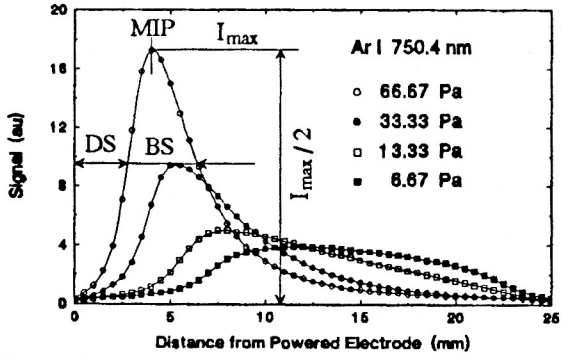

Fig. 1 Spatially resolved time averaged optical emission for Ar I 750.4 nm line.

The measurements of the optical intensity distributions of Ar II 427.8 nm line for different pressure are shown in Fig. 2. These measurements are taken under

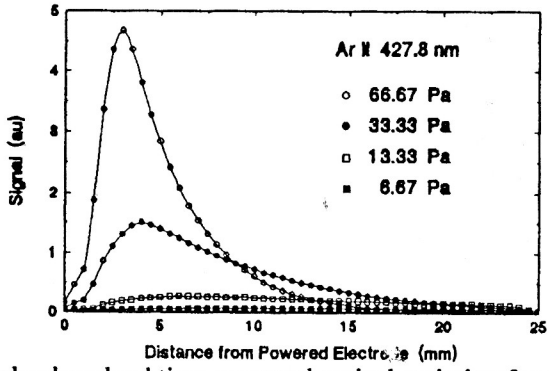

Fig. 2 Spatially resolvedresolved time averaged optical emission for Ar II 427.8 nm line

same conditions as the measurements of Ar I line and show similar behaviour. The intensities of both Ar I and Ar II lines are highly dependent on the discharge pressure. As the pressure is increased the most intense regions of emission shift toward the powered electrode and the well defined sheats (dark zone near the electrode surface) are formed.

The characteristic of the spatially resolved emission between the electrodes is defined by three parameters: Maximum Intensity position (MIP), Dark Space (DS) and Bright space (BS), which are showed in Fig. 1. Pressure dependence of the three defined parameters for Ar I 750.4 nm line with applied pea-to-peak rf voltage of 200 V is shown in Fig. 3. The same for Ar II 427.8 nm line is shown in Fig. 4.

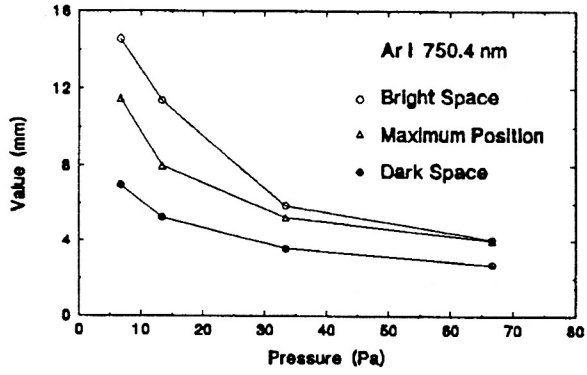

Fig. 3 Pressure dependence of three parameters for Ar I 750.4 nm line

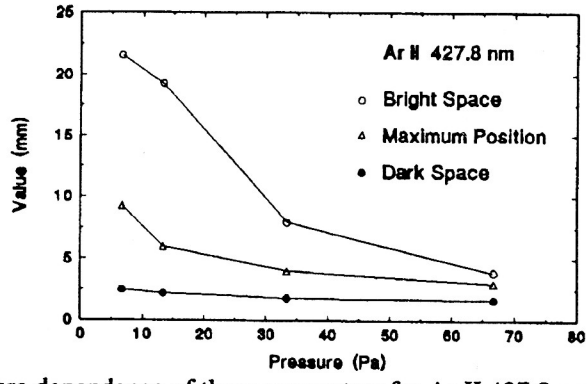

Fig. 4 Pressure dependence of three parameters for Ar II 427.8 nm line

From these measurements one ca conclude:

- Emission intensity at the electrodes (positions 0 and 25 mm in Figs. 1 and 2) is not zero (after noise subtraction), which implies that the plasma extends outside the electrode region.

- Spatially resolved profiles of both Ar I and Ar II lines show considerable pressure dependence.
- The maximum intensity position of the Ar II line is closer to the powered electrode than maximum intensity positions of the Ar I line.

The last conclusion is the most important one. This in contradiction with the intuitive picture that can be produced for secondary electron sustained discharge. In that picture electrons get accelerated from zero energy and thus should excite transitions with lower thresholds first. An explanation of this apparent inverted distribution of the emission is offered in Ref. Petrović *et al.* (1995).

Acknowledgment

This work was performed in the Atomic Physics Division of the Physics Laboratory of the National Institute of Standards and Technology, Gaithersburg, USA. The author would like to thank J. R. Roberts for their help in performing the measurements.

References

Djurović, S., Roberts, J. R., Sobolewski M. A. and J. K. Olthoff, J. *Res. Natl. Stand. Technol.* 98, 159 (1993).

Einspruch, N. G. and Brown, D. M. : 1984, *VLSI Electronics Microstructure Science*, Academic Press, New York.

Hargis, P. J., Greenberg, K. E., Miller, P. A., Gerardo, J. B., Torcznski, J. R., Riley, M. E., Hebner, G. A., Roberts, J. R., Olthoff, J. K., Whetstone, J. R., Van Brunt, R. J., Sobolewski, M. A., Anderson, H. M., Splichal, M., Mock, J. L., Bletzinger, P., Garscadden, A., Gottscho, R. A., Selwyn, G., Dalvie, M., Hidenreich, J. E., Butterbaugh, J. W., Brake, M. L., Passow, M. L., Pender, J., Lujan, A., Elta, M. E., Graves, D. E. B., Sawin, H. H., Kushner, M. J., Verdeyen, J. T., Horwath, R. and Turner, T. R. : 1994, *Rev. Sci. Instrum.* 65, 140.

Miyake, S., Shimura, N., Makabe T. and Itoh, A. : 1992, *J. Vac. Sci. Technol.* A10, 1135.

Morgan, R. A. : 1985, *Plasma Etching in Semicondutor Fabrication*, Elsevier, Amsterdam.

Petrović, Z. Lj., Bzenić, S., Jovanović J. and Djurović, S. : 1995, *J. Phys. D: Appl. Phys.* 28, 2287.

Powell, R. A. : 1984, *Dry Etching for Microelectronics*, North-Holland, Amsterdam.

Tokonami, T. and Makabe, T. : 1992, *J. Appl. Phys.* 72, 3323.

Publ. Astron. Obs. Belgrade No. 61 (1998), 99 – 102 *Poster paper*

ВЛИЯНИЕ ХАРАКТЕРА РАЗЛЕТА ПАРОВ МИШЕНИ НА ОБРАЗОВАНИЕ ПРИПОВЕРХНОСТНОЙ ЛАЗЕРНОЙ ПЛАЗМЫ

В.В.ЕФРЕМОВ, Л.Я.МИНЬКО, Ю.А.ЧИВЕЛЬ, А.Н.ЧУМАКОВ
Институт молекулярной и атомной физики Национальной Академии наук Беларуси, 220082 Минск, Беларусь
E-mail lrpd@imaph.bas-net.by

Резюме. Обнаружена и исследована размерная зависимость порогов приповерхностного лазерного плазмообразования, обусловленная боковым разлетом паров мишени из области воздействия.

1. ВВЕДЕНИЕ

Образование приповерхностной лазерной плазмы, существенно изменяющее характер взаимодействия лазерного излучения (ЛИ) с облучаемыми материалами, является предметом многочисленных исследований. Экспериментально выявлена степенная зависимость времени начального плазмообразования от плотности мощности ЛИ в импульсе, хорошо соблюдающаяся при лазерном воздействии на ряд поглощающих материалов в условиях квазиодномерного разлета образующейся плазмы (Козлова Н.Н., и др., 1975; Бессараб А.В. и др., 1978; Данилычев В.А. и др., 1980; Чивель Ю.А. и Чумаков А.Н., 1983). Предложены эмпирические и теоретические обобщения обнаруженных закономерностей, описывающие также зависимость времени образования плазмы от формы лазерных импульсов (Берченко Е.А. и др., 1981,1984; Минько Л.Я. и др., 1984; Минько Л.Я. и Чумаков А.Н., 1991; Борец-Первак И.Ю., Воробьев В.С.: 1995), а также влияние условий лазерного воздействия на особенности образования приповерхностной лазерной плазмы (Даньщиков Е.В. и др., 1982, 1985). В то же время особенности приповерхностного плазмообразования в условиях перехода к трехмерному разлету плазмы вплоть до струйного ее истечения почти не исследованы.

Настоящая работа посвящена исследованию влияния характера разлета паров мишени на пороги испарения и плазмообразования при импульсном лазерном воздействии (λ = 1,06 мкм) на плоские полированные мишени из алюминия и алюминиевых сплавов в воздухе нормальной плотности.

2.ЭКСПЕРИМЕНТАЛЬНЫЕ РЕЗУЛЬТАТЫ И ИХ ОБСУЖДЕНИЕ

В экспериментах использовался моноимпульсный лазер на неодимовом стекле с энергией в импульсе до 50 Дж. Переход от квазиодномерного к трехмерному разлету паров мишени осуществлялся изменением пятна облучения в диапазоне 0,25÷4 мм и длительности лазерных импульсов от микросекундной (τ = 0,35 мкм) до наносекундной (τ = 60 нс). Благодаря изменению как диаметра пятен облучения, так и длительности лазерных импульсов обеспечивалась возможность разделения влияния на пороги плазмообразования характера разлета паров мишени с одной стороны, и собственно размеров пятна облучения - с другой. Распределение плотности мощности ЛИ на плоских мишенях в пятнах облучения 1÷4 мм было близко к прямоугольному с неравномерностью не хуже 20%, а в пятнах диаметром менее 0,5 мм - дифракционным.

Экспериментально изучены зависимости времени начала испарения и плазмообразования от размеров пятна облучения и плотности мощности ЛИ для лазерных импульсов двух типов с крутизной переднего фронта 350 и 80 нс (рис.1). Момент начала испарения и плазмообразования устанавливался по достижению некоторой пороговой яркости свечения паров и эрозионной плазмы (Минько Л.Я., Чивель Ю.А., Чумаков А.Н., 1985). В частности, за порог испарения принималось достижение в пятне облучения яркостной температуры 2700 К, соответствующей температуре кипения алюминия при нормальных условиях. Обнаружен существенный рост порогов испарения и плазмообразования при пятнах облучения менее 0,5 мм. Для всех исследованных пятен облучения при интенсивности до $1{,}5 \cdot 10^3$ МВт/см^2, наблюдалась однотипная степенная зависимость (Минько Л.Я. и др., 1984) времени начала испарения и образования плазмы от плотности мощности ЛИ, что свидетельствует об эрозионном характере начального плазмообразования. Пороговые для плазмообразования плотности мощности ЛИ составляют 25 и 50 МВт/см^2 при τ = 350 и 80 нс соответственно (d=4 мм).

При переходе к пятнам диаметром 0,25 мм (τ = 350 нс) пороги плазмообразования возрастает до 80 МВт/см^2, а пороги испарения повышаются при этом почти вдвое независимо от длительности лазерных импульсов. Сравнение пороговых плотностей энергии испарения и плазмообразования в пятнах облучения диаметром 1-4 мм для лазерных импульсов различной длительности приводит к приближенной зависимости $E \sim \tau^{0,7}$.

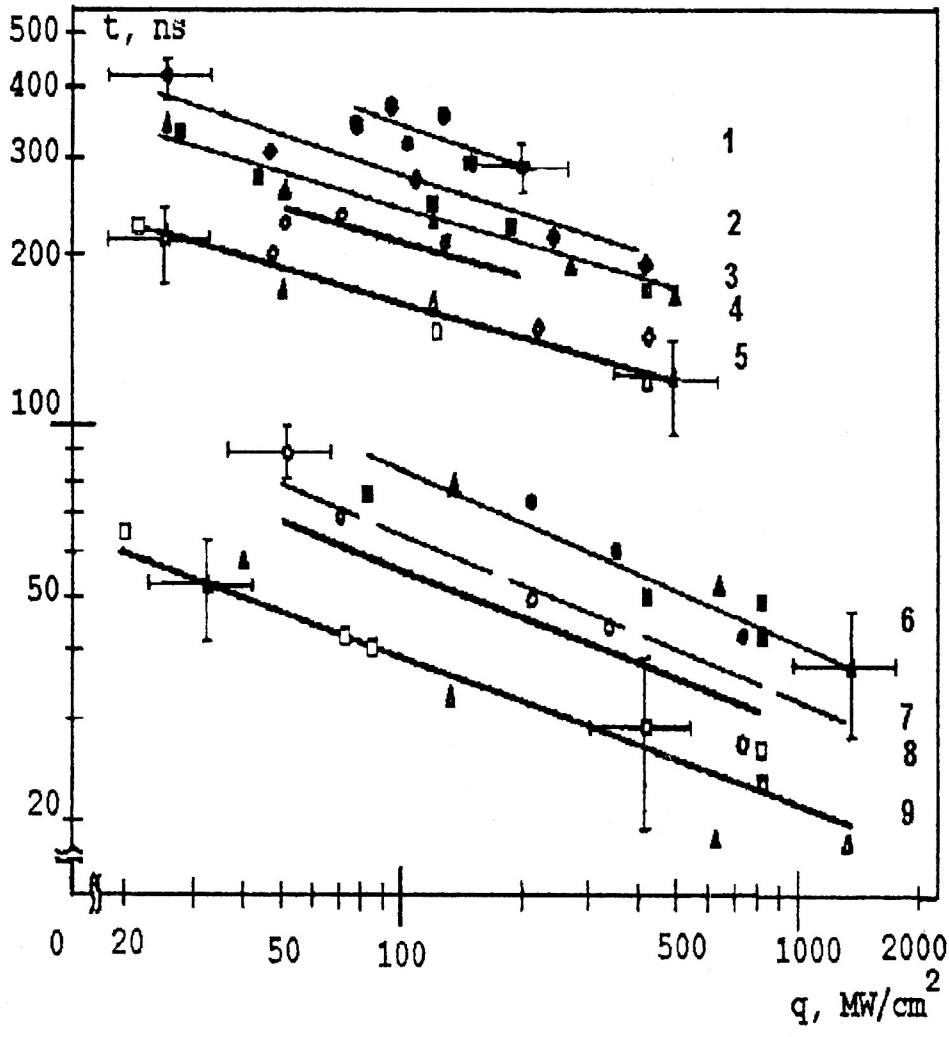

Рис. 1. Начало испарения - 4,5,8,9 (светлые символы □ , Δ , ◊ , O); начало плазмообразования - 1-3,6,7 (темные символы □ , Δ , ◊ , O); диаметр пятна облучения - 4 (□), 1 (Δ), 0,5 (◊) и 0,25 мм (O); длительность фронта лазерного импульса 350 (1-5) и 80 нс (6-9).

Обнаруженная размерная зависимость порогов плазмообразования наблюдается лишь в условиях существенно неодномерного разлета, реализующего при воздействии лазерных импульсов с τ = 350 нс, тогда как

размерная зависимость порога испарения наблюдается и в условиях квазиодномерного разлета (τ =80 нс). Таким образом, экспериментально обнаружена размерная зависимость порогов плазмообразования, обусловленная боковым разлетом паров мишени из области воздействия. Наблюдаемая зависимость порогов плазмообразования осложнена возрастанием порогов испарения в малых пятнах облучения ($d < 0,5$ мм), что указывает на локальный характер начального испарения.

ЛИТЕРАТУРА

Берченко Е.А., Кошкин А.В., Соболев А.П., Федюшин Б.Т.: 1981, *Квантовая электроника*, **8**, №7, 1582.

Берченко Е.А., Кошкин А.В., Соболев А.П., Федюшин Б.Т.: 1984, *Квантовая электроника*, **11**, №4, 842.

Бессараб А.В., Романов В.М., Самылин В.А., Фунтиков А.И.: 1978, *ЖТФ*, **48**, № 8, 1751.

Борец-Первак И.Ю., Воробьев В.С.: 1995, *Квантовая электроника*, **22**, 763.

Данилычев В.А., Зворыкин В.Д., Холин И.В., Чугунов А.Ю.: 1980, *Квантовая электроника*, **7**, №12, 2599.

Даньщиков Е.В., Дымшаков В.А., Лебедев Ф.В., Рязанов А.В.: 1982, *Квантовая электроника*, **9**, №8, 1703.

Даньщиков Е.В., Дымшаков В.А., Лебедев Ф.В., Рязанов А.В.: 1985, *Квантовая электроника*, **12**, №9, 1863.

Козлова Н.Н., Петрухин А.И., Суляев В.А.: 1975, *Квантовая электроника*, **2**, №7, 1390.

Минько Л.Я., Чумаков А.Н., Чивель Ю.А.: 1984, *Квантовая электроника*, **11**, №11, 2241.

Минько Л.Я., Чивель Ю.А., Чумаков А.Н.: 1985, *Ж. прикл. спектроскопии*, **42**, 55.

Min'ko L.Ya., Chumakov A.N.: 1991, *Proceedings of the SPIE. Optical Radiation Interaction with Matter*, **1440**, 166.

Чивель Ю.А., Чумаков А.Н.: 1983, *Ж. прикл. спектроскопии*, **39**, 159.

Publ. Astron. Obs. Belgrade No. 61 (1998), 103 – 106 *Poster paper*

ABLATION OF TiN COATINGS BY TEA-CO_2 LASER BEAM

B.Gaković, M.Trtica, T.Nenadović, S.Petrović-Stepanović and N.Mijatović
The Institute of Nuclear Sciences "Vinča", P.O.B. 522, 11001 Belgrade, Yugoslavia

1. Introduction

Although the laser-beam interaction on thin films/coatings is used in many areas of technology, a better understanding of interaction kinetic is required. The surface features during the interaction processes depend on the beam characteristics but also on the physical and thermomechanical properties of target and the surrounding atmosphere of the bombarded target.

Laser sputtering causes rapid removal of surface material and many combine thermal and collisional effects. Process may be divided into laser induced ablation which presents high-yield sputtering process and laser induced desorption which include low-yield sputtering. The process of laser beam target interaction can be described in terms of heat model including few characteristic stages: absorption of the laser beam and transformation of its energy in radiative or non-radiative processes, heating of the target without damage, ejection of material from the interaction region, formation of the plume above the surface and finally rapid cooling when interaction occurs (Kelly et al. 1992).

In many application material processing relies on the heating effect due to the absorption of the beam energy which is characterized by photon energy, pulse duration and fluence F (J/cm^2). The amount of the absorbed energy depends on the optical and thermal characteristics of target. It increases with decreasing the wavelength ($E=hc/\lambda$). The reflectivity of the most metals in the optical range of wavelengths reaches 70-95% of incident radiation. At the wavelength 10.6 μm that corresponds to the TEA-CO_2 laser beam the reflectivity on polished metal can be higher (Rykalin et al. 1988)

The analyses of the laser beam induced changes allow us to determine the threshold damage on different coatings, the damage area induced by different shape of the laser pulses, and the mechanism of the interaction.

2. Experimental

In this work the laser induced surface modifications of thin film studies were carried out by pulsed, UV preionized, TEA carbon-dioxide laser. The laser operated with nontypical CO_2/X, X= N_2/H_2; H_2 gas mixtures. The presence of hydrogen in the laser makes that efficiency of the system greater in comparison when it has been absent. The laser gave multimode output of a pulse repetition of 1Hz. The beam cross-section was typically of quadratic form so that spatial-uniform distribution of intensity can be assumed. Output pulse was in the interval from 3 to 40 mJ for CO_2/H_2 gas mixture and FWHM = 80 ns.

The bombardment of coatings was performed with focused laser beam. The NaCl lens with focal length of 6.0 cm ensured the focusing on the target. Surface area of the laser spot of 0.0008 cm^2 was measured optically. The laser beam interacted with coating on zero incident angle.

The TiN layer (thickness = 0.85 μm) was deposited by reactive d.c. ion sputtering from a 99.98% titanium target, on polished austenitic stainless steel AISI 316 type (Gaković et al. 1998).

The coating characterization has been performed by X-ray diffraction analysis, wavelength dispersive - XRD and energy dispersive analysis – EDX. For morphology studies the SEM analyses has been employed. We used both, the secondary electron (SE) and backscattered electron (BSE) detectors.

3. Results and Discussion

XRD as well as EDAX analysis done before laser irradiation of TiN coatings have confirmed its polycrystalline structure and stoichiometric composition. The surface topography of TiN coatings was homogeneous relatively dense with spherical growth features on the surface. Analyses of the cross section have shown columnar crystal structure typical for low temperature zone, presented in a three zone model of structure. This have been expected since the deposition temperature (T = 473 K) was lower than 0.3 from the melting temperature of material (T_m = 3220 K). The grain sizes varied from few tens to one hundred nanometers.

Investigation of TiN coating morphological changes, induced by the laser radiation, has shown their dependence on laser fluence, number of pulses and laser pulse shape. In this work we present the results of 20 and 340 TEA CO_2 laser pulses interaction with TiN/AISI layer.

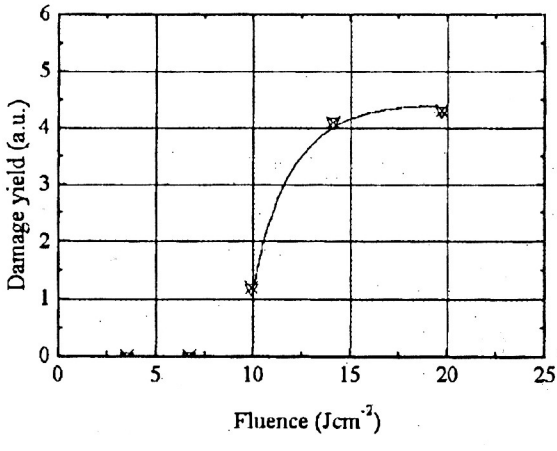

Fig. 1. Damages yield as a function of the fluence for twenty laser pulses.

Three types of interaction were obtained depending on the incident laser fluence. At the beginning target acted as a mirror for laser radiation (reflectivity 97%) and laser pulses were reflected without noticeable changes on the target surface. A damage threshold defined as the minimum fluence that creates a detectable damage on the surface. In this experiment the registered damage threshold was observed after twenty accumulated pulses The obtained value of 9.9 J/cm^2 is presented on Fig.1.

Finally the action of 340 laser pulses with fluences of 14 J/cm^2 and laser intensity I ≈170 MW/cm^2 leads to important changes in morphology of TiN coating, Figure 2. (a-c). During the laser action on the coating the three zones in damage area, can be distinguish.

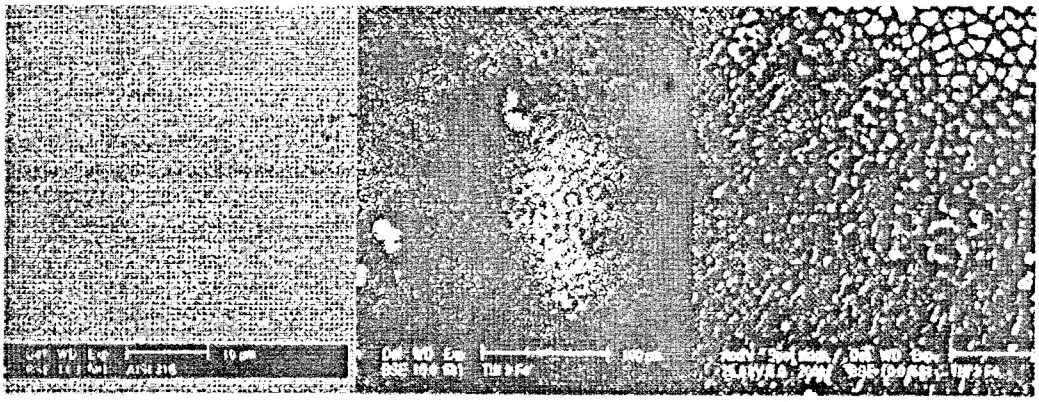

Fig. 2 (a-c). The morphology of TiN coating changes induced by 340 pulses of TEA CO_2 laser: a- as deposited coating surface, b- central part of the spot and c- rim of the spot periphery.

SEM analyses have shown that the target surface of this type of interaction shows signs of superficial melting. Heating in the zone of interaction must be the primary process of laser sputtering ablation (Nenadović et al. 1992).

Each shot after twenty pulses ignites a discharge in front of the target. The emitted particles above the target surface form a plume. The plume above the surfaces is always present after about twenty pulses. It increases up to 3-4 mm after about 100 pulses. The present of the plum suggests that there are also a thermal effects in sputtering (desorption and ablation) connected with induced surface morphology.

The X-ray analyses have shown that the composition of heated area differs from those of as deposited materials. The processes form an alloy layer of a specific composition. The analyses (EDAX) of the composition (^{w}/o) of the targets are presented on the Table 1. The obtained composition do not improve the cutting properties of laser bombarded coatings.

Table 1. The EDAX analyses of the targets.

	Ti	N	Fe	Cr	Ni	(Mo,Mn,Si)
substrate AISI 316	-	-	66.27	17.74	12.65	3.43
coating TiN on AISI 316	49.05	24.88	17.25	5.20	3.16	0.47
dark area in the bombarded zone	68.33	-	21.05	6.63	3.99	-
bright area in the bombarded zone	6.92	-	59.37	16.04	11.68	5.99

4. Conclusions

The interaction of the radiation of laser radiation of TiN coatings can be summarized as follows:

- Laser induced processes in central part of the spot cause the decomposition of the coatings and wave like structure in the interaction area. The distance between two following waves is about 10 μm, which corresponds to the wavelength of TEA CO_2 laser radiation.
- In the outer zones pulse shots produced thermally activated changes: material removal out of the interaction region and droplet formation. Solidified droplets melting of TiN are noticeable. Subsequently fast heating and cooling during multi-pulse laser bombardment cause the grain growth in the bombarded zone.

REFERENCES

Kelly R., Miotello A., Baren B., Gupta A. and Casey K., 1992, *Nuclear Instruments and Methods in Physical Research* B 65, 187.

Gaković B., Rakočević Z., Nenadović T., Peruško D, Trtica M, 1998, *Solid State Phenomena* Vols. 61-62, 357

Nenadović T., Mihać T., Rakočević Z., 1992, *Thin Solid Films* Vol. 218, 247.

Rycalyn N., Uglov A., Zuev I. Kokora A., Laser and Electron Beam Material Processing, Handbook, Mir Publisher Moscow, 1988.

Publ. Astron. Obs. Belgrade No. 61 (1998), 107 – 110 *Poster paper*

TANGENTIAL FLOW MIP SOURCE WITH DESOLVATION SYSTEM

S. JOVIĆEVIĆ, M.IVKOVIĆ,Z.PAVLOVIĆ, N. KONJEVIĆ
Institute of Physics, 11 080 Belgrade, P.O.Box 68, Yugoslavia
E-mail: konjevic@atom.phy.bg.ac.yu

Abstract. In this paper we present the description of a tangential flow microwave induced plasma source witch enables generation a temporally and spatially stable discharge, located in the center of the discharge tube. In such a configuration etching of the tube walls and thermal losses are greatly reduced. The desolvation systems which is also described enables enhancement of the detection limits of analytical species, whose spectral lines are overlapped by OH bands.

1. INTRODUCTION

After the introduction of the Beenakker (1976) cylindrical resonant cavity microwave-induced plasmas (MIP) has received considerable attention as an excitation source for atomic emission spectroscopy (see e.g. Q. Jin et al. 1997). This cavity, which operates at 2.45 GHz in the TM_{010} mode, make possible the generation of a plasma at atmospheric pressure in argon or helium. Further modification of this cavity by Van Dalen et all. (1978) enables more efficient excitations of various elements in aqueous solutions.

It was noticed that at input power above 50 W plasma moves to the wall of the tube. Same spatial distortion of the plasma is observed at higher support gas flow rates also. This characteristic of MIP has several detrimental effects. Plasma, which touches the inner wall of the discharge tube will etch the wall, and shortens the tube lifetime. Etching may also lead to analyte memory effects due to occlusion of salt particles at the etched surface. The plasma also has a tendency to wander about the inner wall of the discharge tube making difficulties to couple the plasma image to a monohromator. Therefore, it would be desirable to obtain a plasma discharge which is temporally and spatially steady and which do not lie along the discharge tube wall to reduce etching and thermal losses.

The introduction of aqueous solution of investigated samples results in a existence of very intense OH bands. Such a bands overlap low intensity spectral lines of analytical samples, and in this way reduce detection limits. For some elements this problem is so pronounced that analytical line detection is practically impossible. In such case it is desirable to remove water from sample gas before entering discharge vessel. The method for obtaining dry and spatially and temporally stable plasma is presented in this paper.

2. EXPERIMENT

We used commercially avaiable Van Dalen et all. (1978) modification of the Benakeers (1976) cylindrical resonant cavity (model HMW 25-471) supplied via coaxial cable by the 300 W, 2.45 GHz microwave generator GMW 24-302DR (both

produced by AHF analysentechnik, Tübingen,Germany). The resonant cavity with inner diameter 88 mm and depth 7.65 mm is made from silver electroplated brass. The microwave power is coupled into the cavity by the inner conductor of the coaxial cable, which ends like an antenna inside the cavity. Variable capacitive coupling is obtained by variation of distance between end of the antenna and opposite wall of the inner part of the cavity. This allows transformations of the plasma impedance to the impedance of the coaxial cable and getting an optimal matching of the load to the generator. Tuning of the cavity resonance frequency, is acheived by adjusting the radially mounted ceramic stub, in order to compensate dielectric effects induced by different plasma conditions.

Tangential flow torch In applied configuration spatial distortion is eliminated by using discharge tube similar to the tangential flow MIP torch reported by A. Bollo-Kamara (1985). This torch, constructed entirely from quartz, utilizes a concentric tube arrangement, with a thread insert to generate a tangential flow. The thread is fused to the inner and then sealed to the outer tube. We also use two concentric tubes, made from Al oxide, separated by the cooper wire (see Fig 1). These tubes (outer diameters 4 and 2mm) are fixed by stainless steel body and holding nut via graphite gasket. Windings of the cooper wire are the same as coils of a A.Bollo-Kamara (1981) threaded insert.

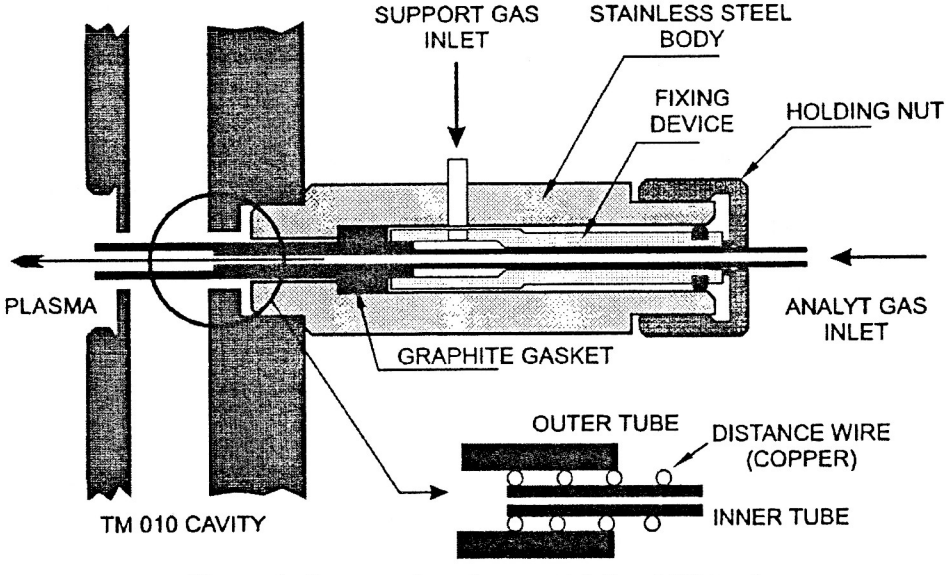

Figure 1. Cross section of tangential flow MIP torch

The optimal positioning of the Al oxide tubes are shown in Figure 1. Analyte sample gas goes through the inner tube while the plasma support gas is introduced through the outer sleeve and exit from the cooper wire windings with a spiral trajectory. In such a manner, by increasing the flow rate of support gas, discharge behaves as a rod like filament, suspended in the center of the discharge tube, extending the length of the cavity. Once this so called "suspended plasma" is formed the gas flow

rate can be decreased to the lower values. The obtained discharge is spatially and temporally stable and separated from tube walls.

Desolvation system This used desolvation system is similar to the one described by Veillon et all. (1968) see Figure 2. It consists of right angle pneumatic ICP nebulizer, spray chamber, evaporating chamber and modified Liebig-Graham condenser.

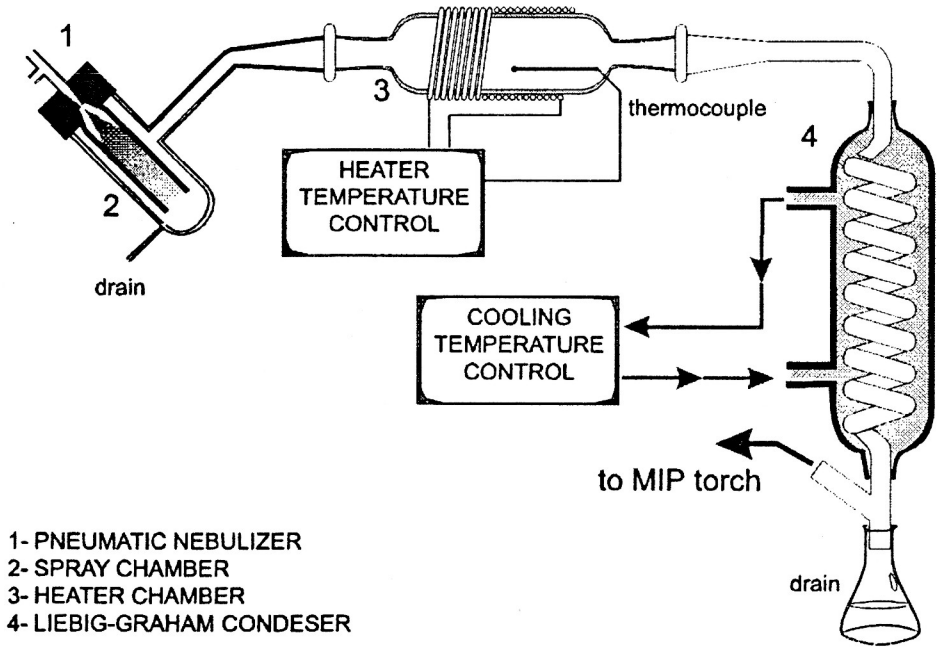

Figure 2. The desolvation system

For generation of aerosols from aqueous solution of analyzed samples we used Meinhard right angle pneumatic ICP nebulizer. Aerosols produced from this nebulizer have both extremely wide drop size ranges and very turbulent gas flow patterns [Browner et all.1984]. In order to reduce in this way generated random fluctuations of spectral line intensities dual tube Scott-type (1974) spray chamber was used [see Fig.2]. The purpose of the central tube is to separate the forward and reverse aerosol flows, the latter produced as a result of the low pressure in the region of high aerosol velocity. Evaporation of water was realized by the use of glass chamber heated to the temperature of 300 C and controlled by thermocouple and corresponding electronics. The water vapor is then condensed by Liebich Graham condenser cooled by water, which temperature is sustained at 3 C. Water droplets are accumulated in the drain and dry gas with analytic sample is lead to the discharge tube. This desolvation system removes water vapor from discharge, what is verified by lowering of the OH band spectra by two orders of magnitude (see Figure 3).

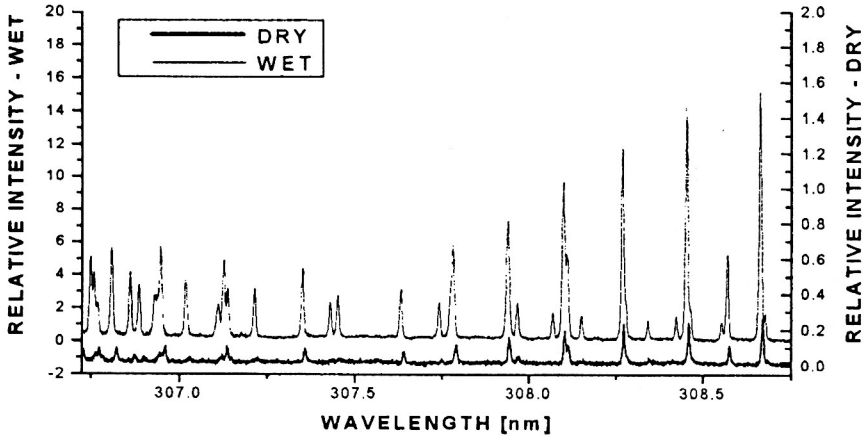

Figure 3. OH band spectra in wet and dry nebulizer gas

Surprisingly a little effects to the intensity of the analytical sample spectral linesis noticed. The drying of the nebulizer gas makes MIP discharge more stable and detection limits enhanced.

REFERENCE.

Beenakker C.I.M., 1976, *Spectrohimica Acta* 31B, 483
Bollo-Kamara A, Codding E.G., 1981, *Spectrohimica Acta* 36B, 973
Browner R.B., Boorn A.W., 1984, *Anal. Chem.* 56, 786
Jin Q, Duan Y, Olivares J.A. (1997), *Spectrohimica Acta* 52B, 131
Scott R.H., Fassel V.A, Kniseley R.N., Nixon D.A. 1974, *Anal.Chem,* 46, 75
Van Dalen J.P.J, de Lezenne Coulander P.A, de Galan L, 1978, *Spectrohimica Acta* 33B, 545
Veillon C, Margoshes M, 1968, *Spectrohimica Acta* 23B, 553

Publ. Astron. Obs. Belgrade No. 61 (1998), 111 – 114 *Poster paper*

ON THE USE OF RELATIVE LINE INTENSITIES OF FORBIDDEN AND ALLOWED COMPONENTS OF THE He I 447.1 nm LINE FOR ELECTRIC FIELD MEASUREMENTS

M. M. KURAICA, N. KONJEVIĆ, M. ĆUK and B. M. OBRADOVIĆ
Faculty of Physics, University of Belgrade, 11001 Belgrade, P.O.Box 368, Yugoslavia

1. INTRODUCTION

Recently we have reported measurements of electric field strength in the cathode fall region of an analytical glow discharge, determined from Stark splitting and shifting of three visible He I lines and their forbidden components (Kuraica *et al.*, 1997). In this paper, we present the results of an attempt to use relative line intensities of the He I 447.1 nm allowed line ($2p\ ^3P^0$ - $4d\ ^3D^0$) and its forbidden component ($2p\ ^3P^0$ – $4f\ ^3F^0$) for the measurement of electric field strength in the cathode fall region of the same analytical glow discharge (GD) in helium-hydrogen mixture. For determination of electric field strengths we calculated the He I relative line intensities following classical Foster's paper (Foster, 1927). An experimental testing of electric field measurements in helium-hydrogen mixture is performed using Stark spectroscopy of the hydrogen Balmer H_β line (Videnović *et al.*, 1996).

2. EXPERIMENT

The experimental setup is presented schematically in Fig.1. Our discharge source, a modified Grimm GD is laboratory made and described in detail elsewhere (Kuraica *et al.*, 1992, 1997). Here, for completeness, minimum details will be given. The hollow anode 30 mm long with inner and outer diameters 8.00 mm and 13 mm, has a longitudinal slot (15 mm long and 1 mm wide) for side-on observations along the discharge axis. The water cooled cathode holder has an exchangeable iron electrode, 18 mm long and 7.60 mm in diameter, which screws tightly into its holder to ensure good cooling. A gas flow of about 300 cm^3/min of helium-hydrogen mixture (95% He : 5% H_2) is sustained at a pressure of 200 Pa by means of needle valve and a two-stage mechanical vacuum pump. To run the discharge a 0-2 kV, 0-100 mA current stabilized power suply is used. A ballast resistor of 10 kΩ is placed in series with the discharge and the power supply.

After polarization with a Glan-Thomson prism or a plastic polarizer, the radiation from the discharge source is focused with unity magnification (8 cm focal length achromat lens) onto the entrance slit of the scanning monochromator-photomuliplier system, see Fig.1. For electric field intensity axial distribution measurements, the discharge tube is translated in ≈0.1 mm steps by a stepping motor, so that the discharge image obtained through the observation slot is translated in the plane of the entrance slit (30 μm) of the monochromator. For the spectral recordings, 4 m Hilger and Watts Ebert type spectrometer with inverse dispersion of 0.242 nm/mm is used. All spectra are recorded with 30 μm entrance and exit slits, giving a Gaussian instrumental profile with 0.022 nm half-width. The monochromator is equipped with a stepping motor which enables minimum wavelength change in steps of 0.0028 nm. For radiation detection, a photomultiplier with Peltier cooling is used. A lock-in signal amplification technique is employed. The entire experiment is controlled by a PC. The same computer is used for data acquisition and analysis.

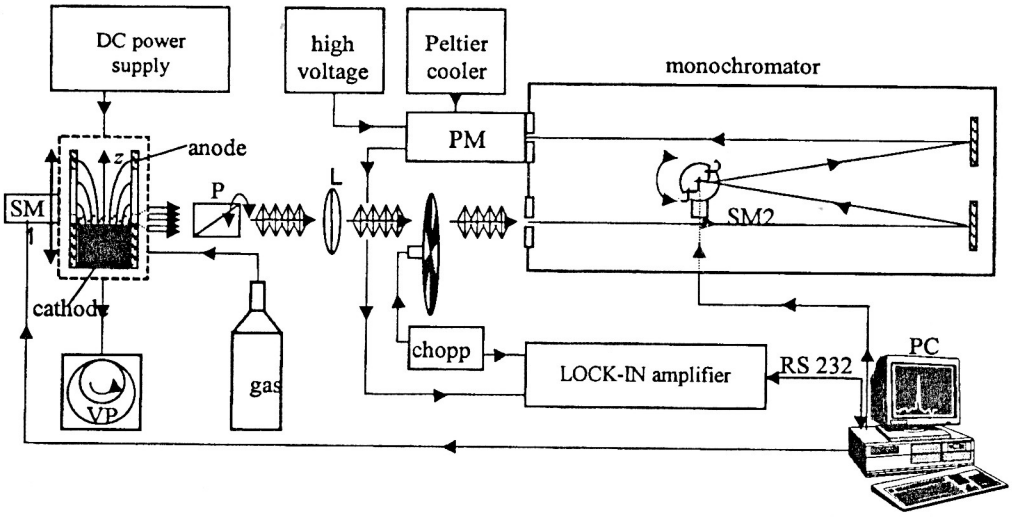

Fig. 1. Schematic diagram of the central part of Grimm GDS and experimental setup for side-on observations. Symbols: VP - vacuum pump, SM 1 and SM 2 - stepping motors; P - polarizer; L - lens; PM - photomultiplier.

3. RESULTS AND DISCUSSION

As an illustration of the influence of electric field strength on the He I 447.1 nm allowed line and its forbidden component intensities, typical π-polarized spectra recorded in the cathode fall region of our GD, at electric field strength 12.1 kV/cm, is given in Fig.2. Both, allowed and forbidden lines marked in this figure contain two π-components which cannot be resolved in our experimental conditions, see Fig.2. The third feature, marked with *ff* in Fig.2, originates from the discharge protruding through the longitudinal observation slot into the field free space (Kuraica *et al.*, 1997). Therefore, in order to estimate the total intensity of unresolved two π-components of allowed line, it is necessary to subtract the radiation intensity of the *ff* feature from the overall profile. This is done by fitting the experimental data with two independent Gaussian profiles. Than, from the whole fit, the area of the *ff* profile is subtracted. The results of forbidden-to-allowed He I π-profile intensity ratios, measured along the cathode fall region of our GD (at various electric field strengths, determined from H_β line shapes at same positions, see Kuraica *et al.*, 1997), are given in Fig.3. The solid line in Fig.3. represents our calculation of theoretical intensity ratios for this line following Foster (1927).

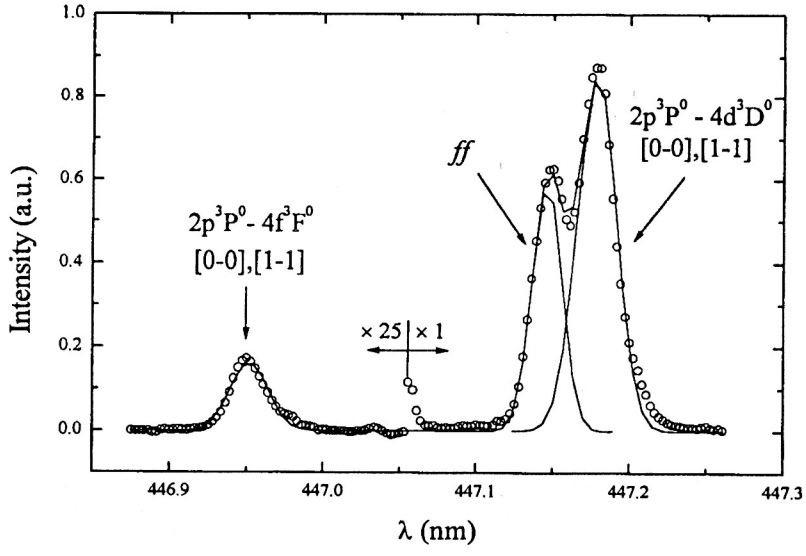

Fig.2. Typical π-polarized spectra recording of the He I 447.1 nm allowed line and its forbidden component at electric field strength of 12.1 kV/cm in the cathode fall region.

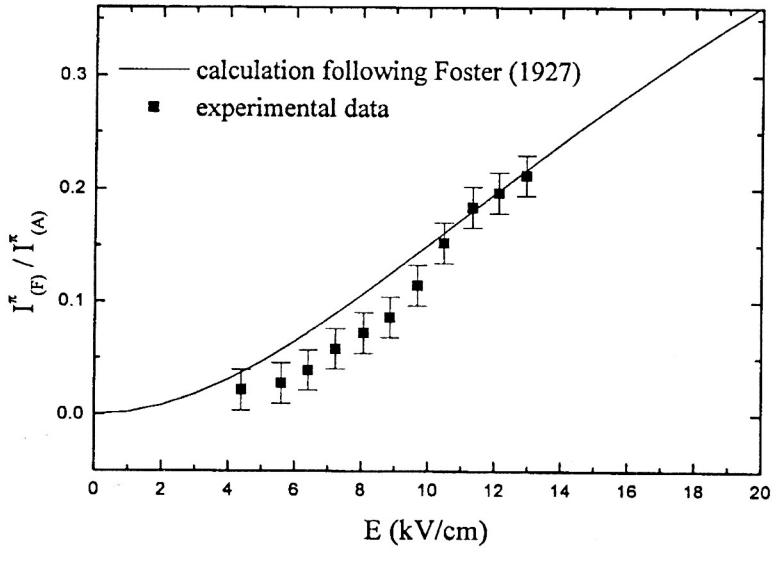

Fig.3. Comparison of experimental and theoretical intensity ratios of π-components of the He I 447.1 nm allowed and its forbidden line.

Electric field strength is determined from the H_β line shapes at same positions (Videnović *et al.*, 1996). From the comparison of our experimental and theoretical data in Fig.3, one may conclude that, in spite of some difficulties like e.g. deviation from theoretical predictions at low electric field strengths, intensity ratios of the π-components of forbidden and allowed He I 447.1 nm line may be used for electric field measurements. At low electric fields, the partial overlapping of the the *ff* feature with allowed line makes the substraction of the *ff* line impossible, which results in increasing the allowed line total intensity. Consequently, the intensity ratio shows systematical decrease at low electric fields.

REFERENCES

Foster J.S., 1927, *Proc. Roy. Soc. London Ser. A* **117,** 137.
Kuraica M, Konjević N., Platiša M. and Pantelić D., 1992, *Spectrochim. Acta B* **47,** 1173.
Kuraica M.M. and Konjević N.,1997, *Appl. Phys. Lett.* **70,** 1521.
Kuraica M.M., Konjević N. and Videnović I.R., 1997, *Spectrochim. Acta B* **52,** 745.
Videnović I.R., Konjević N. and Kuraica M.M.,1996, *Spectrochim. Acta B* **51,** 1707.

Publ. Astron. Obs. Belgrade No. 61 (1998), 115 – 117 *Poster paper*

ON THE 455.254 nm N II SPECTRAL LINE STARK WIDTH. PRESENT STATUS

V. MILOSAVLJEVIĆ and S. DJENIŽE
Faculty of Physics, University of Belgrade
P.O.B. 368, 11001 Belgrade, Serbia, Yugoslavia

1. INTRODUCTION

Existence of the singly ionized nitrogen (N II) spectral lines in a great number of various star spectra make them interesting for diagnostic purposes. A number of the papers (Day and Griem 1965; Berg *et al.* 1967; Jalufka and Craig 1970; Purcell and Barnard 1984; Pittman and Konjević 1986) deals with the Stark width measurements of the 455.254 nm N II spectral line that belong to 3d-4f transition (multiplet No. 58). The existing experimental values lie between 18 000 K and 36 000 K electron temperature and show mutually scatter up to the factor 5. No theoretical Stark FWHM (full-width at half intensity maximum, w) calculations exist for this transition, to the knowledge of the authors (Fuhr and Lesage 1993, and references therein).

The aim of this work is to extend the knowledge of the Stark FWHM of the 455.254 nm spectral line up to 54 000 K electron temperature.

2. EXPERIMENT

The modified version of the linear low pressure pulsed arc (Djeniže *et al.* 1990; Djeniže *et al.* 1998; Milosavljević and Djeniže 1998) has been used as a plasma source. A pulsed discharges driven in a quartz discharge tube of 5 mm inner diameter and has 6.2 cm effective plasma length. The tube has end-on quartz windows. On the opposite side of the electrodes (Fig. 1 in Djeniže *et al.* 1998) the glass tube was expanded in order to reduce erosion of the glass wall and also sputtering of the electrode material onto the quartz windows. The working gas was nitrogen and oxygen mixture (83% N_2 + 17% O_2) at 70 Pa filling pressure in flowing regime. Spectroscopic observation of isolated spectral line was made end-on along the axis of the discharge tube. A capacitor of 14 μF was charged up to 3.0 kV. The line profile was recorded by a shot-by-shot technique following the procedure described earlier (Djeniže *et al.* 1990). The photomultiplier signal was digitized using oscilloscope, interfaced to a computer. A standard deconvolution procedure (Davies and Vaughan 1963) was used. The deconvolution procedure was computerized using the least square algorithm. The Stark width was measured with ±15% error. The plasma parameters were determined

using standard diagnostics methods. The electron temperature was determined from the ratios of the relative intensities of the 348.49 nm NIV to 393.85 nm N III and the previous N III to 399.50 nm N II spectral line, assuming the existence of LTE, with an estimated of ±12% error. All the necessary atomic parameters were taken from Wiese *et al.* (1966). The electron density decay was measured using a well-know single wavelength He-Ne laser interferometer for the 632.8 nm transition with an estimated error of ±7%.

3. RESULT AND DISCUSSION

The observed Stark FWHM of the 455.254 nm N II spectral line is 0.256 nm ±15% at T= 54 000 K electron temperature and $N = 2.8 \times 10^{23}$ m^{-3} electron density. Experimental Stark FWHM (taken from various papers and our measured value) dependence on the electron temperature, at electron density of $N = 1 \times 10^{23}$ m^{-3}, is presented graphically in Fig. 1.

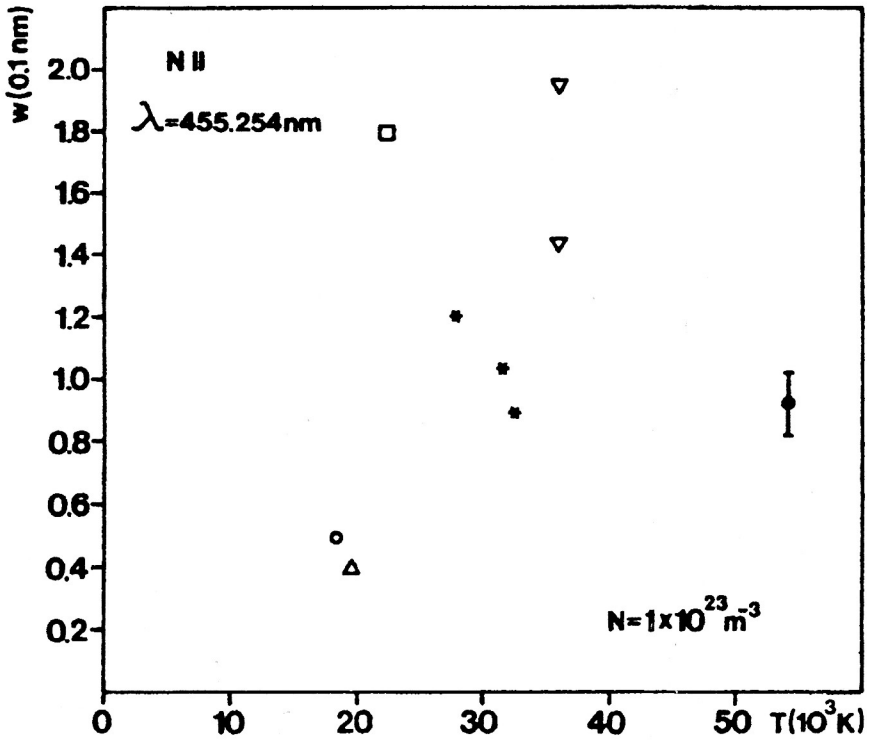

Fig. 1. Measured Stark FWHM vs electron temperature: Δ, Day and Griem (1965); □, Berg *et al.* (1967); ○, Jalufka and Craig (1970); ∇, Purcell and Barnard (1984); ∗, Pittman and Konjević (1986); •, this work. The error bar includes the width and electron density uncertainties.

It is evident that the existing experimental results show mutually scatter. Berg *et al.* (1967) and Purcell and Barnard (1984) have measured the highest Stark FWHM values in comparison to the results of other authors. Our new Stark FWHM value at 54 000 K electron temperature follows the trend estimated by the results of Pittman and Konjević (1986). Results from Day and Griem (1965) and Jaulfka and Craig (1970), at about 20 000 K electron temperature, lie under other experimental data. Theoretical calculations of the Stark FWHM value of the 455.254 nm N II spectral line would be helpful.

Acknowledgements

This research is a part of the project "Plasma Spectroscopy" supported by Ministry of Science and Technology of the Republic of Serbia.

References

Berg, H.F., Ervens, W., Furch, B.: 1967, *Z. Phys.* **206**, 309.
Davies, J.T., Vaughan, J.M.: 1963, *Astrophys. J.*, **137**, 1302.
Day, R.A., Griem, H.R.: 1965, *Phys. Rev.* **140**, A1129.
Djeniže, S., Srećković, A., Platiša, M., Konjević, R., Labat, J., Purić, J.: 1990, *Phys. Rev.* A **42**, 2379.
Djeniže, S, Milosavljević, V., Srećković, A.: 1998, *JQSRT*, **59**, 71.
Fuhr, J.R., Lesage, A.: 1993, Bibliography on Atomic Line Shapes and Shifts, (July 1978 through March 1992) NIST Special Publication 366 Supplement 4 US DC National Institute of Standards and Technology.
Jalufka, N.W., Craig, J.P.: 1970, *Phys. Rev.* A **1**, 221.
Milosavljević, V., Djeniže, S.: 1998, *Astron. Astrophys. Suppl. Series*, **128**, 197.
Pittman, T.L., Konjević, N.: 1986, *JQSRT*, **36**, 289.
Purcell, S.T., Barnard, A.J.: 1984, *JQSRT*, **32**, 205.
Wiese, W.L., Smith, M.W., Glennon, B.M.: 1966, "Atomic Transitition Probabilities" NSRDS NBS 4 Vol.1 (Washington, DC:US Govt Printing Offices).

Publ. Astron. Obs. Belgrade No. 61 (1998), 118 – 122 *Poster paper*

ON THE IONIZING SOURCES IN SPIRAL GALAXIES: II. THE CENTER OF THE MILKY WAY

V. MILOŠEVIĆ–ZDJELAR[1], S. SAMUROVIĆ[1] and M.M. ĆIRKOVIĆ[2,3]

[1]*Public Obs., Gornji Grad 16, Kalemegdan, 11000 Belgrade, Yugoslavia*
E–mail vesnamz@afrodita.rcub.bg.ac.yu
E–mail srdjanss@afrodita.rcub.bg.ac.yu

[2]*SUNY at Stony Brook, Stony Brook, NY 11794-3800, USA*
[3]*Astronomical Observatory, Volgina 7, 11160 Belgrade 74, Yugoslavia*
E–mail cirkovic@sbast3.ess.sunysb.edu

1. INTRODUCTION

The overall shape of our galaxy, Milky Way, has mainly been revealed – it is classified as a SAB(rs) type galaxy with a bar (Kuijken 1996, and references therein; Gyuk 1996), weak rings and a four arms spiral structure (Valée 1995).

A model for the rotation curves of spiral galaxies by Sofue (Sofue 1996), could be applied to the Milky Way introducing:

- nuclear mass component (scale radius $r \sim 100 - 150$ pc, mass $M \sim 3 - 5 \times 10^9$ $M_\odot$),
- central bulge ($r \sim 0.5 - 1$ kpc, $M \sim 10^{10}$ $M_\odot$),
- disk ($r \sim 5 - 7$ kpc, thickness ~ 0.5 kpc , and $M \sim 1 - 2 \times 10^{11}$ $M_\odot$),
- massive halo ($r \sim 15 - 20$ kpc, $M \sim 2 - 3 \times 10^{11}$ $M_\odot$).

The fifth component could be added (Sofue 1996) for the Milky Way – the very nucleus ($r \sim 30$ pc, $M \sim 10^7 M_\odot$) with a "dark" mass at a dynamical center of the Galaxy ($r \leq 0.01$ pc, $M \simeq 2.6 \times 10^6 M_\odot$).

The distribution and influence of different ionizing sources throughout the Galaxy (even some local like the great Gum Nebula) could be described by the Taylor-Cordes model (TC93) (Taylor and Cordes 1993), with Galactic center (GC) component added (Lazio and Cordes 1998, hereafter LC98), using a number density of free electrons in the interstellar medium as a parameter of ionization. In this contribution we discuss the fifth (GC) component that becomes dominant from the galactocentric distance of 0.5 kpc towards the GC.

The opened question remains whether the "dark mass" in GC is directly responsible for the high ionization of that region, or only indirectly through the accretion disk, if it is a supermassive black hole (BH).

2. THE CENTER OF THE MILKY WAY

The complete activity of the GC region has been studied for almost two decades now, and numerous nonthermal and thermal sources have been revealed. All of them contribute to the total electron density of the last component in the equation that represents the overall estimate of electron density (n_e) distribution (TC93, LC98):

$$n_e(x,y,z) = n_1 g_1(r)\mathrm{sech}^2(z/h_1) + n_2 g_2(r)\mathrm{sech}^2(z/h_2) +$$
$$+ n_a \mathrm{sech}^2(z/h_a) \sum_{j=1}^{4} f_j g_a(r, s_j) + n_G g_G(u) + n_{GC} g_{GC}(r) h_{GC}(z) \qquad (1)$$

where r is the Galactocentric distance projected onto the plane and is equal $r = (x^2 + y^2)^{1/2}$, the sum goes over four spiral arms, n_i, $i = 1 \ldots 5$ denotes the density in different regions, f_i, $i = 1 \ldots 4$ are scale factors, g_i, $i = 1 \ldots 5$ are functions of position, h_i, $i = 1 \ldots 4$ are scale heights and z is the height above the galactic plane. The detailed description of each component is given in TC93 and LC98.

The GC component has a following shape:

$$n_{GC} g_{GC}(r) h_{GC}(z) = (10\ \mathrm{cm}^{-3}) \times e^{-\left(\frac{r}{0.15}\right)^2} \times e^{-\left(\frac{z}{0.075}\right)^2} \qquad (2)$$

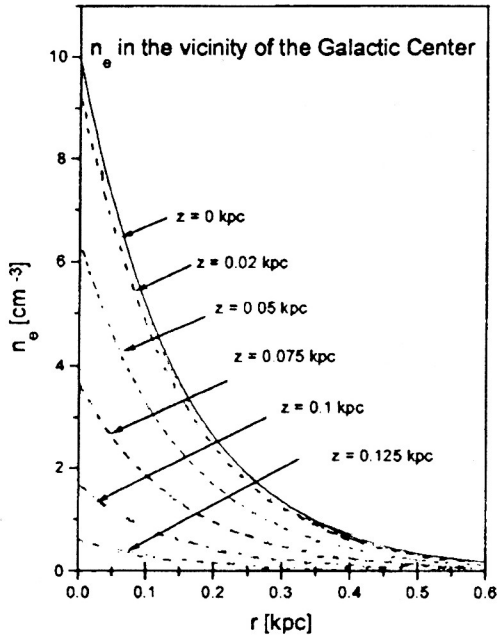

Fig. 1. Dependence of electron density n_e as a function of Galactocentric radius r in the vicinity of the GC (up to $\sim$ 500 pc) for different heights above the galactic plane – z, according to LC98.

The overall contribution of the GC component to the total electron density n_e of the Galaxy, according to eq. (2), is shown in Fig. 1. The problem of the ionization throughout a spiral galaxy is briefly discussed in Samurović, Ćirković, Milošević-Zdjelar and Petrović (1998) (Paper I).

Electron densities as functions of r are presented in TC93 (in their Fig. 3).

Local contributions from the GC area come from a complex set of sources. At a dynamical center of the Milky Way lies a nonthermal synchrotron radio-source SgrA*, of yet unrevealed nature, surrounded with thermal orbiting plasma SgrA West (within a Central Cavity, $r \sim 1$ pc), which is ionized by IRS 16, a cluster of hot HeI/HI (spectral type O) stars in the vicinity of GC ($r \sim 0.6$ pc) (Zylka *et al.*, 1995). Cavities like this one are usual features around stellar associations which blow out surrounding interstellar matter by stellar winds, leaving hot rarefied gas cavity surrounded with envelope of neutral and ionized gas (Bochkarev and Ryabov 1997). In our case the envelope is a Circum-Nuclear Disc beginning at the outer edge of SgrA West (the Arc) at ($r \sim 1.7$ pc) and extending as far as 12 pc. SgrA West complex consists of a three arm minispiral and an extended ionized component, and contributes with $n_e \sim 10^4$ cm^{-3} (minispiral) and 10^3 cm^{-3} (extended component) (Beckert *et al.*, 1996).

Some other local features of the smaller scale, like the Bullet (Yusef-Zadeh et al 1998), and the Sickle (Yusef-Zadeh *et al.*, 1997b), contribute the $n_e \sim 10^4$ cm^{-3} and 10^2 cm^{-3}, respectively.

Another contribution of $n_e \sim 6$ cm^{-3} (Koyama *et al.*, 1996) comes from a probable supernova remnant SgrA East located 30 pc behind the GC. It is heated by a cluster of hot O stars behind SgrA West (Sofue 1993). There have been some attempts to describe its unusual feature, more energetic than supernova, as a Seyfert-like activity like in the nuclei of some other spiral galaxies (LaRosa and Kassim 1985). SgrA East is physically interacting with a "50 km s^{-1} molecular cloud" forming new stars in the areas of collision, and is considered to be the source of the high energy activity of the GC (Yusef-Zadeh 1997a). The GC region ($r \sim$ few hundred pc) is responsible for 10% of the total star forming rate of the entire Galaxy (Sofue 1993).

The contribution of SgrA complex to the total electron density is $n_e \sim 6$ cm^{-3}, and it drops outside of that area to 0.3-0.4 cm^{-3}.

One of the largest luminous HII plasma/molecular region in the GC vicinity is SgrB2 at a distance of 100 pc from GC. It consists of several active star forming regions with numerous associated dense HII regions (Gordon *et al.*, 1993). Besides SgrB2, within the Nuclear Disc ($r \sim 200$ pc, thickness 50 pc), there are several other HII (SgrC, D, and E), and star forming regions.

ASCA observations detected strong Kα lines from highly ionized various elements, and showed presence of high temperature plasma over the GC region (Koyama *et al.*, 1996).

On the large scale, hot plasma is distributed symmetrically along the galactic plane with a strong concentration at the GC. X-ray spectra obtained from ASCA showed high energy (10 keV) spectra of the similar shape over the emission region (Koyama *et al.*, 1996). Their results show that energy generation rate resembles the rates at the active galactic (Seyfert-like) nuclei, having a large mass concentration at the GC.

Weaker thermal emission is detected extending 80 pc along the Galactic plane on both sides of GC. Vertical to the Galactic plane, various thermal arched filaments extending more than 100 pc, are detected along magnetic field, having turbulent motion, preferably towards the GC. Similar vertical structures exist in other galaxies (Sofue 1993).

3. THE NATURE OF SgrA^*

Motions of the ionized gas can not reveal characteristics of the central object as the stars can, because the gas is influenced by the magnetic field. Also, high temperature plasma can not be bound by the galactic gravity.

By proper motions of the stars within central 0.01 pc one can draw conclusions about the mass and nature of the central object (Yusef-Zadeh 1998). The most recent research (Eckart and Genzel 1997) finds the value of stellar proper motion greater than 1000 km s^{-1} and undoubtedly estimates the central mass: 2.6 $\times 10^6$ $M_\odot$.

Different models could be applied to the SgrA^* – a central "dark mass". If we consider a black hole model, we have to examine all the problems related to such an object. Radio-emission detected from GC due to cyclo-synchrotron and synchrotron radiation is consistent with a theoretical prediction of an accreting disk around a 10^6 $M_\odot$ BH (Bower and Backer 1998). There are few models successfully applicable to it:

- advection dominated accretion (Narayan *et al.*, 1995, Lasota 1998)
- spherical accretion (Melia 1994).

The crucial problem related to the BH model is low X and γ-ray flux detected from SgrA^*. The strongest source in the vicinity of GC is 1E 1740.7-1942, hard X-ray source, and a strong source of annihilation 511 keV line (e.g. Wehrse *et al.*, 1996), but it is not coinciding with SgrA^* (it is situated in a dense molecular cloud 50' away from GC). It shows all the features (similar shape and luminosity) as CygX-1, another BH in a Milky Way.

There have recently been some quite different approaches to the "blackness" of the SgrA^*. We briefly mention here the recent proposal that SgrA^* is a neutrino ball, i.e. there is no BH – instead there is a ball made of self- gravitating, degenerate neutrinos with the same total mass of 2.5×10^6 $M_\odot$ (Tsiklauri and[B Viollier 1998a,b). These neutrinos have masses $m_\nu \geq 12$ keV/c^2 (for $g = 2$) and $m_\nu \geq 14.3$ keV/c^2 (for $g = 1$), where g is the spin degeneracy factor. These neutrinos are, according to cosmological constraints, decaying thus producing X-ray emission lines. Another way to distinguish the existence of the neutrino ball is to examine in detail the trajectory of stars in the vicinity of the GC. If there is the BH the trajectory will be an ellipse with the BH at the focus, while in the case of the neutrino ball the center of the ellipse will be the center of the ball.

References

Beckert, T., Duschl, W.J., Mezger, P.J. and Zylka, R.: 1996, *Astron. Astrophys.*, **307**, 450.
Bochkarev, N. and Ryabov, M.: 1997 *Astrophys. Space Sci.* **252**, 309.
Bower, G.C. and Backer, D.C.: 1998, *Astrophys. J.* **496**, 97.

Eckart, A. and Genzel, R.: 1997, *MNRAS*, **284**, 576.
Gordon, M.A., Berkermann, U., Mezger, P.J., Zylka, R., Haslam, C.G.T., Kreysa, E., Sievers, A. and Lemke, R.: 1993, *Astron. Astrophys.*, **280**, 208.
Gyuk, G.: 1996, preprint astro-ph/9607134.
Koyama, K., Maeda, Y., Sonobe, T., Takeshima, T., Tanaka, Y., Yamauchi, S.: 1996, *PASJ*, **48**, 249.
Kuijken, K.: 1996, in *IAU Coll. 157*, eds. R. Buta, D.A. Crocker, B.G. Elmegreen, ASP, San Francisco, 504.
LaRosa, T., N., Kassim, N., E.: 1985, *Astrophys. J.*, **299**, L13.
Lasota, J.-P.: 1998, *Phys. Rep.* (to be published), preprint astro-ph/9806064.
Lazio, T.J.W. and Cordes, J.M.: 1998 *Astrophys. J.*, **497**, 238 (LC98).
Melia, F.: 1994, *Astrophys. J.*, **426**, 577.
Samurović, S., Ćirković, M.M., Milošević-Zdjelar, V. and Petrović, J.: 1998, *Proceedings of 19th Symposium of the Physics of the Ionized Gases*, submitted (Paper I).
Sofue, Y.: 1993, NATO adv. school "The Nuclei of Normal Galaxies: Lessons from the Galactic Center", Ringberg Schloss Tegernsee, preprint astro-ph/9309046.
Sofue, Y.: 1996, *Astrophys. J.*, **458**, 120.
Taylor, J.H. and Cordes J.M.: 1993 *Astrophys. J.* **411**, 674 (TC93).
Tsiklauri, D. and Viollier, R.D.: 1998a, *Astrophys. J.*, submitted (preprint astro-ph/9805272).
Tsiklauri, D. and Viollier, R.D.: 1998b, *Astrophys. J.*, **500**, 591 (preprint astro-ph/9805273).
Valée, J.P.: 1995, *Astrophys. J.* **454**, 119.
Wehrse, R., Duschl, W. J., Hof M., and Tscharnuter, W. M.: 1996, *Astron. Astrophys.*, **313**, 457.
Yusef-Zadeh, F., Purcell W. and Gotthelf, E.: 1997a, *IAUS* **184**, 196.
Yusef-Zadeh, F., Roberts, D.A. and Wardle, M.: 1997b, *Astrophys. J.* **490**, 83.
Yusef-Zadeh, F., Roberts, D.A. and Biretta, J.: 1998, *Astrophys. J.*, **499**, 159.
Zylka, R., Mezger P.G., Ward-Thompson, D., Duschl, W.J. and Lesch, H.: 1995, *Astron. Astrophys.*, **297**, 83.

Publ. Astron. Obs. Belgrade No. 61 (1998), 123 – 126 *Contributed paper*

Явления на поверхности и их влияние на процессы приповерхностного низкопорогового плазмообразования при импульсном высокоэнергетическом лазерном воздействии

Минько Л.Я., Чивель Ю.А.
Институт Молекулярной и Атомной Физики НАН Беларуси
220072, Беларусь, г.Минск, пр.Ф.Скарины 70

Аннотация Экспериментально изучено изменение состояния поверхности в процессе воздействия импульсного лазерного излучения и влияние возникающих поверхностных структур на процессы приповерхностного плазмообразования.

1. Введение

К настоящему времени установлена и подтверждена эрозионная природа начального плазмообразования у поверхности твердых тел при импульсном лазерном воздействии (см. например Гречихин Л.И., Минько Л.Я., 1967; Брунов В.В. и др., 1986; Минько Л.Я. и др., 1988). Пороговые параметры приповерхностного плазмообразования существенно зависят от длительности, длины волны, интенсивности воздействующего ЛИ и условий воздействия.

В данной работе предоставлены результаты исследований пороговых зависимостей плазмообразования и влияния состояния поверхности на процессы начального разрушения поверхности и плазмообразования в широком диапазоне длин волн и длительностей импульсов воздействующего ЛИ.

2. Эксперимент

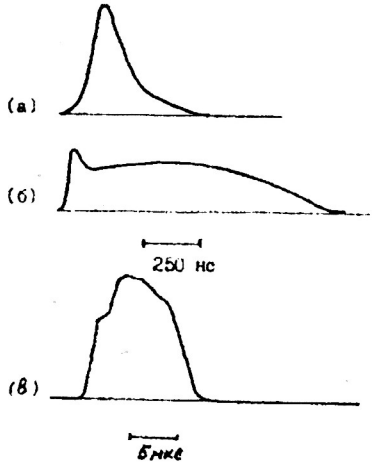

Рис.1. Формы импульсов лазерного излучения а - Nd лазера, б - CO_2-лазера, в - родаминового лазера.

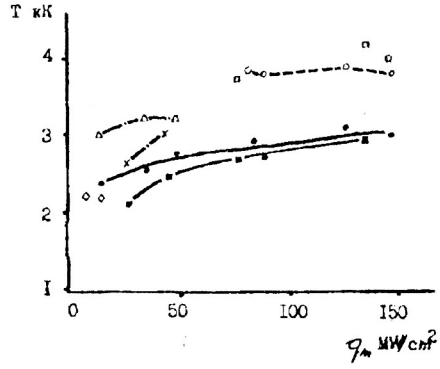

Рис.2. Зависимость температуры поверхности в пятне облучения в момент начала разрушения (● - Д16Т, ■ -Zn, ▲ - Bi), температуры поверхности в момент плазмообразования (○ - Д16Т, □ - Zn) от максимальной плотности мощности ЛИ.

Эксперименты были выполнены при атмосферном давлении и в вакууме с использованием лазерной системы на неодимовом стекле, генерирующей моноимпульсы длительностью ~40нс и 300нс (рис. 1). Ряд экспериментов выполнен на электроионизационном CO_2-лазере с длительностью импульса ~1мкс и родаминовом лазере с длительностью импульса ~10мкс (рис. 1).

В качестве мишеней использовались механически полированные образцы из алюминия А99, дюралюминия Д16Т, цинка, висмута, индия. Контроль состояния поверхности в процессе воздействия и определение пороговых характеристик плазмообразования осуществлялось посредством измерения динамических характеристик зеркальной, диффузной, рассеянной компонент отраженного ЛИ, температуры поверхности и давления на поверхности в пятне облучения с временным разрешением ~10^{-8}с. Использовались датчики давления в режиме "генератора тока". Калибровка датчиков давления осуществлялась с помощью лазерной ударной трубки. Состояние поверхности до и после воздействия изучалось методами оптической и растровой электронной микроскопии, проводился рентгеноструктурный анализ поверхностного слоя материалов.

3. Результаты и обсуждение

Исследования морфологии и распределения дефектов на поверхности механически полированных образцов показали, что основная масса дефектов с характерным размером ~0,5÷1мкм и концентрацией ~$10^6 \div 10^7$см$^{-2}$ это царапины, оставленные зернами абразива и частицы абразива (Al_2O_3) внедренные в поверхность. Плотность дефектов достаточно высока и можно предположить, что высота неровностей рельефа также ~1мкм при периоде 1-10мкм. Проведенные комплексные эксперименты позволили выявить особенности начального разрушения поверхности. Показано, что локальность повреждений в области пятна облучения в испарительных режимах в большей степени определяется неравномерностью облучения, нежели распределением дефектов, что можно было предполагать, имея ввиду высокую их концентрацию. Установлено, что независимо от длительности лазерных импульсов ($\tau_{1/2}$=40-300нс, λ=1,06мкм) в процессе воздействия, до момента плазмообразования яркостная температура поверхности достигает значений 3000°-4000°К (рис.2). Нарастание заметного поглощения в парах начинается при этом уровне температур. Переход паров из состояния практически полной прозрачности в сильнопоглощающую плазму в зависимости от крутизны фронта импульса ЛИ происходит за времена ~10^{-8}с (τ=40нс) и ~10^{-7}с (τ=300нс). На развитие плазмообразования в парах существенное влияние оказывает боковая волна разрежения. При переходе от квазиодномерного к трехмерному разлету паров, а это наблюдается при пятнах облучения $\leq$0,2мм($\tau_и$~300нс) происходит увеличение времени задержки плазмообразования (Ефремов В.В. и др., 1988) и пороговых для плазмообразования плотностей мощности ЛИ (рис.3).

Ранее (L.Ya. Min'ko, Yu.A. Chivel, 1993) нами установлено "взрывное" разрушение поверхности металлов за времена ~10^{-8}с с выбросом частиц конденсированной дисперсной фазы и появлением на поверхности микроструктур размером 1-10мкм с термоизолированными фрагментами размером ≤1мкм. Для ряда металлов разрушение имеет место при температурах поверхности ниже точки кипения в области температур ≥2000°К (рис. 2). Показано, что такое низкопороговое разрушение обусловлено объемной неоднородностью твердого тела. Пороги плазмообразования в этих условиях определяются уже не только начальным состоянием поверхности, но и возникшей поверхностной структурой с характерной для металлов плотностью ~10^6см$^{-2}$.

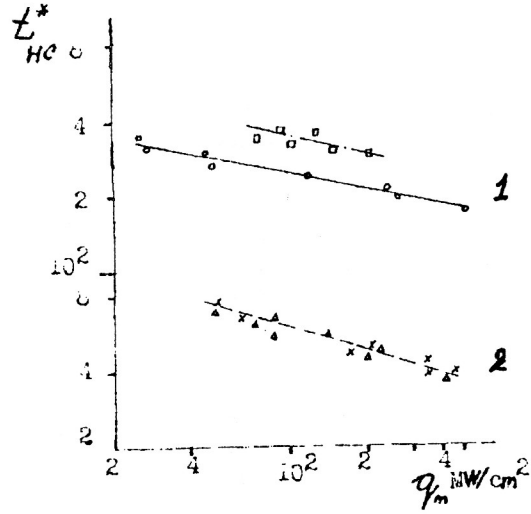

Рис.3. Время начального плазмообразования на дюралюминиевой мишени в воздухе в зависимости от максимальной плотности мощности ЛИ (1,06мкм):
1. $\tau_и$=300нс
   - ○ - диаметр пятна облучения - 4мм
   - □ - диаметр пятна облучения - 0,25мм
2. $\tau_и$=40нс:
   - △ - диаметр пятна - 4мм
   - x - диаметр пятна - 0,25мм

При воздействии ЛИ микрочастица или теплоизолированный дефект на поверхности существенно повлияет на плазмообразование в том случае, если их нагрев и испарение протекают быстрее основы металла. Согласно экспериментальным данным, размеры выбрасываемых частиц < 1мкм. Расчеты времени нагрева частиц до $T_{кип}$, времени ее испарения с учетом высокой поглощательной способности частиц размером $\lambda>d>\lambda/6$ (λ=1,06мкм) при интенсивностях ЛИ в диапазоне пороговых для плазмообразования значений ~10^8 Вт/см^2 ($\tau_и$=40нс; λ=1,06мкм) и ~10^7 Вт/см^2 ($\tau_и$=300нс; λ=1,06мкм) показали, что испарение произойдет за времена соответственно ~10^{-8}с и ~10^{-7}с, на переднем фронте импульса ЛИ, что хорошо согласуется с экспериментом. На локальный характер испарения указывают и результаты измерений давления в испарительных режимах воздействия излучения Nd-лазера с $\tau_и$ = 40 нс. Измеренные значения амплитуды импульсного давления в пятне облучения значительно меньше значений полученных из предположения о равновесном характере фазового перехода в пределах пятна облучения.

Перекрытие отдельных облачков пара, возникших на микронеоднородностях, при скорости звука в паре ~10^5см/с произойдет за ~10^{-8}с и в дальнейшем геометрия течения, влияющая на порог плазмообразования будет определятся размером всего пятна, что и подтверждается экспериментом (рис.3).

По результатам измерений времени задержки плазмообразования были рассчитаны пороговые параметры: мгновенная плотность мощности в момент плазмообразования и удельные энергетические затраты на плазмообразование E*/S (рис.4). Установлено, что в условиях воздействия импульсов ЛИ длительностью <1мкс плазмообразование носит нестационарный характер, т.е. имеет место при интенсивностях ЛИ превосходящих пороговые и условием плазмообразования является превышение некоторой плотности E*/S, необходимой вероятно для испарения дефектов. Зависимость времени плазмообразования от максимальной плотности мощности ЛИ q_m в этом случае хорошо описывается степенной зависимостью $t^* \approx \beta\sqrt{\tau}/q_m$. Для длинных импульсов, плазмообразование носит квазистационарный характер и плазма возникает в струе паров с установившейся структурой. При сформировавшейся газодинамической структуре паровой струи для плазмообразования необходимо превышение некоторой пороговой плотности мощности ЛИ q_m^*, что особенно ярко проявляется для импульсов сложной формы.

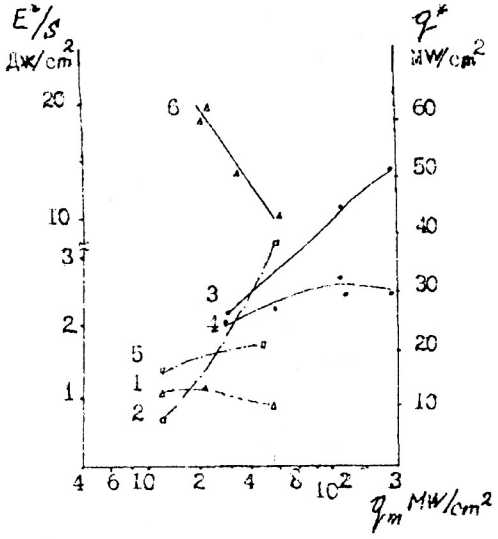

Рис.4. Зависимость параметров плазмообразования от максимальной плотности мощности ЛИ:
1. q* - 1- Д16Т (λ=0,59мкм - родамин),
2- Д16Т (λ=1,06мкм; $\tau_и$=300нс)
3- In (λ=10,6мкм; $\tau_и$=1мкс)
2. E*/S: 4,5,6 - Д16Т (λ=1,06мкм), In (λ=10,6мкм), Д16Т (λ=0,59мкм)

Литература

Гречихин Л.И., Минько Л.Я.: 1967, ЖПС, т.14, 720
Брунов В.В., Горбунов А.А., Конов В.И.: 1986, ЖПС. т.44 ,845.
Минько Л.Я.,Чумаков А.Н., Чивель Ю.А.: 1988, Квант.электроника,т.15,1619.
L.Ya.Min'ko, Yu.A.Chivel:1993, Proc. ICPIG XXI, vol 1,135.
L.Ya.Min ko, Yu.A.Chivel: 1996, Proc. SPIE, vol.2713,361.
Ефремов В.В., Минько Л.Я., Чивель Ю.А., Чумаков А.Н., 1988, Тез. докл. III Всес. конф. "Взаим. изл., плазм. и электр. потоков с веществом, 172

Publ. Astron. Obs. Belgrade No. 61 (1998), 127 – 130 *Contributed paper*

КВАЗИСТАЦИОНАРНЫЙ ПРИПОВЕРХНОСТНЫЙ ОПТИЧЕСКИЙ РАЗРЯД ПРИ РАЗЛИЧНЫХ ДАВЛЕНИЯХ ОКРУЖАЮЩЕГО МИШЕНЬ ГАЗА

Л.Я.МИНЬКО, В.И.НАСОНОВ
Институт молекулярной и атомной физики,
Ф.Скарины 70, 220072 Минск, Беларусь

Аннотация. Экспериментально исследована динамика развития квазистационарного приповерхностного оптического разряда при воздействии квазинепрерывного излучения неодимового лазера (q=0,1-10 Вт/см^2) на Д16Т, А99 и Bi в воздухе (1 атм) и азоте (до 17 атм) Установлен вид зависимостей от q начальных испарения и плазмообразования, а также яркостной температуры эрозионных факелов. Выявлены и проанализированы два вида периодических неустойчивостей плазмообразования и неустойчивость развития плазмы, связанная с q(t), в течение лазерного импульса.

Настоящая работа посвящена экспериментальному исследованию квазистационарного приповерхностного оптического разряда (КПОР), реализуемого при воздействии квазинепрерывного лазерного излучения (ЛИ) (λ=1,06 мкм, $\tau \sim$ 1,5 мс) на дюралюминий Д16Т, алюминий А99 и висмут (Bi) в режиме формирования недорасширенного лазерного эрозионного плазменного факела (ЛЭПФ) в атмосфере воздуха нормального давления и азота давлением до 17 атм. Плотность мощности ЛИ q в зоне воздействия диаметром $\sim$ 3,5 мм изменялась в диапазоне 0,1 - 10 МВт/см^2.

Экспериментально прослежена динамика процессов, сопровождающих лазерное воздействие от стадии начального испарения через промежуточную стадию неустойчивого плазмообразования до стадии установившегося состояния КПОР. Выявлены и изучены особенности в развитии приповерхностной плазмы и оптического разряда, тесно увязанные с физико-химическими свойствами материала мишени, режимом и условиями воздействия на поверхность. При воздействии на мишени в воздухе получены количественные данные об

энергетических зависимостях начального испарения и приповерхностного плазмообразования . Первоначальное плазмообразование (рис.1,2, кривые 2), проявляя свою эрозионную природу, всегда развивалось спустя некоторое время относительно начала испарения (рис.1, 2, кривые 1).

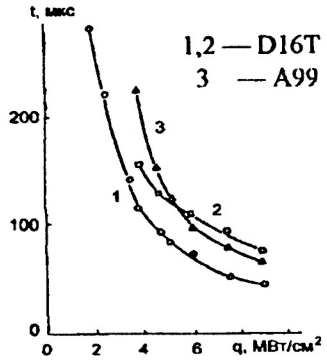

Рис.1

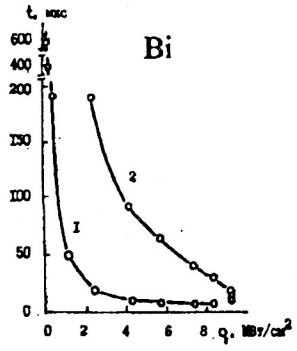

Рис.2

На основе изучения отражения ЛИ в условиях существования КПОР установлено, что вклад плазмы в поглощение ЛИ не велик, а регистрируемая экранировка поверхности мишени факелом обусловлена главным образом поглощением и рассеянием излучения частицами эрозии мишени. При воздействии на Д16Т показано, что связанные с этим энергетические потери, а также потери, обусловленные разлетом факела, могут компенсироваться тепловым действием самого факела на поверхность вследствие переизлучения части энергии плазмой, увеличивающегося с ростом q, а также вкладом инициируемой в приграничных с воздухом областях факела реакции горения частиц , повышающей температуру факела и его излучающую способность. В результате при воздействии ЛИ на Д16Т в диапазоне q = 4-8 МВт/см^2 запаздывание начала плазмообразования относительно начала испарения остается примерно постоянным (рис. 1). Существенные отличия в поведении порогов начального плазмообразования с мишенями из Д16Т и А99 в пределах

рассматриваемого диапазона q можно объяснить на основе различного вклада примесных компонент сплава Д16Т в плазмообразование в начале и в конце диапазона (Min'ko and Nasonov , 1996). С висмуговой мишенью (рис. 2) при изменении q имеет место резко нелинейная зависимость запаздывания начала плазмообразования относительно начала испарения. Уменьшение задержки начала образования плазмы относительно начала испарения при увеличении q с Bi, вероятно, можно объяснить тем, что при более высоких q в ходе воздействия в относительно однородном мелкодисперсном эрозионном факеле Bi легче достигаются пороговые условия развития плазмы (Минько и Насонов, 1996; Минько и Насонов, 1998).

Данные высокоскоростных съемок и измерений интенсивности свечения ЛЭПФ показали, что для всех материалов существуют интервалы q, внутри которых при каждом q образование плазмы в эрозионном факеле имеет неустойчивый характер.. Выявлены и изучены два вида неустойчивостей периодического характера - высокочастотные с периодом в несколько микросекунд и относительно медленные с периодом в несколько десятков микросекунд.. Неустойчивости связаны с неоднородностью теплофизических свойств мишеней и характером их разрушения, с дискретным, неравномерным поступлением частиц в факел и его экранирующим действием, с высокочастотными колебаниями интенсивности ЛИ, имеющими место на огибающей реального квазинепрерывного лазерного импульса, а также с неустойчивостью локального перегрева поверхности, вызванной тепловой контракцией при теплообмене между нагретой (выше температуры плавления) поверхностью и плазмой.

С мишенью из Д16Т при $q \geq 3{,}5$ МВт/см^2 обнаружены неустойчивости развития плазмы в течение лазерного импульса, обусловленные пороговым характером плазмообразования, связанным с мгновенной плотностью мощности q(t), энергетическим вкладом реакции горения частиц эрозии мишени и экранирующим действием факела

на поверхность. Отмечено, что диапазон пороговых значений q, при которых проявляются указанные неустойчивости, определяется разбросом оптических свойств поверхности и степенью однородности мишеней.

Динамику процессов, сопровождающих лазерное воздействие на мишени в воздухе при изменении q иллюстрирует поведение яркостных температур эрозионных факелов, представленных на рис. 3 и 4. Так, например, с висмутом участок AB соответствует испарительной стадии воздействия, BC - предпробойному состоянию паров, CD - неустойчивому плазмообразованию, DE - устойчивому развитию КПОР, EF - просветлению КПОР.

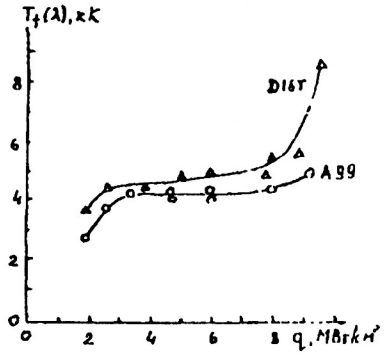

Рис.3.

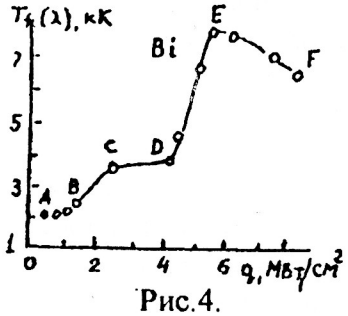

Рис.4.

В экспериментах с мишенями из Д16Т и Bi в атмосфере азота получены количественные данные, указывающие на уменьшение выноса массы вещества из зоны воздействия и снижение (в несколько раз) скорости фронта плазменного образования при повышении давления газа от 1 до 17 атм.. При достижении некоторого порогового значения q ЛИ в ходе воздействия удаление фронта плазменного образования от поверхности сохраняется постоянным, а КПОР оказывается «прижатым» к поверхности и тем самым способствующим поддержанию процесса лазерно-плазменного воздействия на мишень.

Литература

Min'ko L.Ya, Nasonov V.I.: 1996, Chem. Phys. vol.(15), 435

Минько Л.Я., Насонов В.И.: 1996, Publ. Obs. Astron. Belgrade. 53, 125

Минько Л.Я., Насонов В.И.: 1998, Журн. прикл. спектр. (65), 126

Publ. Astron. Obs. Belgrade No. 61 (1998), 131 – 134 *Poster paper*

PLASMA BROADENED 433.3 nm AND 433.5 nm Ar I SPECTRAL LINES

D. NIKOLIĆ, S.DJUROVIĆ, Z. MIJATOVIĆ,
R. KOBILAROV AND N. KONJEVIĆ*
Institute of Physics, Trg D. Obradovića 4, 21000 Novi Sad, Yugoslavia
Institute of Physics, P.O. Box 68, 11080 Belgrade, Yugoslavia
E-mail: dnikol@unsim.ns.ac.yu

Abstract. Two close plasma broadened spectral lines of neutral argon, 433.3 nm and 433.5 nm were experimentally investigated. Obtained widths and shifts were compared with the results of other authors. Some discrepancies with the results of other authors are explained by rough approximation in deconvolution procedure used by other authors.

1. INTRODUCTION

Many experimental papers are devoted to study of neutral argon spectral lines (Konjević et al. 1976, 1984, 1990) in order to obtain Stark broadening parameters. A few questions about the accuracy of existing data is still opened. This accuracy is influenced by several procedures: *a)* spectral intensity measurements, *b)* wavelength measurements and *c)* separation of different line broadening mechanisms. In the last one the critical is deconvolution of Gaussian (instrumental + Doppler) and Stark broadened profile $j_{A,R}(x)$ which is asymmetric and defined as (Griem 1974):

$$j_{A,R}(x) = \frac{1}{\pi}\int_0^\infty \frac{H_R(\beta)d\beta}{1+((\lambda-(\lambda_0+d_e))/w_e - A^{4/3}\beta^2)^2}$$

where x is reduced wavelength, $H_R(\beta)$ is microelectric field distribution, R is dimensionless parameter and A is ion broadening parameter. Incorrect deconvolution procedure introduce systematic error in line width measurements up to 25 %. This is particularly important when strongly asymmetric lines, like Ar I 433.3 nm and 433.5 nm lines, are in the question.

The aim of this study was to obtain Stark broadening parameters of Ar I 433.3 nm and 433.5 nm lines, reliable as much as possible.

2. EXPERIMENTAL

Particular attention was paid on precise spectral intensity measurements, since this is the first step in the measurements and produces unrecoverable errors. Wall stabilized arc, as very stable plasma source, was used. The arc operated under atmospheric pressure with 99 % Ar + 1 % H_2 gas mixture. H_2 was introduced for plasma diagnostics purposes. An averaging technique (Mijatović et al. 1995) for spectral intensity measurements was applied introducing the error less than 1%.

Radiation from the arc was focused 1:1 onto the entrance slit of 1-m monochromator equipped with 1200 g/mm grating, photomultiplier and stepping motor. The

accuracy of wavelength settings was 0.0025 nm. The height of entrance slit was 0.3 mm while width of entrance end exit slit was 20 μm resulting in 0.018 nm instrumental width. Plasma was observed side-on at twelve positions along the plasma column radius.

Geissler tube was used for shit measurements (Mijatović et al. 1995).

Plasma electron densities ranging (0.74 - 2.90)$\times 10^{16}$ cm^{-3} were determined from H_β line width (Vidal et al. 1974), while the temperatures ranging 9000 - 10800 K were determined from plasma composition data (White et al. 1958).

After Abel inversion numerical procedure for deconvolution (Nikolić et al. 1998) was applied. Contribution of Van der Waals and resonance broadening was extracted also.

3. RESULTS AND DISCUSSION

An example of experimental line profiles (after Abel inversion) is presented in Fig. 1, together with the reference line used for shift measurements. As it can be seen from the Fig. 1 fitted profile (Gaussian + $j_{A,R}(x)$) is in very good agreement with measured ones. This agreement ensures high quality data of width and shift measurements.

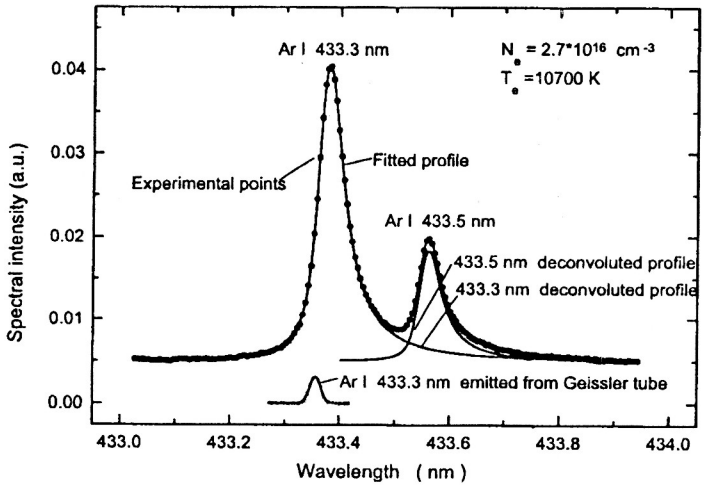

Figure 1. An example of experimental, fitted and deconvoluted line profiles of 433.3 nm and 433.5 nm lines.

The obtained widths and shifts for 433.3 nm line are plotted versus electron density in Fig. 2. Experimental results of other authors (Bues et al. 1966-67; Musielok 1994) are included also together with the errors ranging 15 - 30 % (30 % is presented) estimated by critical reviews (Konjević et al 1976, 1984 and 1990). The exception is result taken from Musielok (1994). For this point the error of 10 % stated by the author is taken. Theoretical data for this line are not available.

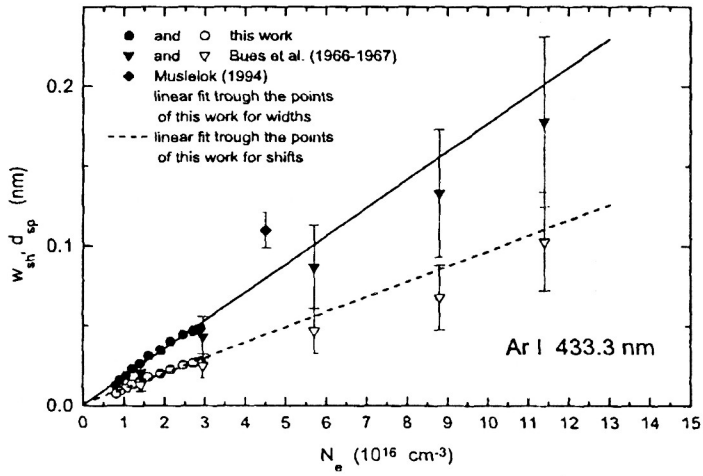

Figure 2. Measured widths and shifts of Ar I 433.3 nm line vs electron density. Full symbols - widths, open symbols - shifts.

As it can be seen from Fig. 2 agreement between experimental results is inside error bars. It should be noted that deconvoluton procedures used in '60 and '70-ties have not taken asymmetry of the lines into account.

Ratios of measured to theoretical values (Griem 1974) for widths and shifts of 433.5 nm versus electron density is given in Fig. 3. Results of other authors (Bues et al. 1966-67: Schulz and Wende 1968) are also included together with the errors estimated by (Konjević and Roberts 1976).

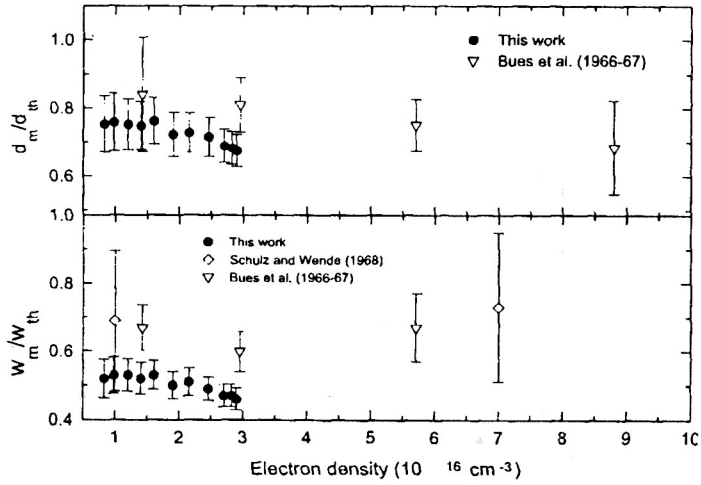

Figure 3. Ratios of measured to theoretical values of shift and width of Ar I 433.5 nm line vs electron density.

Disagreement between results of this work and the results of other authors is considerable in the case of Ar I 433.5 nm line. Results of other authors are

systematically higher in both cases, shifts and widths. This can be explained by overlapping of the 433.3 nm and 433.5 nm lines. It can be seen from Fig. 1 that vicinity of neighbour line influences much more the shape of 433.5 nm line, while the shape of 433.3 nm line is almost uninfluenced. This is due to the difference in intensity of these two lines. Contribution of blue wing of weaker line (less than one half) to the intensity and shape of stronger one is almost negligible, while the contribution of red wing of stronger line to the intensity and shape of the weaker one is considerable. From Fig. 1 can be seen that the last influence contributes in wider and more shifted weaker line (compare fitted profile and separated profile of weaker line).

Finally, it can be concluded that, besides quality in spectral intensity measurements, in case overlapping lines, correct procedures for separation and deconvolution of the investigated lines must be applied in order to obtain high precision data.

References

Bues I., Haag T. and Richter J.: 1966-67, *Laboratoriumsbericht aus dem Institut für Experimentalphysik der Universität Kiel.*

Griem H.R.: 1974, *Spectral Line Broadening by Plasmas*, Academic, New York.

Konjević N. and Roberts J.R.: 1974, *J. Phys. Chem. Data* **5**, 209.

Konjević N. Dimitrijević M.S. and Wiese W.L.: 1984, *J. Phys. Chem. Data* **13**, 619.

Konjević N. and Wiese W.L.: 1990, *J. Phys. Chem. Data* **19**, 1307.

Mijatović Z., Konjević N. Kobilarov R. and Djurović S.: 1995, *Phys. Rev E* **51**, 613.

Musielok J.: 1994, *Acta. Phys. Pol. A* **86**, 315.

Nikolić D., Mijatović Z., Kobilarov R., Djurović S. and Konjević N.: 1998, *Contributed Papers of 19th SPIG*, to be published.

Schulz P. and Wende B.: 1968, *Z. Phys.* **208**, 116.

Vidal C.R., Cooper J. and Smith E.W.: 1973, *astrophys J. Suppl. Ser. No. 214* **25**, 37.

White W.B., Jonson S.M. and Dantzig G.B.: 1958, *J. Chem. Phys.* **28**, 751.

Publ. Astron. Obs. Belgrade No. 61 (1998), 135 – 138 *Poster paper*

ELECTRON-IMPACT BROADENING PARAMETERS FOR ASTROPHYSICALLY IMPORTANT Eu II LINES

L. Č. POPOVIĆ and M. S. DIMITRIJEVIĆ
Astronomical Observatory, Volgina 7, 11160 Belgrade 74, Yugoslavia
E–mail lpopovic@aob.aob.bg.ac.yu
E–mail mdimitrijevic@aob.aob.bg.ac.yu

Abstract. Electron-impact widths and shifts for four astrophysically important lines of singly ionized europium have been calculated by using the modified semiempirical method. The influence of the electron-impact mechanism on line shape in a hot star atmosphere has been tested.

1. INTRODUCTION

The lines of ionized rare earth elements are present in spectra of hot CP stars (see e.g. Kupka *et al.* 1996, Golbmann *et al.* 1997, Ryabchikova *et al.* 1997, etc). Considering that in the layers of a hot star atmosphere Stark broadening mechanism can be the main impact broadening mechanism, Stark broadening parameters are needed in numerous problems concerning line formation in stellar atmospheres. Here we present the Stark broadening parameters for four astrophysically important Eu II lines. The spectral lines of singly ionized europium are present in solar as well as in stellar spectra (see e.g. Grevesse and Blanquet 1969, Molnar 1972, Adelman 1987, Mathys and Cowley 1992, etc.). Here we direct our attention to several lines which are very strong in CP star spectra.

Due to the lack of known energy levels as well as of realiable transition probabilities for this emitter, the approximative method can be applied for Stark broadening parameter calculations. Here we have applied the modified semiempirical approach – MSE (Dimitrijević and Konjević 1980, Dimitrijević and Kršljanin 1986, Popović and Dimitrijević 1996ab).

2. METHOD OF CALCULATION

Taking into account very complex spectra of Eu II, as well as that higher levels have no designation, we were able to calculate the electron-impact broadening parameters only for 6s-6p transitions by using the modified semiempirical approach (Dimitrijević and Konjević 1980, Dimitrijević and Kršljanin 1986). Due to the complex spectrum we have applied here this method as it was described in Popović and Dimitrijević (1996). We have estimated also the electron-impact width for Eu II ($5d^9D_6^0 - 6p^9P_5$)

λ =6645.064 Å line by using the MSE approach with the estimation of the perturbation of the partialy known $5f$ levels (in accordance with Popović and Dimitrijević (1998)).

Table 1. Stark full widths (FWHM) and shifts for Eu II lines as a function of temperature. The electron density is $10^{23}\mathrm{m}^{-3}$.

Transition	T (K)	W (nm)	d (nm)
	5000.	0.451E-01	-0.391E-02
$6s^9S_4^0 - 6p^9P_5$	10000.	0.314E-01	-0.278E-02
	20000.	0.219E-01	-0.198E-02
$\lambda = 381.967$ nm	30000.	0.179E-01	-0.161E-02
	40000.	0.158E-01	-0.142E-02
	50000.	0.146E-01	-0.132E-02
	5000.	0.557E-01	-0.169E-01
$6s^9S_4^0 - 6p^9P_4$	10000.	0.388E-01	-0.122E-01
	20000.	0.270E-01	-0.897E-02
$\lambda = 412.970$ nm	30000.	0.221E-01	-0.759E-02
	40000.	0.195E-01	-0.688E-02
	50000.	0.181E-01	-0.654E-02
	5000.	0.570E-01	-0.173E-01
$6s^9S_4^0 - 6p^9P_4$	10000.	0.397E-01	-0.125E-01
	20000.	0.276E-01	-0.916E-02
$\lambda = 420.505$ nm	30000.	0.226E-01	-0.776E-02
	40000.	0.200E-01	-0.705E-02
	50000.	0.185E-01	-0.671E-02

Transition	T (K)	W (nm)
	5000.	0.930E-01
$5d^9D_6^0 - 6p^9P_5$	10000.	0.644E-01
	20000.	0.447E-01
$\lambda = 664.505$ nm	30000.	0.367E-01
	40000.	0.327E-01
	50000.	0.306E-01

Atomic energy levels needed for calculations were taken from Martin *et al.* (1978). Matrix elements have been calculated by using the method of Bates and Damgaard (1949). Since for nonet terms the line factors are not presented in the tables of Oertel and Shomo (1968), they have been calculated as

$$\Re_{\mathrm{line}} = \sqrt{2J+1}\sqrt{2J'+1}\left\{\begin{matrix} S & J & L \\ 1 & L' & J' \end{matrix}\right\}$$

where S is the total spin; J and J' are total angular momentum quantum numbers; while L and L' are total azimuthal quantum numbers. The quantum numbers of perturbing level are denoted with the primes.

3. RESULTS AND DISCUSSION

In Table 1. the results of our calculation are presented as a function of temperature, for an electron density of $10^{23}\mathrm{cm}^{-3}$. We have tested also the importance of the electron-impact broadening effect in stellar atmospheres. As an example of this influence we have synthesized line profile for Eu II λ=6645.064 Å line using SYNTH code and the Kurucz's model of stellar atmosphere with T_{eff} = 10000 K and $log g$=5.0. The synthesized line profiles are shown in Fig. 1. As one can see from Fig. 1, the electron-impact effect causes that equivalent width is larger. Consequently, for the determination of elemental abundance by comparing the observed to the synthetic spectra one should take into account this effect, especially in the case when europium is overabundant (see e.g. the case of silicon in Lanz *et al.* 1988). The detailed discussion of the electron- impact broadening effect in stellar atmospheres will be discussed elsewhere (Popović *et al.* 1998).

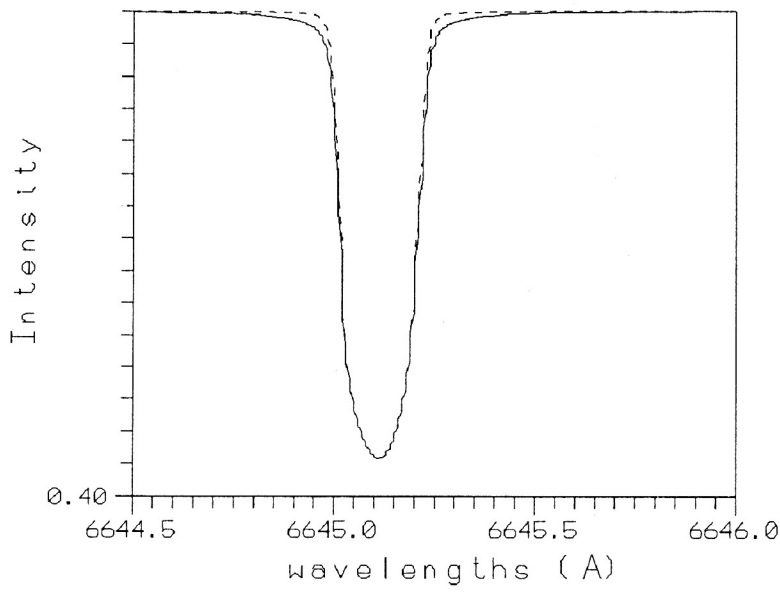

Fig. 1. The synthesized profile of Eu II λ=6645.05 Å: profile shown by full line has been calculated when the electron-impact width is taken into account, and the dashed profile without this width.

References

Adelman, S J.: 1987, *in Elemental Abundance Analyses*, Proc. of the IAU working group on Ap stars Workshop (Eds. S.J. Adelman and T. Lanz) p. 58.

Bates, D.R., and Damgaard, A.: 1949, *Phil. Trans. Roy. Soc. London*, Ser. A, **242**, 101.

Dimitrijević, M.S., Konjević, N.: 1980, *J. Quant. Spectrosc. Radiat. Transfer*, **24**, 451.

Golbmann, M., Kupka, F., Weiss, W.W. and Mathys, G.: 1997, *Astron. Astrophys.* **319**, 630.
Grevesse, N. and Blanquet, G.: 1969, *Solar Phys.* **8**, 5.
Kupka, F., Ryabchikova, T.A., Weiss, W.W., Kursching, R., Rogel, J. and Mathys, G.: 1996, *Astron. Astrophys.* **308**, 886.
Lanz, T., Dimitrijević, M.S., and Artru, M.-C.: 1988, *Astron. Astrophys.* **192**, 249.
Martin, W.C, Zalubas, R. and Hagan, L.: 1978, *Atomic Energy Levels*, NSRDS-NBS, Vol. **60**, Washington D.C.
Mathys, G. Cowley, C.R.: 1992, *Astron. Astrophys.* **253**, 199.
Molnar, H.: 1972, *Astron. Astrophys.* **20**, 69.
Oertel, G.K., Shomo, L.P.: 1968, *Astrophys J. Suppl. Series*, **16**, 175.
Popović, L.Č. and Dimitrijević, M.S.: 1996a, *Phys. Scr.* **53**, 325.
Popović, L.Č. and Dimitrijević, M. S.: 1997, In: The Physics of Ionized Gas, (eds. B. Vujičić, S. Djurović and J. Purić) p.477.
Popović, L.Č., Dimitrijević, M.S.: 1998, *in preparation.*
Ryabchikova, T.A., Landstreet, J.D., Gelbmann M.J., Bogova, G.T., Tsymbal V.V. and Weiss W.W.: 1997, *Astron. Astrophys.* **327**, 1137.

Publ. Astron. Obs. Belgrade No. 61 (1998), 139 – 142 *Poster paper*

LONG-TERM H_β LINE PROFILE VARIATION IN Akn 120

L. Č. POPOVIĆ[1], N. TRAJKOVIĆ[1], A. KUBIČELA[1], V. T. DOROSHENKO[2], S. G. SERGEEV[3], E. BON[1] and I. STANIĆ[4]

[1]*Astronomical Observatory, Volgina 7, 11160 Belgrade 74, Yugoslavia*
[2]*Crimean Astrophysical Observatory, Nauchny, Ukraine*
[3]*Sternberg Astronomical Institute, Moskow, Russia*
[4]*Imtel Computers & Digital Radio, Belgrade, Yugoslavia*

Abstract. Long-term H_β line shape variation in spectra of Akn 120 is discussed. We have analysed the H_β line shape from 96 spectra observed from 1977. till 1990. The H_β line has been fitted with two broad and one narrow gaussians troughout the whole considered period. The broad components of H_β and shelf cause the H_β line shape variation. Two broad gaussians of H_β may suggest existence of two broad line region in Akn120 – central part.The mean redshift of H_β line amounts to 213 kms^{-1}.

1. INTRODUCTION

Optical spectra of Seyfert 1 galaxies (Sy1) usually show significant emission lines and continuum variabilities. Investigations of these variations may bring more information about the structure of Broad Line Regions (BLRs) in them (e.g. Peterson 1993).

One of the Sy1 galaxies which has a large-amplitude variability in continuum and in spectral line shapes is Akn120 (Peterson *et al.* 1985, Peterson and Cota 1987, Winge *et al.* 1996).

Here we present the preliminary results of our analysis of H_β line shape variation in Akn120.

2. THE DATA AND ANALYSIS

We have analysed 96 spectra in the wavelength interval 4500-5300 Å obtained by K. K. Chuvaev on 2.6 m Shajn telescope at Crimean Astrophysical Observatory (CrAO) during the period 1971-1990 (HJD 2443435 till 2447944).

All spectra were scanned on two-coordinate CrAO microphotometer. The further treatment, including the correction for film and sky background, instrumental spectral sensitivity, as well as wavelength and flux calibration were made using the SPE data reduction package, developed by S.G. Sergeev. The wavelength calibration was based on the night sky lines and narrow emission lines of the galaxy. The redshift of Akn120 was accepted equal to z=0.03428 (Foltz *et al.* 1983).

In order to investigate the long-term variability of H_β line shape and to take into consideration the big gaps in the observations, spectra have been divided into 10 groups (see Table 1).

Table 1. Time-distribution and number of the observed spectra (in Heliocentric Julian Days – HJD.)

group	1	2	3	4	5	6	7	8	9	10
from HJD 2440000 +	3435	3790	4173	4522	4881	5263	5619	5997	6853	7832
till HJD 2440000 +	3574	3934	4289	4672	5054	5412	5734	6088	7124	7944
mean HJD 2440000 +	3474	3879	4229	4577	4958	5331	5695	6058	7014	7888
numbers of spectra	14	14	9	5	15	12	11	6	6	4

The spectra within groups have been averaged. In the mean spectra noises and some short-term variability are to some extent suppressed and possible long-lasted features better expressed. The local continuum in two narrow zones around 4900 and 5260 Å was interpolated with a straight line. The mean spectra have been normalized to this continuum.

The broad H_β line has two peaks shifted blueward and redward from the line center defined by the narrow emission lines. The peaks are more or less clearly resolved. Besides, the H_β is blended with OIII(4959,5007) and some other emission lines (Jackson and Browne 1989, Meyers and Peterson 1985).

3. RESULTS AND DISCUSSION

In order to decrease the number of free parameters, some relations among the fitting gaussians have been established a priori (Popović and Mediavilla 1997). Namely, the three gaussians representing two narrow OIII lines and a narrow H_β component are preconditioned to have the same systemic redshift (z=0.03248, according to Foltz *et al.* 1983), and the intensity ratio of the two OIII lines has been supposed to be 1 : 3.03 . Also, the ratio of the full widths of these two lines and narrow H_β component are fixed in proportion with their wavelengths as

$$\frac{W_{H_\beta}}{4861} = \frac{W_{4959}}{4959} = \frac{W_{5007}}{5007},$$

where W_{H_β} is width of H_β narrow component, W_{4959} and $W_{(5007)}$ are widths of the two OIII(4959,5007) lines.

We obtained the best fit with six gaussians (Figure 1). During the considered period, in all groups, H_β can be resolved into three components. Two of them are broad with the full width from 654 to 1707 kms^{-1} (red peak) and from 3225 to 3328 kms^{-1} (blue peak) and one, narrow, is about 550 kms^{-1} wide.

The slow time-variations of H_β broad gaussian shifts can be noticed in the sense that the red peak progressively decreases its line-of-site velocity, while the blue one exhibits a minimum during the observed period (Figure 2).

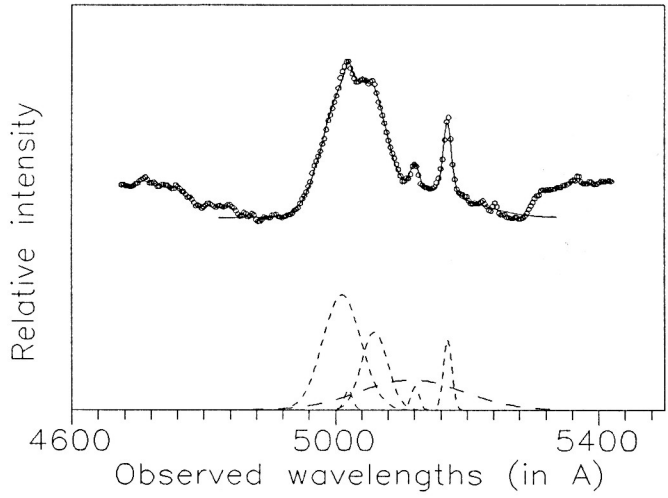

Fig. 1. The data of the seventh group of the mean spectra as an example of decomposition of the Hβ and OIII lines. (o o o) – observed data, (—) - the best fit, (- - -) - gaussians of the resolved spectral lines, (– –) - the broadest gaussian (shelf).

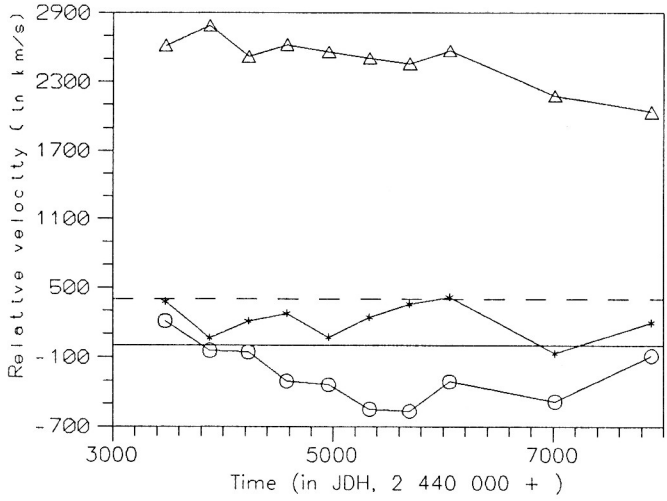

Fig. 2. The line-of-site velocities of the blue and red gaussians (circles and triangles respectively) relative to the narrow Hβ component having the systemic redshift z=0.03248 (the horizontal solid line) are shown as functions of time. The asterisks are the weighted mean of the red and blue broad Hβ wings. The dashed line represents the gravitational redshift estimated by Peterson *et al.* (1985).

The presence and behavior of two broad gaussians in Hβ line may indicate the existence of two broad line regions in Akn120, as it was suggested by Gaskell (1983, 1996) for the 3C390.3 – type of galaxies. However, in all considered groups, the intensity

of the blue H_β gaussian is higher than intensity of the red one. It is an accordance with the curves in Figure 3. Alternatively, these results can be taken as a kind of a "blue boosted, redshifted" spectral line usually connected with a rotating disk (e.g. Stuchlik, 1998).

The overall redshift of H_β line is in a way presented by the weighted mean of the blue and the red wing line-of-sight velocities, asterisks in Figure 2. The areas under the corresponding gaussians were taken as weights. This velocity averaged amounts to 213 kms^{-1}. It is slightly lower than the value of 400 kms^{-1} found by Peterson *et al.* (1985) as the gravitational redshift of Akn120.

The detailed discussion of the obtained results will be presented elsewhere (Popović *et al.* 1998).

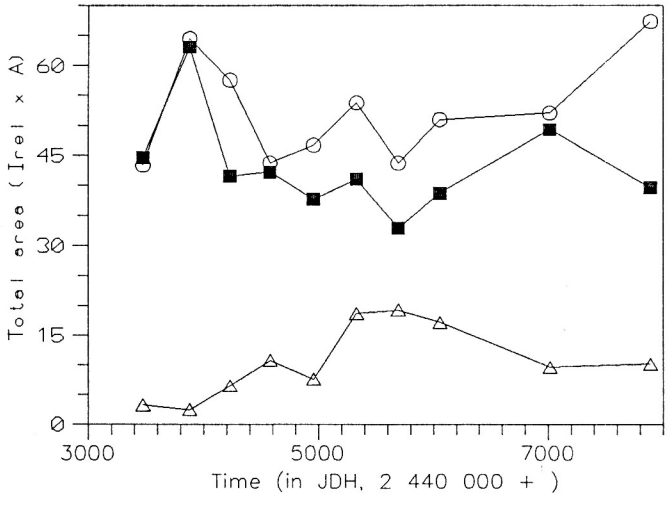

Fig. 3. The areas of the red broad H_β gaussian (triangles), blue broad gaussian (circles), and shelf (filled squares) as functions of time.

References

Foltz, C.B., Wilkes, B.J. and Peterson, B.M.: 1983, *Astrophys. J.* **88**, 1703.
Gaskell, C.M.: 1983, Proc. 24th Liege Intern. Ap. Colloquium, Univ. de Liege, Liege, 473.
Gaskell, C.M.: 1996, *Astrophys. J. Lett.* **464**, 107.
Jackson, N. and Browne, I.W.A.: 1989, *MNRAS* **236**, 97.
Meyers, K.A. and Peterson, B.M.: 1985, *PASP* **97**, 734.
Peterson, B.M.: 1993, *PASP* **105**, 247.
Peterson, B.M. and Cota, S.A.: 1987, *Astrophys. J.* **94**, 7.
Peterson, B. M., Meyers, K.A., Capriotti, E.R, Foltz, C.B., Wilkes, B.J., Miller, H.R.: 1985, *Astrophys. J.* **292**, 164.
Popović, L.Č. and Mediavilla, E.: 1997, *Publ. Astron. Obs. Belgrade* **57**, 95.
Popović, L.Č., Trajković, N., Kubičela, A., Doroshenko, V.T., Sergeev, S.G., Bon, E. and Stanić, I.: 1998, in preparation.
Stuchlik, Z.: 1998, Proc. 20th Stellar Conference, eds. Dushek, J. and Zejda, M., N. Copernicus Obs. and Planetarium, Brno, 147.
Winge, C., Peterson, B.M., Pastoriza, M.G. and Storchi-Bergman, T.: 1996, *Astrophys. J.* **469**, 648.

Publ. Astron. Obs. Belgrade No. 61 (1998), 143 – 146 *Poster paper*

STARK BROADENING MECHANISM IN ATMOSPHERES OF A, DA AND DB TYPE STARS

L.Č. POPOVIĆ, D. TANKOSIĆ and M.S. DIMITRIJEVIĆ
Astronomical Observatory, Volgina 7, 11160 Belgrade 74, Yugoslavia
E-mail :lpopovic@aob.aob.bg.ac.yu
E-mail :dtankosic@aob.aob.bg.ac.yu
E-mail :mdimitrijevic@aob.aob.bg.ac.yu

Abstract. The influence of Stark broadening mechanism on Au II (λ=1740.48Å) and Ti II (λ= 3761.32Å) lines originating in layers of A, DA and DB type star atmospheres, have been considered.

1. INTRODUCTION

It was noted in several papers that Stark broadening mechanism is the main broadening mechanism in hot star atmosphere (see e.g. Dimitrijević 1989, Popović and Dimirtijević 1996a). Also, this mechanism may be important in the case of cooler stars as e.g. solar type stars (see Vince *et al.* 1985) especially in photospheric and subphotospheric layers.

It is very important to consider and to take into account the Stark broadening parameters in the case of the chemical abundance determination in the atmospheres of magnetic, CP stars and white dwarfs by using the atmosphere model method (see Hohlova 1994).

We have discussed here the importance of Stark broadening mechanism in stellar plasma with the help of Kurucz's (1979) model atmosphere of an A type star (T_{eff}=10000K, log$g$=4) and with models of DA (T_{eff}=10000K, log$g$=6) and DB (T_{eff}=15000K, log$g$=7) white dwarfs atmospheres (Wickramasinghe 1972).

2. RESULTS AND DISCUSSION

Considering that Au II (λ=1740.48Å) and Ti II (λ= 3761.32Å) lines have been used for gold and titanium abundance determination, respectively (for gold see e.g. Fuhrmann 1988, Adelman 1994, Wahlgren *et al.* 1995 and for titanium see e.g. Guthrie 1987, Boyarchuk and Savanov 1987), in CP stars, we have tested the influence of Stark mechanism on widths of these lines in layers of three hot star types.

We consider here Stark broadening mechanism with the help of an A-type (T_{eff}=10000 K, log$g$=4), DA(T_{eff}=10000K, log$g$=6) and DB (T_{eff}=15000K, log$g$=7) atmosphere models. Also, we use the Stark broadening parameters (Popović *et al.*

1998, Tankosić *et al.* 1998) calculated here, within the modified semiempirical approach (Dimitrijević and Konjević 1980, Popović and Dimitrijević 1996b).

The results of our investigation are presented in Figs. 1-3 and in Tables 1 and 2. As one can see from Fig. 1, for the case of hot A type star, Stark broadening mechanism is important for both considered lines. In photospheric layers the Stark broadening line width is one order of magnitude larger than thermal Doppler one. In higher layers of the stellar atmosphere ($\tau \approx$-4) however,the thermal Doppler mechanism is more important.

As we can see from Figs. 2 an 3, in the case of white dwarfs atmospheres Stark broadening mechanism is important in all layers of atmospheres and in deeper atmosphere layers the Stark width is two or three orders of magnitude larger than thermal Doppler width. In Tables 1 and 2 the Stark and thermal Doppler widths for Au II (λ=1740.48 Å) and Ti II (λ=3761.32 Å) lines are shown as functions of optical depth, for an A-type star (T_{eff}=10000K, log$g$=4).

For all three considered atmosphere models Stark broadening effect for ivestigated lines should be taken into account in abundance determination.

Table 1. Thermal Doppler and Stark widths for Au II (λ=1740.48Å) line as a function of optical depth for an A type star (T_{eff}=10000K, log$g$=4).

tau	Stark FWHM[Å]	Thermal Doppler FWHM[Å]
-2.57851	0.786004E-05	0.145411E-03
-1.91422	0.286703E-04	0.149050E-03
-1.53557	0.653420E-04	0.152124E-03
-0.99829	0.356666E-02	0.355163E-03
-0.58649	0.935110E-03	0.196676E-03
-0.08239	0.210489E-02	0.223318E-03
0.09867	0.281302E-02	0.233914E-03

Table 2. Thermal Doppler and Stark widths for Ti II (λ=3761.32 Å) line as functions of optical depth for an A type star (T_{eff}=10000K, log$g$=4).

tau	Stark FWHM[Å]	Thermal Doppler FWHM[Å]
-2.57851	0.680424E-04	0.308503E-03
-1.91422	0.248070E-03	0.316223E-03
-1.53557	0.565113E-03	0.322746E-03
-0.99829	0.413068E-03	0.167404E-03
-0.58649	0.805063E-02	0.417266E-03
-0.08239	0.181118E-01	0.473791E-03
0.09867	0.241986E-01	0.496271E-03

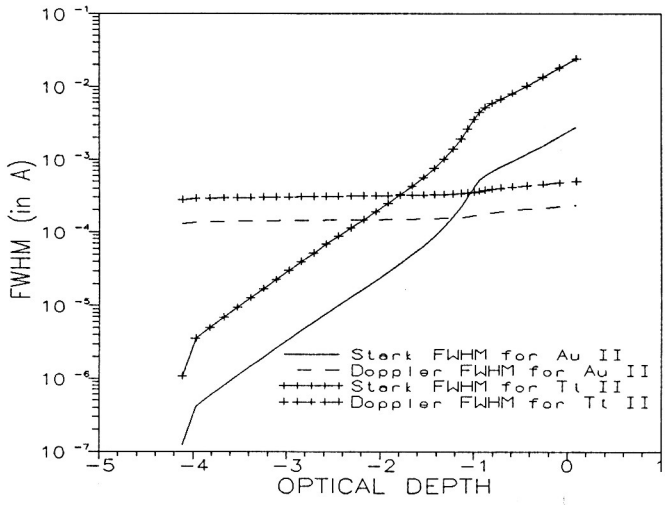

Fig. 1. Thermal Doppler and Stark widths for Au II (λ=1740.48 Å) and Ti II (λ=3761.32 Å) lines as functions of optical depth for an A type star (T_{eff}=10000K, log$g$=4).

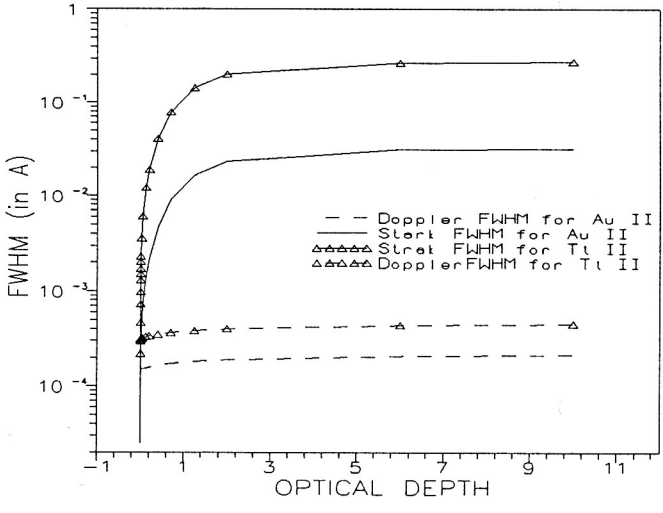

Fig. 2. Thermal Doppler and Stark widths for Au II (λ=1740.48 Å) and Ti II (λ=3761.32 Å) lines as functions of optical depth for DA (T_{eff}=10000K, log$g$=6) white dwarfs.

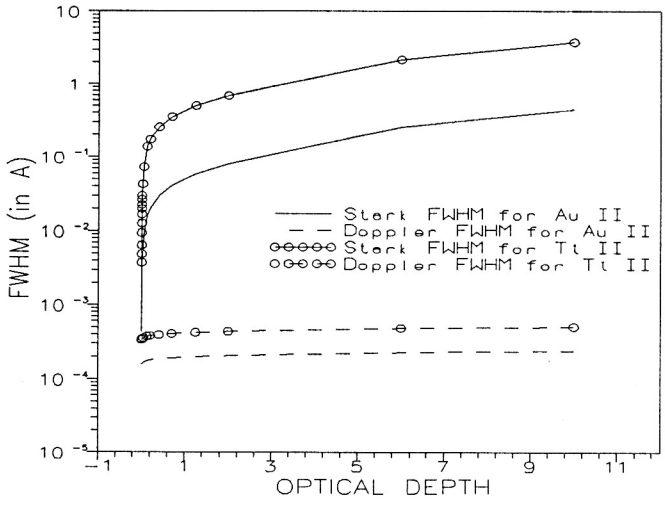

Fig. 3. Thermal Doppler and Stark widths for Au II (λ=1740.48 Å) and Ti II (λ=3761.32 Å) lines as functions of optical depth for DB (T_{eff}=15000K, log$g$=7) white dwarfs.

References

Adelman, S.J.: 1994, *Mon. Not. R. Astron. Soc.*, **266**, 97.

Boyarchuk, A.A, Savanov, I.S.: 1987, in Elemental Abundance Analyses (ed. Adelman S. J. and Lanz T.), Institut d'Astronomie de l'Université de Lausanne, Chavannes-des -Bois, Switzerland.

Dimitrijević, M.S., Konjević, N.: 1980,*JQSRT*, **24**, 454.

Dimitrijević, M.S.: 1989, *Bull. Obs. Astron. Belgrade*, **140**, 111.

Fuhrmann, K.: 1988, *ESA Spec. Publ.*, **282**, 1, 405.

Guthrie, B.N.G.: 1987, in Elemental Abundance Analyses (ed. Adelman S. J. and Lanz T.), Institut d'Astronomie de l'Université de Lausanne, Chavannes-des-Bois, Switzerland.

Hohlova, V.L.: 1994, *Pisma v Astron. Zhurnal*, **20**, 110.

Kurucz, R.L.: 1979, *Astrophys. J. Suppl. Series*, **40**, 1.

Popović, L.Č., Dimitrijević, M.S.: 1996a, *Astron. Astrophys. Suppl. Series*, **120**, 373.

Popović, L.Č. , Dimitrijević, M.S.: 1996b, *Physica Scripta*, **53**, 325.

Popović, L.Č., Tankosić, D., Bon, E., Dimitrijević, M.S.: 1998, Proc. of XIX SPIG, Zlatibor (in press).

Tankosić, D., Popović, L.Č., Dimitrijević, M.S.: 1998, in preparation.

Walhgren, G.M., Lecrone, D.S., Johansson, S.G., Rosberg, M., Brage, T.: 1995, *Astrophys. J.*, **444**, 438.

Wickramasinghe, D.T.: 1972, *Mem. R. Astron. Soc.*, **76**, 129.

Vince, I., Dimitrijević, M.S., Kršljanin, V.: 1985, in Progres in Stellar Spectral Line Formation Theory (ed. Berkman, J., Crivellari, L., Reidel, D.), Dordrecht.

Publ. Astron. Obs. Belgrade No. 61 (1998), 147 – 150 *Contributed paper*

USAGE OF SPECTROSCOPICAL EXPERIMENTS FOR DETERMINATION OF OTHER PLASMA PARAMETERS

M.M. Popović and D.S. Djordjević
Institute of Physics, Pregrevica 118, Zemun, 11080 Beograd, Yugoslavia
E-mail:marko@exp.phy.bg.ac.yu

Abstract: Electrical gas discharge is a source of plasma in many spectroscopic experiments. In this paper it has been shown that those experiments, with some additional measurements, could be used for determination of other plasma parameters, electrical ones before all. There is an example of measurements in cascade arc and Z-pinch.

1. INTRODUCTION

Electrical gas discharge is being used as a plasma source in many experiments with a purpose, before all, to obtain spectroscopic data. Generally used ones are: classical cascade arc, spark, different kinds of pinches, impulse arc, glow discharge, etc. In those discharges meritorious spectroscopic diagnostics could be done, so that temperature and electronic concentration parameters could be correctly determined. Those two values, with measurements of absolute and often only relative radiation intensities in a field observed enable relevant interpretation of spectral line width and shift, continuous discharge origin and intensity, spectral series merging, etc. Due to possibility of reliable interpretation of spectroscopic values, in those measurements other plasma parameters are not being taken into account enough. Very often even basic technical data about discharge, such as volt-ampere characteristics are not being determined.

In this paper at the example of cascade arc and Z-pinch it is shown that in these experiments, with some additional measurements, data about other "useful" values could be obtained. The data about electrical conductivity from an arc

plasma are obtained and compared with the data from an pulse arc measurements. The data from Z-pinch are used for a determination of a very interesting resistant dependence of current during the discharge. A comparison of the data with data from other experiments has been done.

2. WALL-STABILIZED STATIONARY ARGON ARC

A high-pressure wall-stabilized arc used in this experiment predicted especially for spectroscopic measurement is described in Goldbach et al. (1972). A plasma channel (length: 70mm; diameter: 5mm) is inducted within six electrically insulated copper plates (thickness: 10mm).

The plates are water-cooled. The arc is burning between two water-cooled tungsten cylinders. The whole device operated at a chosen pressure within a high-pressure steel cylinder. Four fused silica windows, located in side walls and the electrodes, allow either end-on or side-on observations. The pressure in the chamber was measured by membrane pressure gauge connected to a digital voltmeter. We have used additional procedure for performed electrical measurements. The axial electrical field strength was measured as a function of arc current and pressure. Each plate was individually connected to a stepping switch and the voltage drop between two successive plates was measured using a digital voltmeter. The slope of the linear part of the voltage distribution versus the plasma length yields the axial field strength. This method excludes electrode drops in the plasma field determination. The arc current was measured using a shunt in the power line, Goldbach et al. (1978).

In that way, with known arc current, axial component of the electrical field strength and corresponding radial temperature distribution T(r) we were able to determine electrical conductivity by well known procedure, Popović (1986). The electrical conductivity value obtained by the procedure is presented at Fig. 1. in form $\sigma(T, p=\text{const.})$ and compared with the value obtained in pulse arc.

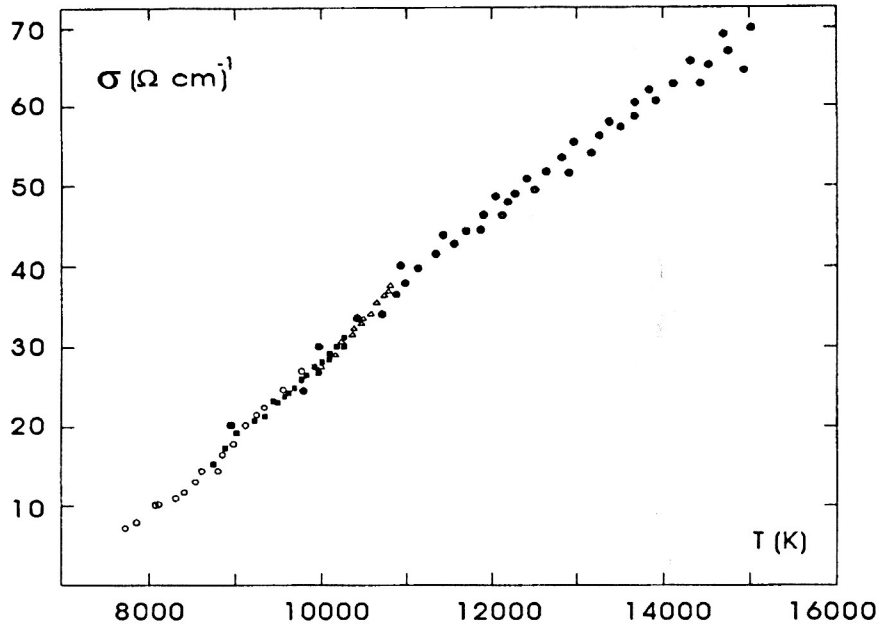

Fig. 1. Plasma electrical conductivity: O - wall stabilized arc E=15V/cm; ■ -wall stabilized arc E=18V/cm ; Δ- wall stabilized arc E=23V/cm; ● - pulsed arc.

3. RESISTANCE OF THE BEGINNING OF HIGH CURRENT DISCHARGES

The knowledge of the main discharge characteristics (current, resistance, voltage, etc.) during the transition period between a breakdown and a steady state regime of high current discharge is interesting both for practical purposes (calculation of circuit elements) and for physical reasons (comprehension of the main processes occurring in the discharge). Many papers have studied the development of the spark, suggesting models and relations between different quantities, for instance resistance and current, Popović et al. (1976) to be used. In order both to investigate dependence between particular parameters and especially to determine a function R(i,d,r,t) we have used Z-pinch, which is mainly applied in spectroscopic measurements, Fig. 2.

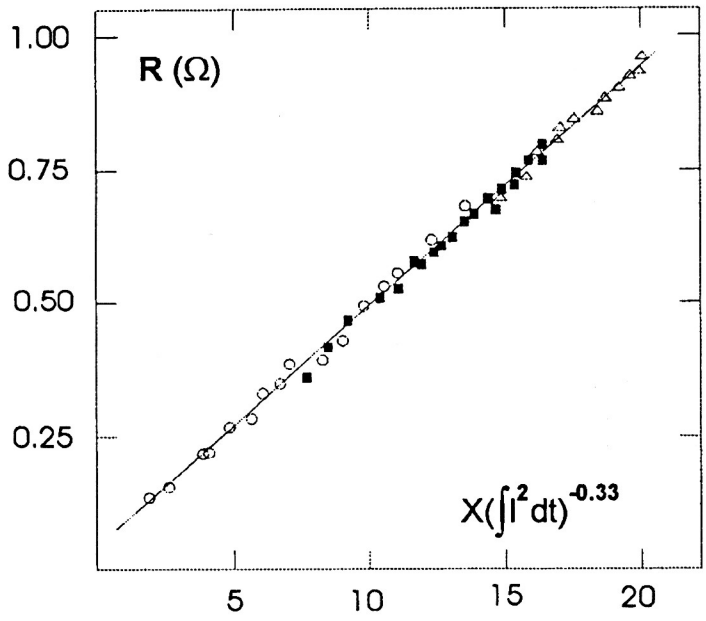

Fig. 2. Resistance versus current integral in case Z-pinch for different lenghts: o X = 5 cm, ■ X = 10 cm, Δ X = 15 cm

4. CONCLUDING REMARKS

It is shown that spectroscopic experiments with electrical gas discharge as a plasma source could be used for determination of other, particularly electrical plasma parameters.

Acknowledgment: This paper is supported by the Ministry for Science and Technology of Republic of Serbia.

References

Goldbach C., Nollez G. and Peyruraux R.: 1972, JQSRT **12,** 1089.
Goldbach C., Nollez G., Popović S. and Popović M.M.: 1978, Z. Naturforsch. 33a,11.
Popovic M. M. et al.: 1976, *in Gas Discharge* (ed. C. Grey Morgan), IEE Conf. Publ. No. 143. London.
Popović M.M. and Popović S.:1986, in Strongly Coupled Plasma Physics (eds. F.J. Rogers and H. E. Dewit), Plenum Press, N.Y.

Publ. Astron. Obs. Belgrade No. 61 (1998), 151 – 154 *Poster paper*

STARK PARAMETER GENERAL REGULARITIES FOR THE ION LINES

J. PURIĆ[1] and M. ŠĆEPANOVIĆ[2]

[1] *Faculty of Physics, University of Belgrade, P. O .Box 368, 11001 Belgrade, Yugoslavia*
[2] **Faculty of Sciences and Mathematics, University of Montenegro, P. O.Box 211, 81000 Podgorica, Yugoslavia*

1. INTRODUCTION

Stark widths and shifts published data (Griem, 1974; Dimitrijević, 1998, 1993.a,b; Dimitrijević and Sahal-Bréchot,1992. a,b,c,d, 1993.a,b,c,d, 1996; Dimitrijević *et al.* 1994, 1996, Popović and Dimitrijević 1996; Popović *et al.* 1993.) and their dependence on the upper level ionization potential (Purć, 1996; Purć *et al.* 1993.) χ are used here to demonstrate the existence of the other kinds of regularities within similar spectra of different elements and their ionization stages. The emphasis is on the Stark parameter dependence on the rest core charge and the electron temperatures for the lines from similar spectra. The found relations connecting Stark broadening and shift parameters and upper level ionization potential, rest core charge and electron temperature were used for a prediction of new Stark broadening data, avoiding much more complicated procedures. For opacity calculations and investigation of stellar atmosphere, when a large number of line broadening data was required, present investigation are useful in enlarging the number of needed data. This field of research remains largely open to other demonstrations of regularities and similarities, as long as one can relate the same kind of spectroscopic transition. Also, the obtained dependencies can be used as an additional criterion for checking accuracy of the particular theoretical and experimental data from different sources.

Stark widths dependencies on the rest core charge and electron temperatures within spectral lines originating from 2p-nd (n=3,4,5); 2s-np (n=2,3); 2p-3s; 3d-np (n=4,5); 3d-4f; 3p-nd (n=3,4,5); 3p-ns (n=4,5); 3s-np (n=3,4,5); 4s-np (n=4,5); 4p-nd (n=4,5); 4p-5s; 5p-5d; 5s-5p under the same plasma conditions have been found and discussed here. After being well established and checked using existing theoretical (Purć 1996) data the dependencies can be used to predict additional Stark broadening data for the lines for which there is neither theoretical nor experimental data so far.

2. REGULARITIES

In order to investigate Stark parameters regularities an accurate set of theoretical and experimental data is needed for a multiplet, supermultiplet transition array, homologous, isoelectronic and isonuclear sequences or the same type of transition along

the Periodical system of elements for different stages of ionization under the same plasma conditions characterized by particular electron density and electron temperature. Therefore the Stark parameters dependencies on the electron density and electron temperature has to be well determined to make it possible to normalize data given for different temperatures and densities to particular ones at which the other types of regularities have to be investigated. Of special interest are dependencies on the rest core charge of the emitter within isoelectronic or isonuclear sequences or on the nuclear charge number within particular transition of homologous group of atoms or ions and on the upper level ionization potential in all the above mentioned cases.

The Stark parameter dependence on the electron density is well established and in the case of nonhydrogenic emitters is linear. However, Stark paramter dependence on the electron temperature is of different kind from line to line in every spectrum. Therefore, the correction to temperature dependence has to be done with a great care for all data used in particular case of the verification of certain type of mentioned dependencies. For instance instead of usually used temperature dependencies as $T^{-1/2}$ for ion lines, one has to use the whole spectrum of the functions from line to line of the form:

$$W = f(T) = A + BT^{-C} \tag{1}$$

Different kinds of regularities within Stark parameters of the given spectra can be explained on the bases of their dependencies on the upper level ionization potential (Purć 1996; Purć *et al.* and Refs. therein). A general form of that dependence in the case of the particular transition array along the Periodical table of the elements is:

$$W = N_E f(T) z^c a \chi^{-b} \tag{2}$$

where w is line width in angular frequency units; χ is the corresponding upper level ionization potential expressed in eV; z is the rest core charge of the emitter seeing by the electron undergoing transition. Coefficients a, b and c are independent of the temperature, ionization potential and the electron density for a particular transition.

The procedure for Stark broadening data predictions was described elsewhere (Purć 1996; Purć *et al.* and Refs. therein). A comprehensive set of Stark broadening data of the investigated ions has been used here to demonstrate the existence of Stark width data regularities within this group of spectral lines.

3. RESULTS AND DISCUSION

It has been verified that the Eq. (2) is appropriate for all the investigated transitions in all groups of the ions, above mentioned, at different temperatures and electron densities. Namely, it was found that the best fit can be obtained if $f(T)$ is taken as given by Eq. (1) instead $T^{-1/2}$. As an example, the reduced Stark width:

$$W^* = w f(T) z^{-c/a} \chi^{-b} \tag{3}$$

as the function of the inverse value of the upper level ionization potential χ of the corresponding transition is given in Fig. 1 for all of that transitions.

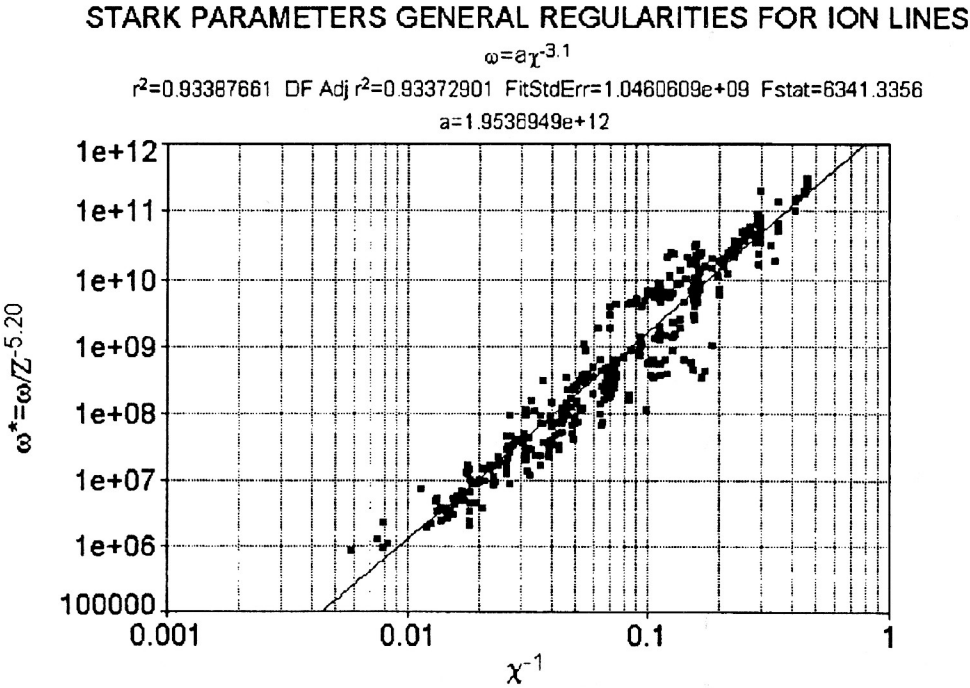

Fig. 1

By a comparison of the above described regularities and those presented elsewhere (Dimitrijević 1993a). one can conclude that the method used here differs in the choice of the variable conveying atomic structure information. Prior work (Purć *et al.* and Refs. therein) was based on the hydrogenic model. Consequently, it used integer principal quantum numbers instead of the upper level ionization potential. Although both parameters take into account the density of states perturbing the emitting state, the advantages of the present method are: (i) χ based trend analyses achieve better fits; (ii) in χ values the lowering of the ionization potential (Teller 1937) is taken into account, predicting merging with continuum when the plasma environment causes a line's upper state ionization potential to approach zero; and (iii) the ω dependence on χ is theoretically expected (Purć 1996).

The corresponding correlation's factor was almost equal to unity. Less then 17% of all our data correspond to values that are twice bigger than prediction values. Therefore, the Eq. (3) can be used to calculate Stark widths of the multiply charged ion from this transition of different elements along the Periodic table of the elements not calculate so far taking T and χ in K and eV, respectively. All data is at an electron density $N_e = 1 \times 10^{23}$ m^{-3} for different temperatures being normalised using the Eq. (1) at $T = 10^5$ K.

4. CONCLUSION

Stark parameters dependence on the upper level ionization potential, after being well established within particular transition array can be used for prediction of the parameters for the corresponding ion of heavier elements where not available so far. The electron-impact widths predicted by intratransition arrays regressions analyses are of the same accuracy as the accuracy of the results used in the course of the calculation of coefficients a, b and c from Eq. (2). In order to generate widths for lines of heavier elements from this types of transitions one has to find the upper level ionisation potential for that lines and substitute it in the Eq. (3) using the coefficient as anb b obtained from Fig. 1 and taking that the coefficient c=5.20. This method used here is computationally simple, involving each line's upper level ioniation potential and one multiplicative and one exponential fitting parameter per the investigated group of spectral lines originating from all of the investigated transition arrays, for the given emitter, temperatures and electron densities. Such method is conductive to the method's incorporation into mathematical simulations of stellar atmosphere opacities.

References

Blagojević, B., Popović, M. V., Konjević, N., Dimitrijević, M.S.: 1994, *Physical Review* E, **50**, 2986.

Griem, H.R.: 1974, Spectral Line Broadening by Plasmas New York; Academic.

Dimitrijević, M.S.: 1988, *Astron. Astrophys. Suppl. Series*, **76**, 53.

Dimitrijević, M.S.: 1993a, *Astron. Astrophys. Suppl. Series*, **100**, 237.

Dimitrijević, M.S.: 1993b, *Astro. Lett. And Communications*, **28**, 381.

Dimitrijević, M.S., Sahal-Bréchot, S.: 1992a, *J.Q.S.R.T*, **48**, 397.

Dimitrijević, M.S., Sahal-Bréchot, S.: 1992b, *Astron. Astrophys. Suppl. Series*, **96**, 613.

Dimitrijević, M.S., Sahal-Bréchot, S.: 1992c, *Astron. Astrophys. Suppl. Series*, **95**, 109.

Dimitrijević, M.S., Sahal-Bréchot, S.: 1992d, *Astron. Astrophys. Suppl. Series*, **93**, 359.

Dimitrijević, M.S., Sahal-Bréchot, S.: 1993a, *Astron. Astrophys. Suppl. Series*, **101**, 587.

Dimitrijević, M.S., Sahal-Bréchot, S.: 1993b, *J.Q.S.R.T.* **49**, No 2, 157.

Dimitrijević, M.S., Sahal-Bréchot, S.: 1993c, *Astron. Astrophys. Suppl. Series*, **99**, 585.

Dimitrijević, M.S., Sahal-Bréchot, S.: 1993d, *Astron. Astrophys. Suppl. Series*, **100**, 237.

Dimitrijević, M.S., Sahal-Bréchot, S.: 1996, *Physica Scripta*, **54**, 50.

Dimitrijević, M.S., Djurić, Z., Mihajlov, A.A.: 1994, *J. Phys. D: Appl. Phys.* **27**, 247.

Dimitrijević, M.S., Djeniže, S., Srećković, A., Platiša, M.: 1996, *Physica Scripta*, **53**, 545.

Inglis, D.R., Teller, E.: 1937, *Astrophys. J.* **90**, 439.

Popović, L.Č., Dimitrijević, M.S.: 1996, *Physica Scripta*, **53**, 325.

Popović, L.Č., Vince, I., Dimitrijević, M.S.: 1993, *Astron. Astrophys. Suppl. Series*, **102**, 17.

Purć, J.: 1996, *Journal of Applied Spectroscopy*, **63**, 816.

Purć, J., Miller, M.H., Lesage, A.: 1993, *Astrophys. J.* **416**, 825.

Publ. Astron. Obs. Belgrade No. 61 (1998), 155 – 158 *Contributed paper*

OPTICAL AND SPECTROSCOPIC INVESTIGATIONS OF ARC DISCHARGE AT FULLERENE SYNTHESIS

V.D. Shimanovich, I.P. Smyaglikov, A.I. Zolotovsky, S.M. Pankovets
Institute of Molecular and Atomic Physics,
National Academy of Sciences of Belarus
Scoryna Av. 70, 220072 Minsk, Belarus, phone (017) 2841434

Abstract. Quasi-periodic time-spatial structure of an arc was found out in a mode of fullerene synthesis. Spatial distributions of the spectral component radiation of arc plasma were studied, and radial profiles of temperature were measured. Mechanism of cathode deposit formation is also discussed.

1. INTRODUCTION

The most perspective approach to study the processes of fullerene formation is an experimental determination of plasma characteristics of the arc between graphite electrodes in inert gases at lowered pressures. Saito and Inagaki (1993) observed only C_2 bands and lines of C and C^+ in emission spectra of such arc. Afanasiev et al. (1994) measured average over discharge gap temperature of plasma by molecular bands of C_2 and CN, and found it to be T = 5000-7000 K, depending on the discharge mode. Similar temperatures were obtained by Huczko et al. (1995) for AC arc. All this results based on assumptions about stability of the arc plasma. However, according to Finkelnburg and Maekker (1961), the DC arc is a non-uniform and non-stationary plasmoid in many operation modes.

The research of pulsation characteristics of carbon arcs at current I = 60÷100 A and helium pressures P_0 = 1÷500 Torr was carried out in the present work. The 6 mm rods of pure graphite were used as electrodes, the discharge gap amounted ~5 mm and the arc voltage was U = 20÷40 V.

2. TIME-SPATIAL STRUCTURE OF THE ARC

The change of shape of electrodes during the discharge is one of possible reasons of the arc plasma instability. Within the first several seconds after arc ignition, relatively uniform layer of carbon deposit is formed on the cathode. At the subsequent discharge stages the deposit is grew on periphery of the cathode end face and its lateral surface. Two areas are distinctly observed in the section of cathode deposit. The internal part of deposit has some millimetres in diameter and represents friable structure, consisting of a mix of nanoparticles, nanotubes and amorphous carbon (see for example Ebbesen and Ajayan (1992)). The hard external metallic-grey shell is formed from needle and sector

structures focused mainly in a direction of their growth. For some arc modes there is a hollow crater in the central zone of cathode deposit. The formation of cathode deposit may result in changing the mode of cathode operations and discharge parameters during a work cycle of fullerene synthesis.

The faster processes in the near-electrode regions of discharge result in pulsations of plasma parameters. In the present work, pulsation characteristics were studied with the help of high-speed camera in modes of imaging and continuous scanning with time resolution up to 1 μs. The analysis of obtained data shows, that the considered carbon arc may operate in two modes, distinguished by time-spatial structure. The first mode concerns to the diffuse symmetric stationary arc channel with uniform anode erosion, and other represents non-uniform and non-stationary structure with quasi-periodic pulsations of brightness with frequency 10÷20 kHz. As the high-speed imaging has shown, the diameter of current-conducting channel decreases in this mode, and the channel is bent and continuously displaced in space like moving "spiral" arc, described by Asinovsky et al. (1976).

The transition of arc into non-stationary mode is accompanied by voltage drop of 4÷6 V and by considerable rise of plasmoid brightness. The brightness pulsations correspond to voltage pulsations with amplitude 0.5÷2 V. When increasing the duration of non-stationary stage, the pulsation is increased in frequency and disturbed in periodicity. The mode transition occurs spontaneously every 0.5÷5 ms and does not depend on discharge external parameters. Times of existence of the modes, structure and frequency of pulsations in the non-stationary stage of discharge depend on pressure, kind of gas as well as on arc current. At $P_0 = 100$ Torr the total duration of non-stationary mode is approximately equal to that of arc in stationary stage. At pressure lower 1 Torr only the non-stationary mode exists.

3. EMISSION SPECTRA OF THE ARC AND PLASMA DIAGNOSTICS

The emission spectra of arc plasma were registered in visible and UV areas by diffraction and prism spectrographs with reverse linear dispersion 6 Å/mm. It was found that spectra do not contain components of radiation of other molecules, except for earlier observable C_2 and CN. In addition to the data of Afanasiev et al. (1994) and Saito and Inagaki (1993), the band near λ = 2320 Å was found out in UV area. This band, according to Landsverk (1939), belongs to molecule C_2 or molecular ion C_2^+. It is necessary to note also registration of the line of carbon double ion at λ = 2296 Å.

The intensities of spectral component have approximately identical distributions over the arc radius. The distinctions are observed in distributions over length of discharge. Molecule CN radiates approximately equally over whole discharge gap. For bands C_2 and lines of carbon atoms and ions, the

maxima of radiation are observed in near-electrode regions. The intensity of C_2 near the anode is much higher than that near the cathode, and the radiation of ions is located in cathode region in the main. The molecular band close $\lambda =$ 2320 Å emitted mainly near the cathode.

In the present work the radial distributions of arc temperature were measured in approximation of stationary equilibrium plasma. The radial distributions of spectral emissivity were calculated by Abel inversion of registered integrated chordal intensities. The measurements were carried out by Fowler-Milne method from band edges of C_2 5165 and 4737 Å for arc cross-section at distance ~1 mm from the anode at initial helium pressure in the chamber P_0 = 1 and 100 Torr. The results of measurements by different molecular bands are well consistent. Instrumental uncertainty of temperature determination does not exceed 10%. Maximal plasma temperature was found to be T = 4100 and 4500 K, for initial helium pressure P_0 = 1 and 100 Torr respectively. Temperature of plasma monotonously falls down to periphery of the discharge. The temperature profile at P_0 = 1 Torr lies below by ~500 K relatively the profile at P_0 = 100 Torr.

4. DISCUSSION

The results of performed optical and spectroscopic investigations of the arc discharge in fullerene synthesis mode may be interpreted in view of properties of plasma with carbon particles as follows.

The plasma parameters are determined by processes at electrodes. The electrons, emitted by the heated up cathode, ionize the gas at collisions. The formed ions under action of an electrical field are directed to the cathode and take part in creation of deposit on its surface. According to Abrahamson (1974) the important role in the cathode deposit formation may belong to carbon crystallites arising from erosion of the anode. When heating in plasma the crystallites get a positive charge due to thermoemission. Thus, the cathode deposit is a result of deposition of the ions and positively charged carbon particles, accelerated by an electrical field, as well as of physical and chemical transformations during high temperature growth and subsequent cooling.

Instability of arc in question is substantially caused by a competition of physical processes under entering of carbon vapour and particles from the anode into the arc and removing them from a zone of the discharge. At small content of carbon atoms and crystallites in plasma, the quasi-periodic fluctuations of plasma arise from development of overheating instability, described by Alexandrov and Ruhadze (1976). This accompanied by contraction of cylindrical arc channel into spiral-like one with an anode spot formation, that lead to rising of input energy density on the anode surface. The increase of erosive flow results in rising the plasma thermal conductivity, therefore the

overheating instability is dumped and non-stationary arc passes into the stationary mode. The increase of electron emission due to heated carbon particles reduces the current density near anode and also promotes the suppression of overheating instability. The arc mode transition repeats repeatedly during all time of the arc discharge existence.

The obtained emission spectra of the arc appear to be superposition of spectra of plasma both in stationary and non-stationary modes. The molecules C_2 and CN are the coolest components of plasma of considered discharge. Their radiation may be attributed to the stationary mode with uniform anode erosion. The excitation of ion lines in spectra is apparently due to increase of temperature in the non-stationary arc. Thus, it is possible to assume that measured radial temperature distributions correspond to the stationary mode of arc discharge.

The obtained information on processes in carbon arc at the lowered pressure of helium should be taken into account when measuring the plasma parameters, developing the models of fullerene formation in the arc and designing the reactors for fullerene synthesis.

This work was carried out under support of the Fund of fundamental investigations of Belarus.

References:

Abrahamson J.: 1974, *Carbon* **12**, 111.

Afanasiev D., Blinov I., Bogdanov A., Djuzhev G., Karataev V. and Kruglikov A.: 1994, *J. Technical Physics* **64**, № 10, 76 (*in Russian*).

Alexandrov A.F. and Ruhadze A.A.: **1976**, *Physics of high current electrodischarge sources of light*, Moscow (*in Russian*).

Asinovsky E.I., Afanasiev A.A. and Pakhomov E.P.: 1976, *Reports of Academy of Sciences of USSR* **231**, 326 (*in Russian*).

Ebbesen T.W. and Ajayan P.M.: 1992, *Nature* **358**, 220.

Finkelnburg V. and Maekker G.: 1961, *Electrical arcs and thermal plasma*, Moscow (*in Russian*).

Huczko A., Lange H., Resztak A. and Buszewski P.: 1995, *High Temp. Chem. Proc.* **4**, 125.

Landsverk O.G.: 1939, Phys. Rew. **56**, № 8. 769.

Saito Y. and Inagaki M.: 1993, *Jpn. J. Appl. Phys.* **32**, L954.

Publ. Astron. Obs. Belgrade No. 61 (1998), 159 – 162 *Poster paper*

ON THE STARK WIDTH REGULARITIES IN THE Ar II SPECTRUM: 4s-4p AND 3d-4p TRANSITIONS

A. SREĆKOVIĆ and S. DJENIŽE
Faculty of Physics, University of Belgrade
P.O.B. 368, 11001 Belgrade, Serbia, Yugoslavia

1. INTRODUCTION

The great number of the papers (Fuhr and Lesage 1993, and references therein; Pellerin *et al.* 1997) devoted to the Stark width of the singly ionized argon (Ar II) spectral lines testify to their topicality in the plasma diagnostic. The aim of this paper is to establish regularities of Stark HWHM (half-width at half intensity maximum, w) along a one type of the quantum transition in the Ar II spectrum. Namely, with the established regularities a quick and reliable estimation of the Stark HWHM values is possible that have not yet been measured or calculated. We have established trends of the Stark HWHM within 4s-4p and 3d-4p type of transitions. In view of these regularities new measurements of these Stark HWHM values can be recommended.

2. REGULARITIES

The simplest way to estimate values of Stark HWHM is to use the established regularities of w along the same type of quantum transition in the ionic spectra (Djeniže *et al.* 1989 and references therein). On the basis of the existing experimental Stark HWHM values of the spectral lines that belong to 4p-4d transition in the Ar II spectrum it was found (Djeniže *et al.* 1989) that simple analytical relationship exists between w and corresponding upper-level ionization potential (I) of a particular spectral line for the same type of the transition. The found relationship, normalized to a $N = 1 \times 10^{23}\ \mathrm{m}^{-3}$ electron density, is of the form:

$$w = aT^{-1/2}I^{-b} \quad (\mathrm{rad/s}). \tag{1}$$

The upper-level ionization potential I (in eV) specifies the emitting ions, while the electron temperature T (in K) characterizes the assembly. The coefficients a and b are independent of I and T. The found form in the case of the 4p-4d transition is presented in Djeniže *et al.* (1989). This relationship was confirmed by new w experimental results (Srećković and Djeniže 1998). On the basis of Eq. (2) in Djeniže *et al.* (1989) it was possible to predict w values for the spectral lines that have not been measured

or calculated before. These predictions were summarized in Srećković and Djeniže (1998). In the meantime, since 1989, the results of the new Stark HWHM values have been published for various transitions of the singly ionized argon. These values, and those before 1989, enable establishing the trend of the Stark HWHM values along the 4s-4p and 3d-4p transitions. In Figs. 1 and 2 we present, graphically, the reduced Stark widths ($wT^{1/2}$) vs the inverse value of the upper-level ionization potential (1/ I) for: 4s-4p and 3d-4p type of transitions, respectively. The necessary atomic data were taken from Wiese *et al.* (1969).

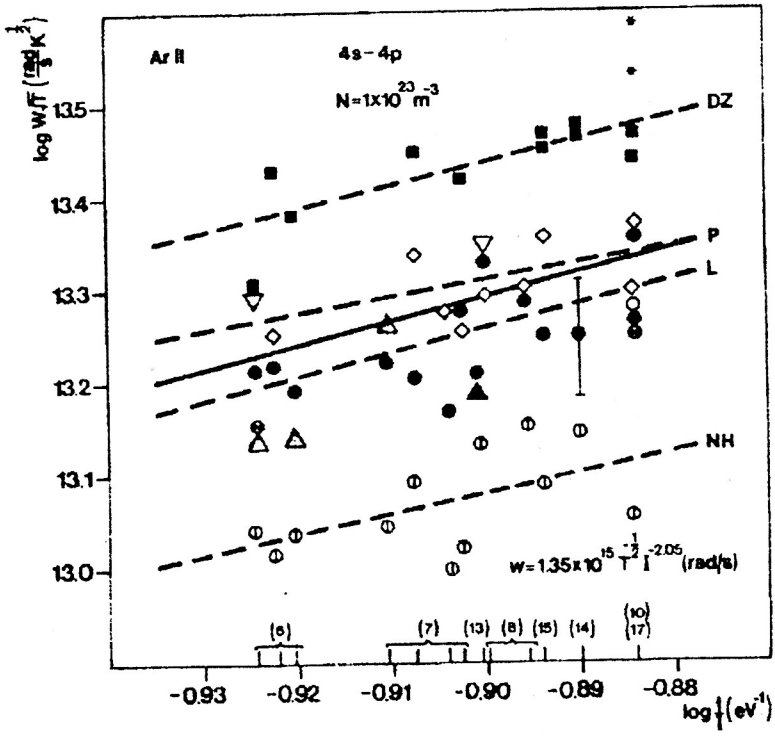

Fig. 1. Reduced Stark HWHM ($wT^{1/2}$) vs inverse value of the upper-level ionization potential at 1×10^{23} m^{-3} electron density. —, established trend; •, Labat *et al.* 1974 (L); Φ, Nick and Helbig 1986 (NH); ■, Dzierżega and Musiol 1994 (DZ); ◇, Pellerin *et al.* 1997 (P); ○, Djeniže *et al.* 1989; ▲ , Konjević *et al.* 1970; ▽, Chapelle *et al.* 1968; Δ, Vitel and Skowronek 1987; ⊗, Aparicio *et al.* (1997); *, Mazing and Vrubljovskaia (1962).

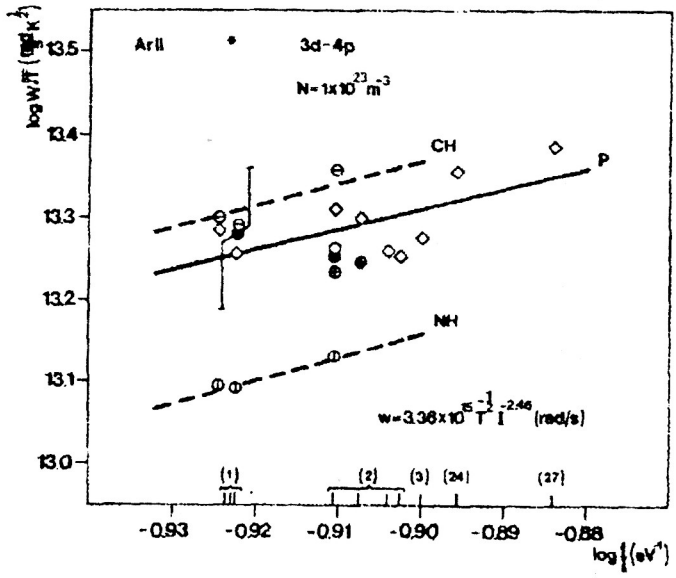

Fig. 2. Same as in Fig. 1. Complement: Θ, Chapelle *et al.* 1967 (CH); ⊕, Lhuissier (1987).

An evident scatter exists between experimental Stark HWHM values. However, one can conclude that in the selected particular experiments (L, NH, DZ, P, CH) (Labat *et al.* 1974; Nick and Helbig 1986; Dzierżega and Musiol 1994; Pellerin *et al.* 1997, Chapelle *et al.* 1967) the measured Stark HWHM values follow also regularities described by Eq. (1) (dashed lines in Figs. 1 and 2). The full lines show their averaged values. In order to ilustrate the magnitude of the scatter of the reduced Stark HWHM values we have their uncertainties (± 20%), like error bars, presented in Figs 1 and 2. The averaged values can be expressed by formulae:

$$w_{4s-4p} = 1.35 \times 10^{15} T^{-1/2} I^{-2.05} \quad \text{(rad/s)}. \tag{2}$$

$$w_{3d-4p} = 3.36 \times 10^{15} T^{-1/2} I^{-2.46} \quad \text{(rad/s)}. \tag{2}$$

3. CONCLUSION

On the basis of the existing experimental data we have established trends for Stark HWHM values for spectral lines that belong to 4s-4p and 3d-4p transitions. The evident scatter between results of particular experiments can be explained on the basis of various uncertainties of the electron density and temperature measurements in these experiments. It should be pointed out that these experiments were performed with various plasma sources and the plasma parameters were obtained using various diagnostics methods. In any case, new measurements of the Stark HWHM values for spectral lines that belong to 4s-4p and 3d-4p transitions would be helpful.

Acknowledgements

This research is a part of the project "Plasma Spectroscopy" supported by Ministry of Science and Technology of the Republic of Serbia.

References

Aparicio, J.A., Gigosos, M.A., Mar, S., Gonzales, V.R.: 1997, "Spectral Line Shapes", Vol. 9, 151, AIP Conf. Proceed. 386, Woodbury, New York.

Chapelle, J., Cabannes, F., Blandin, J.: 1968, *JQSRT*, **8**, 1201.

Chapelle, J., Cabannes, F., Blandin, J.: 1967, *C.R.H. Acad. Sci.*, Ser. B **264**, 853.

Djeniže, S., Malešević, M., Srećković, A., Milosavljević, M., Purić, J.: 1989, *JQSRT*, **42**, 429.

Dzierżega, K., Musiol, K.: 1994, *JQSRT*, **52**, 747.

Fuhr, J.R., Lesage, A.: 1993, Bibliography on Atomic Line Shapes and Shifts, (July 1978 through March 1992) NIST Special Publication 366 Supplement 4, US DC National Institute of Standards and Technology.

Konjević, N., Labat, J., Ćirković, Lj., Purić, J.: 1970, *Z. Phys.* **235**, 35.

Labat, J., Djeniže, S., Ćirković, Lj., Purić, J.: 1974, *J. Phys.* B., **7**, 1174.

Lhuissier, J.F.: 1987, Thesis, Ruen, France (unpublished).

Mazing, M.A., Vrubljovskaia, N.A.: 1962, Optik. Spektroskop. (in Russian), XIII, 308.

Nick, K.P., Helbig, V.: 1986, *Phys. Scripta*, **33**, 55.

Pellerin, S., Musiol, K., Chapelle, J.: 1997, *JQSRT*, **57**, 377.

Srećković, A., Djeniže, S.: 1998, *Proceed. the 19th SPIG*, Zlatibor, Serbia, Yugoslavia.

Vitel, Y., Skowronek, M.: 1987, *J. Phys.* B. **20**, 6477.

Wiese, W.L., Smith, M.W., Miles, B.M.: 1969, "Atomic Transition Probabilities", Vol. II, NSRDS-NBS 22 (U. S. Government Printing Office, Washington, DC.).

Publ. Astron. Obs. Belgrade No. 61 (1998), 163 – 166 *Poster paper*

POWERFUL SHOCK WAVES RADIATION IN AIR I

K.L. STEPANOV, L.K. STANCHITS, Y.A. STANKEVICH

Heat & Mass Transfer Institute, ul. Brovky, 15, 220072, Minsk, Belarus
E-mail kls@hmti.ac.by

Abstract. Problems related to the structure and radiation of a strong shock waves propagating in the Earth's atmosphere with velocities D≤50 km/s at heights H≤50 km are considered in this paper on the basis of real thermodynamic and optical properties of air. Data on shock adiabatic curves of air obtained both in the supposition of complete thermodynamic equilibrium of air behind the shock wave front, and with account of possible transparency of gas for self radiation are presented. The hierarchy of scales of various physical processes in a shock wave permitting to simplify solution of the problem concerning the front structure is considered. The modes of SW propagation, profiles of parameters, spatial scales, spectral and integrated radiation fluxes have been determined for various heights and velocities.

1. Hugoniot adiabatic curves. The condition of gas behind the shock wave front (SWF) is determined by thermodynamic parameters prior to break and the magnitude characterizing the wave's amplitude (for example its velocity D). If the equation of state is represented as that for ideal gas $\varepsilon = (\gamma - 1)^{-1} p / \rho$, the jump of pressure, density and temperature at the shock wave is determined by equations:

$$\frac{p_1}{p_0} = \frac{\gamma_0 M^2 + 1}{\gamma_1 + 1} + \frac{1}{\gamma_1 + 1}\sqrt{\gamma_0^2 M^4 - 2\gamma_0\left(\frac{\gamma_1^2 - 1}{\gamma_0 - 1} - 1\right) + \gamma_1^2}\,, \qquad (1)$$

$$\frac{\rho_1}{\rho_0} = \frac{(\gamma_1 + 1)p_1 + (\gamma_1 - 1)p_0}{(\gamma_0 + 1)p_0 + (\gamma_0 - 1)p_1}\frac{\gamma_0 - 1}{\gamma_1 - 1}, \qquad \frac{T_1}{T_0} = \frac{\mu_1}{\mu_0}\frac{p_1}{p_0}\frac{\rho_0}{\rho_1}, \qquad M = \frac{D}{\sqrt{\gamma_0 p_0 / \rho_0}}$$

Here M is the Mach number, index 0 corresponds to the state in front of the shock wave, 1 – to the state behind its front. The equation of the shock adiabatic curve represented as $\varepsilon_1 - \varepsilon_0 = (p_0 + p_1)\left(\rho_0^{-1} - \rho_1^{-1}\right)/2$, can be numerically calculated. The parameters of undisturbed air were taken from the CIRA atmosphere model. Composition and thermodynamic functions of air were determined according to equations of ionized and chemical equilibrium in Debye approximation of the large canonical ensemble (Romanov 1995). The results are presented in figs.1,which illustrates the dependence of temperature T_1 and compression $\delta = \rho_1 / \rho_0$ on shock wave velocity at various altitudes.

At sufficient transparency of plasma for its own radiation when absorption and emission processes are not compensated, spontaneous decay of excited levels, the processes of a photo- and dielectron recombination result in deviation from boltzmann population and shift ionization equilibrium in plasma to smaller ionization degree (Romanov 1988, Panasenko 1995). The shock adiabatic curves calculated as per the radiative-collision model in the supposition of a full transparency of plasma are shown in fig.2. Their comparison with equilibrium data is presented here in as well. As seen from the curves, noticeable differences in temperature and compression in SWF are observed at altitudes over 40-50 km. If partial reabsorbtion of radiation, which reduces the contribution of

radiative transitions in level population, is taken into account, the distinctions of shock adiabatic curves are maintained at altitudes H =60 km.

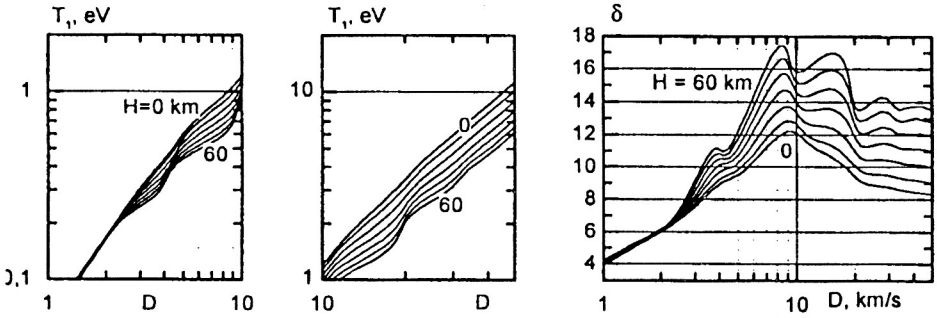

Fig. 1. Dependence of T_1 and compression δ from SW velocity D at various altitudes.

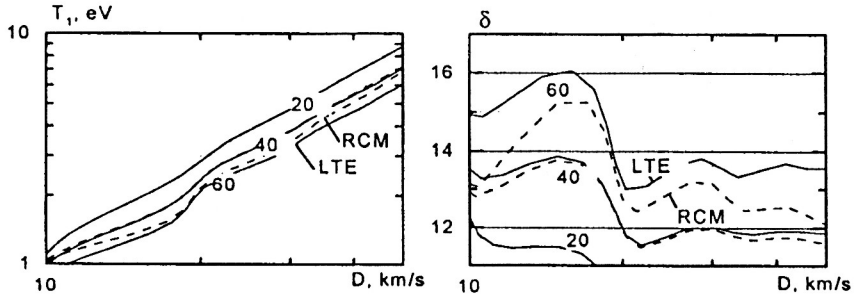

Fig. 2. Shock adiabatic curves of air at H=20, 40 and 60 km, obtained in LTE approximations and as per the RCM- model for transparent plasma.

2. The structure of a powerful SW front. Analysis of hierarchy of scales describing various physical processes indicates (Stepanov et al. 1998) that the largest scale of length is associated with plasma heat radiation free lengths. The radiation free length exceeds the scale of lengths of dissociation and ionization, the area of relaxation of electrons and heavy particles temperatures to uniform plasma temperature as well as the length of the zone, where electronic thermal conduction is considerable. Further it is supposed, that the dissociation and ionization processes «monitor» the medium's temperature and density, that the temperatures T_e=T_i, electronic thermal conduction is small as compared to radiation transfer. Therefor the problem concerning the structure can be formulated as a problem concerning radiation relaxation in the front of a powerful SW (Zeldovich 1966). Further we shall assume that the thickness of shock compressed gas behind the front is adequately for it to be optically dense. The structure of a SW having velocity D, is described by a set of gas dynamics and radiation transfer equations

$$\rho u = \rho_0 D\,, \quad p + \rho u^2 = p_0 + \rho_0 D^2\,, \quad \varepsilon + \frac{p}{\rho} + \frac{u^2}{2} + \frac{S}{\rho_0 D} = \varepsilon_0 + \frac{p_0}{\rho_0} + \frac{D^2}{2} + \frac{S_0}{\rho_0 D} \tag{2}$$

$$\mu \frac{dI_\nu}{dx} = \kappa_\nu (I_{\nu p} - I_\nu)\,, \qquad S_\nu = \int_{(4\pi)} I_\nu \Omega \, d\Omega\,, \qquad S = \int_0^\infty S_\nu d\nu \tag{3}$$

As the laws of conservation of mass and impulse determine linear dependence of pressure on the magnitude of inverse compression $p = p_0 + \rho_0 D^2 (1-\eta)$, $\eta = \rho_0 / \rho$, it is

possible to construct the tabulated equations $\varepsilon(T)$, $p(T)$, $\rho(T)$, dependent from one variable and describing the modification of gas characteristics in a wave. Then we find the relationship between T and S

$$S = S_0 - \rho_0 D F(T), \quad F(T) = \varepsilon(\eta) - \varepsilon_0 - \frac{p_0}{\rho_0}(1-\eta) - \frac{D^2}{2}(1-\eta)^2, \quad \eta = \eta(T) \tag{4}$$

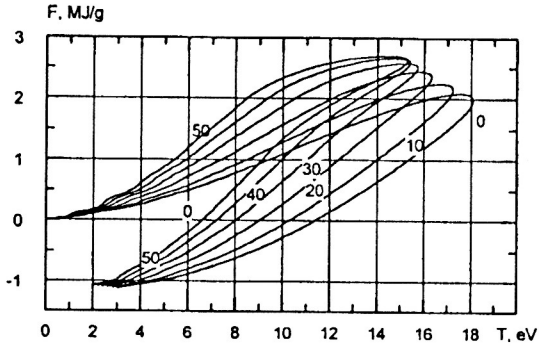

Fig. 3. F(T) for SW with D=50 at various H.

Function F(T) for a SW with a given velocity for various H is shown in fig.3. Flux $S = S_0$, i.e. $F(T_0) = 0$ corresponds to the initial state; in equilibrium state behind the SW front $S_1 = 0$ and $F(T_1) = S_0 / (\rho_0 D)$. As $S_0 < 0$, the final temperature behind the wave front will be less than if there was no outgoing radiation. If the energy emitted is neglected in comparison with the hydrodynamic energy flux ($S_0 << \rho_0 D^3 / 2$) T_1 is determined by condition $F(T_1) = 0$.

3. Diffusion "gray" approximation. In order to find a solution of the equations of radiation transfer and hydrodynamics it is necessary to set "good" initial profiles of parameters, to solve equations of spectral transfer, to determine radiation flux S and to construct a converging iterative process. Such a distribution of parameters can be found by considering the transfer in a gray diffusion approximation. The appropriate equations

$$\frac{dS}{d\tau} = c(U_p - U), \qquad S = -\frac{c}{3}\frac{dU}{d\tau}, \qquad U_p = \frac{4\sigma T^4}{c}, \tag{5}$$

where τ is the "average" optical variable ($d\tau = \kappa dx$), with account for of energy conservation law (5) can be reduced to a phase plane equation

$$\frac{dU}{dT} = -3\left(\frac{\rho_0 D}{c}\right)^2 \frac{F'(T)\left(F(T) - S_0/(\rho_0 D)\right)}{U_p(T) - U} \tag{6}$$

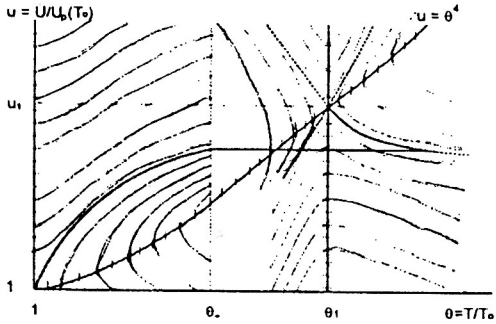

Fig. 4. The phase plane of (6) at $S_0 = 0$.

The phase plane of (6) is given in fig.4. Points of initial (0) and final (1) states are singular for (6) should satisfy conditions $T = T_i$: $U = U_p(T_i)$ $F(T_i) = 0$ $i = 0,1$. After the problem on the phase plane is solved, it is possible to find the distribution of T, ρ, S along τ counted from the SWF. The profiles of T and S along τ are shown in figs. 5 at H=50 km for SWs having velocities D=50, 30 and 20 km/s. Note a considerable difference in optical thickness of the warming up layer and relaxation area behind SWF.

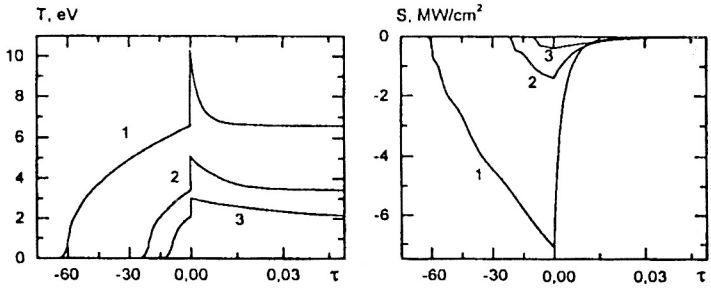

Fig.5. Distributions of T and S along τ. H= 50 km. 1-D=50 km/s, 2-D=30 km/s, 3-D=20 km/s.

4. Radiation transfer in real spectrum. The recalculation of gas-dynamic profiles from the optical variable τ to a spatial coordinate x was performed with account of the character of radiation transfer in various layers. In super critical amplitude waves temperature $T(\tau)$ varies weakly on scale $\Delta\tau = 1$ in the warming up zone. Radiation heat transfer occurs here in the mode of radiation thermal conductivity. Therefore it is natural to use the Rosseland free length. The distances from the viscous jump upwards along the flow were found by ratio $dx = L_R d\tau$. The Planck coefficient was used as the recalculation scale in the vicinity of the SW front and in the front part of the warming up zone ($dx = K_P^{-1} d\tau$). In the iterative process the most complicated problem is to obtain a self-consistent solution in the neighborhood of the front and periphery of the warming up zone. Here it is necessary to determine the average absorption coefficient $\overline{K}$, ($\Delta x = \Delta\tau / \overline{K}$) by averaging κ_ν on the field of self radiation.

Integral representation of the flux was used to describe radiation transfer

$$S_\nu^+(\tau_\nu) = 2\int_{\tau_\nu}^{\tau_1} S_{\nu p}(\tau')\left[\exp\left(-(\tau_\nu - \tau')\right) - (\tau_\nu - \tau')E_1(\tau_\nu - \tau')\right] d\tau' + S_{\nu 0}^+(\tau_\nu) \qquad (7)$$

$$S_\nu^-(\tau_\nu) = 2\int_{\tau_1}^{\tau_\nu} S_{\nu p}(\tau')\left[\exp\left(-(\tau' - \tau_\nu)\right) - (\tau' - \tau_\nu)E_1(\tau' - \tau_\nu)\right] d\tau' + S_{\nu 0}^-(\tau_\nu) \qquad (8)$$

The integral radiation was determined by direct integrating on spectrum. It overlapped the range of quantum energies, in which plasma radiation is considerable. In the range of quantum energies $E < 17.35$ eV, 560 spectral groups were taken, the averaging interval was 250 cm^{-1} (0.031 eV). Starting at 17.35 eV scale was used, on which the averaging spacing was set by a ratio $\Delta E_i = E_0 \cdot 10^{(i-560)/500}$, where $E_0 = 8.\cdot 10^{-2}$ eV. Thus 1300 spectral groups in the range of radiation transfer energy were used (fig.6).

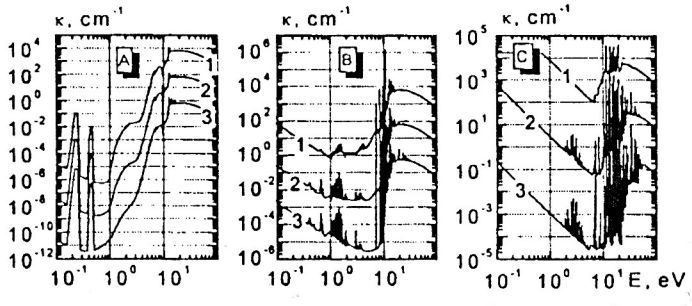

Fig. 6. Absorption coefficients of air. T=3·10³ K (A), 10⁴ B), 3.16 eV (C). 1 - $\rho_1 = 1.23\cdot 10^{-2}$ g/cm³, 2 - $\rho_2 = 10^{-2}\rho_1$, 3 - $\rho_3 = 10^{-4}\rho_1$.

Publ. Astron. Obs. Belgrade No. 61 (1998), 167 – 170 *Poster paper*

POWERFUL SHOCK WAVES RADIATION IN AIR II

K.L. STEPANOV, L.K. STANCHITS, Y.A. STANKEVICH

Heat & Mass Transfer Institute, ul. Brovky, 15, 220072, Minsk, Belarus
E-mail kls@hmti.ac.by

5. Calculation results. Further we shall consider the spatial structure of shock waves. Fig.7 illustrates the results of calculations of physical characteristics in the warming up zone before the shock wave at altitudes 30 km (in this case for convenience the wave is moving from left to right). The dependence on distance from the front of temperature, radiation flux, degrees of dissociation and ionization of air and compression in shock waves being propagated at velocities D = 50, 40 and 30 km/s is shown. Waves with such D at H>30 km are supercritical ones. Comparison of the dependence of a radiation flux and parameters α_D, α_i shows that maximum flow divergences correspond to sections where intensive gas disassociation and ionization takes place. As seen from the plots, disassociation and ionization waves are sufficiently strongly separated in space.

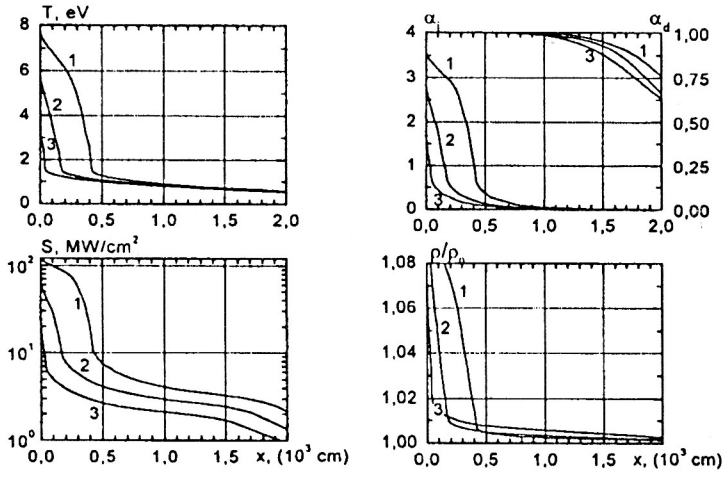

Fig. 7. Spatial parameter profiles at altitude H=30 km.
1 - D=50 km/s,
2 - D=40 km/s,
3 - D=30 km/s.

First of all it is necessary to note the very strong dependence of warming up area spatial scales on altitude. In particular, the ratio of distances from the front, at which temperature T=1 eV, at appropriate velocities is equal $(X_{50}/X_{40})_{T=1} \approx 40$ and $(X_{50}/X_{30})_{T=1} \approx 1.6 \cdot 10^3$ for all D>30 km/s. The ratio of distances, where the air completely is dissociated, $(X_{50}/X_{40})_{\alpha_d=1} \approx 35$ and $(X_{50}/X_{30})_{\alpha_d=1} \approx 1.5 \cdot 10^3$ and also poorly depends on the SW velocity. The ratio of distances from the front, on which single ionization of gas (α_i=1) is achieved, is equal $(X_{50}/X_{40})_{\alpha_i=1} = 40-50$ and $(X_{50}/X_{30})_{\alpha_i=1} = (2-5) \cdot 10^3$ At alteration of the altitude from H=40 to H =50 km the air density is reduced ba a factor of 4, and the ratio of densities at altitudes 30 and 50 km is $\rho_{30}/\rho_{50} = 18$. If it is taken into account that in the range of temperatures T = 1-10 eV the average Rosseland path of radiation is well approximated by dependence $L_R \sim \rho_0^{-\beta}$ where $\beta \approx 1.5$, it appears that it increases $(L_{50}/L_{40})_R = 8$ and $(L_{50}/L_{30})_R = 76$ times.

Therefor, the ratio of warming up area scales at various altitudes is approximately $(X_{H_1} / X_{H_2})_{T=1} = [(L_R / \rho_0)_{H_1} / (L_R / \rho_0)_{H_2}]$. Estimated data on the mass of the air layer heated by radiation (the area with $T \geq 1$ eV) for the considered modes of SW propagation are presented in Table 2 ($M \approx \rho_0 X_{T=1}$).

Table 1. Mass of gas heated by shock wave radiation (g/cm^2)

	D=50 km/s	D=40 km/s	D=30 km/s
H=50 km	1.5+0	1.0+0	7.0-1
H=40 km	1.5-1	1.0-1	7.0-2
H=30 km	1.5-2	1.0-2	7.0-3

The structure of SWs at altitude H=20 km with D=20 and D=50 km/s is presented in fig.8. In distinction from the previous data, the parameter profiles are given here for the area behind the SW front too. The following parameters are presented: temperature, radiation flux S and radiation flux in the "visible" area of the spectrum S_{vis} (1.5<E<6.5 eV, up to band Schumann-Runge), degrees of ionization and dissociation, free length in the visible range averaged on the local spectrum of radiation l_{vis}.

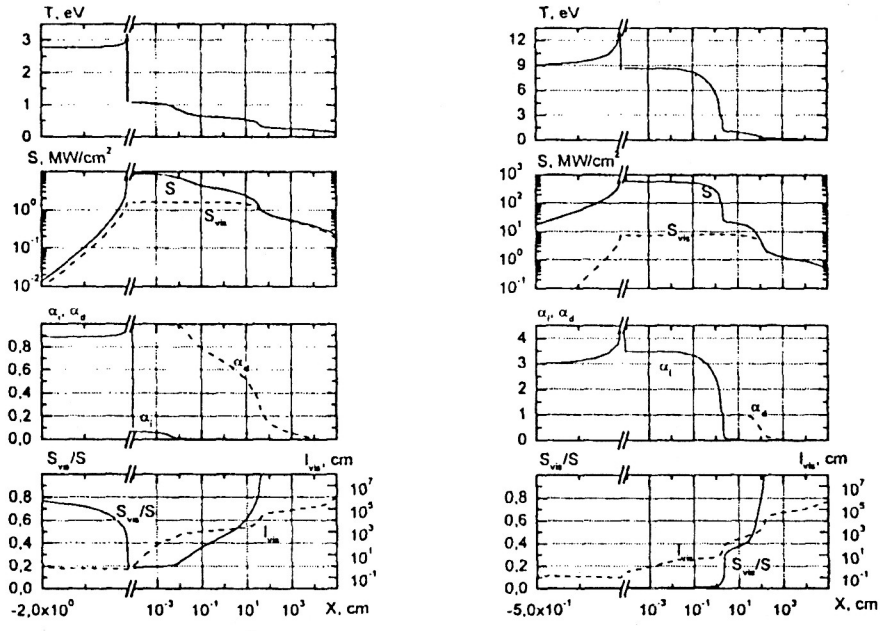

Fig. 8. Shock wave structure at H=20 km. **A** - D=20 km/s, **B** - D=50 km/s.

It is seen that at D=20 km/s "visible" radiation contain at SWF near 15% of full flux, at distance from front 40 cm radiative flux is completely "visible". For wave with D=50 km/s this part contain not much larger 1% at SWF and is completely "visible" at 10^2 cm from it. It is interesting nonmonotone alteration of the degree of ionization α_i. For ex-

ample, for H=20 km and D=50 km/s in precursor zone near SWF α_i =3.5, behind front is 4.2 and in final state α_i =3.

The spectra of radiation of shock waves at various distances from the viscous jump are presented on fig.9 and 10 for series D and H. The spectra of black-body radiation with equilibrium temperature T_1 and peak temperature T_+ are specified on the wave front. It is seen that for quantum with $E \leq 7$ eV the temperature peak is optically transparent, the radiation in this area is close to Planck radiation with T_1. The radiation flux in spectral lines is closer to $B_E(T_+)$. As a whole, the temperature peak radiates a spectrum characteristic for semitransparent layer.

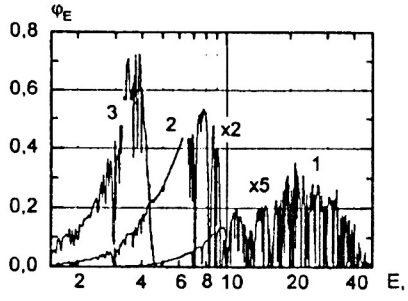

Fig. 9. Normalized spectrum of SW with D=50 km/s at H=30 km. 1 - distance from SWF x=50cm S=107 MW/cm^2; 2 - x=10^3, S=4; 3 - x=10^4, S=0.27.

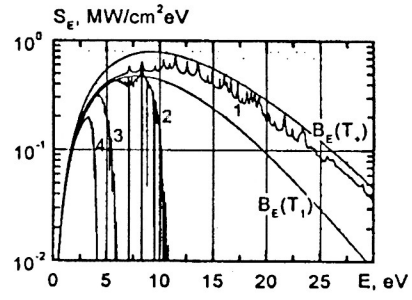

Fig. 10. Spectral radiation flux of SW with D=20 km/s at H=20 km. 1 - x=0, S=8.76 MW/cm^2; 2 - x=4 cm, S=2.92; 3 - x=55, S=0.93; 4 - x=9.2·10^3, S=0.405.

The space distributions of spectral and integrated radiation fluxes are determined by opacity of the air. At adequately large distances the entire radiation is concentrated in the visible area of the spectrum. The absorption coefficient in this range is small in comparison with other spectrum sections where the SW radiates. At temperatures ~ 10^3 K the absorption coefficient (Avilova, 1970; Landshoff, 1969) poorly depends on T, its dependence on quantum energy and density can be approximated by expression $\lg \kappa_E = E(4.33 - 0.66E) - 11.4 + 1.5\lg(\rho/\rho_0)$, where quantum energy E in eV and $\rho_0 = 1.23 \cdot 10^{-3}$ g/cm^3. The free length (with E=3 eV) in "cold" air at H= 30 km is ~ 10^7 cm.

At analysis of radiation exiting to "infinity" it is conventionally assumed that cold air is transparent for visible light. Noticeable absorbtion begins in the Schumann-Runge band at wave lengths $\lambda \leq 190$ nm. Large though final free lengths of visible radiation cause heating of gas up to temperatures T~(1-3)·10^3 K at large distances, the radiation flux is exponentially reduced. Therefore, the largest physical scale, which is the distance from the SW front to the boundary of the air dissociation area, can be adopted as the width of the warming zone. The radiation exiting from this boundary (conditionally $\alpha_d \approx 0.05$) is in the visible spectrum band and weakly excites the initial medium parameters. It may be considered as exiting to "infinity". When noticeable dissociation of air before the front is absent, the radiation exiting from the SW front practically is not screened. In this case the shock wave radiates as a black body with equilibrium tempera-

ture T_1, and the radiation flux to "infinity" is equal to the fraction of the visible spectrum of the total radiative flux σT_1^4. The flux of radiation exiting to "infinity" S_∞ and its fraction relative to the hydrodynamic flow of energy S_G thus calculated are contained in table 2. The results for S_∞ and α indicated in the usual font, were obtained according to

Table 2. SW energy flow $S_G = \rho_0 D^3 / 2$ (MW/cm^2), flux S_∞ and ratio $\alpha = S_\infty / S_G$ (%)

		D				
H		50	40	30	20	10
50	S_G	6.375	3.264	1.377	4.08-1	5.1-2
	S_∞	1.2-2	9.7-3	7.2-3	4.8-3	2.5-3
	α	1.88-1	2.97-1	5.23-1	1.18	4.9
40	S_G	2.54+1	1.30+1	5.495	1.628	2.035-1
	S_∞	5.2-2	4.1-2	3.1-2	2.07-2	1.04-2
	α	2.05-1	3.4-1	6.16-1	1.39	5.1
30	S_G	1.15+2	5.888+1	2.484+1	7.360	9.20-1
	S_∞	2.55-1	2.03-1	1.53-1	1.02-1	4.7-2
	α	2.22-1	3.45-1	6.2-1	1.4	5.1
20	S_G	5.556+2	2.845+2	1.200+2	3.556+1	4.445
	S_∞	1.32	1.08	8.08-1	5.37-1	**1.0-1**
	α	2.37-1	3.8-1	6.73-1	1.51	**2.81**
10	S_G	2.619+3	1.341+3	5.657+2	1.676+2	2.095+1
	S_∞	6.96	5.57	4.19	2.8	**1.28-1**
	α	2.66-1	4.15-1	7.4-1	1.67	**6.9-1**
0	S_G	7.688+3	3.936+3	1.660+3	4.920+2	6.15+1
	S_∞	2.21+1	17.7	12.9	8.61	**1.65-1**
	α	2.88-1	4.5-1	7.77-1	1.75	**2.68-1**

criterion $\alpha_d \approx 0.05$. For weaker shock waves (D=10 km/s, H=20 and 10 km) the gas before the front is not dissociated, and $S_\infty = \beta_{vis} \sigma T_1^4$ (bold font).

References

Romanov G.S., Stankevich Yu.A., Stanchits L.K.and Stepanov K.L.: 1995 Int. J. Heat Mass Transfer,.38, 545.

Romanov G.S., Stepanov K.L.and Stanchits L.K.: 1988 Sov. Plasma Physics, **14**, 1383.

Panasenko L.N., Romanov G.S., Stankevich Yu.A. and Stepanov K.L.: 1995 Russsian Engineer-Physical J, **68**, 569.

Stepanov K.L., Stanchits L.K., Stankevich Yu.A.: 1998, Preprint of Heat & Mass Transfer Institute №2, Minsk.

Zeldovich Ya.B., Raiser Yu.P. Physics of Shock Waves and High Temperature Hydrodynamic Phenomena. Moscow, Nauka, 1966.

Avilova I.V., Biberman L.M., Vorob'ev V.S. at al. The Optical Properties of Hot Air. Moscow, Nauka, 1970.

Landshoff R.K.M., Magee J.L. Thermal Radiation Phenomena. V.1. Radiative Properties of Air. N.Y.-W. 1969.

Publ. Astron. Obs. Belgrade No. 61 (1998), 171 – 174 *Contributed paper*

STUDIES ON RELAXATION PROCESSES IN LASER-PRODUCED PLASMA

N.V. Tarasenko
Institute of Molecular and Atomic Physics National Academy of Sciences of Belarus, 70 Scaryna Ave., 220072 Minsk, Belarus
E mail: lldp@imaph.bas-net.by

Abstract. Based on the results of quantitative spectroscopic diagnostics the character of relaxation of parameters (n_e, T_e, n_a) of recombining laser produced plasma has been analyzed.

Laser-produced plasmas in the recombination phase have been used for formation of atomic, molecular and cluster beams, for generation of laser oscillations, as X-ray and vacuum ultraviolet sources etc. (Schriever *et al,* 1998, Ohyanagi *et al,* 1996). For optimization of these applications and refined management of ablation plume characteristics it is of great importance the understanding the character of plasma parameters relaxation.

In the present paper based on diagnostics of plasma composition and its spatial-temporal changes at different irradiation conditions relaxation aspects of laser-produced plasma dynamics have been examined. The main attention has been focused on the temporal evolution of parameters (n_e, T_e, n_a) of recombining laser produced plasma, relaxation dynamics of the ionized and atomic states of Al after action of the excimer XeCl laser radiation (λ=308nm) on the Nd:YAG laser-ablated aluminum plume, the elucidation of self-regulating regime of recombining laser-produced plasma evolution with a frozen ionization state in the late stages.

Details of the experimental apparatus employed in studies of laser-produced plasma composition have been described elsewhere (Burakov *et al,* 1997). Briefly, plasma was produced by focusing of a Nd:YAG laser radiation (1064nm, 10ns, 100mJ, 10^8-10^9 W/cm^2) on the surface of the metallic (Al, Ti) samples in the helium (air) atmosphere at pressures of 0.1-500 Torr. Relaxation dynamics of the ionized and atomic states was studied by the time-resolved emission spectroscopy and laser-induced fluorescence (LIF) techniques. The electron density (n_e) was determined from the emission linewidth measurements according to the Stark broadening theory. The shapes of some selected lines were analyzed at different delay times (with respect to the leading edge of the laser pulse) in order to obtain the

temporal evolution of n_e. The electron temperature (T_e) was deduced by the relative intensities of lines from a given state of ionization.

Optical observation of the plasma emission was performed by imaging the section of the plasma plume onto the entrance slit of monochromator equipped by the fast photomultiplier. The emission spectra of plasma were recorded in the UV and visible region (spectral resolution of $\Delta\lambda \geq 3 \bullet 10^{-2}$nm) at different distances from the target surface. The detection of the photomultiplier signals was accomplished by a transient digitizer, connected to a personal computer for data processing, storage and analysis.

For LIF measurements a tunable dye laser radiation at the fundamental wavelength (560 - 630 nm) or its second harmonic was used to probe the ground state atoms and ions with the regular delay times after ablating laser pulse.

The emission spectra, electron temperature and density are found to be influenced by the irradiation conditions and ambient atmosphere. The profiles of the AlI 396.15nm line for different delays and the temporal evolution of electron density deduced from Stark broadening of this line are shown in the Fig.1.

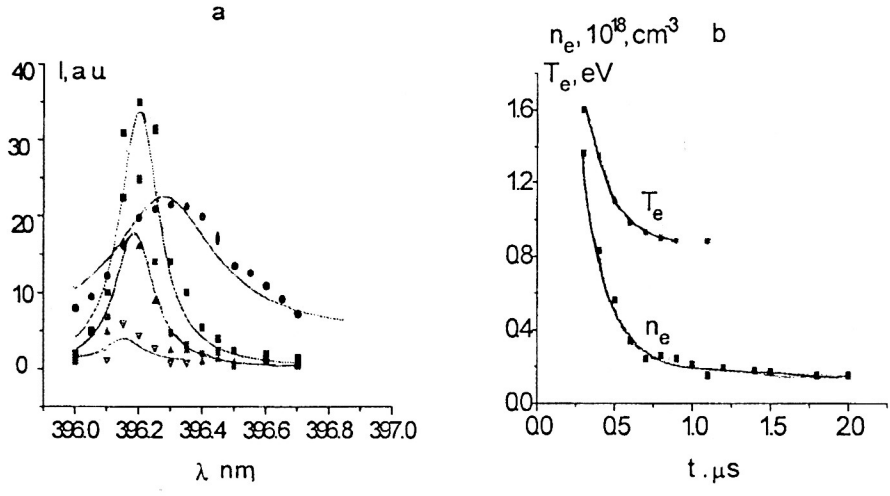

Fig.1. (a) AlI 396.15nm line Stark profiles at delays 0,4(•), 0,7(■), 1,0(Δ), and 2 μs (∇) after the ablating laser pulse and (b) time evolution of electron density (n_e) and temperature (T_e) in aluminum/air plasma at distance of 0.5mm from the target and laser irradiance of 500 MW/cm^2.

The temporal evolution of n_e for each distance can be characterized by an approximately biexponential decrease. The initial more fast decay rate can

be attributed to the propagation of the recombining plasma, while the slow decay is preferably due to the recombination processes. The electron temperature rapidly decreases in the time interval where maximal line emission is observed. After this time T_e is not practically changed with time, showing that there is a quasistationary equilibrium between the rates of cooling of electrons and their recombination heating.

The similar behavior of recombination dynamics with a very slow recombination of ions with electrons in the late stage has been observed in recombining titanium/air laser produced plasma. The characteristic recombination time essentially exceeded the gasdynamical expansion one. So, plasma has had time to fly apart without a complete recombination. It is supported by the temporal dependence of relative concentrations of ions and atoms as determined by fluorescence measurements. Such situation in recombination dynamics called "frozen" ionization is caused by decreasing of electron density and delivering the kinetic energy to them in the recombination process and as result there exist a tendency to maintain the plasma temperature.

Relaxation dynamics of the excited atomic states of Al after action of the excimer XeCl laser radiation (λ=308nm) on the Nd:YAG laser-ablated aluminum plume was studied by measuring the time histories of the AlI 396.15nm emission line. The relaxation rates were found to be dependent on distance from the target and XeCl laser pulse delays. The more shorter duration of the AlI 396.15nm signal, its faster decrease at longer delays and the change of the spectral shape (Fig.2) were observed. The results obtained indicated that the resonant photoionization of the Al atoms via $3^2D_{3/2}$ level with radiative recombination (predominantly at short delays), and collisional deexcitation of laser excited atomic level ($3d^2D_{3/2}$) with the excitation transfer to the adjacent $4p^2P^0$ levels resulting in the cascade of emission transitions $4p^2P^0$-$4s^2S$-$3p^2P^0$ were the most probable mechanisms of populating of Al ($4s^2S_{1/2}$) level.

So, time-resolved spectroscopic diagnostics of the recombining laser produced plasma allowed us to make some conclusions concerning character of relaxation of its parameters (n_e, T_e, n_a). The investigations showed, that it possible to distinguish two main stages in the time and space evolution of laser-induced plasma in gas environment. The first stage is associated with a plasma expansion. Plasma evolution in this stage is ruled mainly by processes with charged species (ionization by electron impact, and three-body electron-ion recombination). At the end of this stage plasma involving

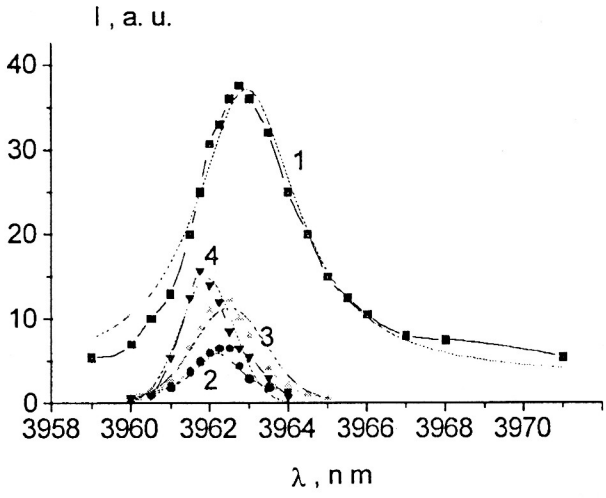

Fig.2. The XeCl laser produced AlI 396.15nm emission line profiles at delays 3 (2), 20 (3) and 46 μs (4) after the ablating Nd:YAG laser pulse and the AlI 396.15nm line profile from the Nd:YAG laser produced plasma in 150 Topp He atmosphere at the Nd:YAG laser irradiance of 500MW/cm^2 and the XeCl laser radiation intensity of 60MW/cm^2.

electrons and multicharged ions is turned to plasma consisting of atoms (molecules) and one-charged ions (predominantly in ground states). The processes that govern the ablation plume-gas dynamics in this stage are chemical kinetics of the ablated species with background gas, material or thermal diffusion in background gas, and cluster/particulate formation (condensation) as plasma cools.

The work has been supported by the Belorussian Foundation for Fundamental Researches under grant F95 -110.

References

Schriever G., Mager S., Naweed A., Engel A., Bergman K., and Lebert R.: 1998, *Appl. Optics* **37,** 1243.

Ohyanagi T., Miyashita A., Murakami K., and Yoda O.: 1996, *Jpn.J. Appl.Phys.* **35**, 3436.

Burakov V.S., Bokhonov A.F., Naumenkov P.,A., Nedel'ko M.I., and Tarasenko N.V.: 1998, *Zh. Prikl. Spectrosk.* **65,** 426.

Publ. Astron. Obs. Belgrade No. 61 (1998), 175 – 178 *Poster paper*

THE INFLUENCE OF THE FINE STRUCTURE TO THE HYDROGEN BALMER LINE SHAPES IN THE CONDITIONS TYPICAL FOR THE ANALYTICAL GLOW DISCHARGE CATHODE FALL REGION

I. R. VIDENOVIĆ and M. M. PLATIŠA
Faculty of Physics, University of Belgrade, P.O.Box 368, 11001 Belgrade, Yugoslavia

Abstract. The influence of the fine structure to the shapes of the hydrogen Balmer H_β and H_γ lines in the external electric field strengths in the range 0 - 20 kV/cm, and excited hydrogen atoms temperature ranging from 0.1 to 300 eV is studied. No significant deviations of the line shapes calculated with and without fine structure influence has been encountered. The reasonable accuracy of the simple symmetrical Stark manifold for the cathode fall region diagnostic purposes is approved.

1. INTRODUCTION

Knowledge of the external electric field axial distribution is essential for the diagnostics of the cathode fall region (CFR) of a glow discharge. The nonintrusive spectroscopic method for the determination of the electric field distribution in the CFR of various types of glow discharges have been employed in several recent experimental studies (Barbeau and Jolly, 1991; Ganguly and Garscadden, 1991; Donkó *et al.*, 1994; Videnović *et al.*, 1996). This method is based on the polarization-dependent Stark splitting coupled with Doppler broadening of hydrogen Balmer lines. The influence of the fine structure to the Stark profiles of the hydrogen H_β line is first investigated by Lüders (1951), providing Stark patterns of polarized H_β profiles for the electric fields of 2, 4 and 6 kV/cm. For the same electric field strengths, our previous studies (Videnović *et al.*, 1996, Videnović and Platiša, 1998) showed that, when the temperature of the emitters - excited hydrogen atoms exceed 5 eV, the effects of the fine structure splitting to the line shapes of both hydrogen Balmer H_β and H_γ lines may be neglected. In this paper, we extend our previous calculations to the electric field range of 0 - 20 kV/cm and excited H atoms temperature range of 0.1 - 300 eV, with intention to cover all conditions typical for the analytical glow discharge CFR (see Videnović *et al.*, 1996).

2. THEORY

2.1. SYMMETRICAL STARK SPLITTING

Both semiclassical and quantum mechanical theory of the linear Stark effect, applied to the hydrogen and hydrogen-like emitter, yield the same result (Condon and Shortley, 1977): each energy level is splitted into equidistant sub-levels. Therefore, the hydrogen spectral lines consist of numerous components which are polarized either linearly, parallel to the vector of external field $\vec{F}$ (π-components), or circularly, in the plane perpendicular to $\vec{F}$ (σ-components). The relative wavelength positions of these components are proportional to the electric field strength and form the characteristic symmetrical Stark pattern. In numerical modeling of Stark profiles of hydrogen lines we assumed that plasma broadening effects in the CFR of a glow discharge may be neglected. Thus, to each Stark component we have assigned a Gauss function only which takes into account the instrumental and Doppler broadening. The overall profile is calculated as the superposition of all components. A de-

tailed explanation of the theoretical basis of these calculations one can find in Videnović *et al.* (1996).

2.2. FINE STRUCTURE COMPONENTS AND INTENSITIES

For the calculation of hydrogen atom eigenvectors and eigenvalues, the perturbed Hamiltonian in the external electric field $\vec{F}$ is taken, with eigenvalues E_ν obtained by solving the Schrödinger equation. The intensities of the components including fine structure splitting of the transition $n \rightarrow n'$ are given by the relationship (Gigosos and González, 1998)

$$I_{nn'} = 2\,\mathrm{Re}\,\mathrm{tr}(\vec{d}_{n'n} \cdot U_n^+ \vec{d}_{nn'} U_{n'}) \,, \tag{1}$$

where $\vec{d}_{nn'}$ is the nn' box of the atom dipole momentum operator that connects the group of states n with the n' one and U_n is the evolution operator of the group of states with main quantum number n for a given configuration of the static electric field. Using the projector P_ν on the subspace of states with eigenvalue E_ν, one obtains:

$$I_{nn'} = 2\mathrm{Re}\sum_{\nu}\sum_{\nu'} \exp\left[-\frac{i}{\hbar}(E_\nu - E_\nu^{'})t\right] \mathrm{tr}\,(\vec{d}_{n'n} \cdot P_\nu \vec{d}_{nn'} P_{n'}) \,. \tag{2}$$

The inclusion of the Z components of the vector $\vec{d}_{nn'}$ yield intensities of the π transitions, while X and Y components yield intensities of the σ transitions.

3. RESULTS

For the quantitative characteristics of the H_β and H_γ line profiles, we used the full half-width $\Delta\lambda$ and the distance between strongest maximums $\Delta\lambda_{pp}$, see Videnović *et al.* (1996), Videnović and Gigosos (1998). For the H_γ (σ) profiles, for numerical reasons, $\Delta\lambda$ only is calculated. The electric field and temperature dependencies of the line profiles parameters are shown in Figs. 1 and 2.

By intercomparison of the surfaces at the left-hand and right-hand side of both figures, one may, at first sight, recognize them as identical. That approves once again that the fine structure splitting does not play an important role in the spectroscopic diagnostics of the CFR of a glow discharge, which employs Stark profiles of hydrogen lines. The usage of simple symmetrical Stark manifold of hydrogen lines enables quick estimation of the local electric field strength in the CFR and, by fitting the experimental profiles with theoretical ones, the temperature of the excited hydrogen atoms.

In addition, by analyzing the surfaces in Fig. 1, one may conclude that the halfwidth of all profiles depends linearly both, on the electric field strength and on the excited H-atoms temperature, for $T_H < 10$ eV. In absence of high-resolution spectral equipment, this feature can be used in determination of low electric fields, near the negative glow region, where Stark profiles has no distinguished maximums (see Videnović *et al.*, 1996).

ACKNOWLEDGMENT

The authors gratefully acknowledge private communication with Dr. Marco Antonio Gigosos, providing fine structure components and intensities.

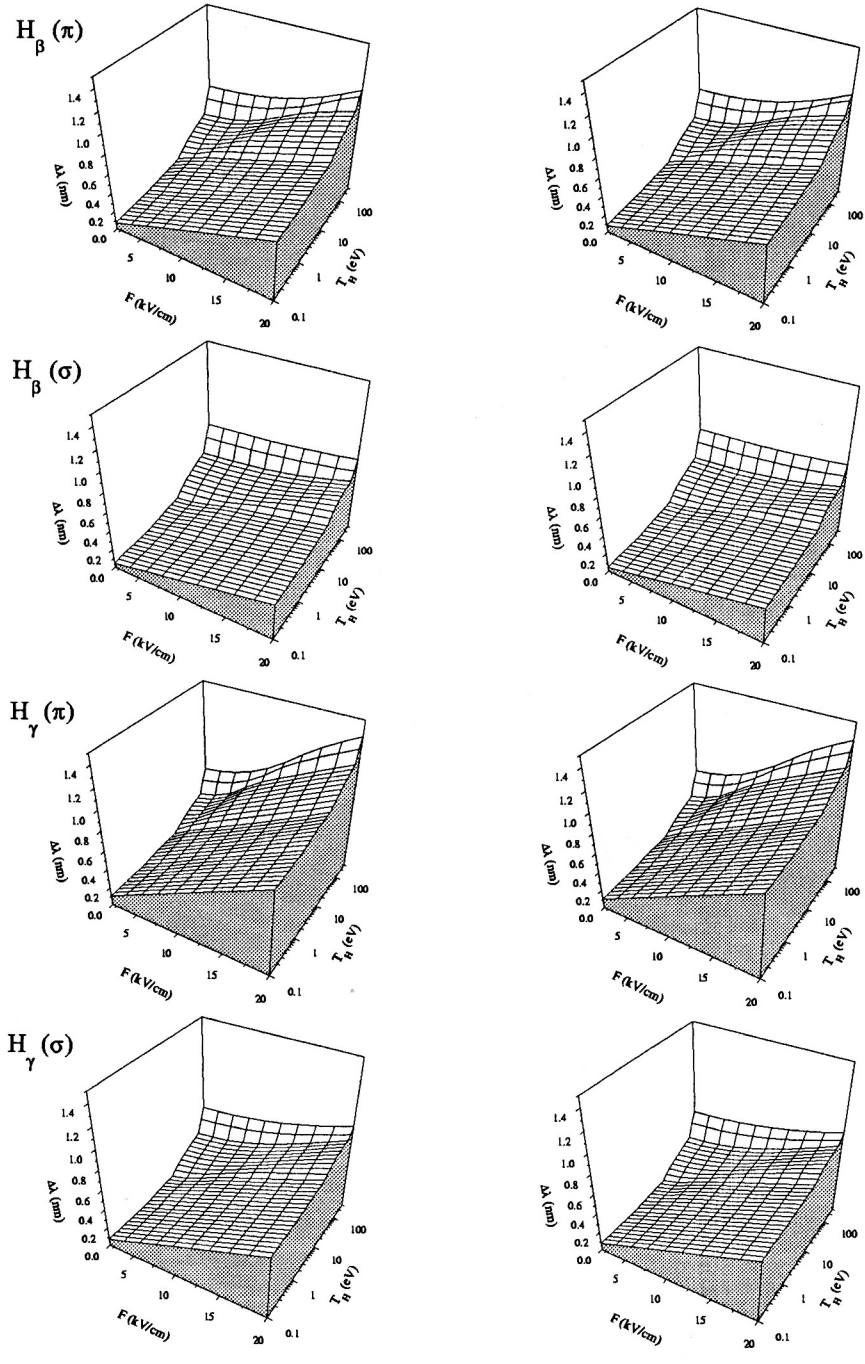

Fig. 1. The electric field strength (F) and emitter temperature (T_H) dependencies of the polarized hydrogen Balmer H_β and H_γ profiles halfwidth ($\Delta\lambda$), calculated upon symmetrical Stark manifold (left-hand side graphs) and including fine structure influence (right-hand side graphs).

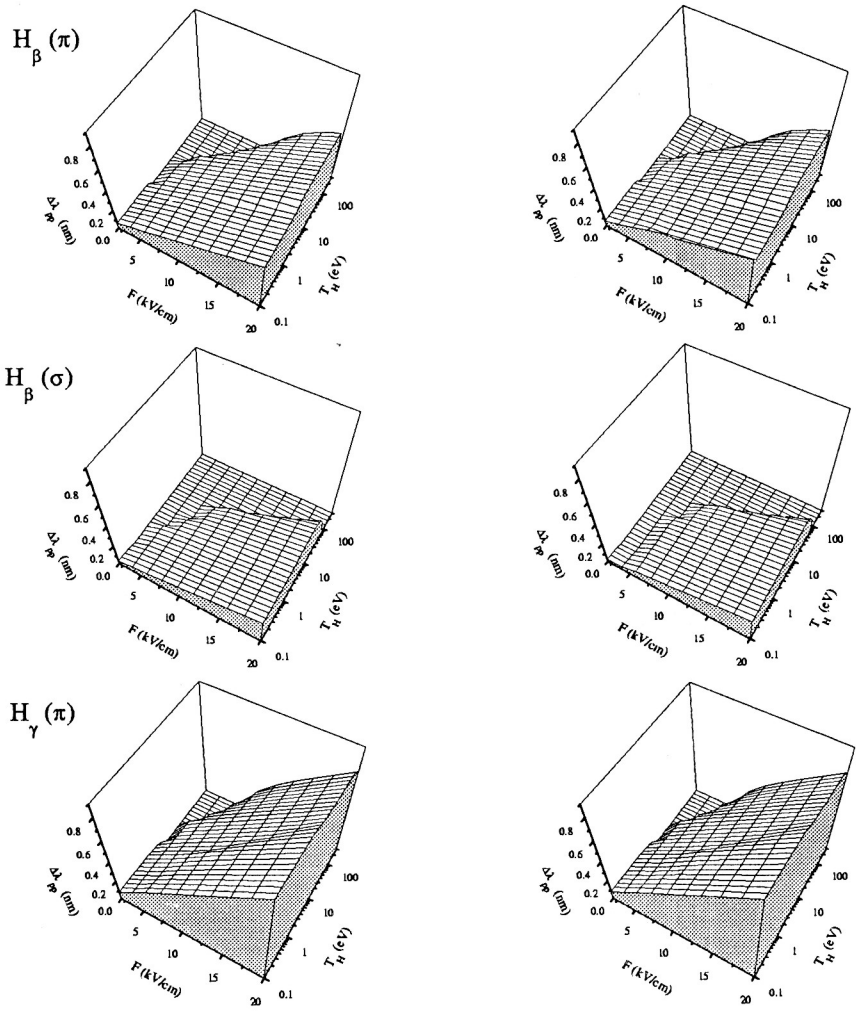

Fig. 2. Same as in Fig. 1, but for the distance between strongest maximums ($\Delta\lambda_{pp}$). For numerical reasons, this parameter is not calculated for the H_γ (σ) profile.

REFERENCES

Barbeau C., Jolly J., 1991, *Appl. Phys. Lett.* **58**, 237.

Condon E. U., Shortley G. H., 1977, *The Theory of Atomic Spectra*, University Press, Cambridge.

Donkó Z., Rózsa K., Tobin R. C., Peard K. A., 1994, *Phys. Rev. E* **49**, 3283.

Ganguly B. N., Garscadden A., 1991, *J. Appl. Phys.* **70**, 621.

Gigosos M. A., González M. A., 1998, *Phys. Rev. E* (to be published).

Lüders G., 1951, *Ann. Phys.* **8**, 301.

Videnović I. R., Konjević N., Kuraica M. M., 1996, *Spectrochim. Acta Part B* **51**, 1707.

Videnović I. R., Platiša M. M., 1998, *Contributed papers*, 19th SPIG, Zlatibor, Yugoslavia, August 31 - September 4, 1998 (in press).

Publ. Astron. Obs. Belgrade No. 61 (1998), 179 – 182 *Poster paper*

SHOCK FRONT VELOCITY IN MODIFIED MAGNETICALLY DRIVEN T-TUBE

B. VUJIČIĆ, S. DJUROVIĆ, DJ. KALOCI, I. SAVIĆ

Institute of Physics, Trg Dositeja Obradovića 4, 21000 Novi Sad, Yugoslavia

1. INTRODUCTION

The magnetically driven shock tubes (Wright, 1961; Colb, 1957) has been widely used as a plasma source for spectroscopic investigation of atomic processes in plasma, plasma dynamics behind a shock front, plasma chemistry etc.

The parameters of the shocked gas behind the shock front (flow velocity, gas pressure and temperature) strongly depends on shock front velocity thus, changing the front velocity one can change parameters of the plasma produced in a T-tube. Because the shock velocity depends only on the voltage across the discharge electrodes and ambient pressure of the gas it is possible to produce the moving plasma with requested parameters by change those two parameters.

It is clear that the velocity of the shock front appears as a magnitude of primary importance in shock tubes.

2. EXPERIMENT

The plasma source used in this experiment is a small magnetically driven T-tube made of glass with an inner diameter of 27 mm. The end of the tube 160 mm from the discharge electrodes is connected with glass balloon 160 mm in diameter. The sock front produced in a tube expands through the balloon heating the gas.

The T-tube energized from a low inductance 4 μF capacitor bank which was charged between 9 kV and 18 kV. The discharge current is critically dumped and initiated by a 10 kV trigger pulse via spark gap. The filling gas was a pure hydrogen under a pressure between 100 Pa and 500 Pa.

The method of velocity measurement is modified and improved method used earlier (Djurović, 1980; Djurović, 1997). The apparatus set-up is shown in Fig. 1. The image of the central part of the T-tube along the tube axis is focused (1:1 magnification) on a plane, where is placed precise positioner P. The two narrow tubules are placed on the positioner on the mutual distance of $\Delta x = 15$ mm and coupled on pfhotomultiplier via optical fibers.

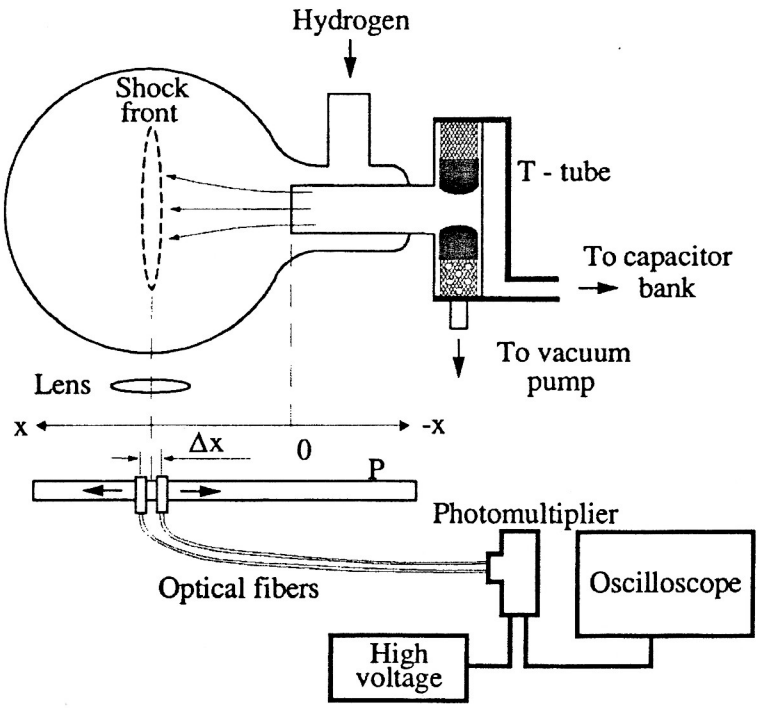

Fig. 1 Apparatus set-up

By changing position of the lens it is possible to focus any position along the line parallel to the tube axis.

3. RESULTS AND DISCUSSION

The passage of the luminous front image of a shock wave across the front ends of the tubules changes the photomultiplier signal. The signal from photomultiplier was led to the digitized oscilloscope and its typical form is shown in Fig. 2.

The time interval $\Delta t = t_2 - t_1$ between two maxima t_1 and t_2 is the time during which the incident shock front pass the distance Δx between the tubules. In this way the shock front velocity on the observed point along the tube axis can be obtained as $v = \Delta x/\Delta t$.

The time interval Δt was measured at different positions along the tube axis (with 5 mm steps) starting from x = - 20 mm (see Fig. 1).

The evaluated velocities of the shock front versus position x along the tube axis for three different filling pressures of hydrogen are presented in Fig. 3.

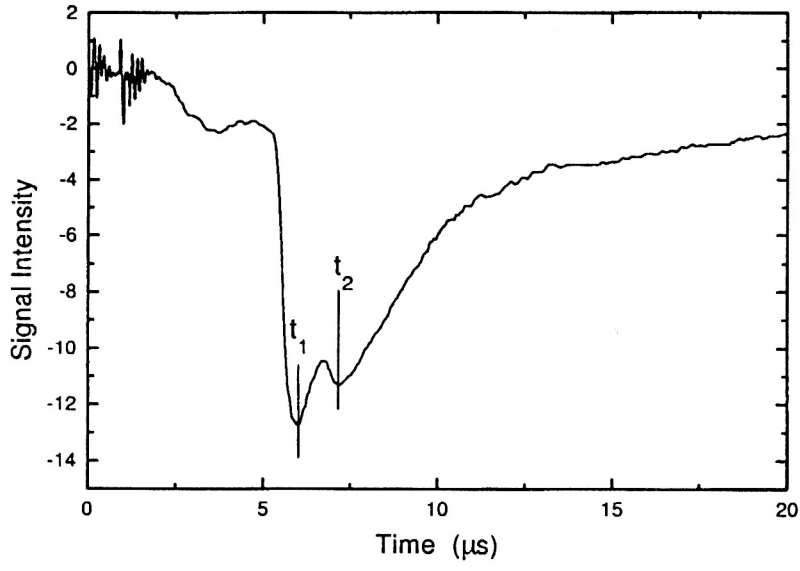

Fig. 2 Signal from oscilloscope

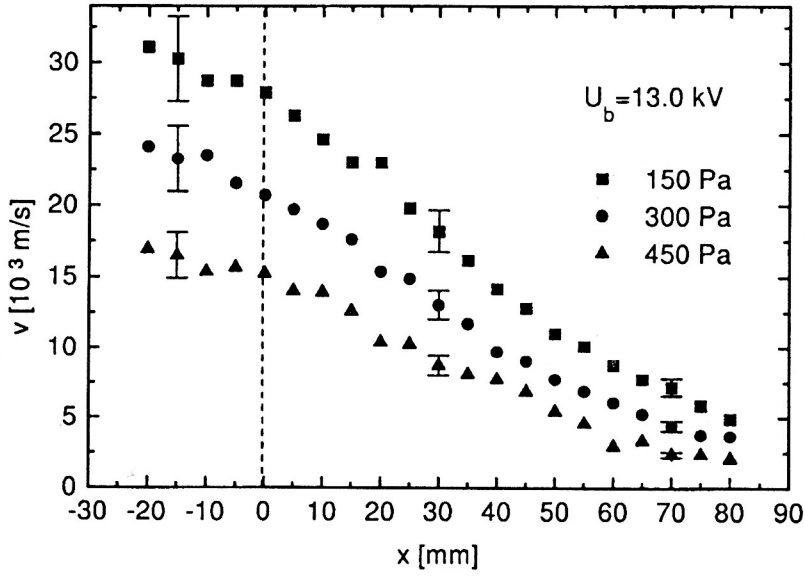

Fig. 3 Shock front velocity along tube axis for different gas pressures

The shock front velocity for the given gas pressure and position depends on the voltage across discharge electrodes. This dependence is presented in Fig. 4.

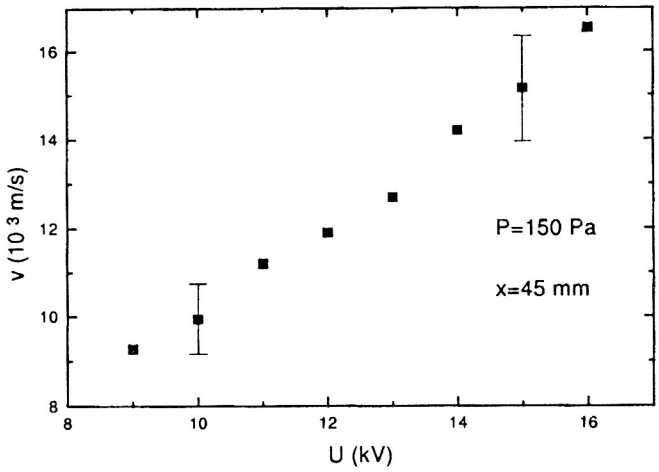

Fig. 4 Shock front velocity vs voltage across discharge electrodes

The error bars in Figs. 3 and 4 represent evaluated uncertainties in velocity determination which lies between 6% and 10%.

This preliminary measurements show that shock front velocity in the modified T-tube can change by varying the gas pressure and voltage between the electrodes. For the pressures P > 500 Pa in the case of the hydrogen measured velocities become unreliable especially for long distances from zero point (Fig. 1).

References

Djurović, S., Mijatović, Z., Pavlov, M., Kobilarov, R. and Vujičić B. T., Zhurnal Prikladnoj Spektroskopii **64**, 566 (1997).

Djurović, S. Pavlov, M., Rev. Res. Fac. Sci. Novi Sad **10**, 263 (1980).

Kolb, A. C., Phys Rev. **107**, 345 (1957).

Wright, J. K.: 1961, Shock Tubes, John Wiley & Sons, New York.

PROGRAM OF THE 2nd YUGOSLAV-BELARUSSIAN SYMPOSIUM ON PHYSICS AND DIAGNOSTICS OF LABORATORY AND ASTROPHYSICAL PLASMAS

SATURDAY (September, 5th)

9^{00} - 9^{30} OPENING CEREMONY

Chairman: M. S. Dimitrijević

9^{30} G. S. Romanov: *Theoretical Investigations of High - Temperature Multicharge Plasma.*

10^{00} J. Purić, R. Atanasijević, M. Ćuk: *Plasma Focus Experiment in Yugoslavia.*

10^{30} V. M. Astashynskii, L. Ya. Min'ko, M. Ćuk, M. M. Kuraica, J. Purić: *Compact Quasi-Stationary Plasma Accelerator as a Source of Plasma for Atomic Spectroscopy.*

10^{45} V. D. Shimanovich, I. P. Smyaglikov, A. I. Zolotovsky, S. M. Pankovets: *Optical and Specroscopic Investigations of Arc Discharge at Fullerene Synthesis.*

11^{00}-11^{30} Coffee break

Chairman: V. I. Arkhipenko

11^{30} A. A. Mihajlov: *Electric Characteristics of the Total Ionized Plasmas in Constant and Time-Variable External Fields.*

12^{00} V. K. Goncharov, M. V. Puzyrev, A. F. Chernyavskii: *The Parameters and Phase Composition Control of Laser Erosion Jets with an Employment of Electric and Electromagnetic Fields.*

12^{30} Z. Mijatović, D. Nikolić, S. Djurović, R. Kobilarov and N. Konjević: *Stark Broadening of Neutral Argon Lines in Plasmas.*

13^{00}-15^{00} Lunch break

Chairman: J. Purić

15^{00} V. I. Arkhipenko, L. V. Simonchik, S. M. Zgirovskii: *The Effect of Cathode Temperature on the Electric Field Intensity Distibution in Chatode Fall Region of the Kiselevskii Plasma Source.*

15^{30} L. Č. Popović: *Spectral Line Investigation of Active Galactic Nuclei (AGNs) at Belgrade Astronomical Observatory.*

16^{00} L. Ya. Min'ko, Yu. A. Chivel: *Surface Phenomena and Their Influence on Near-Surface Low-Threshold Plasma Formation Under the High-Energy Action on Solids.*

16^{15}-16^{45} Coffee break

Chairman: V. K. Goncharov

16^{45} M. M. Škorić: *Self-organization Processes in Plasmas.*

17^{15} L. Ya. Min'ko: *Radiative Plasmadynamics as a New Direction in Plasma Physics.*

17^{45} M. M. Popović, D. Djordjević: *Usage of Spectoscopical Experiments for Determination of Other Plasma Parameters.*

18^{00}-19^{00} Poster section

20^{00} CONFERENCE DINNER

SUNDAY (September, 6th)

Chairman: L. Ya. Min'ko

10^{00} A. N. Chumakov, N. A. Bosak: *Multipulse Near-Surface Optical Discharge as an Effective Source of Erosive Plasma.*

10^{30} E. Ershov-Pavlov, K. Stepanov, L. Stanchits, Yu. Stankevich: *Emission of an Atmospheric Pressure Arc in a Gas Flow.*

11^{00} D. M. Šulić: *Characteristics of Guiding VLF Waves by Field-Aligned Irregularities in the Magnetosphere.*

11^{30} N. V. Tarasenko: *Studies of Relaxation Processes in Laser-Producted Plasma.*

11^{45} CLOSING OF THE CONFERENCE

AUTHORS INDEX

LIST OF PARTICIPANTS

Ананин С.И., Институт молекулярной и атомной физики Национальной Академии наук Беларуси, Минск, Беларусь

Antanasijević R., Institute of Physics, Zemun-Belgrade, Yugoslavia

Arkhipenko V.I., Institute of Molecular and Atomic Physics National Academy of Sciences of Belarus, Minsk, Belarus

Arsenijević J., Astronomical Observatory, Belgrade, Yugoslavia

Асташинский В.М., Институт молекулярной и атомной физики Национальной Академии наук Беларуси, Минск, Беларусь

Авраменко В.Б., Институт молекулярной и атомной физики Национальной Академии наук Беларуси, Минск, Беларусь

Барихин Б.А., Гродненский госуниверситет, Гродно, Беларусь

Blagojević B., Institute of Physics, Zemun-Belgrade, Yugoslavia

Bon E., Astronomical Observatory, Belgrade, Yugoslavia

Босак Н.А., Институт молекулярной и атомной физики Национальной Академии наук Беларуси, Минск, Беларусь

Chernyavskii A.F., Scientific-Research Institute of Applied Physical Problems, Minsk, Belarus

Ćirković M.M., SUNY at Stony Brook, Stony Brook, NY, USA; Astronomical Observatory, Belgrade, Yugoslavia

Ćuk M., Faculty of Physics, University of Belgrade, Belgrade, Yugoslavia

Čelebonović V., Institute of Physics, Zemun-Belgrade, Yugoslavia

Чивель Ю.А., Институт молекулярной и атомной физики Национальной Академии наук Беларуси, Минск, Беларусь

Чумаков А.Н., Институт молекулярной и атомной физики Национальной Академии наук Беларуси, Минск, Беларусь

Dimitrijević M.S., Astronomical Observatory, Belgrade, Yugoslavia

Djeniže S., Faculty of Physics, University of Belgrade, Belgrade, Yugoslavia

Djordjević D., Institute of Physics, Zemun-Belgrade, Yugoslavia

Djordjević D.S., Institute of Physics, Zemun-Belgrade, Yugoslavia

Djurić Z., Institute of Physics, Zemun-Belgrade, Yugoslavia and Dept. of Materials, Oxford University, Oxford, Great Britain

Djurović S., Institute of Physics, Novi Sad, Yugoslavia

Doroshenko V.T., Crimean Astrophysical Observatory, Nauchny, Ukraine

Ефремов В.В., Институт молекулярной и атомной физики Национальной Академии наук Беларуси, Минск, Беларусь

Ershov-Pavlov E.A., Institute of Molecular and Atomic Physics National Academy of Sciences of Belarus, Minsk, Belarus

Gaković B., Institute of Nuclear Sciences "Vinča", Belgrade, Yugoslavia

Goncharov V.K., Scientific-Research Institute of Applied Physical Problems, Minsk, Belarus

Иванов А.Ю., Институт молекулярной и атомной физики Национальной Академии наук Беларуси, Минск, Беларусь

Ivković M., Institute of Physics, Zemun-Belgrade, Yugoslavia
Joksimović D., Institute of Physics, Zemun-Belgrade, Yugoslavia
Jovićević S., Institute of Physics, Zemun-Belgrade, Yugoslavia
Kaloci DJ., Institute of Physics, Novi Sad, Yugoslavia
Kobilarov R., Institute of Physics, Novi Sad, Yugoslavia
Konjević N., Institute of Physics, Zemun-Belgrade, Yugoslavia
Костюкевич Е.А., Институт молекулярной и атомной физики Национальной Академии наук Беларуси, Минск, Беларусь
Kubičela A., Astronomical Observatory, Belgrade, Yugoslavia
Kuraica M.M., Faculty of Physics, University of Belgrade, Belgrade, Yugoslavia
Кузьмицкий А.М., Институт молекулярной и атомной физики Национальной Академии наук Беларуси, Минск, Беларусь
Маньковский А.А., Институт молекулярной и атомной физики Национальной Академии наук Беларуси, Минск, Беларусь
Marković S., Astronomical Observatory, Belgrade, Yugoslavia
Mihajlov A.A., Institute of Physics, Zemun-Belgrade, Yugoslavia
Mijatović N., Institute of Nuclear Sciences "Vinča", Belgrade, Yugoslavia
Mijatović Z., Institute of Physics, Novi Sad, Yugoslavia
Milosavljević V., Faculty of Physics, University of Belgrade, Belgrade, Yugoslavia
Milošević–Zdjelar V., Public Observatory, Kalemegdan, Belgrade, Yugoslavia
Минько Л.Я., Институт молекулярной и атомной физики Национальной Академии наук Беларуси, Минск, Беларусь
Насонов В.И., Институт молекулярной и атомной физики Национальной Академии наук Беларуси, Минск, Беларусь
Недолугов В.И., Институт молекулярной и атомной физики Национальной Академии наук Беларуси, Минск, Беларусь
Nenadović T., Institute of Nuclear Sciences "Vinča", Belgrade, Yugoslavia
Nikolić D., Institute of Physics, Novi Sad, Yugoslavia
Obradović B.M., Faculty of Physics, University of Belgrade, Belgrade, Yugoslavia
Pankovets S.M., Institute of Molecular and Atomic Physics National Academy of Sciences of Belarus, Minsk, Belarus
Панусевич Е.З., Гродненский госуниверситет, Гродно, Беларусь
Pavlović Z., Institute of Physics, Zemun-Belgrade, Yugoslavia
Petrović-Stepanović S., Institute of Nuclear Sciences "Vinča", Belgrade, Yugoslavia
Platiša M.M., Faculty of Physics, University of Belgrade, Belgrade, Yugoslavia
Popović L.Č., Astronomical Observatory, Belgrade, Yugoslavia
Popović M.M., Institute of Physics, Zemun-Belgrade, Yugoslavia
Popović M.V., Institute of Physics, Zemun-Belgrade, Yugoslavia
Purić J., Faculty of Physics, University of Belgrade, Belgrade, Yugoslavia
Puzyrev M.V., Scientific-Research Institute of Applied Physical Problems, Minsk, Belarus
Романов Г.С., Академический научный комплекс "Институт тепло- и массообмена им. А.В. Лыкова" Академии наук Беларуси, Минск, Беларусь
Sahal-Bréchot S., Observatoire de Paris, Meudon Cedex, France
Samurović S., Public Observatory, Kalemegdan, Belgrade, Yugoslavia

Savić I., Institute of Physics, Novi Sad, Yugoslavia
Sergeev S.G., Sternberg Astronomical Institute, Moscow, Russia
Shimanovich V.D., Institute of Molecular and Atomic Physics National Academy of Sciences of Belarus, Minsk, Belarus
Simonchik L.V., Institute of Molecular and Atomic Physics National Academy of Sciences of Belarus, Minsk, Belarus
Smyaglikov I.P., Institute of Molecular and Atomic Physics National Academy of Sciences of Belarus, Minsk, Belarus
Srećković A., Faculty of Physics, University of Belgrade, Belgrade, Yugoslavia
Stanchits L.K., Heat and Mass Transfer Institute, Minsk, Belarus
Stanić I., Intel Computers and Digital Radio, Belgrade, Yugoslavia
Stankevich Y.A., Heat and Mass Transfer Institute, Minsk, Belarus
Stankevich Yu.A., Heat and Mass Transfer Institute, Minsk, Belarus
Stepanov K.L., Heat and Mass Transfer Institute, Minsk, Belarus
Šćepanović M., Faculty of Sciences and Mathematics, University of Montenegro, Podgorica, Yugoslavia
Škorić M.M., Institute of Nuclear Sciences "Vinča", Belgrade, Yugoslavia; National Institute for Fusion Science, Toki-shi, 509-5292, Japan
Šulić D.M., Astronomical Observatory, Belgrade, Yugoslavia
Tankosić D., Astronomical Observatory, Belgrade, Yugoslavia
Tarasenko N.V., Institute of Molecular and Atomic Physics National Academy of Sciences of Belarus, Minsk, Belarus
Trajković N., Astronomical Observatory, Belgrade, Yugoslavia
Trtica M., Institute of Nuclear Sciences "Vinča", Belgrade, Yugoslavia
Васильев С.В., Институт молекулярной и атомной физики Национальной Академии наук Беларуси, Минск, Беларусь
Videnović I.R., Faculty of Physics, University of Belgrade, Belgrade, Yugoslavia
Vujičić B., Institute of Physics, Novi Sad, Yugoslavia
Zgirovskii S.M., Institute of Molecular and Atomic Physics National Academy of Sciences of Belarus, Minsk, Belarus
Zolotovsky A.I., Institute of Molecular and Atomic Physics National Academy of Sciences of Belarus, Minsk, Belarus

№ 1 (1947)
ЕФЕМЕРИДЕ 98 МАЛИХ ПЛАНЕТА ЗА 1947 ГОДИНУ
ÉPHÉMÉRIDES DE 98 DES PETITES PLANÈTES POUR L'AN 1947

№ 2 (1947)
ЕФЕМЕРИДЕ 106 МАЛИХ ПЛАНЕТА ЗА 1948 ГОДИНУ
ÉPHÉMÉRIDES DE 106 DES PETITES PLANÈTES POUR L'AN 1948

№ 3 (1949)
ЕФЕМЕРИДЕ 106 МАЛИХ ПЛАНЕТА ЗА 1949 ГОДИНУ
ÉPHÉMÉRIDES DE 106 DES PETITES PLANÈTES POUR L'AN 1949

№ 4 (1951)
P. M. Djurković, B. M. Ševarlić et Z. M. Brkić
ОДРЕЂИВАЊЕ ГЕОГРАФСКЕ ШИРИНЕ АСТРОНОМСКЕ ОПСЕРВАТОРИЈЕ У БЕОГРАДУ, 1947
DETERMINATION DE LATITUDE DE L'OBSERVATOIRE ASTRONOMIQUE DE BELGRADE, 1947

№ 5 (1957)
B. M. Ševarlić
SUR LE PROBLÉME DE LA VARIATION DES LATITUDES ET DU MOUVEMENT DU PÔLE INSTANTANÉ DE ROTATION À LA SURFACE DE LA TERRE

№ 6 (1961)
Ljubiša A. Mitić
COOSCILLATIONS DES PENDULES ASTRONOMIQUES

№ 7 (1961)
Zaharije M. Brkić
ПРИЛОГ ИСПИТИВАЊИМА СИСТЕМАТСКИХ УТИЦАЈА НА АСТРОНОМСКО ОДРЕЂИВАЊЕ ВРЕМЕНА
CONTRIBUTION AUX ÉTUDES DES INFLUENCES SYSTÉMATIQUES À LA DÉTERMINATION ASTRONOMIQUE DE L'HEURE

№ 8 (1961)
B. M. Ševarlić
ПРОМЕНЕ ГЕОГРАФСКЕ ШИРИНЕ АСТРОНОМСКЕ ОПСЕРВАТОРИЈЕ У БЕОГРАДУ ОД 1949.0 – 1957.0
VARIATIONS DE LA LATITUDE DE L'OBSERVATOIRE ASTRONOMIQUE DE BEOGRAD DE 1949.0 – 1957.0

№ 9 (1961)
Branislav M. Ševarlić
PRILOG ISPITIVANJU PROMENA GEOGRAFSKIH ŠIRINA BEOGRADA
CONTRIBUTION A L'ETUDE DES VARIATIONS DE LA LATITUDE DE BEOGRAD

№ 10 (1964)
Vasilije Oskanjan
THE UV CETI VARIABLE STARS

№ 11 (1965)
P. M. Djurković, M. Protić, J. Arsenijević, A. Kubičela, O. Kovačević, R. Grujić, Lj. Dačić, M. Djokić, Č. Čepinac
OBSERVATIONS DU SOLEIL EN 1957, 1958 ET 1959 A L'OBSERVATOIRE ASTRONOMIQUE DE BEOGRAD

№ 12 (1968)
Editor: P. M. Djurković
SIMPOZIJUM ASTRONOMA JUGOSLAVIJE POVODOM 75. GODIŠNJICE OSNIVANJA ASTRONOMSKE OPSERVATORIJE U BEOGRADU (1887 - 1962)

№ 13 (1967)
G. Teleki
A CONTRIBUTION INTO THE RESEARCH OF ASTRONOMICAL REFRACTION AND ITS ANOMALIES ON THE BASIS OF AEROLOGICAL MEASUREMENTS CARRIED OUT IN BEOGRAD

№ 14 (1968)
RADOVI NA ISPITIVANJU FUNDAMENTALNIH ASTROMETRIJSKIH INSTRUMENATA, NJIHOVIH ORGANA I PRIBORA
TRAVAUX SUR L'EXAMEN DES INSTRUMENTS ASTROMETRIQUES FONDAMENTAUX, DE LEUR ORGANES ET ACCESSOIRES

№ 15 (1968)
Aleksandar Kubičela
UNE MODIFICATION DU SPECTROGRAPHE CHROMOSPHERIQUE A PLAQUE MOBILE

№ 16 (1969)
Editor: P. M. Djurković
RADOVI PRIKAZANI NA IV KONGRESU MATEMATIČARA, FIZIČARA I ASTRONOMA, OKTOBRA 1965 U SARAJEVU

№ 17 (1972)
Sofija N. Sadžakov, Dušan P. Šaletić
CATALOGUE OF DECLINATIONS OF THE LATITUDE PROGRAMME STARS (KŠZ)

№ 18 (1974)
Editor: G. Teleki
THE PRESENT STATE AND FUTURE OF THE ASTRONOMICAL REFRACTION INVESTIGATIONS
Proceedings of the Study Group on Astronomical Refraction of the International Astronomical Union Commission 8

№ 19 (1974)
Georgije M. Popović
THE FIRST GENERAL CATALOGUE OF DOUBLE-STAR OBSERVATIONS MADE IN BELGRADE, 1951–1971

№ 20 (1975)
Editor: Dj. Teleki
ZBORNIK RADOVA NACIONALNE KONFERENCIJE JUGOSLOVENSKIH ASTRONOMA - 1973, BEOGRAD
PROCEEDINGS OF THE NATIONAL CONFERENCE OF YUGOSLAV ASTRONOMERS - 1973, BELGRADE

№ 21 (1975)
S. Sadžakov, D. Šaletić
DECLINATIONS AND THE PROPER MOTIONS OF THE STARS OF THE INTERNATIONAL LATITUDE SERVICE ON THE BASIS OF MERIDIAN CATALOGUES FROM 1929 TO 1972.

№ 22 (1975)
Ivan Pakvor
ISPITIVANJE NAGLAVAKA VELIKOG PASAŽNOG INSTRUMENTA ASTRONOMSKE OPSERVATORIJE U BEOGRADU
PIVOT-EXAMINATIONS OF BELGRADE OBSERVATORY'S LARGE TRANSIT INSTRUMENT

№ 23 (1975)
Lj. A. Mitić
PRIPREMNI RADOVI NA VELIKOM PASAŽNOM INSTRUMENTU BEOGRADSKE OPSERVATORIJE
PREPARATION OF THE LARGE TRANSIT INSTRUMENT OF THE BELGRADE OBSERVATORY FOR REGULAR OBSERVATION

№ 24 (1978)
Sofija N. Sadžakov
IZVEDENI KATALOG ŠIRINSKIH ZVEZDA (IKŠZ)
GENERAL CATALOGUE OF LATITUDE STARS (IKŠZ)

№ 25 (1978)
Danilo J. Zulević
PRILOG STATISTIČKOM ISPITIVANJU UTICAJA ODNOSA MASA KOMPONENATA NA DINAMIČKE PUTANJSKE ELEMENTE (e, P, a) KOD VIZUELNO DVOJNIH ZVEZDA
STATISTICAL INVESTIGATION OF THE RELATION BETWEEN THE MASS RATIO AND THE DYNAMICAL ORBITAL ELEMENTS e, P, a OF THE VISUAL BINARIES

№ 26 (1979)
Editor: Dj. Teleki
ZBORNIK RADOVA III NACIONALNE KONFERENCIJE
JUGOSLOVENSKIH ASTRONOMA, BEOGRAD, 1977.
PROCEEDINGS OF THE III NATIONAL CONFERENCE
OF YUGOSLAV ASTRONOMERS, BELGRADE, 1977.

№ 27 (1979)
S. N. Sadžakov
ISPITIVANJE SISTEMATSKIH GREŠAKA TIPA $\Delta\delta_\alpha$ ŠIRINSKIH
POSMATRANJA RAZNIH OPSERVATORIJA NA OSNOVU NJIHOVOG
UPOREDJIVANJA SA BEOGRADSKIM IZVEDENIM KATALOGOM
ŠIRINSKIH ZVEZDA I FOTOGRAFSKIM KATALOGOM AGK3

INVESTIGATION OF THE SYSTEMATIC $\Delta\delta_\alpha$ - TYPE ERRORS IN LATITUDE
OBSERVATIONS OF VARIOUS OBSERVATORIES BY THEIR COMPARISON
WITH BELGRADE GENERAL CATALOGUE OF LATITUDE STARS AND THE
PHOTOGRAPHIC CATALOGUE AGK3

№ 28 (1980)
Jelisaveta Arsenijević
POLARIZACIJA ZRAČENJA NEKIH HLADNIH SUPERDŽINOVA

№ 29 (1982)
Editors: G. Teleki, B. Ševarlić
EPITOME FUNDAMENTORUM ASTRONOMIAE, Pars II
Photographic Catalogues and Charts of Star Positions

№ 30 (1981)
S. N. Sadžakov, D. P. Šaletić, M. D. Dačić
KATALOG ZVEZDA PROGRAMA SFZT
CATALOGUE OF NPZT PROGRAMME STARS

№ 31 (1981)
ASTROKLIMATSKA ISTRAŽIVANJA ZA IZBOR MESTA VISINSKE STANICE
ASTRONOMSKE OPSERVATORIJE U BEOGRADU
ASTROCLIMATIC EXPLORATIONS FOR SITE SELECTION OF THE HIGH
ALTITUDE STATION OF THE BELGRADE OBSERVATORY

№ 32 (1984)
Vojislava Protić-Benišek
MERKUROVI PROLAZI I PARALAKSA SUNCA
TRANSITS OF MERCURY AND SOLAR PARALLAX

№ 33 (1985)
Editor: G. M. Popović
ZBORNIK RADOVA VI NACIONALNE KONFERENCIJE
JUGOSLOVENSKIH ASTRONOMA, HVAR, 1983.
PROCEEDINGS OF THE VI NATIONAL CONFERENCE
OF YUGOSLAV ASTRONOMERS, HVAR, 1983

№ 34 (1986)
Božidar Popović
EQUATIONS DES PERTURBATIONS DES ELEMENTS HELIOCENTRIQUES VECTORIELS DES ORBITES DES PETITES PLANETES ET COMETES

№ 35 (1987)
Editor: G. Teleki
PROCEEDINGS OF THE WORKSHOP ON REFRACTION DETERMINATION IN THE OPTICAL AND RADIO ASTROMETRY, LENINGRAD, USSR, 1985

№ 36 (1989)
STO GODINA ASTRONOMSKE OPSERVATORIJE U BEOGRADU

№ 37 ((1989)
Vladimir Kršljanin
ŠTARKOV POMAK JONSKIH LINIJA KOD TOPLIH ZVEZDA
ION LINES STARK SHIFTS IN SPECTRA OF HOT STARS

№ 38 (1990)
S. N. Sadžakov, M. D. Dačić
BEOGRADSKI KATALOG DVOJNIH ZVEZDA
BELGRADE CATALOGUE OF DOUBLE STARS

№ 39 (1990)
Milan S. Dimitrijević
ISTRAŽIVANJA OBLIKA SPEKTRALNIH LINIJA U JUGOSLAVIJI 1962 – 1985
(Bibliografija i indeks citata)
LINE SHAPES INVESTIGATIONS IN YUGOSLAVIA 1962 – 1985
(Bibliography and citation index)

№ 40 (1990)
Editors: G. Teleki and B. Ševarlić
EPITOME FUNDAMENTORUM ASTRONOMIAE, Pars III
Parallaxes, Proper Motions and Radial Velocities

№ 41 (1991)
Milan S. Dimitrijević
ISTRAŽIVANJE OBLIKA SPEKTRALNIH LINIJA U JUGOSLAVIJI II
(1985 – 1989)
(Bibliografija i indeks citata)
LINE SHAPES INVESTIGATIONS IN YUGOSLAVIA II (1985 – 1989)
(Bibliography and Citation Index)

№ 42 (1991)
Gojko Djurašević
ISPITIVANJE AKTIVNIH TESNIH DVOJNIH SISTEMA
NA OSNOVU FOTOMETRIJSKIH MERENJA
INVESTIGATION OF ACTIVE CLOSE BINARIES
BASED ON PHOTOMETRIC MEASUREMENTS

№ 43 (1992)
Editors: O. Atanacković-Vukmanović and M. S. Dimitrijević
Astronomska opservatorija u Beogradu
AKTIVNOSTI I KRATKI SADRŽAJI RADOVA 1980 – 1990
Astronomical Observatory in Belgrade
ACTIVITIES AND ABSTRACTS OF PAPERS 1980 – 1990

№ 44 (1993)
Editors: M. S. Dimitrijević and D. Djurović
ZBORNIK RADOVA X NACIONALNE KONFERENCIJE
JUGOSLOVENSKIH ASTRONOMA, 22 – 24 SEPTEMBAR 1993
PROCEEDINGS OF THE X NATIONAL CONFERENCE
OF YUGOSLAV ASTRONOMERS, BELGRADE, SEPTEMBER 22 – 24, 1993

№ 45 (1993)
B. Jovanović, L. Djurović, M. Jovanović
HOMOGENIZOVANI SISTEM UT_{BLI} ZA PERIOD 1964 – 1986
HOMOGENEOUS SYSTEM UT_{BLI} FOR 1964 – 1986

№ 46 (1994)
Luka Č. Popović
ŠTARKOVO ŠIRENJE SPEKTRALNIH LINIJA TEŠKIH JONA
U SPEKTRIMA TOPLIH ZVEZDA
STARK BROADENING OF HEAVY ION SPECTRAL LINES
IN SPECTRA OF HOT STARS

№ 47 (1994)
Milan S. Dimitrijević
ISTRAŽIVANJE OBLIKA SPEKTRALNIH LINIJA U JUGOSLAVIJI
I SRBIJI III (1989 – 1993)
(Bibliografija i indeks citata)
LINE SHAPES INVESTIGATIONS IN YUGOSLAVIA
AND SERBIA III (1989 – 1993)
(Bibliography and citation index)

№ 48 (1995)
Editors: O. Atanacković-Vukmanović and M. S. Dimitrijević
ISTRAŽIVANJA U ASTRONOMIJI I
RESEARCHES IN ASTRONOMY I

№ 49 (1995)
Editors: I. Vince, M. S. Dimitrijević and L. Balázs
PROCEEDINGS OF THE FIRST HUNGARIAN–YUGOSLAV
ASTRONOMICAL CONFERENCE
April 26–27, 1995, Baja Hungary

№ 50 (1995)
Editors: M. S. Dimitrijević and L. Č. Popović
PROCEEDINGS OF THE FIRST YUGOSLAV CONFERENCE
ON SPECTRAL LINE SHAPES
September 11–14, 1995, Krivaja, Yugoslavia

№ 51 (1996)
Editors: M. S. Dimitrijević and L. Č. Popović
Астрономска Опсерваторија у Београду
АКТИВНОСТИ И КРАТКИ САДРЖАЈИ РАДОВА (1991 – 1995)
Astronomical Observatory in Belgrade
ACTIVITIES AND ABSTRACTS OF PAPERS (1991 – 1995)

№ 52 (1996)
Milan S. Dimitrijević
БЕОГРАДСКА АСТРОНОМСКА ОПСЕРВАТОРИЈА У 1995
BELGRADE ASTRONOMICAL OBSERVATORY IN 1995

№ 53 (1996)
Editors: V. S. Burakov and M. S. Dimitrijević
PROCEEDINGS OF THE FIRST BELARUSSIAN–YUGOSLAVIAN
SYMPOSIUM ON PHYSICS AND DIAGNOSTICS
OF LABORATORY & ASTROPHYSICAL PLASMA
PDP–I'96
July 1 – 3, 1996, Minsk, Belarus
In memoriam of M. A. Elyashevich, academician of Belarus AS

№ 54 (1996)
Editors: M. Vukićević-Karabin and Z. Knežević
ЗБОРНИК РАДОВА XI НАЦИОНАЛНЕ КОНФЕРЕНЦИЈЕ
ЈУГОСЛОВЕНСКИХ АСТРОНОМА
Београд, 9 – 11, октобар 1996
PROCEEDINGS OF THE XI NATIONAL CONFERENCE
OF YUGOSLAV ASTRONOMERS
Belgrade, October 9 – 11, 1996

№ 55 (1997)
Milan S. Dimitrijević
БЕОГРАДСКА АСТРОНОМСКА ОПСЕРВАТОРИЈА У 1996
BELGRADE ASTRONOMICAL OBSERVATORY IN 1996

№ 56 (1997)
Editors: M. S. Dimitrijević, J. Milogradov-Turin and L. Č. Popović
РАЗВОЈ АСТРОНОМИЈЕ КОД СРБА
DEVELOPMENT OF ASTRONOMY AMONG SERBS

№ 57 (1997)
Editors: Luka Č. Popović and Milivoje Ćuk
PROCEEDINGS OF THE SECOND YUGOSLAV CONFERENCE
ON SPECTRAL LINE SHAPES
September 29 – October 2, 1997, Bela Crkva, Yugoslavia

№ 58 (1997)
Milan S. Dimitrijević
LINE SHAPES INVESTIGATIONS IN YUGOSLAVIA
AND SERBIA IV (1993 – 1997)
(Bibliography and citation index)
ISTRAŽIVANJE OBLIKA SPEKTRALNIH LINIJA U JUGOSLAVIJI
I SRBIJI IV (1993 – 1997)
(Bibliografija i indeks citata)

№ 59 (1998)
Milan S. Dimitrijević
БЕОГРАДСКА АСТРОНОМСКА ОПСЕРВАТОРИЈА У 1997
BELGRADE ASTRONOMICAL OBSERVATORY IN 1997

№ 60 (1998)
Editors: M. S. Dimitrijević and L. Č. Popović
PROCEEDINGS OF THE 4th YUGOSLAV-ROMANIAN
ASTRONOMICAL MEETING
(4th YuRoAM)

ZADUŽBINA ANDREJEVIĆ

ZADUŽBINA ANDREJEVIĆ je neprofitna i nevladina institucija, osnovana 1994. godine a registrovana 1995. godine od strane Ministarstva kulture Republike Srbije. Njeni ciljevi su:

1. Pomaganje stvaralaštva u svim naučnim oblastima i disciplinama.
2. Pružanje pomoći i podrške talentovanim naučnim stvaraocima u objavljivanju njihovih prvih naučnih dela - magistarskih teza i doktorskih disertacija.
3. Stvaranje fonda aktuelnih naučnih knjiga i časopisa iz svetske nauke.
4. Podsticanje razvoja jugoslovenske naučne kritičke misli.

ZADUŽBINA objavljuje najbolje radove talentovanih naučnika Jugoslavije koji se biraju putem javnih konkursa. Do sada je bilo pet konkursa, na kojima je učešće uzelo više od 400 autora. Iz prva tri konkursa štampane su 52 monografije. U toku je štampanje naučnih dela koja su odabrana na IV konkursu (16 disertacija i 10 magistarskih teza), dok je izbor najboljih disertacija i magistarskih teza iz V konkursa u toku. Do sada je publikovano 60 monografija iz svih naučnih oblasti.

Izabrane doktorske disertacije se štampaju u Biblioteci DISSERTATIO (predsednik Redakcije dr Milan S. Dimitrijević, direktor Astronomske opservatorije u Beogradu) a magistarske teze u Biblioteci ACADEMIA (predsednik Redakcije prof. dr Momčilo Babić, direktor KBC "Bežanijska kosa"). U ove dve redakcije je angažovano 50 profesora univerziteta.

Naučnim radom ZADUŽBINE upravlja Naučni savet (predsednik akademik Miroslav Pantić, generalni sekretar SANU). Članovi su akademici SANU i CANU, predstavnici jugoslovenskih univerziteta i drugi istaknuti naučnici Jugoslavije.

ZADUŽBINA ima svoj program na INTERNETU. U pripremi je stvaranje baze podataka savremene svetske nauke koja će služiti jugoslovenskim naučnicima, prvenstveno mladima.

ZADUŽBINA sva objavljena dela promoviše, kao i njihove stvaraoce, putem medija, naučnih i drugih skupova.

Podržavajući aktivnost ZADUŽBINE, stalno se širi "porodica" zadužbinara i počasnih osnivača, koja danas broji preko trista članova - fizičkih i pravnih lica, što se registruje na izdanjima ovih biblioteka, dok se sponzori upisuju u knjigama čije su izdavanje pomogli.

Predsednik Upravnog odbora,
Prof. dr Kosta Andrejević

EПC

ELECTRIC POWER INDUSTRY OF SERBIA

1998.
ELEKTROPRIVREDA SRBIJE


LAKO JE KAD ZNAŠ...
TOTAL DESIGN
VIESTA
COMPANY
011 693 655

1 9 2 3

ИКАРБУС

11080 ZEMUN
AUTOPUT 24
Tel. 011/609-822 • 600-134

FABRIKA
AUTOBUSA
I SPECIJALNIH
VOZILA
FACTORY OF
BUSES AND
SPECIAL
VEHICLES

ZLATIBOR
SPECIALIZED INSTITUTE
FOR PREVENTION, TREATMENT AND REHABILATION THYROID DISORDERS

WHAT IS ČIGOTA?

ČIGOTA is a popular dietetic and recreational programme which will help you during your stay on the Mt. Zlatibor, lose surplus weight, rest, freshen up, restore fitness and above alllearn to live in a different style – actively and healthy.

This programme, which has been in use since 1989 at the Mt. Zlatibor, was created for you by a group of authors.

I have had the honour and pleasure of being at the head of this team, which besides my associates, also includes distinguished professors of the Belgrade University School of Medicine and School of Physical Training.

The result of our joint effort is a modern treatment based on a well-balanced dieting plan and diversified physical activities.

In other words, the ČIGOTA PROGRAMME is a reliable and efficient way of restoring the disturbed equilibrium between energy intake and consumption.

The proper diets, exercises in the gym and ČIGOTA swimming pool, and long recreational walks, all under specialist supervision, on an ideal altitude of 1,000 metres a.s.l., help you do a lot in only 7 days, not only for your appearance, but for your health, too.

Anyway, come and see for yourself. My associates and I are expecting you.

We'll teach you the ČIGOTA LIFE PHILOSOPHY.

Your cordially, Dr MILISAV ČUTOVIĆ, Manager, ZLATIBOR Institute

WITH ČIGOTA AGAINST OBESITY AND INTO HEALTHY AND ACTIVE LIVING

Obesity is a health problem caused by improper nutrition and wrong life style. It affects all categories of healthy people and is manifest in the form of accumulation of fat reserves.

There are many causes of obesity. Insufficient physical activity, finding full satisfaction in consuming good food, disrupted balance of energy intake and consumption – all that is conductive to exessive body weight which is increasingly difficult to get rid off with time, which is not detrimental only to appearance, but also to health in the first place.

In view of these facts, the ČIGOTA PROGRAMME includes:

- a well-balanced dieting plan,
- a programme of physical activities,
- creation of a group, positive atmosphere and
- basic information on the importance of proper nutrition and recreation.

DIETETIC TREATMENT implies a daily energy deficit caused by consuming foodstuffs that generate 900 to 1,200 cal. Five meals are recommended to be taken daily, at three-hour intervals, consisting of various foodstuffs, without fats and sugar, and with minimum salt.

PROGRAMME OF PHYSICAL ACTIVITIES makes provisions for individual doses of loading by exercises in the gym and swimming pool, and long walks.

The rhythm of these activities is adjusted to the rhythm of meal taking, and they are carried out two to three times daily.

POSITIVE GROUP ATMOSPHERE which is conductive to harmony, improved disposition, incitement of will-power and motivation for, as well as confidence in the possibility of being succesful in the new and healthy life style.

INFORMATION ON THE IMPORTANCE OF PROPER DITS-a series of lectures on the importance and kinds of nutrition, physical exercises, their proportioning, etc., is delivered in the course of every reducing cure.

The thus conceived ČIGOTA programme lasting 7 or 14 days is a reliable and efficient way of controlling body weight, it produces desirable impacts on health, and the same time, it is only the first step towards a fuller and lasting weight control and prevention of the harmful consequences of obesity.

INFORMATION AND RESERVATION:
"ZLATIBOR INSTITUTE – ZLATIBOR
Phone (381 31)841-141, Fax (381 31)841-182
"ČIGOTA" AGENCY, Svetog Save 43, BELGRADE
Phone (381 11)444-31-82, Fax (381 11)459-874
"ČIGOTA" MARKETING AND DEVELOPMENT, Bregalnička 9, BELGRADE, Phone (381 11)402-676 & 403-553, Fax (381 11)401-685

Transport each Friday by ČIGOTA bus. Besides that, you can also use regular bus and railway service, and seasonal helicopter service.


GSM network
coverage
ROAMING
BK
BK

CIP – Каталогизација у публикацији
Народна библиотека Србије, Београд

533.9(063)(082)

YUGOSLAV-Belarussian Symposium on Physics and Diagnostics of Laboratory and Astrophysical Plasma (2 ; 1998 ; Zlatibor)
Proceedings of the Second Yugoslav-Belarussian Symposium on Physics and Diagnostics of Laboratory and Astrophysical Plasmas September 5-6, 1998, Zlatibor, Yugoslavia / edited by M.[Milan] S. Dimitrijević and V. S. Burakov. - Београд :

Astronomical Observatory, 1998 (Belgrade : Portal). - 197 str. : ilustr. ; 24 cm. - (Публикације Астрономске опсерваторије у Београду = Publications of the Astronomical Observatory of Belgrade, ISSN 0373-3742 ; sv. 61)

Tekst na engl. i rus. jeziku. - Tiraž 500. - Bibliografija uz većinu radova. - Summaries. - Registar.
1. Burakov, V. S.
52-7(063)(082) 521-355(063)(082)
539.18(063)(082)
a) Плазма - Зборници b) Астрофизика - Зборници c) Атомска физика - Зборници
ID=66584588